

Department of Electrical and Computer Engineering

**A New Technique to Detect Loss of Insulation Life in Power
Transformers**

Norazhar Bin Abu Bakar

**This thesis is presented for the Degree of
Doctor of Philosophy
of
Curtin University**

May 2016

Declaration

To the best of my knowledge and belief this thesis contains no material previously published by any other person except where due acknowledgment has been made.

This thesis contains no material which has been accepted for the award of any other degree of diploma in any university.

Signature:

Date:

Abstract

Power transformer condition monitoring plays an important role in order to maintain the reliability of power systems operations. Failure of a power transformer could lead to a major disaster affecting the whole transmission and distribution network systems. The quality of the insulation system within power transformers comprising dielectric insulation paper and oil reflects the overall health condition of the transformer. The combination of heat (pyrolysis), moisture (hydrolysis) and air (oxidation) within operating transformers causes oil and paper decomposition which result in a number of gases that relate to the cause and effect of various faults. A gas chromatography (GC) instrument is currently used as a laboratory-based technique to quantify dissolved gases in transformer oil samples. However, the GC technique incurs running costs and requires an expert to conduct the test. Furthermore, due to the complexity of the equipment, GC measurement can only be performed in a laboratory environment hence takes a long time to get the results. On the other hand, the quality of the insulating oil influences the performance and the service life of the transformer. During the oil aging process, oil gets contaminated with dissolved decay products and sludge as a result of the chemical reaction between the mineral oil molecules and oxygen dissolved in oil. Sludge and contamination development in insulating oil can be identified by measuring the interfacial tension (IFT) value of the oil. The ASTM D971 standard (Interfacial Tension of Oil Against Water by the Ring Method) is widely used to measure IFT of insulating oil. However, this technique is very sensitive and if the precautions mentioned in the standard procedure are not carefully followed may result in an incorrect or inconsistent IFT reading. Moreover, the current technique calls for a trained person to conduct the test that requires a relatively expensive piece of equipment and lengthy time to get the results as oil samples have to be sent to an external laboratory which also incurs an additional running cost.

This thesis proposes an alternative method of measuring the IFT and dissolved gases in transformer oil using absorption spectroscopy which can be performed instantly on-site and has the potential to be implemented on-line. Two novel methods were developed: measuring transformer oil IFT using ultraviolet-to-visible (UV-Vis) spectroscopy, and detecting dissolved gases in transformer oil using near-infrared-to-infrared (NIR-IR) spectroscopy. Also, a new fuzzy logic approach to provide a proper asset management decision and predict the remaining operational life of a power transformer based on some routine insulating oil tests such as furan, dissolved gas analysis (DGA), IFT, water content, and operating temperature has been proposed in this thesis.

Acknowledgements

I would like to take this opportunity to express my deep gratitude to my supervisor, Associate Professor Dr. Ahmed Abu-Siada, for his guidance, support and encouragement throughout the duration of my research. His valuable ideas and advice helped me in producing a quality research investigation and also in successfully completing writing of this thesis. I am also thankful to my co-supervisor, Professor Syed Islam for his support.

A special thanks to all Transformer Fitness Pty. Ltd., Australia teams, Mr. Min Zaw, Mr. Gary Lenco and Mr. Mohamed Dihishi for making available their expert knowledge and facilities for completion of my research.

I would like to express my gratitude to my sponsors, Universiti Teknikal Malaysia Melaka (UTeM) and the Malaysian Government for giving me an opportunity to pursue my study at Curtin University. Without their financial support, I would not have been able to undertake my study.

I wish to thank my parents for their encouragement and support. Finally, I would like to express my love and gratitude to my wife, Nor Azura Mohd Nasir and children, Aliyah Khadijah, Muhammad Yusuf and Muhammad Muaz whose understanding and support over the years, has enabled me to complete this research.

List of Publications

It is acknowledged that most of the work in this thesis has been published in the following papers.

Journals Published

- Norazhar Abu Bakar; A. Abu-Siada ; S. Islam; M. El-Naggar, “A New Technique to Measure Interfacial Tension of Transformer Oil using UV-Vis Spectroscopy”, IEEE Transactions on Dielectrics and Electrical Insulation, vol. 22, Issue 2, pp. 1275-1282, April 2015.
- Norazhar Abu Bakar and A. Abu-Siada “A Novel Method of Measuring Transformer Oil Interfacial Tension Using UV-Vis Spectroscopy” IEEE Electrical Insulation Magazine”, vol. 32, no. 1, pp. 7-13, Jan 2016.
- Norazhar Abu Bakar, A. Abu-Siada, and S. Islam “A Review of DGA Measurement and Interpretation Techniques” IEEE Electrical Insulation Magazine”, vol. 30, no. 3, pp. 39-49, April 2014.
- Norazhar Abu Bakar, A. Abu-Siada, N. Das and S. Islam “Effect of Conducting Materials on UV-Vis Spectral Response Characteristics”, Universal Journal of Electrical and Electronic Engineering, vol. 1, no. 3, pp. 81-86, October, 2013.

Journal Submitted

- Norazhar Abu Bakar; A. Abu-Siada, “Fuzzy Logic Approach for Transformer Remnant Life Prediction and Asset Management Decision”, Submitted on March 2016 to IEEE Transactions on Dielectrics and Electrical Insulation (accepted for publication on 11th July 2016).
- Norazhar Abu Bakar; A. Abu-Siada , “A New Method to Detect Dissolved Gases in Transformer Oil using NIR-IR Spectroscopy”, Submitted on May 2016 to IEEE Transactions on Dielectrics and Electrical Insulation.

Conference Papers

- Norazhar Abu Bakar; A. Abu-Siada, S. Islam “A Novel UV-Vis Spectroscopy Application to Measure Interfacial Tension of Transformer Oil”, 2015 IEEE PES General Meeting, July 26-30, 2015 Denver, Colorado, USA.
- Norazhar Abu Bakar, A. Abu-Siada, S. Islam, M. F. El-Naggar, “Effects of Various Transformer Oil Contaminations on Its Spectral Response” proceedings of the International Conference on Condition Monitoring and Diagnosis (CMD2014), 21-25 Sept 2014, Jeju, Korea.
- Norazhar Abu Bakar, A. Abu-Siada and S. Islam, “A Review of Chemical Diagnosis Techniques for Transformer Paper Insulation Degradation”, proceedings of the Australasian Universities Power Engineering Conference , AUPEC’13, Hobart, 29 Sep.-3 Oct., 2013.
- Norazhar Abu Bakar, A. Abu-Siada, “High Voltage Power Transformer Dissolved Gas Analysis, Measurement and Interpretation Techniques”, invited paper, High Voltage Maintenance Forum, Perth, 27-28 November 2013.
- Norazhar Abu Bakar, A. Abu-Siada, “High Voltage Power Transformer Paper Insulation Assessment Techniques”, invited paper, High Voltage Maintenance Forum, Perth, 27-28 November 2013.

Conference Submitted Papers

- Norazhar Abu Bakar, Huize Cui, A. Abu-Siada, and Shengtao Li, “A Review of Spectroscopy Technology Applications in Transformer Condition Monitoring”, proceedings of the International Conference on Condition Monitoring and Diagnosis (CMD2016), 25-28 Sept 2016, Xi’an, China (accepted for presentation).
- Norazhar Abu Bakar, A. Abu-Siada, “Remnant Life Estimation and Transformer Asset Decision Based on UV-Vis Spectral Response”, proceedings of the International Conference on Electrical Machine (ICEM’2016), 4-7 Sept 2016, Lausanne, Switzerland (accepted for presentation).

Table of Contents

Declaration.....	ii
Abstract.....	iii
Acknowledgements.....	iv
List of Publications.....	v
Table of Contents.....	vii
List of Figures.....	xi
List of Tables.....	xv
List of Abbreviations.....	xvii
Chapter 1 Introduction.....	19
1.1 Background and Motivation.....	19
1.2 Research Problem.....	21
1.3 Aim and Objectives.....	23
1.4 Research Methodology.....	24
1.5 Research Significance.....	25
1.6 Thesis Outline.....	26
Chapter 2 Power Transformer Condition Monitoring.....	28
2.1 Introduction.....	28
2.2 Paper Insulation Degradation and Assessment.....	29
2.2.1 Degree of Polymerization (DP).....	30
2.2.2 Carbon Oxides Concentration (CO and CO ₂).....	32
2.2.3 Furan Analysis.....	32
2.2.4 Methanol as a New Chemical Marker for Paper Degradation.....	36
2.3 Dissolved Gas Analysis.....	37
2.3.1 DGA Measurement Technique.....	38
2.3.1.1 Gas Chromatography.....	38
2.3.1.2 Hydrogen On-Line Monitoring.....	41
2.3.1.3 Photo-Acoustic Spectroscopy.....	43
2.3.2 Interpretation of DGA Data.....	45
2.3.2.1 Key Gas Method (KGM).....	45
2.3.2.2 Doernenburg Ratio Method (DRM).....	46
2.3.2.3 Rogers Ratio Method (RRM).....	47
2.3.2.4 IEC Ratio Method (IRM).....	48
2.3.2.5 Duval Triangle Method (DTM).....	48
2.3.2.6 Duval Pentagon Method (DPM).....	50

2.3.3	Artificial Intelligence and DGA	52
2.4	Other Oil Physical and Chemical Tests	54
2.4.1	Interfacial Tension (IFT)	54
2.4.2	Acid Number	55
2.4.3	Water Content	56
2.4.4	Dielectric Strength	57
2.4.5	Oxygen.....	58
2.4.6	Oil Power Factor.....	58
2.5	Spectroscopy.....	59
2.5.1	Principle of Absorption Spectroscopy	61
2.5.1.1	UV-Vis Spectroscopy.....	62
2.5.1.2	IR Spectroscopy	63
2.5.2	Basic Structure of Spectroscopy Instrument.....	64
2.6	Conclusion	66
Chapter 3	A New Technique to Measure Interfacial Tension	67
3.1	Introduction.....	67
3.2	IFT Measurement.....	68
3.3	UV-Vis Spectroscopy Setup	69
3.4	Experimental Results and Discussion	70
3.5	Fuzzy Logic Modelling.....	73
3.6	Accuracy Analysis	77
3.7	Comparison Between ASTM D971 Ring Method and UV-Vis Spectroscopy	79
3.8	Conclusion	79
Chapter 4	A New Method to Detect Dissolved Gases in Transformer Oil using NIR-IR Spectroscopy.....	80
4.1	Introduction.....	80
4.2	Experimental.....	83
4.3	Fuzzy Logic Model Development	89
4.4	Accuracy Analysis	99
4.5	Conclusion	100
Chapter 5	Power Transformer Asset Management and Remnant Life.....	104
5.1	Introduction.....	104
5.2	Transformer Health Condition.....	106
5.3	Proposed Approach.....	108
5.4	Fuzzy Logic Model Development	109
5.4.1	Furan Criticality	111
5.4.2	CO Ratio Criticality	113

5.4.3	Paper Aging Criticality	114
5.4.4	Relative Accelerating Aging Criticality.....	116
5.4.5	Thermal Fault Criticality	118
5.4.6	Electrical Fault Criticality.....	120
5.4.7	Overall Thermal-Electrical Fault Criticality.....	121
5.4.8	IFT Criticality	123
5.4.9	Remnant Life Estimation.....	124
5.4.10	Asset Management Model	126
5.5	Validation of The Proposed Model.....	130
5.6	Conclusion	132
Chapter 6	Conclusions and Future Research.....	135
6.1	Conclusions.....	135
6.2	Future Research Recommendation	136

References.....	138
Appendix A Properties of 55 Transformers Used for IFT.....	147
Appendix B Repeatability Test Results of IFT Measurement	148
Appendix C Properties of various oil types used for the results of Figure 3-8	149
Appendix D Fuzzy Rules: IFT Estimation Model.....	150
Appendix E FTIR Repeatability Test Results.....	151
Appendix F Fuzzy Rules: CO Concentration Estimation Model.....	152
Appendix G Fuzzy Rules: CO ₂ Concentration Estimation Model	153
Appendix H Fuzzy Rules: CH ₄ Concentration Estimation Model	154
Appendix I Fuzzy Rules: C ₂ H ₂ Concentration Estimation Model	155
Appendix J Fuzzy Rules: C ₂ H ₆ Concentration Estimation Model	156
Appendix K Fuzzy Rules: C ₂ H ₄ Concentration Estimation Model	157
Appendix L Fuzzy Rules: Furan Criticality Model.....	158
Appendix M Fuzzy Rules: CO Ratio Criticality Model.....	159
Appendix N Fuzzy Rules: Paper Aging Criticality Model.....	160
Appendix O Fuzzy Rules: Relative Accelerating Aging Criticality Model	161
Appendix P Fuzzy Rules: Thermal Fault Criticality Model	162
Appendix Q Fuzzy Rules: Electrical Fault Criticality Model	163
Appendix R Fuzzy Rules: Overall Thermal-Electrical Fault Criticality Model.....	164
Appendix S Fuzzy Rules: IFT Criticality Model.....	165
Appendix T Fuzzy Rules: Remnant Life Estimation Model.....	166
Appendix U Fuzzy Rules: Asset Management Decision Model	167
Appendix V Transformer Condition	171
V.1 Pre-known Condition of Sixteen Transformers	171
Appendix W Validation Results of Transformer Remnant Life Model	172

List of Figures

Figure 1-1 Transformers In a Power Delivery System	19
Figure 1-2 Power Transformer Population in Western Australia [3].....	20
Figure 1-3 Transformer Failure Rates Based on Years of Service [2].....	21
Figure 1-4 Transformer Insulation Analysis	22
Figure 2-1 Types of faults and associated gases [25]	29
Figure 2-2 Cellulose chain structure of new and deteriorated paper insulation [40] ...	30
Figure 2-3 Tensile strength and DP correlation [41]	31
Figure 2-4 Furanic compounds detectable in transformer oil [52]	33
Figure 2-5 A comparison of the various correlation equations between DP and 2FAL [59].....	35
Figure 2-6 Correlation between furan concentration in transformer oil and its spectrum response parameters [21].....	35
Figure 2-7 Extraction of dissolved gases from insulating oil using the vacuum extraction method [15].....	39
Figure 2-8 Extraction of dissolved gases from insulating oil using the headspace method [15].....	40
Figure 2-9 A basic gas chromatograph [137].....	41
Figure 2-10 Schematic diagram of a hydrogen on-line monitor [17].	42
Figure 2-11 Basic process of photo-acoustic spectroscopy [82].....	43
Figure 2-12 Schematic diagram of a PAS-based DGA system [81].....	44
Figure 2-13 Characteristic absorbance levels of various fault gases [81].....	44
Figure 2-14 Key Gas Method Chart [17]	46
Figure 2-15 Coordinates and fault zones in the DTM [89].....	49
Figure 2-16 Coordinates and fault zones in the DTM 4 [91]	49
Figure 2-17 Coordinates and fault zones in the DTM 5 [91]	49
Figure 2-18 Example of Duval Pentagon representation [143].....	50
Figure 2-19 The Duval Pentagon 1 for the six “basic” faults [143].....	50
Figure 2-20 The Duval Pentagon 2 for the three basic electrical faults PD, D1, and D2 and the four “advanced” thermal faults	51
Figure 2-21 Proposed AI interpretation method [92].....	53
Figure 2-22 Relationship between IFT, acidity and transformer years in service[103].	54
Figure 2-23 Interfacial tension measurement setup based on ASTM D971[13].....	55
Figure 2-24 Energy levels of various electronic transition types.....	63
Figure 2-25 Schematic diagram of a monochromator (prism).....	64
Figure 2-26 Schematic diagram of interferometer	65
Figure 3-1 Experimental setup for UV-Vis spectroscopy.....	69

Figure 3-2 UV-Vis spectral response for various IFT numbers (mN/m) [155].	70
Figure 3-3 Correlation between IFT (mN/m), peak absorbance and maximum wavelength of oil spectral responses [155].	71
Figure 3-4 Correlation between breakdown voltage (kV), peak absorbance and maximum wavelength of oil spectral response [155].	71
Figure 3-5 Correlation between water content (mg/kg), peak absorbance and maximum wavelength of oil spectral response [155].	72
Figure 3-6 Correlation between acidity (mgKOH/g), peak absorbance and maximum wavelength of oil spectral response [155].	72
Figure 3-7 Spectral response of new transformer oil samples of different types [155].	73
Figure 3-8 Basic fuzzy logic system architecture [140].	74
Figure 3-9 Absorbance, bandwidth and IFT membership functions [140].	75
Figure 3-10 Graphical representation of the developed fuzzy logic rules correlating absorbance and bandwidth with IFT value [140].	75
Figure 3-11 An example of the calculation of IFT based on Fig. 3-11 and (3-2) [140].	76
Figure 3-12 IFT as a function of bandwidth and peak absorbance, according to the fuzzy logic model [140].	77
Figure 3-13 Comparison of ASTM D971 and fuzzy logic values of IFT for each of twenty oil samples.	77
Figure 4-1 NIR absorption spectrum of CO, CO ₂ , CH ₄ , and C ₂ H ₂ based on HITRAN database [153].	81
Figure 4-2 IR absorption spectrum of CO, CO ₂ , CH ₄ , C ₂ H ₆ , C ₂ H ₄ , and C ₂ H ₂ based on HITRAN and NIST database [153, 154].	82
Figure 4-3 Absorbance spectra for various oil samples with different CO concentrations at 2250-2000cm ⁻¹ region.	84
Figure 4-4 Absorbance spectra for various oil samples with different CO concentrations in the 6450-6100cm ⁻¹ region.	84
Figure 4-5 Absorbance spectra for various oil samples with different CO ₂ concentrations in the 2400-2250cm ⁻¹ region.	85
Figure 4-6 Absorbance spectra for various oil samples with different CO ₂ concentrations in the 7000-6850cm ⁻¹ region.	85
Figure 4-7 Absorbance spectra for various oil samples with different CH ₄ concentrations in the 3200-2721cm ⁻¹ region.	86
Figure 4-8 Absorbance spectra for various oil samples with different CH ₄ concentrations in the 6000-5800cm ⁻¹ region.	86
Figure 4-9 Absorbance spectra for various oil samples with different C ₂ H ₂ concentrations in the 1400-1300cm ⁻¹ region.	87
Figure 4-10 Absorbance spectra for various oil samples with different C ₂ H ₂ concentrations in the 6600-6500cm ⁻¹ region.	87
Figure 4-11 Absorbance spectra for various oil samples with different C ₂ H ₆ concentrations in the 1500-1400cm ⁻¹ region.	87

Figure 4-12 Absorbance spectra for various oil samples with different C ₂ H ₄ concentrations in the 1000-900cm ⁻¹ region.....	88
Figure 4-13 Input and output variables' MFs for CO fuzzy model	90
Figure 4-14 Developed fuzzy rules for CO estimation	90
Figure 4-15 CO estimation surface graph.....	91
Figure 4-16 Input and output variables' MFs for CO ₂ fuzzy model	91
Figure 4-17 Developed fuzzy rules for CO ₂ estimation.....	92
Figure 4-18 CO ₂ estimation surface graph.....	92
Figure 4-19 Input and output variables' MFs for CH ₄ fuzzy model	93
Figure 4-20 Developed fuzzy rules for CH ₄ estimation.....	93
Figure 4-21 CH ₄ estimation surface graph.....	94
Figure 4-22 Input and output variables' MFs for C ₂ H ₂ fuzzy model.....	94
Figure 4-23 Developed fuzzy rules for C ₂ H ₂ estimation.....	95
Figure 4-24 C ₂ H ₂ estimation surface graph	95
Figure 4-25 Input and output variables' MFs for C ₂ H ₆ fuzzy model.....	96
Figure 4-26 Developed fuzzy rules for C ₂ H ₆ estimation.....	96
Figure 4-27 C ₂ H ₆ estimation surface graph	97
Figure 4-28 Input and output variables' MFs for C ₂ H ₄ fuzzy model.....	97
Figure 4-29 Developed fuzzy rules for C ₂ H ₄ estimation.....	98
Figure 4-30 C ₂ H ₄ estimation surface graph	98
Figure 4-31 The proposed overall fuzzy logic estimation model.....	99
Figure 5-1 Flow chart of the proposed approach	109
Figure 5-2 Fuzzy decision tree concept	110
Figure 5-3 Proposed fuzzy logic asset management decision model.....	110
Figure 5-4 Input and output variables' MF for furan fuzzy model	111
Figure 5-5 Developed fuzzy rules for paper life estimation based on furan	112
Figure 5-6 Paper life estimation surface graph	112
Figure 5-7 Input and output variables' MF for CO ratio fuzzy model.....	113
Figure 5-8 Developed fuzzy rules for paper deterioration based on CO ratio	113
Figure 5-9 Paper deterioration surface graph.....	114
Figure 5-10 Input and output variables' MF for paper aging criticality fuzzy model	115
Figure 5-11 Developed fuzzy rules for paper aging criticality	115
Figure 5-12 Paper aging criticality surface graph.....	116
Figure 5-13 Input and output variables' MF for relative accelerating aging fuzzy model	116
Figure 5-14 Developed fuzzy rules for relative accelerating aging	117
Figure 5-15 Relative accelerating aging surface graph.....	117
Figure 5-16 Input and output variables' MF for thermal fault fuzzy model	118

Figure 5-17	Developed fuzzy rules for thermal fault criticality based on ethylene and ethane	119
Figure 5-18	Thermal fault surface graph	119
Figure 5-19	Input and output variables' MF for electrical fault fuzzy model.....	120
Figure 5-20	Developed fuzzy rules for electrical fault criticality based on methane and acetylene.....	120
Figure 5-21	Electrical fault surface graph.....	121
Figure 5-22	Input and output variables' MF for overall thermal-electrical fault fuzzy model	121
Figure 5-23	Developed fuzzy rules for overall thermal-electrical fault criticality....	122
Figure 5-24	Overall thermal-electrical fault surface graph.....	122
Figure 5-25	Input and output variables' MF for IFT criticality fuzzy model	123
Figure 5-26	Developed fuzzy rules for contamination criticality based on IFT	123
Figure 5-27	Contamination criticality surface graph	124
Figure 5-28	Input and output variables' MF for transformer remnant life (D1) fuzzy model	124
Figure 5-29	Developed fuzzy rules for transformer remnant life estimation (D1) ...	125
Figure 5-30	Transformer remnant life (D ₁) surface graph	125
Figure 5-31	Input and output variables' MF for asset management decision fuzzy model	126
Figure 5-32	Developed fuzzy rules for asset management decision (D ₂ and D ₃)	126
Figure 5-33	Asset management decision (D ₂) surface graph.....	127
Figure 5-34	Asset management decision (D ₃) surface graph.....	128
Figure 5-35	Comparison between proposed model and real transformer condition ..	132
Figure 5-36	Relationship between model transformer remnant life estimation and transformer real condition.....	132

List of Tables

Table 1-1 Transformer Causes of Failure and Losses [2]	20
Table 2-1 Correlation between DP and mechanical strength [8]	31
Table 2-2 Correlation between furan spectral response and DP level [29].....	35
Table 2-3 Advantages and disadvantages of various paper diagnostic methods [138].....	37
Table 2-4 Comparison of GC, Hydrogen On-line Monitor and PAS [137].....	45
Table 2-5 DRM Concentration Ratios [28].....	46
Table 2-6 Dissolved Gas Concentrations (L1) for the DRM [46]	47
Table 2-7 Revised Suggested RRM Diagnoses [137].....	47
Table 2-8 Suggested IRM diagnoses [87].....	48
Table 2-9 Comparison of KGM, DRM, RRM, IRM, DTM and DPM	51
Table 3-1 Comparison results between actual and estimated IFT for 20 oil samples..	78
Table 3-2 Comparison between IFT measurement based on ASTM D971 method and proposed UV-Vis Spectroscopy.....	79
Table 4-1 Spectrum range for each fault gas	82
Table 4-2 Comparison between actual (GC) and estimated (fuzzy model) gas concentration for 20 oil samples	102
Table 4-3 Comparison of GC, hydrogen on-line monitor, PAS and the proposed spectroscopy methods	103
Table 5-1 Proposed parameters for transformer remnant life and asset management decision model	108
Table 5-2 Proposed transformer asset management decision code.....	129
Table 5-3 Fuzzy logic model output with criticality code proposed.....	134

List of Abbreviations

2-ACF	2-Acetylfuran
2-FAL	2-Furan
2-FOL	2-Furfurol
5-HMF	5-Hydroxy Methyl-2-furfural
5-MEF	5-Methyl-2-furfural
ABS	Peak Absorbance
ASTM	American Society for Testing and Materials
BDV	Average Breakdown Voltage
BW	Bandwidth
C ₂ H ₂	Acetylene
C ₂ H ₄	Ethylene
C ₂ H ₆	Ethane
CH ₄	Methane
CO	Carbon Monoxide
CO ₂	Carbon Dioxide
COG	Centre of Gravity
DGA	Dissolved Gas Analysis
DP	Degree of Polymerization
FT	Fourier Transforms
FRA	Frequency Response Analysis
GC	Gas Chromatography

H ₂	Hydrogen
HITRAN	High-resolution Transmission Molecular Absorption Database
HPLC	High-Performance Liquid Chromatography
IEC	International Electrotechnical Commission
IEEE	Institute of Electrical and Electronics Engineers
IFT	Interfacial Tension
IR	Infrared
MeOH	Methanol
MF	Membership Function
M/DW	Moisture per Dry Weight
N ₂	Nitrogen
NIR	Near-Infrared
NIST	National Institute of Standards and Technology, United States
O ₂	Oxygen
PAS	Photo-Acoustic Spectroscopy
TDCG	Total Dissolved Combustible Gas
UV	Ultraviolet
Vis	Visible

Chapter 1 Introduction

1.1 Background and Motivation

A power transformer is a vital link for any electrical transmission and distribution network, as shown in Figure 1-1. Failure of power transformers could lead to a major disaster affecting the whole power delivery system. Furthermore, an unexpected failure of power transformers could not only cause an electricity shortage to the consumer, but also would involve the loss of millions of dollars for utility companies, industrial failure costs, environmental hazards costs due to oil spillage, and also indirectly to the national security [1]. Based on a report provided in 2003 by the International Association of Engineering Insurers (IMIA), the total losses in five years (from 1997 to 2001) for 94 cases involving power transformer failure, which does not include Business Interruption claims, was about \$286 million [2]. The highest cost was caused by transformer insulation failure, as shown in Table 1-1.

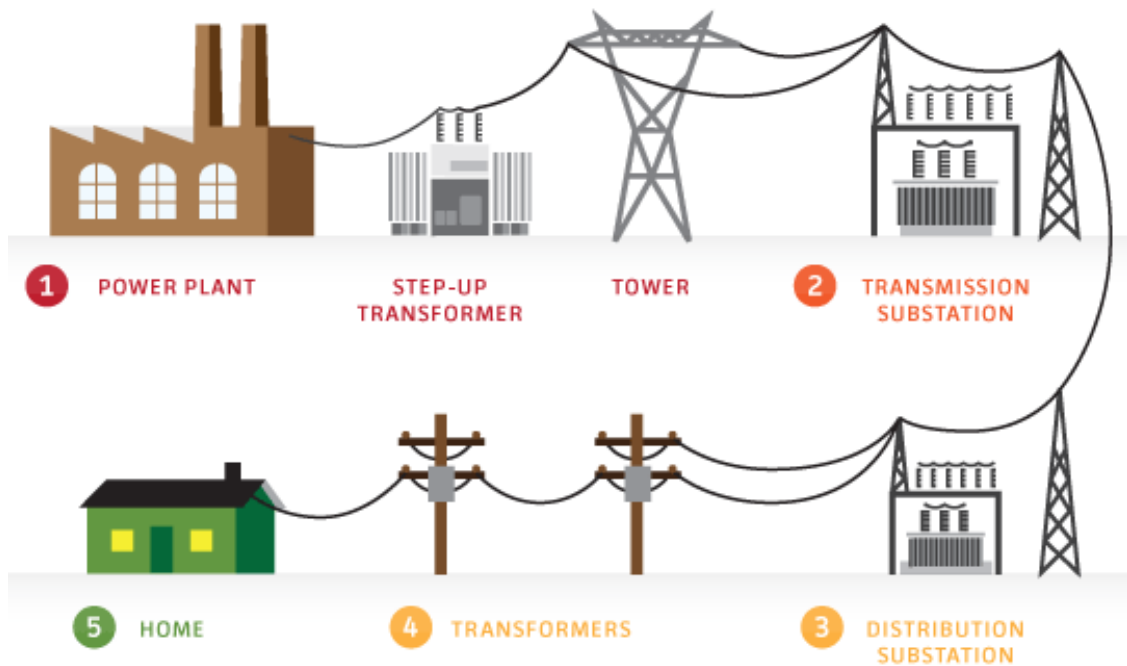


Figure 1-1 Transformers In a Power Delivery System

Another consideration is that, most transformers nowadays are operating either close to or in excess of their design life which is approximately between 35 to 40 years. In fact, the statistics data published by US Department of Energy (2014) shows that the average length of operation of power transformers in the United State is approximately 40 years [1].

Table 1-1 Transformer Causes of Failure and Losses [2]

Cause of Failure	Number	Total Cost
Insulation Failure	24	\$149,967,277
Design/ Material/ Workmanship	22	\$64,696,051
Unknown	15	\$29,776,245
Oil Contamination	4	\$11,836,367
Overloading	5	\$8,568,768
Fire/ Explosion	3	\$8,045,771
Line Surge	4	\$4,959,691
Improper Maintenance/ Operation	5	\$3,518,783
Flood	2	\$2,240,198
Loose Connection	6	\$2,186,725
Lightning	3	\$657,935
Moisture	1	\$175,000
	94	\$286,628,811

Meanwhile, according to Western Power Australia, in their State of Infrastructure Report 2014/15, the majority of transformers operated in Western Australia are over 30 years old and 11.1% of them are already over 40 years old, as shown in Fig.1-2 [3]. A failure rates analysis in accordance with the transformer failure pattern “bathtub” curve reveals that the possibility of a power transformer failure is increased after 30 years of service, as shown in Figure1-3 [2, 4].

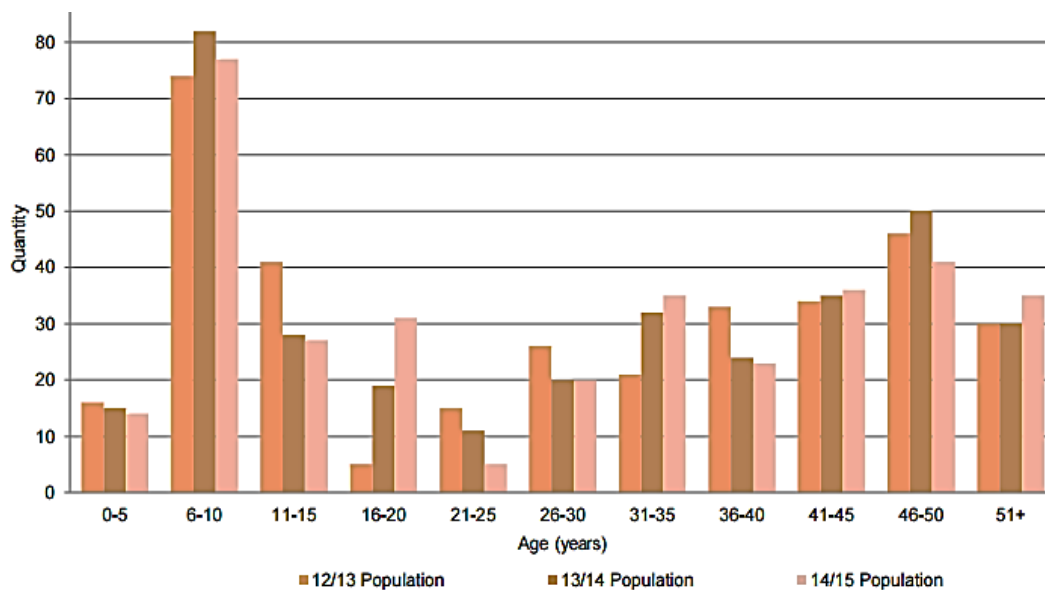


Figure 1-2 Power Transformer Population in Western Australia [3]

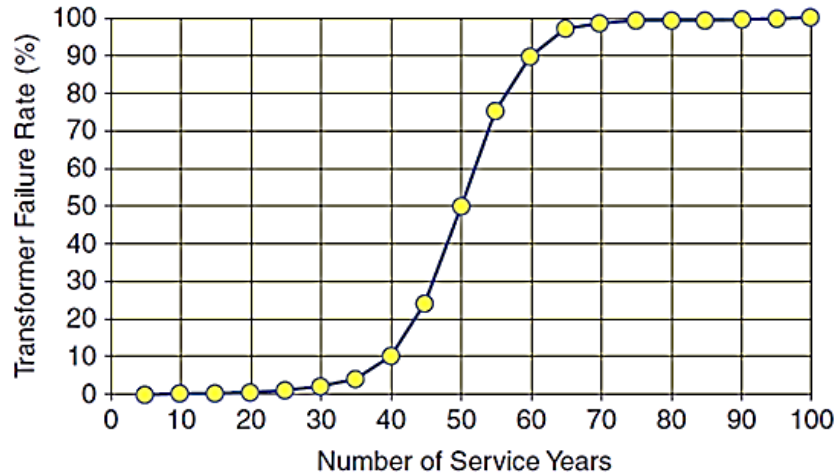


Figure 1-3 Transformer Failure Rates Based on Years of Service [2]

Therefore, a reliable monitoring and diagnostic technique to detect transformer incipient faults is required to avoid catastrophic failures and help in providing efficient predictive maintenance that improves the reliability of the equipment [5]. Often, power transformer health is referred to the quality of its insulation system which consists of paper insulation immersed in insulating oil [6, 7]. Long term degradation of an insulation system occurs mainly through heating (pyrolysis), moisture ingress (hydrolysis) and air ingress (oxidation) [8, 9]. Incipient faults within a transformer can be detected by analyzing samples of its insulating oil, e.g., using dissolved gas analysis and furan analysis [10]. Concurrently, sludge and acids formed in transformer oil affects its quality and potentially increases the rate of insulation paper aging [11]. Thus, IFT and acid number measurements may use as early warnings of insulation aging development [12].

1.2 Research Problem

Several diagnostic techniques have been implemented by industries to assess and monitor the condition of insulation systems of in-service transformers. These assessments can be classified into two groups, electrical and chemical analysis as shown in Fig.1-4. Partial discharge analysis, dielectric breakdown voltage, power factor, time domain polarization, and frequency domain polarization are part of electrical analysis, while water content, acidity, interfacial tension (IFT), degree of polymerization, dissolved gas analysis (DGA), and furan analysis are part of chemical analysis. In practice, water content, acidity, IFT, DGA and furan of transformer insulation oil are frequently monitored during routine maintenance tests, at least once a year for healthy transformers. Meanwhile, for aging or critical transformers, the tests are carried out more frequently.

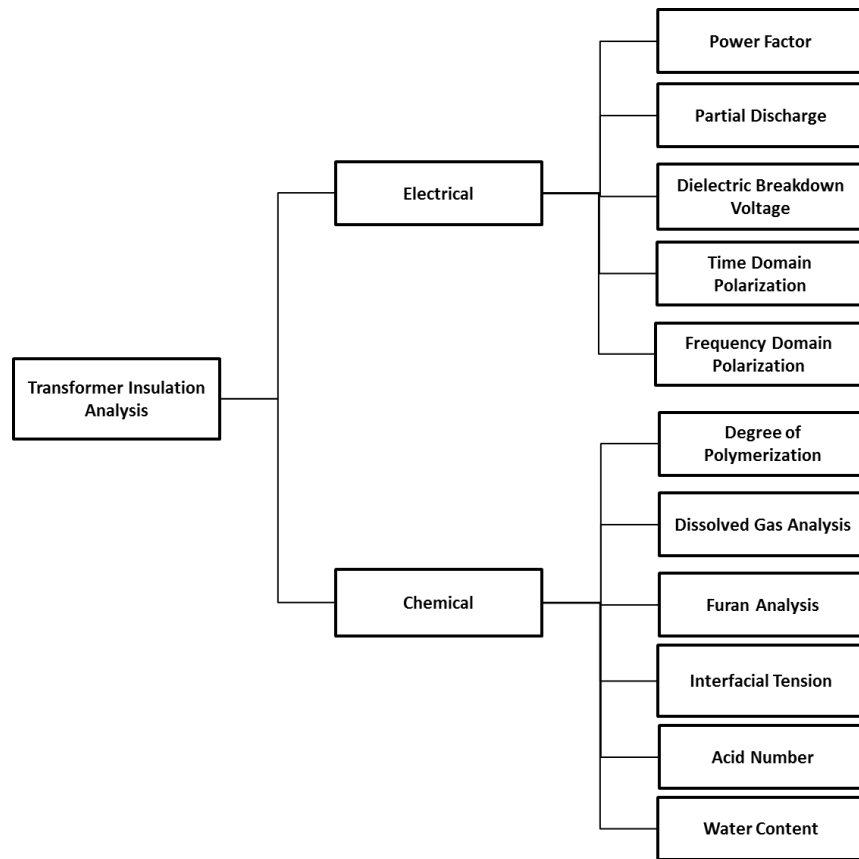


Figure 1-4 Transformer Insulation Analysis

This research is focused on improving the method for diagnoses of the DGA and IFT of transformer insulating oil. Transformer remnant life and asset management decisions based on routine insulating oil testing is also covered in this research. The ASTM D971 standard (Interfacial Tension of Oil against Water by the Ring Method) is widely used to measure the IFT of insulating oil [13].

Soluble polar contaminants and degradation products affect the physical and electrical properties of the insulating oil, thereby lowering the IFT value [13, 14]. The current IFT measurement technique requires great care. Wrong or inconsistent data are likely to be obtained if the precautions mentioned in ASTM D971 standard [13] are not carefully and completely observed. A trained person is required to take the measurements, using an expensive piece of equipment, so that in nearly all cases the oil samples have to be sent to an external laboratory.

On the other hand, gases dissolved in transformer oil can be extracted using ASTM D3612 – Test Method for Analysis of Gases Dissolved in Electrical Insulating Oil by Gas Chromatography [15] or IEC Standard 567- Guide for The Sampling of Gases and of Oil From Oil-Filled Electrical Equipment and For The Analysis of Free and Dissolved Gases.

Current DGA measurement using gas chromatography (GC) can only be done in a laboratory environment due to the complexity of the equipment required where oil samples are to be collected from operating transformers, and transported to the laboratory for gas extraction and measurement processes as stated in ASTM D3612 [15]. Due to the time and costs involved with GC, DGA analysis using this technique is only performed once a year for operating transformers. Frequent DGA testing is only used when significant fault gases have been detected during routine analysis [16].

To overcome the limitation of GC, several new analytical techniques have been introduced, such as the hydrogen on-line monitor and the photo-acoustic spectroscopy (PAS) [16, 17]. Even though both techniques can be implemented on-line, the hydrogen on-line monitor is only capable of detecting a few dissolved gases in transformer oil, whereas the PAS is capable of accurately detecting the gas concentration levels that are influenced by the external temperature and pressure and also affected by vibrations.

In the meantime, the absorption spectroscopy technique which utilizes an electromagnetic effect to determine the energy level and structure of atomic or molecular substance has also been considered for suitability in analysing transformer conditions. Recently, several types of analysis of transformer conditions using absorption spectroscopy techniques have been proposed, such as to analyse the degradation of paper insulation, to estimate the furan concentration in transformer oil, to detect additives and contaminants in insulating oil, and to determine moisture content in insulating oil [18-21]. On the other hand, spectroscopy technologies have also been used to trace the amount of gases concentration either in space or solvent in astrophysics and chemistry fields [22, 23].

1.3 Aim and Objectives

The key aim of this research is to develop a novel reliable cost effective technique to assess the insulation condition of power transformers. The research objectives are listed below:

Objective 1 (a) Investigating the correlation between interfacial tension, acidity, breakdown voltage and water content of transformer oil with its UV-Vis spectral response.

(b) Developing a new technique to measure the interfacial tension of transformer oil using UV-Vis spectroscopy.

Objective 2 (a) Investigating the characteristic of each key gas dissolved in the transformer oil with its NIR-IR spectral response.

(b) Developing a new technique to measure key gases dissolved in transformer oil using NIR-IR spectroscopy.

Objective 3 Developing an expert model to estimate the remnant life and asset management decision of power transformers based on routine insulating oil tests.

1.4 Research Methodology

In respect of the objectives of this research project, the following methodologies are adopted:

- Method for Objective 1: Developing a new technique to measure the interfacial tension of transformer oil using UV-Vis spectroscopy:
 - New and in-service transformer oil collected from utility companies are tested with interfacial tension, acidity, breakdown voltage, and water content in accordance with the current practice standards.
 - Same oil samples are then examined using UV-Vis spectroscopy.
 - The correlation between interfacial tension, acidity, breakdown voltage and water content of transformer oil with its UV-Vis spectral response are investigated.
 - Spectral response results for various interfacial tension numbers are analysed, and the impact of absorbance level and maximum bandwidth are evaluated.
 - The correlation between absorbance level and bandwidth, with the interfacial tension of transformer oil is developed using the fuzzy logic model.
 - The accuracy of the fuzzy logic model developed is validated with other sets of in-service transformer oil.
 - The oil spectroscopy test procedure in this work is conducted in accordance with ASTM E275 [148].

- Method for Objective 2: Developing a new technique to measure the dissolved gases in transformer oil using NIR-IR spectroscopy:
 - Different concentrations of individual key gases dissolved in oil are prepared using new oil in accordance with ASTM D3612 [15] standard and measured with gas chromatography.
 - Same oil samples are then examined using NIR-IR spectroscopy.
 - Spectral response results for each gas with various concentrations are analysed, and the impact of absorbance level and spectral response area in a particular range are evaluated.
 - The correlation between the absorbance level and the spectral response area, with the individual key gases in transformer oil are developed using the fuzzy logic model.

- The oil spectroscopy test procedure in this work is conducted in accordance with the ASTM E2412 [156] and ASTM E1790 [157] standards.
- Method for Objective 3: Developing an expert model to estimate the remnant life and asset management decision of power transformers based on routine insulating oil tests:
 - An expert model to estimate the remnant life of power transformer is developed using the fuzzy logic model.
 - Insulating oil routine tests; DGA, furan, water content, IFT, and operating temperature are used as an input for the fuzzy logic model, and estimates of power transformer life and asset management decisions are the outputs of this model.
 - Fuzzy logic rules are developed based on the correlations reported in the literature and obtained in findings of the previous objective.
 - The fuzzy logic model is developed and simulated using MATLAB/Simulink software.

1.5 Research Significance

Transformers play an important role in power system delivery. Unexpected failure of power transformers is a major disaster for any electricity transmission or distribution network. Furthermore, the growing population of aging power transformers being operated requires regular monitoring and diagnostic testing to minimize the possibility of catastrophic failures occurring. The choice by utility companies of replacing aging transformers with new transformers will be undertaken as a last resort since the price for new transformers is extremely expensive. Moreover, in the highly competitive electricity global market, delaying and maintaining aging transformer in-service is the preferred option compared to replacement. Therefore, a reliable and cost effective diagnostic tool is necessary in order to monitor the health condition of power transformers. Meanwhile, an appropriate asset management decision can extend the operational life of a transformer and minimise the possibility of catastrophic failures.

This thesis proposed two alternative models of measuring the IFT and dissolved gases in transformer oil using absorption spectroscopy. Two novel techniques were developed: measuring transformer oil IFT using ultraviolet-to-visible (UV-Vis) spectroscopy; and detecting dissolved gases in transformer oil using near-infrared-to-infrared (NIR-IR) spectroscopy using a fuzzy logic model approach. The advantage of the proposed techniques

over current practice –ASTM D971 (Interfacial Tension of Oil Against Water by the Ring Method) and the gas chromatography measurement technique– is that they can be conducted instantly on site without the need for trained personnel. Also, the proposed techniques in this research do not incur any running costs, and can be readily implemented on-line for continuous monitoring of the transformer oil condition. A new fuzzy logic approach has also been proposed in this thesis to provide a proper asset management decision and predict the remaining operational life of a power transformer based on some routine insulating oil tests such as furan, DGA, IFT, water content, and operating temperature in evaluating the remnant life and health condition of power transformers. The key advantage of the proposed model in this thesis over previously published models is that all input parameters proposed in the model can potentially be measured on-line or on-site which facilitates a proper and timely maintenance action based on the model output. The model also considers the rate of increase of key parameters that significantly affect transformer health conditions such as furan, carbon monoxide (CO), and IFT.

1.6 Thesis Outline

The aim of the research reported in this thesis is to develop new techniques to detect loss of insulation life in power transformers. There are six chapters in this thesis. The following is an outline of the remaining chapters of the thesis:

- Chapter 2 is a literature review and discussion of the topics related to power transformer condition monitoring of insulation systems, such as paper insulation degradation assessment, DGA measurement technique and interpretation, and oil physical/chemical testing. In addition, the principle of absorption spectroscopy along with its application in transformer condition monitoring is discussed.
- Chapter 3 describes and discusses the development of a new technique to measure the IFT of transformer oil using UV-Vis spectroscopy is discussed. The correlation between the IFT value based on the ASTM D971 method and its oil spectral response is presented. The development of a fuzzy logic estimation model to correlate between oil spectral response parameters and estimated IFT is explained.
- Chapter 4 describes the development of a new technique to identify dissolved gases in transformer oil using NIR-IR spectroscopy. The possibility of detecting some fault gases such as carbon monoxide, carbon dioxide, methane, acetylene, ethylene, and ethane within NIR-IR region is discussed. Then it describes the correlation between each of the gases with its oil spectral response parameters, and the development of the fuzzy logic model in estimating gas concentration based on spectral response.

- Chapter 5 describes the development of transformer remnant life and asset management decision model based on routine insulating oil tests. Then it describes the development of a fuzzy logic model for asset management decision and transformer remnant life based on DGA, furan, IFT, water content and operating temperature results. The validation results of the proposed asset management decision model over actual transformer condition also been discussed in this chapter.
- Finally, in Chapter 6, the overall research conclusion and recommendations for future work are presented.

Chapter 2 Power Transformer Condition Monitoring

2.1 Introduction

Power transformers represent a vital link in any electrical transmission or distribution network. Unexpected failures do not only cause loss of revenue but may lead to a catastrophic failure including environmental hazards due to oil spillage. Therefore, it is essential to adopt appropriate monitoring and diagnostic techniques for incipient fault detection to avoid catastrophic failures and help to provide efficient predictive maintenance that improves the reliability of the equipment [24]. Assessing the condition of transformers with appropriate diagnostic techniques also assists in asset management decisions regarding transformer replacement or rehabilitation. Often, a power transformer's health is related to the quality of its insulation system which consists of paper insulation immersed in insulating oil [6, 7]. Hence, samples of transformer oil and paper insulation are essential sources for detecting incipient and fast developing faults.

Transformer faults generally result from the long term degradation of oil and paper due to the combination of heat (pyrolysis), moisture (hydrolysis) and air (oxidation) [9]. Due to electrical and thermal stresses that an in-service power transformer experiences, oil and paper decomposition occurs resulting in a various gases depending upon the causes of the faults. Gases produced due to oil decompositions are hydrogen (H_2), methane (CH_4), acetylene (C_2H_2), ethylene (C_2H_4) and ethane (C_2H_6); while paper decompositions mainly produce carbon monoxide (CO) and carbon dioxide (CO_2); which can be used as a trigger source for monitoring the condition of paper insulation [25-27]. The characteristics and concentrations of the gases dissolved in transformer oil vary according to the nature of the fault, and hence can be used to identify the type of fault. However, the analysis is not always straightforward as there may be more than one fault present at the same time.

Transformer internal faults are categorised into thermal or electrical where each fault evolves particular characteristic gases and produces energy from low levels to high levels of sustained arcing. Partial discharge which produces H_2 and CH_4 is a low level energy fault, whereas arcing that is capable of generating all gases including C_2H_2 is considered a high level energy fault [25, 27, 28]. The various faults and their characteristic gases they produce are illustrated in Fig. 2-1.

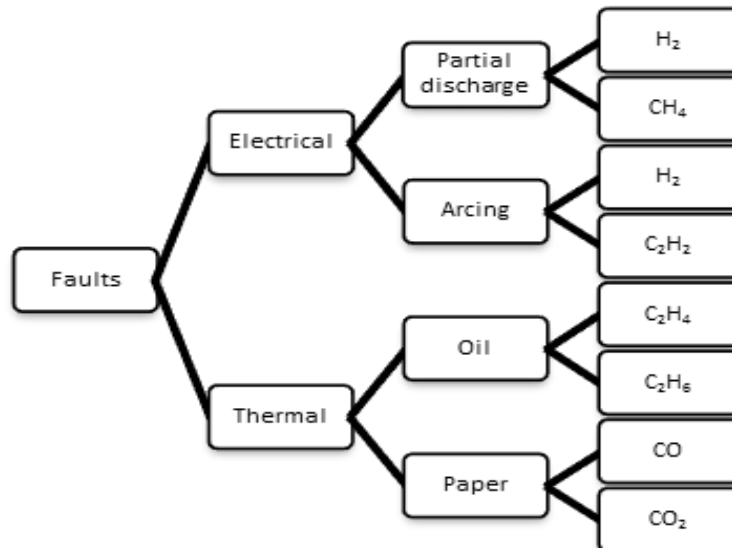


Figure 2-1 Types of faults and associated gases [25]

2.2 Paper Insulation Degradation and Assessment

Paper insulation consists of cellulose, hemi-cellulose, lignin and some mineral substances. According to Abu-Siada, Lai Sin and Islam (2009) [29], paper insulation consists of approximately 90% cellulose, 6-7% hemi-cellulose and 3-4% of lignin; while Schaut, Autru and Eeckhoudt (2011) [9] reported that soft wood Kraft paper consists of approximately 80% cellulose, 12% hemi-cellulose and 8% of lignin and some mineral substances. A dry wood Kraft paper contains 40 to 50% of cellulose, 10-30% hemi-cellulose and about 20-30% lignin [8]. Cellulose is a linear polymer of glucose molecules, which are connected together via glycosidic bonds [30]. When degradation of paper insulation occurs, hydrogen bonds tend to breakdown causing the cellulose molecular chain to shorten. As a result, some chemical products such as CO, CO₂ and furan derivatives are formed and dissolve in the oil. According to Duval, high rates of paper degradation are indicated when the ratio of CO₂/CO is below 6 [31]. However, the application of a CO and CO₂ ratio as an indicator for paper health condition is not reliable due to the long-term oxidation effect of oil that may produce these gases [9]. To overcome this problem, additional tests such as furan analysis or the degree of polymerization (DP) of paper is conducted to examine the health condition of paper. Lately, due to upgraded thermal paper being used in power transformers, which produces less furan derivatives, another possible chemical marker is investigated. According to Jalbert et al. [32] and Schaut, Autru and Eeckhoudt [9], methanol (MeOH) has the potential to be used as a new indicator to monitor the insulation condition of paper.

2.2.1 Degree of Polymerization (DP)

The degree of polymerization (DP) is a direct technique applied to assess the condition of insulating paper in power transformer as stated in IEC 60450 [33]. DP value reveals a strong correlation between the insulation paper deterioration and formation of aging products. The number of anhydro- β -glucose monomers, $C_6H_{10}O_5$ units (also known as DP) in a cellulose chain is a direct indicator of the cellulose decomposition. With the DP technique, the length of the cellulose chain is measured by the average DP based on the viscosity (DP_v) method to determine the quality of cellulose [8, 34]. The viscometer method to determine DP values was introduced by Staudinger in the early 1930's [35] and the correlation of intrinsic viscosity with molecular weight, known as the Mark-Houwink equation, was formulated in 1940 [36]. The intrinsic viscosity of a polymer in a dilute solution correlates with the volume of hydrodynamic sphere of the molecule in solution, which depends on the shape and type of polymer [35]. However, the Mark-Houwink equation is only valid for dilute solutions approximately between 0.1 to 1.0%, since the relationship of DP and intrinsic viscosity is linear within this range only [35]. Therefore, the standard ASTM D4243-99 clearly states that the value of intrinsic viscosity (η) must remain below one [34]. Huggins-Kraemer [36] proposed a technique to measure η based on the concentration of cellulose (g/100ml of solution). In the ASTM D4243 standard procedure, Martin's formula is used to calculate the intrinsic viscosity, which is quite similar to using Huggins-Kraemer's equation. The first standard procedure to measure the average viscometric degree of polymerization was published in 1974 labelled as IEC 450 (labelled later as IEC60450) [33]. Based on IEC 60450, a sample of insulation paper taken when servicing a transformer is required for direct measurement of DP [37]. This paper sample must be taken from locations that have the most rapidly aging paper (hot spot locations) [38]. Emsley et al. [39] developed a first-order kinetic equation that relates the reaction rate at any time with the number of unbroken chain bonds available. Fig. 2-2 shows the cellulose chain structure of new and deteriorated insulating paper.

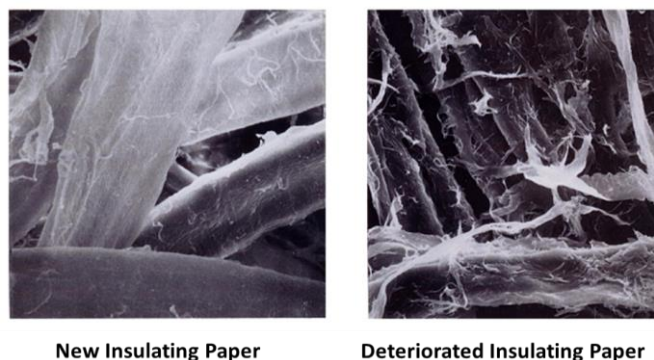


Figure 2-2 Cellulose chain structure of new and deteriorated paper insulation [40]

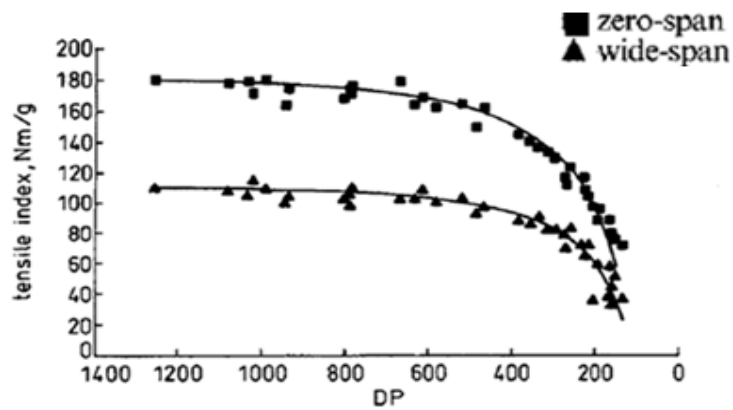


Figure 2-3 Tensile strength and DP correlation [41]

Shroff and Stannett (1985) [41] proved that the paper tensile strength is proportional with the DP value until the transformer gets to the end of life. This result is supported by a study done by Emsley, Heywood, Ali and Xiao (2000) [42] as shown in Fig. 2-3. New Kraft paper has an average length of DP around 1000 to 1500 and the tensile strength is about 1200. When DP value decreases from 1000 to 450, it is considered as a moderate deterioration and the strength is virtually constant. However, when DP value falls below 450, it is an indicator that the mechanical strength of the paper is critical. The paper colour changes to dark brown when DP values are in the range of 200 to 250, and when it reaches a value between 150 to 200, the paper is considered to have no mechanical strength anymore, and therefore the transformer’s life is over [8, 9, 27, 43]. The correlation between the DP of insulation paper and its mechanical strength is summarized in Table 2-1.

Table 2-1 Correlation between DP and mechanical strength [8]

DP Value	Mechanical Strength	Assessment of Transformer
1000 -1500	Greatest (New paper)	Healthy insulation
450 – 1000	Constant (Normal operation)	Moderate deterioration
250 - 450	Critical (Lower requirement)	Extensive deterioration
200 - 250	Nearly loses strength	Crucial deterioration
<200	Zero Strength (End use)	End of life criteria

Gel Permeation is a proposed method that relates DP values with the operation temperature. It is reported that the value of DP begins to decrease at a temperature between 120-140°C, and rapidly decreases with the increase in operating temperature. It goes to end of life criteria at 160-180°C [8].

2.2.2 Carbon Oxides Concentration (CO and CO₂)

An indirect technique for paper insulation assessment is by using a dissolved gas analysis (DGA). As opposed to the Degree of Polymerization method, DGA can be easily applied to an operating transformer [15, 34]. By analyzing the insulating oil of a transformer for specific gas concentrations, its generation rates and total combustible gases can be detected using DGA approaches [44].

Gases dissolved in transformer oil can be extracted using ASTM D3612 – Test Method for Analysis of Gases Dissolved in Electrical Insulating Oil by Gas Chromatography [15] or the IEC Standard 567- Guide for the Sampling of Gases and Oil from Oil-Filled Electrical Equipment and for the Analysis of Free and Dissolved Gases. Tamura et al. [26] reported a strong relationship between the amount of carbon oxides, CO and CO₂, dissolved in transformer oil and the degree of polymerization of insulating paper exist. However, the amount of carbon oxides in insulating oil may also originates from oil decomposition due to long-term oxidation process. De Pablo [45] reported that water and carbon dioxide are the main by-products of the thermal degradation of cellulose. Hence, the ratio of CO₂/CO is normally used as an indicator of thermal decomposition of cellulose [46].

According to the IEEE Standard C57.104, the ratio of CO₂/CO is normally around seven, while the respective values of CO₂ and CO should be greater than 5000 parts per million (ppm) and 500 ppm respectively in order to improve the certainty factor. According to Serveron Corporation (2007) [47], when this ratio is less than 3, it indicates a severe paper degradation. When the ratio exceeds 10, it indicates a fault of temperature less than 150°C. According to Duval et al. [48], faults start to arise when the CO₂/CO ratio is less than 6, while Kan and Miyamoto [49, 50] maintain that it arises at a higher CO₂/CO ratio after considering the absorption phenomenon of CO₂ and CO into paper insulation. Therefore, diagnosing the condition of paper insulation using CO₂/CO is not reliable since carbon oxides may be generated from the long-term oxidation of oil components or could present as a result of an atmospheric leak [51].

2.2.3 Furan Analysis

Furanic compounds that are mainly produced due to paper oxidation and hydrolysis processes could be directly extracted from the oil to characterize the thermal decomposition of insulation paper [31]. Furan concentration in transformer oil depends on the mass ratio between oil and cellulose [44]. Levoglucosan leads to the formation of furfural products at

temperatures above 200°C [19] and the rate of furan production is related to the fractions of glycosidic broken bonds [52]. The level of furanic concentration in oil can be quantified by using High Performance Liquid Chromatography (HPLC) or Gas Chromatography-Mass Spectrometry (GC/MS) based on the American Society for Testing and Material (ASTM D5837 – Standard Test Method for Furanic Compounds in Electrical Insulating Liquids by HPLC; and ASTM D3612 – Test Method for Analysis of Gases Dissolved in Electrical Insulating Oil by Gas Chromatography) [15, 53]. Both techniques are acknowledged to provide accurate and reliable measurement of furan derivative concentration in transformer oil. Five furan derivatives are related with cellulosic insulation degradation in transformer oil: 2-Furfural (2FAL), 2-Furfurol (2FOL), 5-Hydroxy methyl-2-furfural (5HMF), 5-Methyl-2-furfural (5MEF) and 2-Acetyl furan (2ACF), as shown in Fig. 2-4.

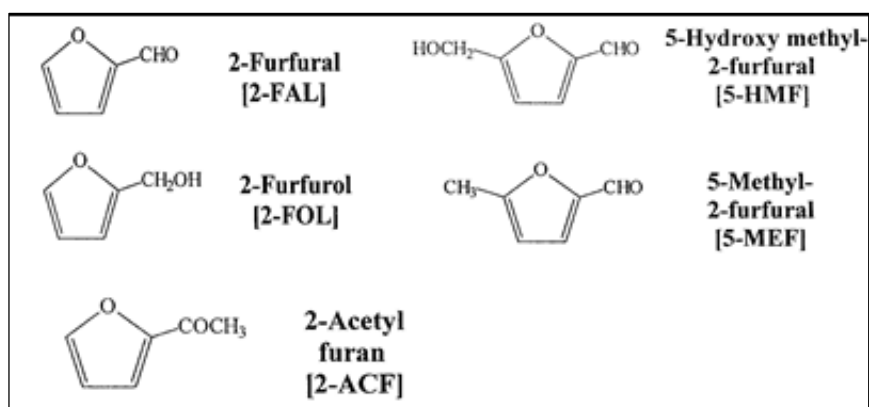


Figure 2-4 Furanic compounds detectable in transformer oil [52]

The first application of furan analysis to assess thermal degradation was initiated by the Central Electricity Generating Board (CEGB) in the UK around the 1980s [54]. According to Scheirs et al. [52], furanic compounds are dominated by 2FAL concentration during hydrolysis degradation of cellulose, and Nevell has identified 2FAL, 5HMF, and 5MEF as the major products of hydrolytic degradation of cellulose for a temperature range of 100-200°C. Measurements from controlled experimental conditions confirmed that the DP value decreases with the increase of furan concentration in transformer oil and there is a logarithmic relationship between the concentration of 2FAL in the oil and the DP [41, 55, 56]. Pahlavanpour et al. [57] reported their research findings that only 2FAL and 5HMF can be detected at a temperature of 120°C either. The concentration of both products continues to increase until the temperature reaches 160°C, after which it starts to decrease. Emsley et al. [55] reported that the concentration of 2FAL is highest in furan products during accelerated aging tests for wood-based paper, cotton-based paper and pure cotton linters. They also reported that the concentration of all furan derivatives increases exponentially with time to a maximum value and then decreases.

Chendong et al. proposed a linear relationship between furfural concentration in a logarithmic scale and DP, as shown below [43].

$$\log(2FAL) = 1.51 - 0.0035(DP_v) \quad (2-1)$$

where 2FAL represents the furfuraldehyde concentration in mg/L.

De Pablo [45] reported the following correlation between 2FAL and DP.

$$DP_v = \frac{7100}{8.88 + 2FAL} \quad (2-2)$$

where 2FAL refers to the furfural concentration expressed in mg/kg of oil. However, it has been noticed that not all winding paper degrades to the same extent, since it depends on the transformer operating conditions. This formula is then revised by Serena [45]. The revised formula is given as:

$$DP_v = \frac{7100}{8.88 + 2FAL + 1} \quad (2-3)$$

Emsley et al. [55], reported that the rate of change of 2FAL concentration in oil is more important than its absolute level. They found that 2FAL concentration increases significantly when DP is below 400, and expressed the production of 2FAL in terms of the reaction rate constant for the exponential portion by using Arrhenius equation. The idea was then improved by Cheim et al. [58] and translated into the mathematical equation below:

$$DP_v = \left(\frac{2FAL}{\lambda} \right)^{\frac{1}{\psi d}} \quad (2-4)$$

where 2FAL is expressed in particle per million (ppm), λ , ψ , and d are constants that depend on the paper type and winding longitudinal temperature gradient [59].

Fig. 2-5 illustrates the correlation of several equations between DP and 2FAL. It can be seen clearly that not all of them are consistent and, in fact, there is a very large difference, especially when compared with the equations proposed by Chendong [43] and De Pablo [45].

Abu-Siada et al. [29] proposed the use of UV-Vis Spectroscopy to measure furan instead of using either HPLC or GC/MS. They found a strong correlation between the furan concentration level and oil the spectral response bandwidth and peak absorbance, as shown in Fig. 2-6. Table 2-2 summarises the relationships between oil spectral response bandwidths and the corresponding DP level [29].

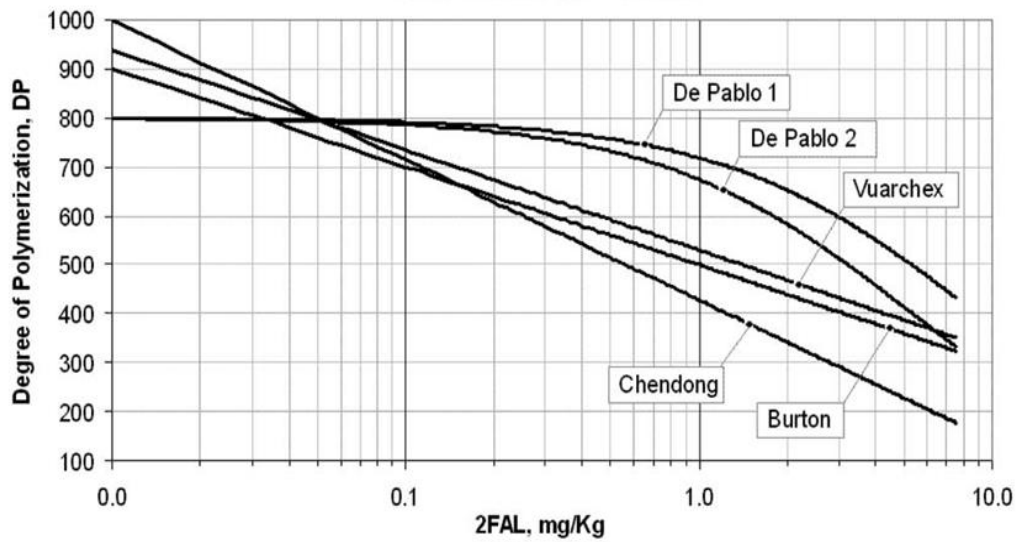


Figure 2-5 A comparison of the various correlation equations between DP and 2FAL [59]

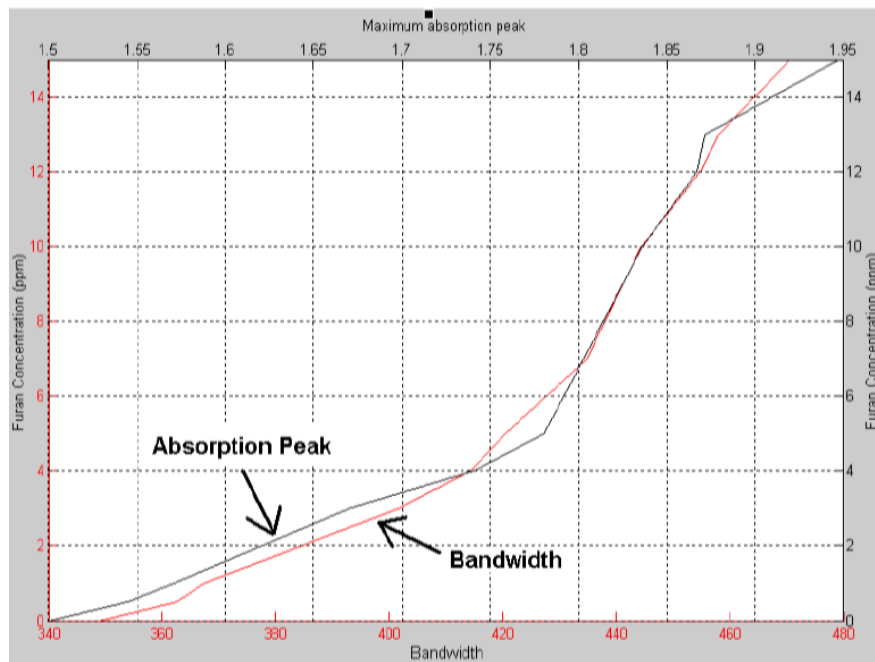


Figure 2-6 Correlation between furan concentration in transformer oil and its spectrum response parameters [21]

Table 2-2 Correlation between furan spectral response and DP level [29]

Bandwidth (nm)	DP Value	Significance
300-350	1200-700	Healthy Insulation
350-365	700-450	Moderate Deterioration
365-445	450-250	Extensive Deterioration
>445	<250	End of Life Criteria

2.2.4 Methanol as a New Chemical Marker for Paper Degradation

With the new thermally upgraded paper and the use of vegetable oil as alternative to mineral oil, the use of 2FAL as a cellulose insulation degradation indicator could be questionable. Several observations and studies [9, 39, 60-62] show that 2FAL detection for thermally upgraded paper is too low. A field study at Manitoba Hydro [63] found that some of the failed transformers' oil samples either did not contain 2FAL or the amount of 2FAL was too low to be detectable.

A few years ago, researchers began investigating the possibility of using Methanol (MeOH) as a chemical degradation marker for paper insulation. Using thermal-ageing tests, Jalbert et al. [32] confirmed that methanol was among molecules detected, suggesting the likelihood it could be used for monitoring paper depolymerization under normal transformer operating conditions. Then, Jalbert et al. [60] reported that 94% of oil samples collected from in service transformers showed the presence of methanol. Those results were supported in further investigations by Gilbert et al. [51] and Schaut, Autru and Eeckhoudt. [9]. Stability and aging tests by Schaut, Autru and Eeckhoudt [9], proved that MeOH is not an oxidation product, and it is formed as a result of paper degradation. The observation also showed that MeOH is not affected by oil aging condition [64]. A comparative study between MeOH and 2FAL showed that MeOH gives a faster indication of the early stages of paper degradation [9]. Schaut, Autru and Eeckhoudt reported that a linear correlation exists between DPV and the formation of MeOH even at early stages of its formation [9].

A kinetic study of the degradation of thermally upgraded papers in oil conducted by Gilbert et al. [51] confirmed a strong correlation between MeOH and the rupturing of 1,4- β -glycosidic bonds of cellulose, hence MeOH can be used as cellulose-degradation indicator. In 2012, Jalbert et al. [65] published a standard procedure for analyzing MeOH resulting from cellulose degradation in mineral oils.

Table 2-3 summarizes the main advantage/disadvantages of all of the condition monitoring techniques discussed above for power transformer solid insulation. Amongst all the techniques for chemical diagnosis, DP value is the most accurate for assessing the condition of paper insulation in power transformer. However, this technique is impractical when it comes to implementing it with in-service transformers because it would require obtaining paper samples from operating transformers. Since CO₂/CO concentration and furan analysis are measured using oil analysis, both of those types of chemical diagnoses have been widely used in industry for the last three decades.

Recently, some studies conducted on thermally upgraded paper used in power transformers revealed the potential use of Methanol as a chemical indicator for paper insulation monitoring. However, this finding is still in the research phase and the technique is not yet fully matured.

Table 2-3 Advantages and disadvantages of various paper diagnostic methods [138]

Method	Advantages	Disadvantages
CO₂/CO	<ul style="list-style-type: none"> Can be easily measured using routine DGA analysis, and can be used as a trigger for further analysis. 	<ul style="list-style-type: none"> May have resulted from oil at normal temperature due to long term oxidation or due to atmospheric leak.
DP	<ul style="list-style-type: none"> Very accurate way to measure the quality of cellulose and paper mechanical strength. 	<ul style="list-style-type: none"> Impractical to apply to in-service transformers and open breath transformers.
Furan	<ul style="list-style-type: none"> The furan level correlates with DP and mechanical strength of paper and can be measured through oil analysis. 	<ul style="list-style-type: none"> Low detection in thermally upgraded paper and vegetable oil; and the result depends on the content of manufactured paper.
MeOH	<ul style="list-style-type: none"> A linear correlation exists between MeOH and DP from an early stage. 	<ul style="list-style-type: none"> Still in research phase and not fully matured.

2.3 Dissolved Gas Analysis

Dissolved gas analysis is used to assess the condition of power transformers. It utilizes the concentrations of various gases dissolved in the transformer oil due to decomposition of the oil and paper insulation. DGA has gained worldwide acceptance as a method for the detection of incipient faults in transformers. Due to the thermal and electrical stresses which the insulation of operating transformers experience, paper and oil decomposition occurs, generating gases which dissolve in the oil and reduce its dielectric strength [15, 39, 44, 64, 66]. Gases generated through oil decomposition include H₂, CH₄, C₂H₂, C₂H₄ and C₂H₆. On the other hand, CO and CO₂ are generated as a result of paper decomposition [25, 46]. Faults such as overheating, partial discharge and sustained arcing produce a range of gases, the concentrations of which can be used to identify faults and estimate their severity.

In 1978, IEEE published guidelines for the detection of gases in oil-immersed transformers, known as ANSI/IEEEEC57.104-1978 [67] which cover instrumentation, sampling procedures, methods for extracting and analyzing gases, and data interpretation.

In 1992, IEEE published further guidelines (IEEE Std C57.104-1991) [46] which deal mainly with interpretation of DGA data; this standard was revised in 2008 (IEEE Std C57.104-2008) [68]. In 1977, IEC published guidelines for the sampling of gases and oil in oil-filled electrical equipment, and the analysis of free and dissolved gases. In 2009, ASTM issued ASTM Standard D3612-02 [15], which deals with analysis of gases dissolved in electrical insulating oil using gas chromatography (GC). GC measurements are always conducted in a laboratory environment because of the complexity of the equipment required; oil samples are collected from operating transformers, and transported to the laboratory for gas extraction and analysis. Vacuum extraction, stripper extraction and headspace sampling are currently used to extract gases from the oil [15]; the Shake Test can also be used [69]. After extraction, the gases are analyzed using GC. Due to the time and costs involved, DGA using GC is usually performed only once a year on operating transformers. More frequent testing is performed only if significant concentrations of fault gases are detected during routine tests [16].

Various techniques for interpretation of DGA data have been developed, e.g., the key gas, Doernenburg ratio, Rogers ratio, IEC ratio and Duval triangle methods. Each of these techniques relies on the accumulated knowledge and experience of various experts, rather than rigorous quantitative scientific models [25, 44] and, therefore, they may yield different diagnoses for the same oil sample. These interpretation techniques are discussed below.

On account of the limitations of the GC approach, several new analytical techniques have been developed, e.g., hydrogen on-line monitoring [70, 71] and photo-acoustic spectroscopy (PAS) [16, 72]. Both require less time than GC analysis. These three techniques are discussed below.

2.3.1 DGA Measurement Technique

2.3.1.1 Gas Chromatography

Gas chromatography has been used to analyze gases dissolved in insulating oil for the last 60 years [17,73]. It has been used regularly by the U.K. Central Electricity Generating Board for monitoring and routine assessment since 1968. It became more popular after IEEE, IEC and ASTM published relevant guidelines. Currently, GC is accepted as the best of the three DGA techniques for measuring the concentrations of gases dissolved in transformer oil, e.g., combustible gases (hydrogen, carbon monoxide, methane, ethane, ethylene, and acetylene), and noncombustible gases (carbon dioxide, nitrogen, and oxygen).

It can also be used to measure the concentrations of gases released into the space above the oil, i.e., into the gas blanket.

As stated above, GC analysis is conducted only in the laboratory environment, following several standards, e.g., those dealing with extraction of the oil sample from the operating transformer, transporting it to the laboratory, and extracting the dissolved gases [15, 67, 74-76]. According to ANSI/IEEE C57.104-1978 [67], oil samples can be stored and transported to the laboratory in calibrated stainless steel cylinders, flexible metal cans, syringes or glass bottles. All the containers must meet stated leak criteria. According to ASTM D923 [76], amber or clear glass bottles may be used, fitted with glass-stoppers or with screw caps incorporating a pulp-board liner faced with tin or aluminum foil, or a suitable oil-resistant plastic such as polyethylene, polytetrafluoroethylene or a fluoro-elastomer. ASTM D3612 [15] states that gases in the oil can be separated using vacuum extraction, stripper column extraction or headspace sampling methods. Vacuum extraction (Fig. 2-7) is suitable for extraction of a fraction of each of the dissolved gases, while stripper column extraction will remove nearly all the gas from each container.

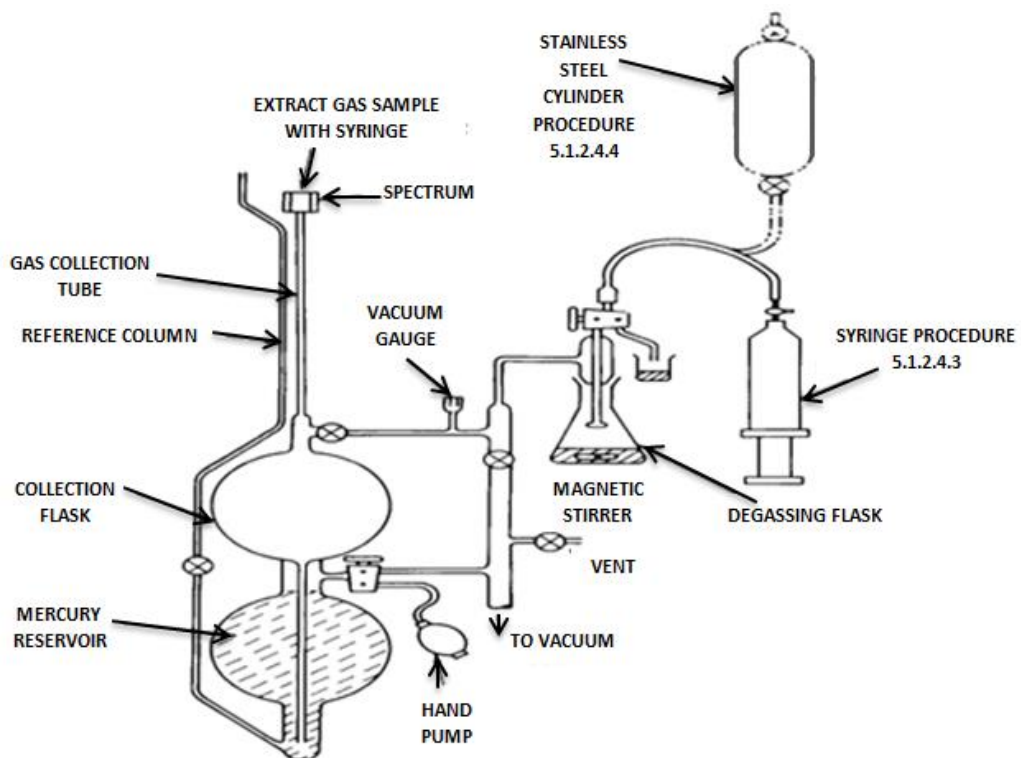


Figure 2-7 Extraction of dissolved gases from insulating oil using the vacuum extraction method [15]

Headspace sampling (Fig. 2-8) will also extract a fraction of each container's headspace gas. Another extraction method, known as the Shake Test, was introduced by Morgan-Shaffer in 1993 [69]. It can extract dissolved gases quickly, even in the field.

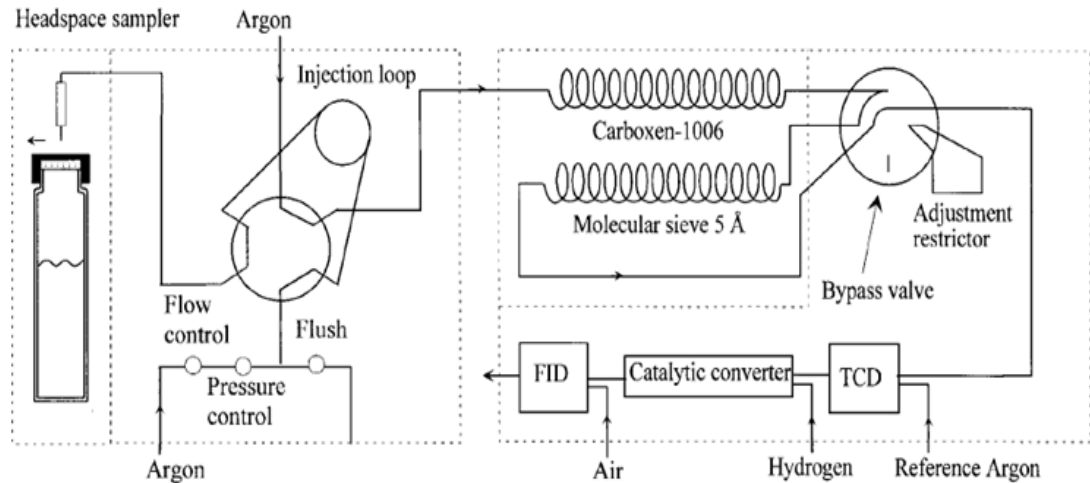


Figure 2-8 Extraction of dissolved gases from insulating oil using the headspace method [15]

A basic gas chromatograph set-up is shown in Fig.2-9. The oil sample is volatilized in the injection port, and its gaseous components separated in the column [73]. A gas entering the column may remain in the gaseous state, i.e., continue to travel with the carrier gas, or dissolve in the liquid on the surface of the stationary phase, or condense on the stationary phase. In the latter two cases, its progress through the column will be much slower than if it continued to travel with the carrier gas. Argon, helium, nitrogen and hydrogen are normally used as carrier gases to transfer the sample from the injector through the columns into the detector [15, 73, 77]. Some of the gaseous components that travel with carrier gas collide and re-enter the stationary phase which is a thin film of thermally stable polymer that is coated on the inner wall of the column. At the same time, the gases that immobilize in the stationary phase travel with the carrier gas. This occurs thousands of times for each gaseous component during its journey along the column. The time taken by each gaseous component to pass through the column (the retention time) varies from component to component, and depends on the temperature of the column and the chemical structure of the stationary phase. The separation characteristics of the columns and the detection sensitivity may vary with the carrier gas [77]. There are two main types of column, namely packed and capillary. Most users prefer capillary columns with a stationary phase coated on the inner wall [73]. Capillary columns have smaller diameters but are longer than packed columns, and therefore have substantially higher separation capacities. Separation capacity is defined as the number of gaseous components which can be separated between the carrier gas and the stationary phase within the column [73]. A smaller diameter and lengthier column will slow down the travel rates of gases; hence, the design of capillary columns allows a longer duration for the separation process. It is essential that the temperature of the column be kept constant, in order to achieve a known and constant separation capacity.

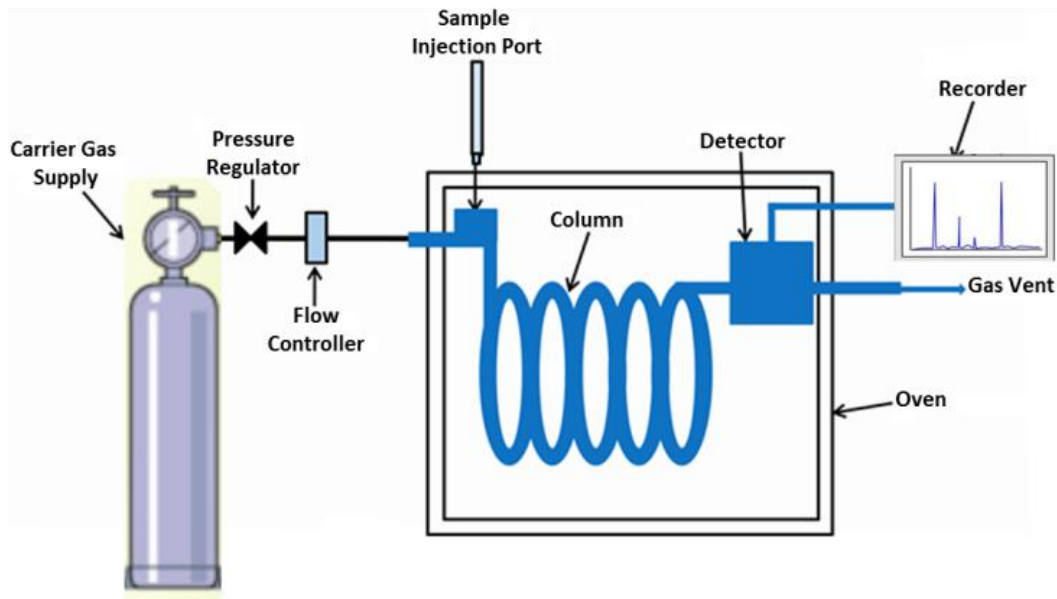


Figure 2-9 A basic gas chromatograph [137]

The gaseous components are washed out of the column one by one, depending on their retention time, and interact with the heated detectors, generating electrical signals [77]. These signals are recorded by a data collection system and plotted against elapsed time, producing a chromatogram. Gases can be identified using the elapsed time, and the concentration of a given gas is determined by the magnitude of the associated electrical signal. Several different types of detector are available, e.g., thermal conductivity, flame ionization, nitrogen–phosphorus, flame photometry, electron capture, atomic emission and electrolytic conductivity [73, 77].

Flame ionization detectors are normally used to detect hydrocarbon and carbon oxide gases, due to their high sensitivity; and thermal conductivity detectors are used to detect permanent gases such as H_2 , O_2 and N_2 [2]. Mass spectrometer detection using electron ionization techniques is very sensitive, and is normally used for measurements of complex gaseous mixtures. Molecules that can also be detected include methyl acetate, 2-methylfuran, phenol, methyl formate, furan, methanol, ethanol, acetone, isopropyl alcohol and methyl ethyl ketone, present in the oil as solids [9, 60, 65, 78].

2.3.1.2 Hydrogen On-Line Monitoring

The hydrogen on-line monitor [17, 79] is a rugged low-cost device introduced by Syprotec and further developed by the Institut de Recherche d'Hydro Quebec (IREQ). It is widely accepted that a majority of faults in oil-filled electrical equipment lead to the generation of hydrogen [46]; the hydrogen on-line monitor therefore focuses on detecting key gases such as hydrogen and carbon monoxide [71].

In this way early detection of faults, especially hot spots, partial discharges and arcing can be achieved. Ethylene and acetylene can also be detected, but with less sensitivity.

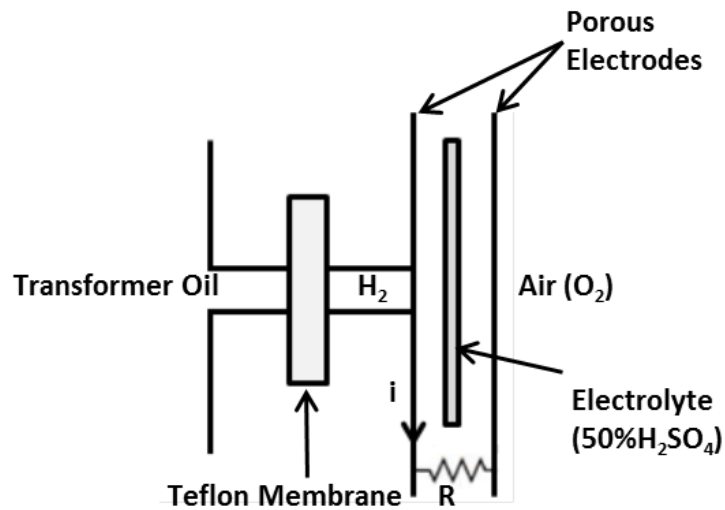


Figure 2-10 Schematic diagram of a hydrogen on-line monitor [17].

A hydrogen on-line monitor consists essentially of a sensor that makes contact with the oil, and an electronic unit. The sensor is placed in a rugged brass housing containing a fuel cell, a temperature sensor and a Teflon membrane (see Figure 2-10). The sensor can be installed on a flange or valve on the transformer's pipe work between the cooling bank and the main tank [17], or on the upper part of the transformer [80]. Hydrogen in the oil permeates through the Teflon membrane, along with atmospheric oxygen, and is chemically burnt in the electrolyte cell, thus generating a small current proportional to the hydrogen gas concentration in the oil. (Simultaneously water is formed as a result of the reaction between hydrogen and atmospheric oxygen). The current is amplified and measured as a voltage drop across the load resistor R connected between two porous electrodes, with the voltage drop yielding the hydrogen gas concentration in the oil. An alarm is activated if the hydrogen concentration reaches a predetermined level. The detection sensitivity of the monitor depends on the percentage of the individual combustible gasses passing through the membrane. These percentages are currently 100 for hydrogen, about 15 for carbon monoxide, 8 for acetylene and 1 for ethylene [17, 80].

Approximately 18,000 hydrogen on-line monitor systems were in operation globally in 2003 [69]. The hydrogen concentration measurement accuracy is $\pm 10\%$ over the temperature range 20 - 40°C [80]. The accuracy diminishes if the monitor temperature varies outside this range, for example as a result of variations in the oil temperature [79]. Although the monitor can detect incipient faults in a power transformer, it cannot identify the fault types.

2.3.1.3 Photo-Acoustic Spectroscopy

In 1880, Alexander Graham Bell observed that a sound was emitted when a thin disk was exposed to mechanically-chopped sunlight [31]; this may be the first recorded observation of the photo-acoustic effect. Subsequently photo-acoustic spectroscopy has been used in various applications such as monitoring of ambient air quality and air pollution from car exhausts. However, its application to monitoring the condition of power transformers is relatively new [12].

The basic principle is that fault gases absorb infrared light energy and convert it into kinetic energy in the form of pressure (sound) waves, which are detected by a microphone [12]. This microphone converts the pressure waves into electrical signals [81]. The photo-acoustic spectrum of the fault gases is obtained by measuring the intensity of the sound waves produced by various infrared wavelengths, with the latter being able to be selected using optical filters. In this way, measurements of the concentrations of various fault gases, e.g., H₂, CO, CO₂, CH₄, C₂H₄, C₂H₂ and C₂H₆ can be obtained [16, 81].

Figure 2-11 shows the basic operating principle, and Figure 2-12 shows some construction details [81].

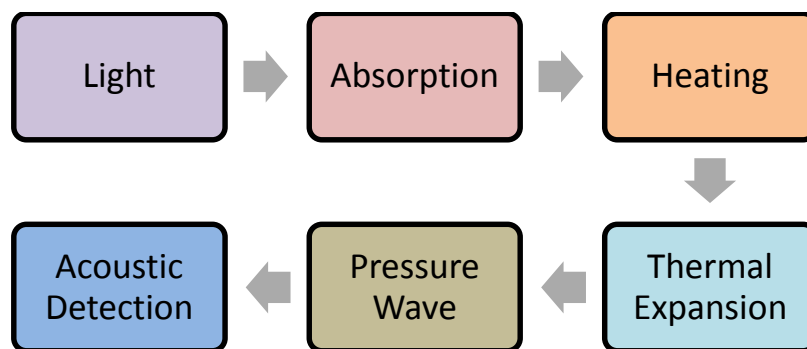


Figure 2-11 Basic process of photo-acoustic spectroscopy [82]

The PAS is a very stable diagnostic tool, suitable for monitoring the condition of power transformers [12]. However, since each fault gas absorbs infrared light at a specific wavelength, selecting the centre wavelength for each gas is a critical process [81].

Fig. 2-13 shows the characteristic absorption of various gases, and water vapor. The detection sensitivity of the equipment varies from gas to gas, and its detection accuracy is influenced by the external environment, e.g., temperature and pressure, and by vibration [83].

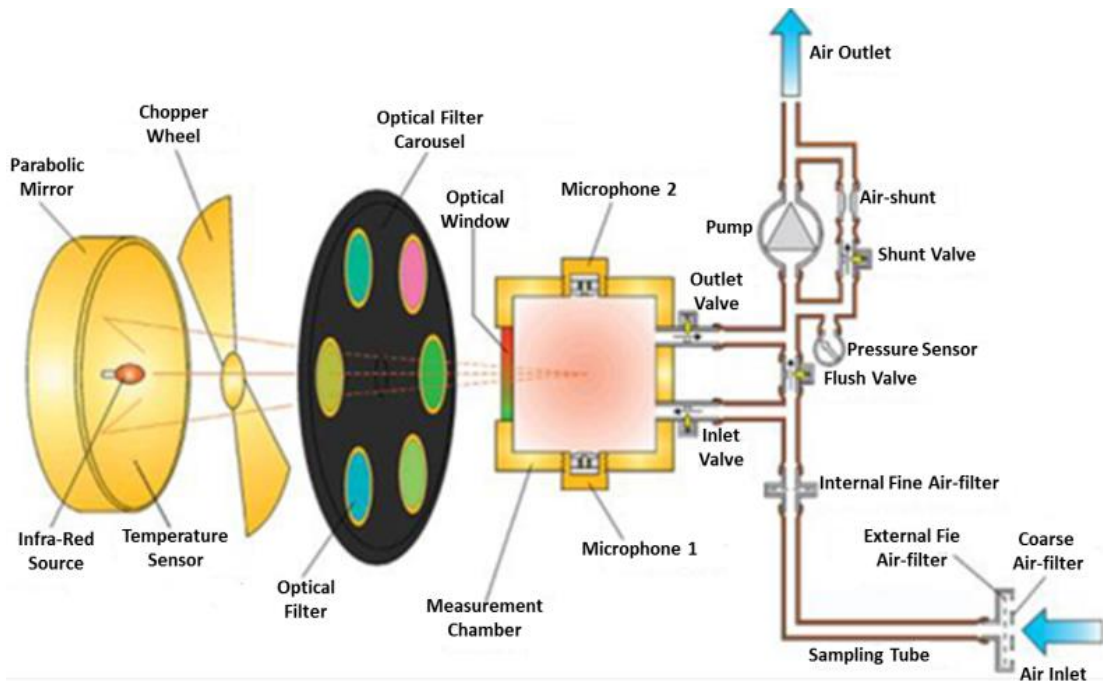


Figure 2-12 Schematic diagram of a PAS-based DGA system [81]

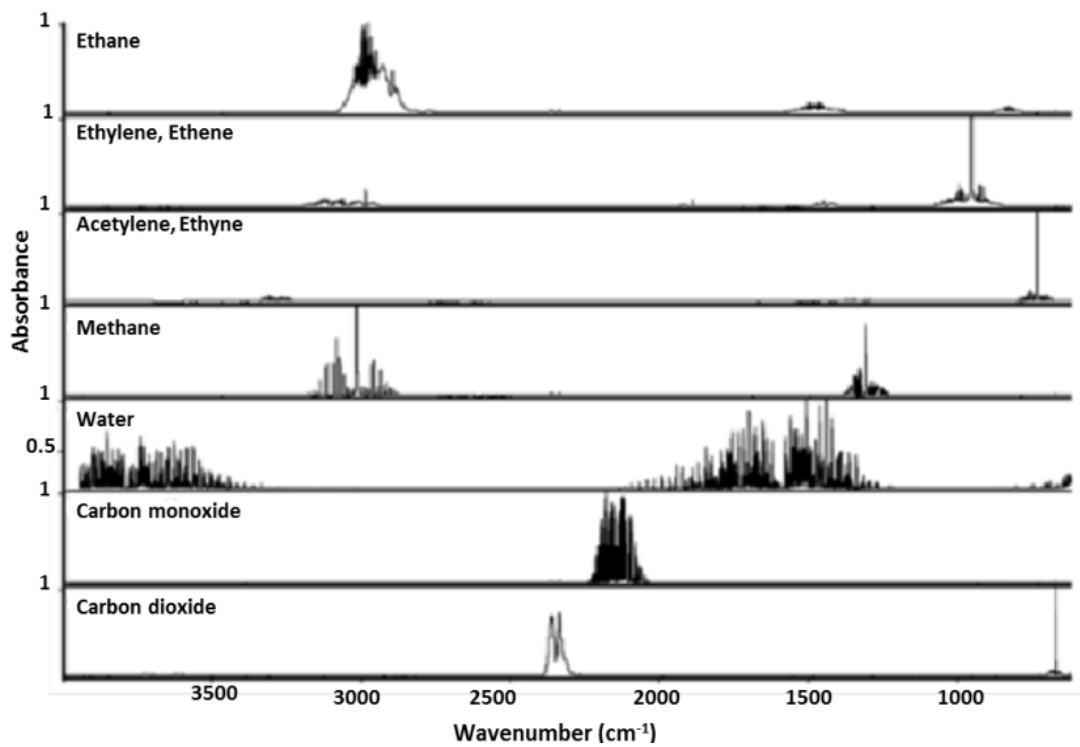


Figure 2-13 Characteristic absorbance levels of various fault gases [81]

A comparison of the advantages and disadvantages of GC, hydrogen on-line monitoring and PAS methods is shown in Table 2-4.

Table 2-4 Comparison of GC, Hydrogen On-line Monitor and PAS [137]

Method	Advantage	Disadvantage
GC	<ul style="list-style-type: none"> • Able to detect and analyze every gas dissolved in transformer oil • Provides highest accuracy and repeatability • Results can be used to identify the fault type 	<ul style="list-style-type: none"> • Can be used only in the laboratory, due to the complexity of the equipment • Long time required to complete a test on a transformer • Expensive • An expert is needed to conduct the test and interpret the data
HYDROGEN ON-LINE MONITOR	<ul style="list-style-type: none"> • Rugged, low-cost and continuous on-line monitoring • Can detect incipient faults 	<ul style="list-style-type: none"> • Can detect only H₂, CO, C₂H₂ and C₂H₄. • Best concentration accuracy only within the monitor temperature range 20 - 40°C • Results cannot be used to identify the fault type
PAS	<ul style="list-style-type: none"> • Continuous on-line monitoring • Can detect and measure the concentration of a wide range of fault gases • Results can be used to identify the fault type 	<ul style="list-style-type: none"> • Results are sensitive to the wave number range of the optical filters and their absorption characteristics • Concentration accuracy influenced by the external temperature and pressure, and by vibration • Still undergoing development

2.3.2 Interpretation of DGA Data

2.3.2.1 Key Gas Method (KGM)

The generation of fault gases within transformer oil requires sufficiently high temperatures (energy) to break chemical bonds in the oil, which then reduces its dielectric insulation strength [84]. The KGM uses the individual concentrations of the six fault gases, shown in Fig. 2-14. The four common fault conditions are distinguished by the quoted percentage concentrations of the six gases. These percentages are based on the practical experience of various experts.

These KGM charts look simple, but they are widely considered to lack sufficient accuracy for diagnosing problems in power transformers [35]. Studies based on an IEC data bank of inspected transformers found that only 42% of KGM diagnoses are correct [47].

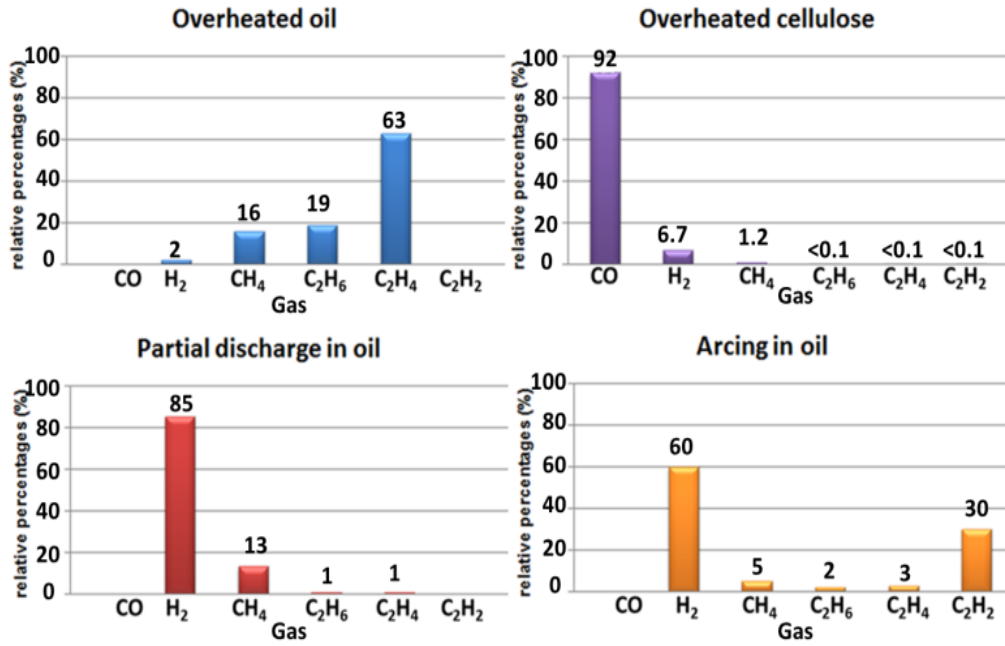


Figure 2-14 Key Gas Method Chart [17]

2.3.2.2 Doernenburg Ratio Method (DRM)

This method [28, 85] utilizes the ratio of gas concentrations to indicate fault types. Predefined limits for the CH₄/H₂, C₂H₂/C₂H₄, C₂H₂/CH₄ and C₂H₆/C₂H₂ ratios are used to interpret the DGA results (see Table 2-5) [28].

Table 2-5 DRM Concentration Ratios [28]

Suggested fault diagnosis	CH ₄ /H ₂		C ₂ H ₂ /C ₂ H ₄		C ₂ H ₂ /CH ₄		C ₂ H ₆ /C ₂ H ₂	
	Oil	Gas Space	Oil	Gas Space	Oil	Gas Space	Oil	Gas Space
Thermal fault	>1	>0.1	<0.75	<1	<0.3	<0.1	>0.4	>0.2
PD	<0.1	<0.01	Not significant		<0.3	<0.1	>0.4	>0.2
Arcing	>0.1 - <1	>0.01 - <0.1	>0.75	>1	>0.3	>0.1	<0.4	<0.2

DRM diagnosis cannot be applied unless the concentration of at least one of the key gases (H₂, C₂H₄, CH₄ and C₂H₂) exceeds twice the relevant limit L1 (see Table 2-6), and the concentration of at least one of the two gases appearing in any one of the four ratios exceeds the relevant limit L1 [46]. The proposed fault diagnosis is based on the ranges of the four ratios shown in Table 2-5.

Table 2-6 Dissolved Gas Concentrations (L1) for the DRM [46]

Key Gas	L1 Concentrations (ppm)
Hydrogen (H ₂)	100
Methane (CH ₄)	120
Carbon Monoxide (CO)	350
Acetylene (C ₂ H ₂)	35
Ethylene (C ₂ H ₄)	50
Ethane (C ₂ H ₆)	65

2.3.2.3 Rogers Ratio Method (RRM)

This method is similar to the DRM. However, while the DRM requires significant concentrations of the fault gases, the RRM can be used provided the concentrations exceed the L1 values in Table 2-6 [46].

Table 2-7 Revised Suggested RRM Diagnoses [137]

Case	C ₂ H ₂ /C ₂ H ₄	CH ₄ /H ₂	C ₂ H ₄ /C ₂ H ₆	Suggested Fault Diagnosis
0	<0.1	>0.1 to <1	<1	Normal
1	<0.1	<0.1	<1	Low energy density PD
2	0.1 to 3	0.1 to 1	>3	Arcing
3	<0.1	>0.1 to <1	1 to 3	Low temperature thermal fault
4	<0.1	>1	1 to 3	Thermal fault < 700°C
5	<0.1	>1	>3	Thermal fault > 700°C

The RRM originally utilized four concentration ratios, namely C₂H₆/CH₄, C₂H₂/C₂H₄, CH₄/H₂, and C₂H₄/C₂H₆, leading to twelve proposed diagnoses [67]. However, the condition C₂H₆/CH₄ <1 held for ten of the twelve suggested diagnoses, i.e., the ratio C₂H₆/CH₄ was of little diagnostic value [85, 86].

This ratio was therefore omitted in the revised IEEE Standard C57.104-1991[46], and the original twelve suggested diagnoses were replaced by six (including the normal state), as shown in Table 2-7 [28]. However, inconsistencies have been reported [25, 44], with the success rate for correct fault type identification being only 58.9 % [25].

2.3.2.4 IEC Ratio Method (IRM)

This method uses the same three ratios as the revised RRM, but suggests different ratio ranges and interpretations, as shown in Table 2-8 [40].

Table 2-8 Suggested IRM diagnoses [87]

Case	Characteristic Fault	C_2H_2/C_2H_4	CH_4/H_2	C_2H_4/C_2H_6
PD	Partial discharges	NS	<0.1	<0.2
D1	Discharges of low energy	>1	0.1-0.5	>1
D2	High energy discharges	0.6-2.5	0.1-1	>2
T1	Thermal faults <300°C	NS	>1 but NS	<1
T2	Thermal faults >300°C and <700°C	<0.1	>1	1-4
T3	Thermal faults >700°C	<0.2	>1	>4
NS = Not significant whatever the value				

A new gas ratio has been introduced, namely, C_2H_2/H_2 to detect possible contamination from on-load tap-changer (OLTC) compartments [88]. Another improvement is 3D graphical representation of ratio ranges, which yields more reliable diagnoses, and diagnoses of faults associated with ratios outside the ranges quoted in Table 2-8 [44].

2.3.2.5 Duval Triangle Method (DTM)

This method was developed from an existing IEC 60599 Ratio method and IEC TC10 databases [40]. It interprets DGA data using graphical representation [89, 90]. It uses the concentrations of CH_4 , C_2H_2 and C_2H_4 , which are plotted along three sides of a triangle [89], as shown in Fig. 2-15. Within the triangle there are seven fault zones, covering partial discharge, thermal faults at various temperatures, and electrical arcing.

According to [25], [34] and [36], the DTM provides more accurate and consistent diagnoses than the other ratio methods. However, careful implementation is needed to avoid incorrect diagnoses [90]. Moreover, since the triangle does not include the fault-free condition, the method cannot be used to detect incipient faults. Duval [91] proposed other versions of DTM, e.g., DTM 2 for oil-type load tap changers, DTM 3 for equipment filled with non-mineral oils, and DTM 4 and DTM 5 as complements of the original DTM for low-temperature faults in transformers. H_2 , CH_4 , and C_2H_6 are used in DTM 4 (Fig. 2-16), and C_2H_4 , CH_4 , and C_2H_6 in DTM 5 (Fig.2-17). DTM 4 and DTM 5 are applicable only when PD, T1, or T2 faults have been identified by the original DTM.

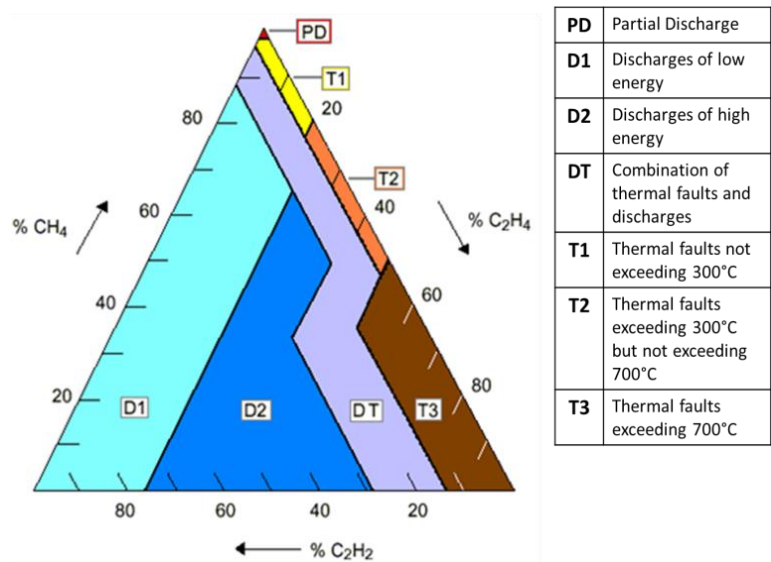


Figure 2-15 Coordinates and fault zones in the DTM [89]

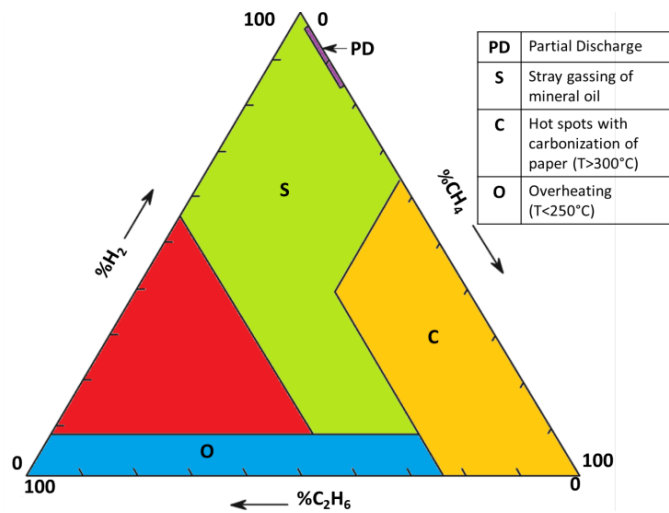


Figure 2-16 Coordinates and fault zones in the DTM 4 [91]

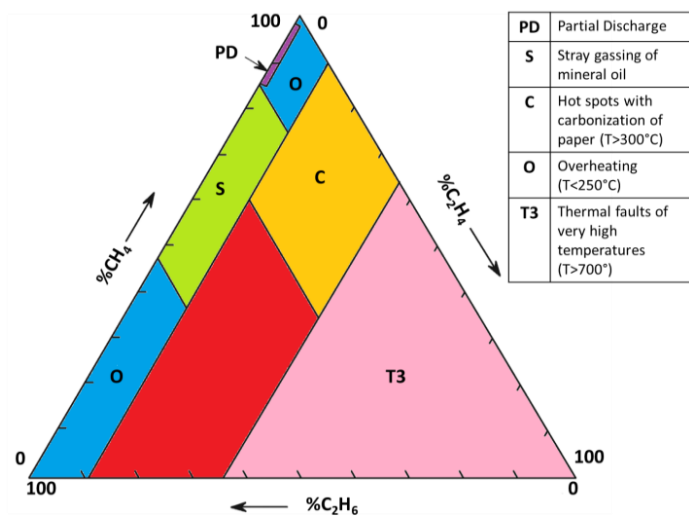


Figure 2-17 Coordinates and fault zones in the DTM 5 [91]

2.3.2.6 Duval Pentagon Method (DPM)

This method was developed as complementary tool for the interpretation of DGA in transformer [143]. According Duval and Lamarre [143], although DPM can be used alone, however it should not replace the function of Duval Triangles 1, 4, and 5 but rather to provide additional information especially for the case of mixtures of faults. In this method, it uses the concentrations of H_2 , CH_4 , C_2H_6 , C_2H_4 , and C_2H_2 , which are plotted along five sides of a pentagon as shown in Fig. 2-18 [143]. Duval Pentagons 1 and 2 are proposed in [143] to identify several fault types based on these five gas concentrations.

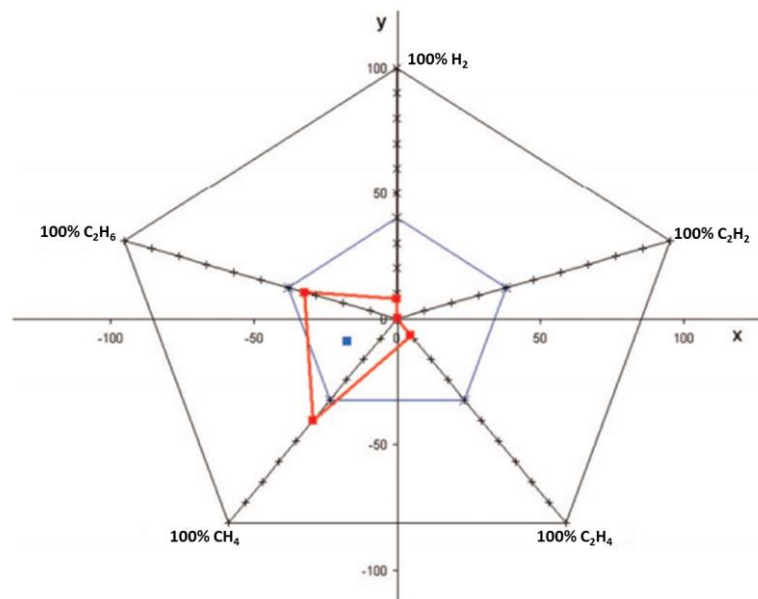


Figure 2-18 Example of Duval Pentagon representation [143].

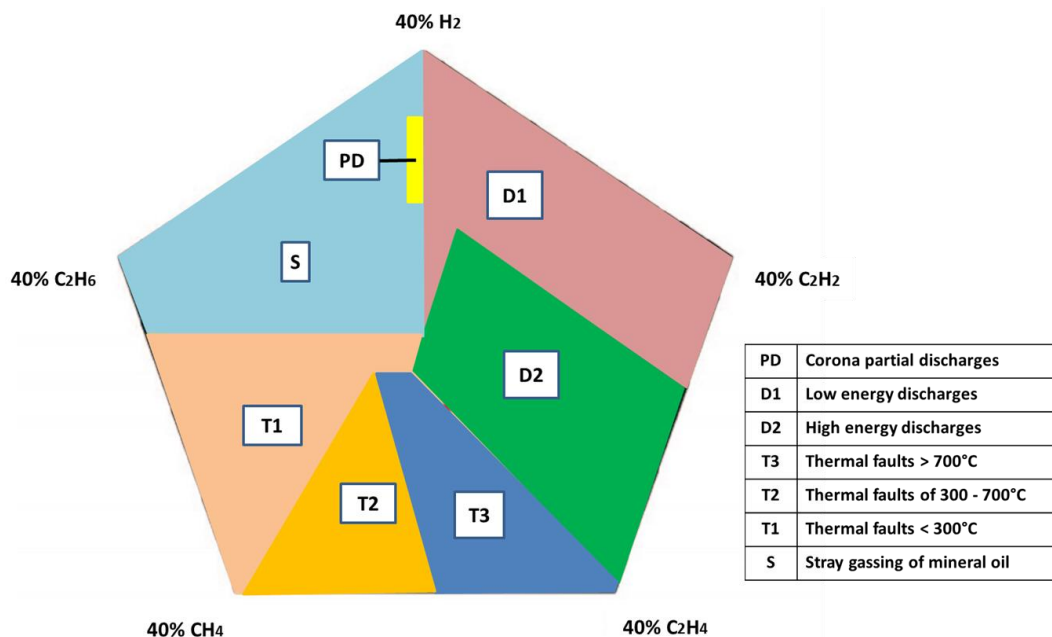


Figure 2-19 The Duval Pentagon 1 for the six “basic” faults [143]

The DPM 1 as shown in Fig. 2-19 is developed corresponding to the six basic electrical and thermal faults used by IEC and IEEE; PD, D1, D2, T1, T2, and T3, plus with stray gassing of mineral oil. Meanwhile, the DPM 2 is developed corresponding to the three basic electrical faults; PD, D1, and D2, and the four more advanced interpretations of thermal faults as shown in Fig. 2-20.

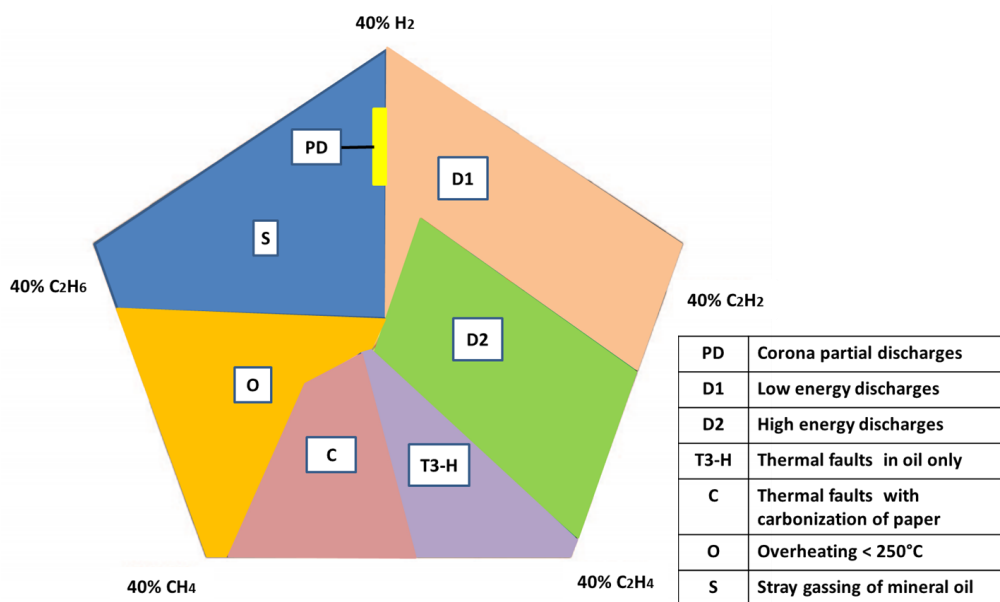


Figure 2-20 The Duval Pentagon 2 for the three basic electrical faults PD, D1, and D2 and the four “advanced” thermal faults

The various DGA interpretation methods discussed above are summarized in Table 2-9.

Table 2-9 Comparison of KGM, DRM, RRM, IRM, DTM and DPM

Types	Method	Fault Types	Gases Involved
KGM	Uses individual gas concentrations, easy to implement, very conservative.	PD, arcing, overheated oil, overheated cellulose.	CO, CO ₂ , H ₂ , CH ₄ , C ₂ H ₂ , C ₂ H ₄ and C ₂ H ₆
DRM	Specifies four gas concentration ratios (CH ₄ /H ₂ , C ₂ H ₂ /C ₂ H ₄ , C ₂ H ₂ /CH ₄ , and C ₂ H ₆ /C ₂ H ₂) to indicate three fault types, and specifies concentration limits to differentiate between faults.	Thermal decomposition, PD, arcing.	H ₂ , CH ₄ , C ₂ H ₂ , C ₂ H ₄ and C ₂ H ₆
RRM	Uses three gas concentration ratios (C ₂ H ₂ /C ₂ H ₄ , CH ₄ /H ₂ , and C ₂ H ₄ /C ₂ H ₆) to indicate five fault types, and specifies concentration limits to differentiate between faults.	PD, arcing, low temperature of thermal fault, thermal <700°C, thermal >700°C.	H ₂ , CH ₄ , C ₂ H ₂ , C ₂ H ₄ and C ₂ H ₆

IRM	Similar to RRM but excludes the C ₂ H ₆ /CH ₄ ratio, indicates six fault types, and specifies concentration limits to differentiate between faults.	PD, low energy discharge, high energy discharge, thermal faults <300°C, 300–700°C, and greater than 700°C.	H ₂ , CH ₄ , C ₂ H ₂ , C ₂ H ₄ and C ₂ H ₆
DTM	Triangular map indicates six faults, however, does not identify a normal state.	PD, low energy discharge, high energy discharge, thermal faults <300°C, 300–700°C, and >700°C.	CH ₄ , C ₂ H ₂ , and C ₂ H ₄
DPM	Pentagon map indicates seven faults, however, does not identify a normal state.	PD, low energy discharge, high energy discharge, thermal faults <300°C, 300–700°C, and >700°C, stray gassing of mineral oil.	H ₂ , CH ₄ , C ₂ H ₂ , C ₂ H ₄ and C ₂ H ₆

2.3.3 Artificial Intelligence and DGA

As stated above, fault diagnosis techniques using fault gas concentrations or ratios thereof are based on the practical experience of various experts, rather than on quantitative evidence-based scientific theory, and may therefore lead to different conclusion for the same oil sample methods [92]. Ratio methods may also fail to diagnose multiple simultaneous fault conditions.

The availability of extensive DGA data has therefore motivated researchers to develop an alternative approach to DGA data interpretation, based on artificial intelligence (AI) techniques [87, 92-99][51]. Fuzzy logic [92, 95, 96] and neural network [87, 93, 97, 99] techniques have been the most popular for this purpose, followed by support vector machine [94, 100, 101] and particle swarm optimization [102] techniques.

Abu-Siada et al. [92] developed an AI model based on a combination of KGM, DRM, RRM, IRM and DTM (Fig. 2-18). KGM is first applied. If the key gas concentrations are less than the L1 concentrations quoted in Table 2-6, the transformer is assumed to be fault free and no further analysis is performed. If the key gas concentrations exceed the L1 concentrations quoted in Table 2-6, the ratio methods and DTM are applied in order to diagnose the fault type. The fault type indicator D is calculated as:

$$D = \frac{\sum_{i=1}^{i=5} A_i D_i}{\sum_{i=1}^{i=5} A_i} \quad (2-5)$$

where D_i (a number in the range 0-10) is the decision value derived from fuzzy logic models based on the i -th method (KGM, DRM, RRM, IRM and DTM) and A_i is the accuracy of the i -th method obtained from an analysis of 2,000 DGA samples with pre-known faults [92]. If any of the ratio methods involves a ratio that is not consistent with the relevant proposed codes, the corresponding D_i is set to zero. D takes a numerical value in the range 0 – 10, where $0 \leq D < 2$ indicates no fault, $2 \leq D < 4$ indicates overheated cellulose, $4 \leq D < 6$ indicates overheated oil, $6 \leq D < 8$ indicates corona in the oil, and $8 \leq D < 10$ indicates arcing in the oil.

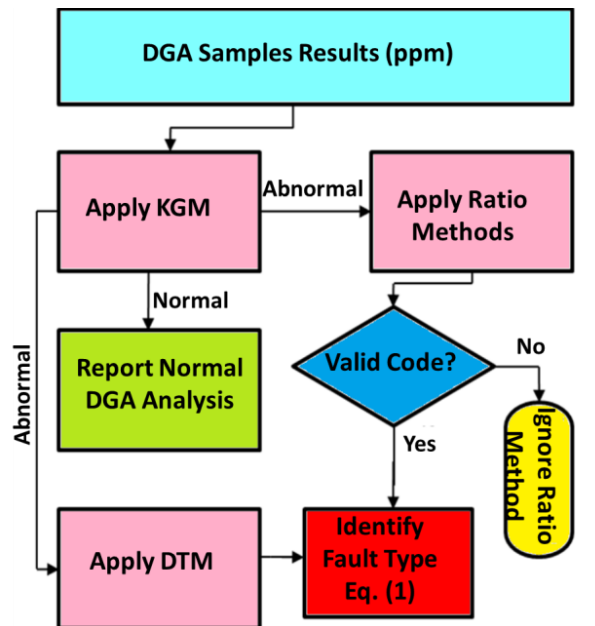


Figure 2-21 Proposed AI interpretation method [92]

As reported in the literature [87, 92, 101, 102], AI approaches provide more accurate and reliable transformer diagnoses than KGM, DRM, RRM, IRM and DTM. However, although a majority of the AI approaches diagnose faults with high accuracy, some of them fail to distinguish between thermal faults in oil and the same faults in cellulose, and engineering judgment is then required [92, 93].

Three methods of measuring the concentrations of fault gases dissolved in transformer oil, namely gas chromatography, hydrogen on-line monitoring and photo-acoustic spectroscopy are compared and discussed in this section. The high accuracy of gas chromatography is widely acknowledged. However, gas chromatography measurements are expensive and time-consuming, and industry therefore tends to favour hydrogen on-line monitoring and photo-acoustic spectroscopy. Hydrogen on-line monitoring can detect incipient faults, but cannot provide detailed fault diagnosis. Photo-acoustic spectroscopy provides more accurate gas concentration data than hydrogen on-line monitoring, but its accuracy may be affected by external gas pressure and vibration.

Several methods are available for the interpretation of DGA data: the Doernenburg, Rogers ratio, IEC ratio, Duval triangle and the Key Gas Method, which are widely used by utilities companies. Unfortunately these methods may yield conflicting diagnoses for the same oil sample. Several artificial intelligence methods have been developed in response to this situation. However, in some cases a certain amount of engineering judgment may be required to obtain a credible diagnosis.

2.4 Other Oil Physical and Chemical Tests

2.4.1 Interfacial Tension (IFT)

The interfacial tension (IFT) test is performed to examine the sludge formation within the oil and is considered as a flag for oil reclamation [11]. Although polar compounds in transformer oil usually have little or no acidity, they can react to form acids which increase the rate of insulation paper ageing as shown in Figure 2-22. IFT and acid number measurements can therefore provide an early warning of such ageing [103].

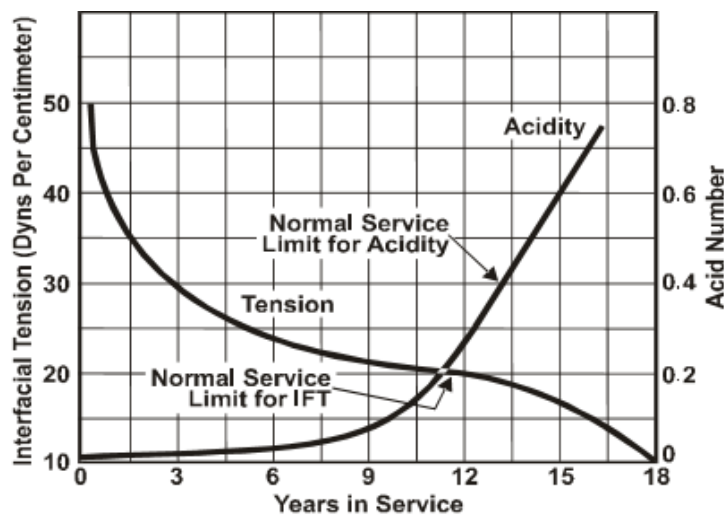


Figure 2-22 Relationship between IFT, acidity and transformer years in service[103].

The ASTM D971 standard (Interfacial Tension of Oil against Water by the Ring Method), as shown in Fig. 2-23, is widely used to measure the IFT of insulating oil [13]. Soluble polar contaminants and degradation products affect the physical and electrical properties of the insulating oil [13, 14], thereby lowering the IFT. According to the ASTM D971 standard, a planar ring of platinum wire with circumference d is immersed in a container filled with water and insulating oil. The force F required to move the ring ten millimetres upwards through the oil-water interface is measured, and the IFT of the oil is then given by F/d [13].

The IFT of new insulating oil is expected to be in the range 40-50 mN/m ; an oil sample with an IFT value less than 25 mN/m is considered to be approaching the end of its useful service lifetime [104]. At this point, the oil is very contaminated and recommended for reclamation to prevent sludging [11]. Sludge starts to form when the IFT value is approximately 22 mN/m and settles on windings, hence affecting the cooling systems of the transformer and causing loading problem as well [12].

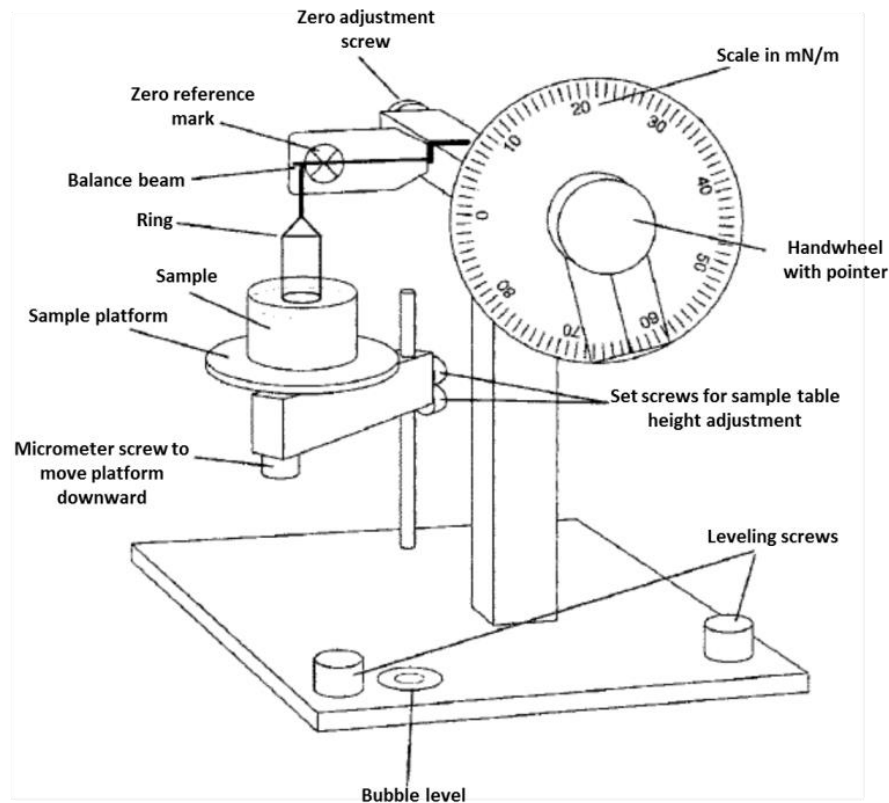


Figure 2-23 Interfacial tension measurement setup based on ASTM D971[13]

The IFT measurement technique requires great care. Wrong or inconsistent data are likely to be obtained if the precautions mentioned in [92] are not carefully and completely observed. A trained person is required to conduct the measurements, using an expensive piece of equipment, so that in nearly all cases the oil samples have to be sent to an external laboratory.

2.4.2 Acid Number

An acid number (acidity) test is performed to determine the acidic degradation components in service-aged oil, and generally used as a guide for oil reclamation or replacement [11]. Acids in transformer oil are formed due to the reaction of oxidation products released by insulation paper and oil that attack the transformer's metal tank and also the paper insulation's cellulose chain [105].

Acids accumulation in the insulating oil leads to the formation of insoluble sludge which reduce the dielectric strength of the oil [106]. Acid content in oil can be measured by chemical titration; the mass of potassium hydroxide (KOH) in milligrams (mg) required to neutralize the acids in 1 gram (g) of the oil sample, also known as the neutralization number (NN) [107]. A higher acid number indicates more acid in the oil. However, there is no direct correlation between acid number and the corrosive tendency of the oil towards metal in electrical power equipment [11]. Furthermore, an acid number does not distinguish between different acids and their strength [106].

New transformer oils contain nearly no acid (the acid number is almost 0 mg KOH/g). However, acid concentration in insulating oil grows as the transformer ages, and sludge begins forming when the acid number reaches 0.40 mg KOH/g [103]; hence, the oil should be reclaimed before the acid number reaches this level. According to IEEE Std. 62-1995 [11], the oil should be reclaimed when the acid number reaches 0.20 mg KOH/g.

The ASTM D974 (Standard Test Method for Acid and Base Number by Color-Indicator Titration) [108] and ASTM D644 (Test Method for Acid Number of Petroleum Products by Potentiometric Titration) [109] describes the procedure for determination of acidity of electrical mineral insulating oil.

2.4.3 Water Content

The dielectric strength of paper insulation significantly reduces when water content within the paper increases. Moreover, the paper insulation will age prematurely if the water concentration is sufficiently high, and may lead to transformer failure if overloaded [110]. Studies show that the rate of aging of a transformer with a high level of oxygen and wet paper insulation is 40 times that of a similar transformer with a low level of oxygen and dry paper insulation [111]. Hence, it is essential to determine the water content of the paper insulation (WCP) and maintain its concentration within safe limits [11].

According to IEEE Std. 62-1995 [11], the paper is considered as dry or within safe limits if the percentage of moisture by dry weight in paper (M/DW) is less than 2%, whereas exceeding this value indicates the paper is becoming wet. Insulation is extremely critical when the WCP reaches 4.5% M/DW, where the paper is excessively wet. Plans should be made for transformer dry out once the WCP reached 2% M/DW, and WCP should never be allowed to go above 2.5% M/DW [12]. However, it is impractical to extract a paper insulation sample from a transformer for measuring the WCP, since it involved removing parts of the transformer insulation.

Therefore, it is a common practice to estimate the WCP value by measuring the water content in the oil (WCO) first, and then correlates the WCO measurement to a WCP value by using equilibrium curves [11]. The Karl Fischer titration technique is widely used to measure the WCO of transformers. IEC 60814 (Insulating liquids - Oil-impregnated paper and pressboard - Determination of water by automatic coulometric Karl Fischer titration) [112] and ASTM D1533 (Standard Test Method for Water in Insulating Liquids by Coulometric Karl Fischer Titration) [113] describe the procedure for determining water content in a transformer oil sample.

2.4.4 Dielectric Strength

A dielectric strength test is performed to determine the dielectric breakdown voltage of transformer insulating oil [11]. Dielectric breakdown voltage is used in assessing the ability of insulating oil to withstand electrical stress without any failure [114]. A low dielectric breakdown voltage indicates the presence of contamination agents such as water, conducting particles, and cellulosic fibers in the oil. However, a high breakdown voltage on the other hand does not guarantee the absence of contamination, as the contamination concentration may not be enough to affect the electric oil characteristics [114].

The ASTM D1816 (Standard Test Method for Dielectric Breakdown Voltage of Insulating Liquids Using VDE Electrodes) [114] and the IEC 60156 standard (Insulating liquids – Determination of the breakdown voltage at power frequency) [115] are widely used to determine the average dielectric breakdown voltage of transformer oil. In this method, the breakdown test uses ac voltage in the power-frequency range from 45 to 65 Hz. A transformer oil sample is placed in the test cell which consists of two spherically shapes electrodes facing each other at a distance of either 1 or 2mm [114].

At the beginning, the voltage across the electrodes is 0V, and it increases at the rate of 0.5kV/seconds until it reached the maximum voltage prior to the breakdown. The tests are repeated **six** times and the mean of maximum voltage is considered as the dielectric breakdown voltage of the sample. According to IEEE Std. C57.106[116], the acceptable minimum breakdown voltage of oil by using ASTM D1816 (with a 1mm electrode gap) is 23 kilovolts (kV) for transformers rated less than 69 kV, and 28 kV for transformers rated within 69 kV to 230 kV. However, the dielectric strength test is not extremely valuable since the cellulose insulation gets destroyed by the moisture in combination with oxygen and heat, before the dielectric strength of the oil indicates any significant defect [12].

2.4.5 Oxygen

Oxygen (O₂) concentration in insulating oil above 2,000ppm may significantly accelerate paper deterioration [12]. Paper insulation with a high level of oxygen in the oil deteriorates 10 times faster than insulation with a low level of oxygen in the oil. Furthermore, the rate of deterioration is worse when combined with wet paper conditions, with the rate of aging of a transformer with high level of oxygen (above 16,500ppm) together with wet paper insulation being 40 times higher than a similar transformer with a low level of oxygen (below 7000ppm) and dry paper insulation [111].

The oil is recommended for rehabilitation (through the transformer being degassed) once the oxygen level in the oil reaches 10,000ppm [12]. Conversely, oxygen only gets in from leaks and paper deterioration, hence high oxygen levels in insulating oil may reflect that a leak has developed either in a bladder or diaphragm in the conservator. Oxygen concentration in insulating oil is normally measured during DGA tests in accordance with ASTM D3612 [15].

2.4.6 Oil Power Factor

An oil power factor test indicates the dielectric loss of insulating oil which suggests there may be a leakage of current associated with watt loss [12]. It is useful for monitoring oil quality and also as an indication of oil contamination or deterioration [117]. A low power factor indicates low dielectric losses while a high power factor indicates deterioration or contamination created by water, carbon, conducting particles, metal soaps, and products of oxidation [12, 117].

Good insulating oil would have a power factor less than 0.5% at 25°C, and further investigation is required once the power factor exceeds 0.5% [12]. The quality of insulating oil is critical and can cause transformer failure when the power factor is greater than 1.0% at 25°C, hence immediate oil treatment or replacement is essential. However, if the power factor is above 2%, then the oil should be removed from service and replaced with new insulating oil.

ASTM D924 (Standard Test Method for Dissipation Factor (or Power Factor) and Relative Permittivity (Dielectric Constant) of Electrical Insulating Liquids) [117] and IEEE C57.106 (IEEE Guide for Acceptance and Maintenance of Insulating Oil in Equipment) [116] standards can be used to determine the power factor of transformer insulating oil.

2.5 Spectroscopy

Spectroscopic techniques are commonly applied to quantify the energy difference between various molecular energy levels to identify the atomic and molecular structures [118]. The spectroscopy method was discovered by Newton in 1740, when he observed the radiation of white light splitting into different colours when passing through a prism [119]. Since that, several researchers have applied the spectroscopy principle to explain various environmental phenomena including spectra of sun, stars, flames, and sparks [119].

Spectroscopy technology became popular after 1852, when Bouguer-Lambert-Beer's Law based on mathematical physics for the quantitative evaluation of spectral absorption measurement which eventually led to the colorimetry, photometry and spectrophotometry techniques [120]. A manually configured spectrophotometry technique for quantitative measurement of the amount of energy absorbed as a function of the incident radiation wavelength has been available since 1943 [121]. Subsequently, a wide range of manual and recording spectrophotometers has become available in the industry market especially in the chemistry field.

In recent years, several researchers attempted to explore the implementation of spectroscopy technology in transformer condition monitoring. In 1999, Shenton et al [122] implemented a spectroscopy technique to analyse the degradation and life aging prediction of polymers which was extended later on to assess the condition and predict the remaining lifetime of paper and oil used in transformer insulation.

Percherancier and Vuarchex [123] employed Fourier Transform Infrared (FTIR) spectrometry to detect additives and contaminants in insulating oil. They discovered the impurities in insulating oil can be detected using FTIR even at a very low concentration level. Koreh et al [18] applied FTIR to studying water clusters in insulating oil where strong O-H absorption is found within the IR region. However, direct measurement of moisture in insulating oil is limited because conventional FTIR is quite insensitive to moisture contents less than 250ppm [124].

The infrared absorption technique has also been proposed for detecting oxidation products in mineral oil [125]. All oxidized products can be identified precisely, either qualitatively or quantitatively in the region $1800\text{--}1650\text{ cm}^{-1}$ [126]. Ali et al [19] used the spectroscopic (FTIR and near-infrared (NIR)) to examine the ageing of cellulose paper and concluded that vibration spectroscopy could potentially be used in monitoring cellulosic material.

This supports an early investigation conducted by Liu et al [127] on Australian cotton cellulose fibers. Based on successful laboratory results reported in the literature [18, 19, 123], Baird et al [128-130] developed a portable spectroscopic probe system that is capable of analyzing insulating oil in power transformers within a visible to near infrared spectroscopy range. The portable spectroscopic system proposed by Baird and his research team was able to evaluate the degree of polymerization of various aged transformer papers and moisture content with adequate precision.

Instead of using a vibrational spectroscopy method (IR spectrum), the American Society for Testing and Material (ASTM) standard proposes using ASTM D6802 (Test Method for Determination of the Relative Content of Dissolved Decay Products in Mineral Insulating Oils by Spectrophotometry) [131] for oil contamination level detection by UV-Vis spectroscopy as an alternative technique for assessing oil conductivity. By this method, as the amount of decayed products dissolved in the oil increases, the area of oil spectral response also increases. However, no specific correlation level has been proposed to associate the spectral response area with the contamination level within an oil sample.

Abu Siada et al [21, 132] introduced a new application of UV-Vis spectroscopy to estimate furan concentration in transformer oil. In developing this technique, the absorbance characteristics of various oil samples of different furan concentrations were observed and correlations of these two dimensions were identified through gene expression programming and fuzzy logic approaches [133]. According to Workman [134], the majority of organic compounds are transparent in the UV-Vis spectra, and their absorbance in this region therefore provides significant information useful for quantitative analysis or compounds identification.

Additionally, the spectroscopy technologies are widely deployed in astrophysics and chemistry to trace an amount of gas concentration either in space or in a solvent. However, the use of spectral response to detect dissolved gases in transformer oil has not yet been investigated. Recent improvements in spectroscopy technology have enabled a wide scanning range from NIR spectrum up to mid-IR spectrum, so the probability of detecting certain gases using spectroscopy has increased.

2.5.1 Principle of Absorption Spectroscopy

A beam of light or electromagnetic radiation that interacts with a substance can be absorbed, transmitted, reflected, scattered, or photoluminescence (PL) can occur. This provides significant information of the molecular structure and energy level transition of the investigated substance [135]. Molecules absorb electromagnetic radiation at various types of transitions, either electronic, rotational or vibrational transitions; which leads to a change in nuclear spin and bond deformation [118]. Each transition mode requires a specific quantity of energy, whereby an electronic mode is associated with a large energy transition, by contrast vibrational and rotational modes are associated with a small energy transition; hence, the different absorption characteristics occur in different regions of the electromagnetic spectrum. Due to the larger amount of energy generated by UV-Vis radiation, absorption which occurs within the UV-Vis spectrum is normally related to a change of electronic transition of the molecule. On the other hand, smaller amounts of energy are associated with IR radiation, therefore the absorption that occurs within the IR spectrum is due to a change of vibrational and rotational transitions of the molecule.

According to quantum theory [118], when a molecule absorbs radiation, its energy E increases proportionally with the energy of the photon as given by:

$$E = h\nu = \frac{hc}{\lambda} \quad (2-6)$$

where h is Planck's constant (6.626×10^{-34} Js), ν is the frequency in s^{-1} , and λ is the wavelength in nanometer (nm), and c is velocity of light.

A different approach is the Beer-Lambert Law (or Beer's Law), which states that the fraction of incident light absorbed by a substance is proportional with the concentration of the absorbing molecules in the light path and the thickness of the sample, and the fraction of the incident light absorbed by a homogeneous medium is independent of the intensity of the incident light [118],[119]. According to the Beer-Lambert Law [135], the amount of light absorbed by a solution or substance can be calculated as:

$$A_{\lambda} = -\log_{10} \left(\frac{I}{I_0} \right) = \epsilon_{\lambda} \cdot c \cdot l \quad (2-7)$$

where, A_{λ} is the light absorbance, I is the intensity of the emergent light, I_0 is the intensity of the incident light, ϵ is the absorbance coefficient of the absorbing species at wavelength λ , c is the concentration of the absorbing species (moles/litre), and l is the path length traversed by the light.

In general, several absorption spectroscopy instruments such as UV-Vis spectroscopy, NIR spectroscopy, IR spectroscopy, and FTIR spectroscopy are developed in accordance with the Beer-Lambert Law. The absorption of electromagnetic radiation spectrum (or light source) is represented by a plot of the absorption intensity versus the wavelength of the light absorbed. The wavelength in the UV-Vis region is usually expressed in nm, while the wavelength in the NIR-IR region is expressed in wavenumbers (cm^{-1}); Note that wavelength in nm = $10^7/\text{wave number in cm}^{-1}$ [118].

2.5.1.1 UV-Vis Spectroscopy

UV-Vis-NIR absorption is related to the measurement of energy absorbed when electrons are promoted from lower to higher energy levels [118]. A molecule is comprised of rotational, vibrational and electronic energy levels, wherein a set of rotational levels which have less energy separations form of vibrational level, while each electronic level is associated with a number of vibrational levels. The UV-Vis spectrum is related to electronic excitation due to the relatively larger amounts of energy associated with the ultraviolet radiation. Hence, the UV-Vis spectrum results reflect the electronic transition associated with the changes that occur either in rotational or vibrational states [136]. Different categories of electronic excitation among the various energy levels within the molecule will reflect the absorption of ultraviolet radiation. These electronic transitions can occur between a bonding (π or σ) or lone-pair orbital (n) and unoccupied non-bonding or antibonding orbital, as shown in Fig.2-24.

Electronic transitions between $\sigma \rightarrow \sigma^*$ (bonding σ to antibonding σ^*) and $n \rightarrow \sigma^*$ (non-bonding atomic orbital to antibonding σ) required relatively higher energy, hence are associated with shorter wavelength radiation (far UV region). On the other hand, electronic transitions for $n \rightarrow \pi^*$ (non-bonding atomic orbital to antibonding π) and $\pi \rightarrow \pi^*$ (bonding π to antibonding π^*) require relatively lower energy, and are normally associated with longer wavelength radiation (UV or Vis region).

The structure of the molecular orbital will influence the probability of a transition occurring. The transition probability is directly proportional with the intensity energy of absorption, therefore the intensity of energy absorption can be estimated when the configuration of the molecular orbitals is recognized [118]. Absorption coefficient ϵ values greater than 10,000 will have a high transition probability, while ϵ values less than 1,000 will have a low transition probability.

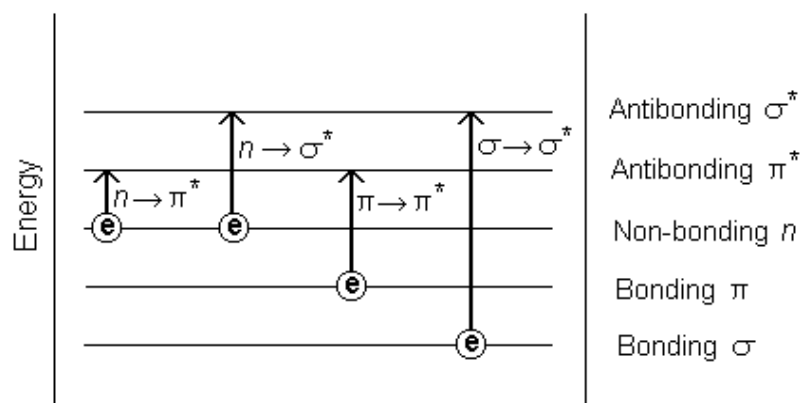


Figure 2-24 Energy levels of various electronic transition types

2.5.1.2 IR Spectroscopy

Infrared spectroscopy gives information on the transition between vibrational and rotational energy levels in molecules, also known as molecular vibrations [118]. Each atom has a different mass which form different strengths of covalent bonds. As a result, the bond vibrates at different frequencies and causes various stretching and bending vibrations in the molecules. During stretching vibrations, the atoms remain in the same bond axis but the distance between the two atoms increases or decreases. However, during bending vibrations, the distance between the atoms remains constant but the position of the atoms changes relative to the original bond axis [118]. Stretching vibrations require higher energy compared to bending vibrations and occur at a higher frequency, while bending vibrations occur at lower frequency. The amplitude of the vibration is increased and radiation energy is absorbed when the infrared light of a certain frequency is incident on the molecule [118].

An infrared spectrum is obtained by finding the corresponding frequency of the molecular vibration from the amount measured of the frequency of the infrared radiation absorbed. Absorption spectra obtained within the normal infrared region (667cm^{-1} to 4000cm^{-1}) contain information about the fundamental harmonic and combination band vibrations; while the shorter wavelength region (4000cm^{-1} to $12,500\text{cm}^{-1}$), which is also known as the near-infrared region, contains the absorption band due to the harmonic overtones of fundamental bands and combination bands. The overtone absorptions are much weaker compared to the fundamental absorptions [135].

The difference between the dipole moments of the molecule in the ground state and the vibrational excited state reflects the intensity of a particular fundamental absorption. The greater the variance in dipole moments, the more intense the fundamental absorption. However, the infrared absorption is inactive when no change in the dipole moment accompanies the vibrations.

2.5.2 Basic Structure of Spectroscopy Instrument

The absorption spectroscopic technique requires the use of instruments which comprise several common components, such as a source of radiation, wavelength selection, detector and signal processor. The source of radiation for the absorption spectroscopic technique is delivered by photons. The most suitable sources of radiation for UV-Vis spectroscopy are hydrogen or deuterium in a discharge tube, which can cover a wavelength ranging from 185nm to 390nm, and a tungsten-filament lamp which is able to cover the visible region ranging from 350nm to 800nm). A small ceramic rod made of either silicon carbide (Glowbar) or Nernst filament, which is heated electrically in a temperature range of 1100-1800°C, is typically used to supply a radiation source for NIR-IR spectroscopy [118].

Wavelength selection is a crucial part of absorption spectroscopy. The effectiveness of spectroscopy is influenced by the ability of the system to select a narrow band of radiation [119]. The three most common features included in the wavelength selection are filtering, dispersing and interferometer. Filtering is the simplest method to isolate a narrow band of radiation from a narrow band of the electromagnetic spectrum using coloured glass, or by applying constructive or destructive interference. However, the filtering method only works for a fixed nominal wavelength and is not recommended for multiple wavelength analysis.

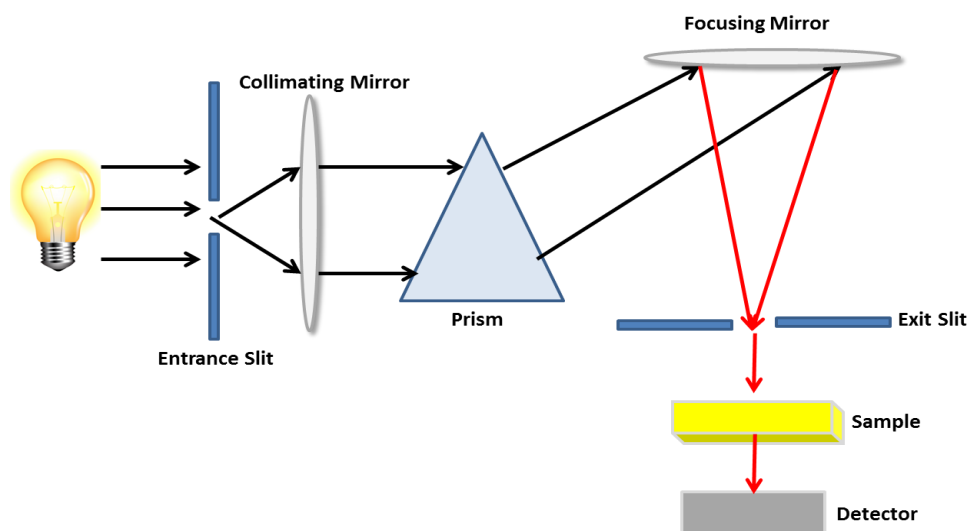


Figure 2-25 Schematic diagram of a monochromator (prism)

The monochromator (dispersing) method using a prism or diffraction grating surface is continuously attuned to the nominal wavelength region. The basic construction of the monochromator (prism) is shown in Fig.2-25.

Radiation from the source enters the monochromator through an entrance slit. The radiation is collected by a collimator mirror and reflects a parallel beam of radiation to a prism or diffraction grating which disperses the radiation. Then, the radiation is focused at the exit slit using a focusing mirror and is passed to the detector. In practice, the prism is normally rotated to cause radiation to move across the exit slit.

Another wavelength selection method involves using interferometers, as shown in Fig.2-26. This approach allows source radiation of all wavelengths to reach the detector simultaneously. A light source emits a light beam of wide wavelength (λ) IR range which is focused on a beam splitter, placed between two fixed and movable mirrors. The movable mirror is moved at a constant velocity v . The beam is split into two directions where half of the beam is reflected to the fixed mirror which reflects it back through the beam splitter to the detector via the tested oil sample. The other half of the beam is transmitted toward the moving mirror which also reflects the beam back to the detector through the splitter and the tested sample.

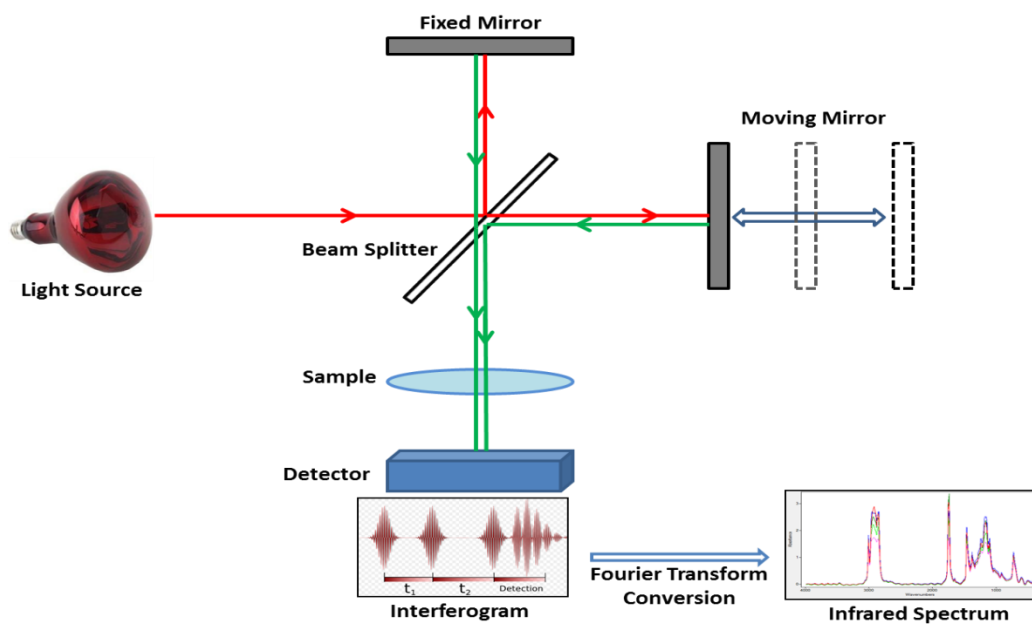


Figure 2-26 Schematic diagram of interferometer

The optical paths distances of the two beams received by the detector are determined by the position of the two mirrors. The detector output will be maximum if the optical path distances of both beams are identical, and minimum if the two optical path distances are different by a value equivalent to half of the wavelength ($\lambda/2$) or out of phase. The detector output signals are detected at a specific interval frequency, f which is determined by the translational velocity of a movable mirror, v and the wavelength of the monochromatic radiation, λ , as shown in (2-8) [118].

The overall detector output as a function of time, also known as the interferogram, will be the sum of the waves for each frequency component. Finally, the interferogram information is converted into a plot of absorption against wavenumber (cm^{-1}) by the computer using the Fourier transform method. In comparison to a monochromator wavelength selection method, an interferometer approach is only applicable to the NIR to IR spectrum, and the approach is known as Fourier Transform spectroscopy.

$$f = 2\nu / \lambda \quad (2-8)$$

The function of the detector is to convert a signal consisting of photons into an easily measured electrical signal. Photoelectric or photomultiplier tubes which contain a photosensitive surface are generally used as detectors for UV-Vis spectroscopy as they can produce an electrical current proportional to the number of photons. Alternatively, a thermal transducer or sensitive thermocouple is used for IR spectroscopy. The absorption of IR photons by a thermal transducer increases its temperature, hence varying one or more of its characteristic properties that is transformed into an electrical signal.

Signal processors which include analog to digital converters, recorders, and computers equipped with a digital acquisition board present the information in a more convenient way for evaluation [118].

2.6 Conclusion

This chapter discussed several techniques to assess transformer health condition based on its insulation system. From the above discussion it can be summarized that although GC can accurately measure the concentration of gas dissolved in oil, however this technique cannot be implemented onsite or on-line. Alternative techniques such as hydrogen on-line monitor and PAS which can be applied online also have their own limitations. Even though hydrogen on-line monitor can detect H_2 , however it's not enough to identify the fault types since it's unable to detect others fault gases like CO, CO_2 , CH_4 and C_2H_6 . In the meantime, PAS which can identify most of the fault gases except H_2 is not fully matured yet and its accuracy is questionable. To overcome this issue, a new technique to detect dissolved gas in transformer oil was proposed and discussed in Chapter 4.

This chapter also discussed the current implementation of spectroscopy technology in transformer condition monitoring. Basic principle of absorption spectroscopy also been reviewed. With remarkable results show by spectroscopy technology, the possibility of measuring IFT using UV-Vis spectroscopy was investigated and discussed in the next chapter.

Chapter 3 A New Technique to Measure Interfacial Tension

3.1 Introduction

This chapter addresses the thesis' Objective 1: Developing a new technique to measure the interfacial tension of transformer oil using UV-Vis spectroscopy.

Reliable monitoring and diagnostic techniques for detecting transformer incipient faults are required in order to help avoid catastrophic failures, and to inform an efficient predictive maintenance program which improves the reliability of the equipment [5, 24]. The overall health of an operating transformer depends largely on the condition of its insulation system [6]. Incipient faults within a transformer can be detected by analyzing samples of its insulating oil, e.g., using dissolved gas analysis and furan analysis [137-139]. Meanwhile, IFT and acid number measurements can provide an early warning of insulation paper ageing activity [103]. Reaction between polar compounds in transformer oil and paper insulation lowered the IFT number and form acids which increase the rate of insulation paper ageing.

The ASTM D971 (Interfacial Tension of Oil against Water by the Ring Method) standard is widely used to measure the IFT of insulating oil [13]. The IFT value reflects the soluble polar contaminations and products of degradation that affect the physical and electrical properties of the insulating oil [14, 141]. The IFT number is the amount of force required to pull a small wire ring upward a distance of one centimeter through a distilled water and oil interface. New or healthy insulating oil is expected to have a high level of IFT in the range of 40 to 50 mN/m, while an oil sample in critical condition would have an IFT less than 25 mN/m [104].

The current IFT measurement technique is very sensitive and may result in a wrong or inconsistent IFT reading if the precautions mentioned in the standard procedure are not carefully followed. Moreover, the current technique calls for specially trained personnel to conduct the test that requires a relatively expensive piece of equipment and it takes a long time to get the results as oil samples have to be sent to an external laboratory which incurs additional running cost.

Spectroscopy technology has demonstrated a remarkable performance in various power transformer condition monitoring applications [16, 21, 128, 137, 142]. This thesis proposes an alternative method to estimate interfacial tension of transformer oil using ultraviolet-to-visible (UV-Vis) spectroscopy along with a fuzzy logic approach. The UV-Vis spectral response of transformer oil can be measured instantly onsite with relatively cheap equipment, does not call for a specially trained personnel to conduct the test and can be implemented online.

Fuzzy logic model is developed based on the information gathered from the UV-Vis spectral response of various transformer oil samples and the corresponding IFT value of each sample that is measured in accordance with the ASTM D971 method. Accuracy of the developed fuzzy logic model is tested using another set of oil samples with wide range of IFT numbers.

3.2 IFT Measurement

An IFT number is determined by the amount of force required to detach a planar ring of platinum wire one centimeter through a water-oil interface, as stated in ASTM D971, and as shown in the IFT setup in Fig. 2-23 [13]. In this technique, distilled water is used as a base layer inside a container in a depth of 10 to 15 mm. The container is placed on a tensiometer platform so that the ring is immersed to a depth not exceeding 6mm into the water. The platform is then slowly pulled down until the ring ruptures the water surface, while the torsion arm is maintained at zero level by increasing the torque on the reading dial.

The oil sample is then carefully floated on the surface of the water until the ring is submerged to a depth of at least 10mm. The platform is then slowly pulled down until the ring ruptures the oil-water interface. Interfacial tension of the oil sample is calculated by:

$$IFT = P \times F \quad (3-1)$$

where *IFT* is the interfacial tension of oil sample in mN/m, *P* is the scale reading of the tensiometer when the ring ruptures the oil/water interface in mN/m, and *F* is a correction factor depending on the ring dimensions and water and oil densities. Since this method is very sensitive, it is essential to carefully follow all the precautions and steps mentioned in the standards. Failure to do so may lead to incorrect and inconsistent results.

3.3 UV-Vis Spectroscopy Setup

Spectroscopy is a powerful non-destructive test that utilizes electromagnetic radiation interaction effect to determine the energy level and structure of atomic or molecular substances [144]. Instead of measuring molecular rotations and vibrations, UV-Vis spectroscopic methods are used to measure an electronic transition corresponding to the excitation of the outer electrons and is used to quantify the transition of metal ions and highly conjugated electronic compounds [135], [145]. In this work, a UV-Vis spectroscopy test is conducted on various transformer oil samples in accordance with ASTM E275 (Standard Practice for Describing and Measuring Performance of Ultraviolet, Visible, and Near-Infrared Spectrometers) [146]. The UV-Vis spectroscopy experimental set up for measuring the spectral response of transformer oil is as shown in Fig 3-1.

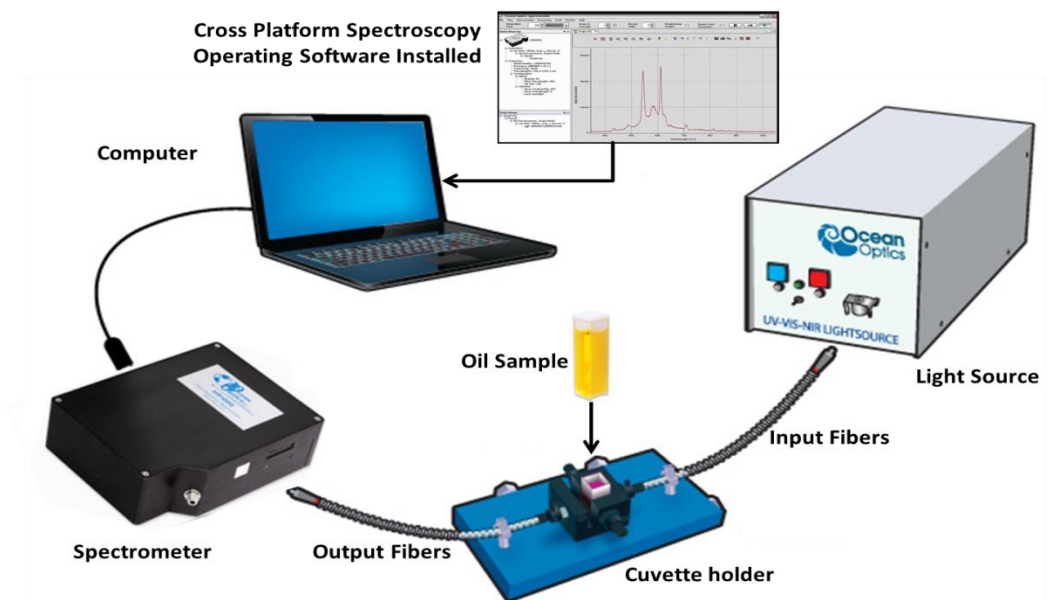


Figure 3-1 Experimental setup for UV-Vis spectroscopy.

A light beam (wavelength λ in the range 200-1100 nm) travels through an optical fiber and enters the oil sample, which is placed in a cuvette. The light interacts with the oil, and the transmitted light passes through a second optical fiber and enters the spectrometer, which is connected to a computer which displays and analyzes the spectral response of the oil sample. The light absorbance A_λ of the oil sample at wavelength λ is related to the ratio of the light intensity transmitted through the oil sample to the light intensity incident on the sample. According to the Beer-Lambert Law [135]

$$A_\lambda = -\log_{10} \left(\frac{S_\lambda - D_\lambda}{R_\lambda - D_\lambda} \right) = \epsilon_\lambda \cdot c \cdot l \quad (2)$$

where S_λ is the light intensity transmitted through the sample, R_λ is the light intensity incident on the sample, D_λ is the intensity detected by the spectrometer with no light incident on the sample, ϵ_λ is the absorbance coefficient of the absorbing species (or molecule) in the oil, c is the concentration of the absorbing species in the oil (gram/litre), and l is the path length of the light through the oil.

3.4 Experimental Results and Discussion

A series of measurements was conducted on fifty-five transformer mineral oil samples that were collected from in-service transformers of various ratings, operating conditions and life spans, using the ASTM D971 method to identify the IFT number of each sample. All examined mineral oil samples are of Shell Diala BX inhibited type that involves an additive to retard the oil oxidation, delay the formation of acids and delay the formation of sludge [147]. The same oil samples were then tested using a laboratory grade spectrophotometer for absorption spectroscopy at 20°C in accordance with ASTM E275 [146, 148]. To calibrate the impact of cuvette on the measurement, the empty cuvette is scanned and the obtained absorbance characteristic is stored as a reference spectral. Then, approximately 2.0 ml of each oil sample is placed into the cuvette and scanned by using the spectrometer. The difference between this spectral response and the reference spectral represents the oil spectral absorbance characteristic. To preserve oil originality, all samples were handled and stored in accordance with ASTM D923 (Standard Practices for Sampling Electrical Insulating Liquids) [76] and were measured within 1 to 2 days after extraction from the transformer. The interfacial tension results obtained using ASTM D971 method are mapped with the spectral response attained for respective oil samples. Samples of oil spectral response measurements are shown in Fig.3-2 where the encircled number represents the IFT value of the corresponding oil sample in mN/m.

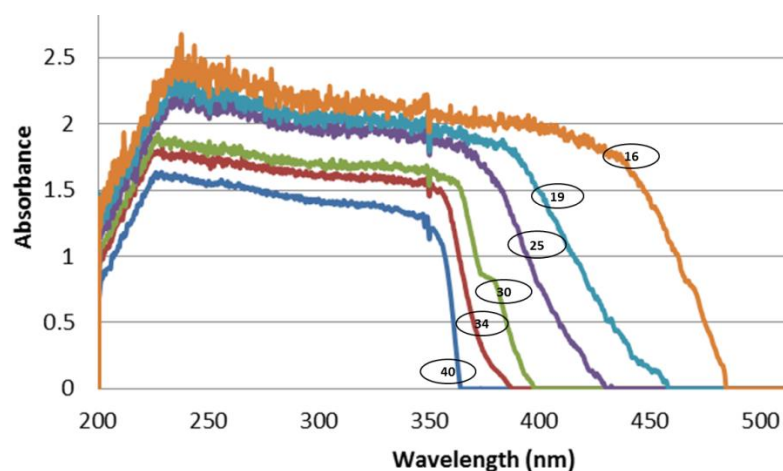


Figure 3-2 UV-Vis spectral response for various IFT numbers (mN/m) [155].

The results show a strong positive correlation between the oil spectral responses and their IFT values, where a new oil sample with an IFT of 40 mN/m exhibits the lowest peak absorbance and the shortest bandwidth. Both parameters increase as the IFT values decrease, as can be seen in Fig.3-2. In Fig. 3-3 which is a 3D plot of the IFT values of various oil samples, the corresponding spectral response parameters (band width and peak absorbance) show a noticeably strong correlation between the IFT number of a transformer oil sample and the oil spectral response.

To investigate the impact of other transformer oil characteristics on their spectral response, the correlations between the oil spectral response parameters and its average breakdown voltage (BDV) [115], water content [112] and acidity [107] were examined, as shown in Figs. 3-4 to 3-6. The obtained results show that apart from IFT, no regular correlation exists between other studied transformer oil characteristics and oil spectral response parameters.

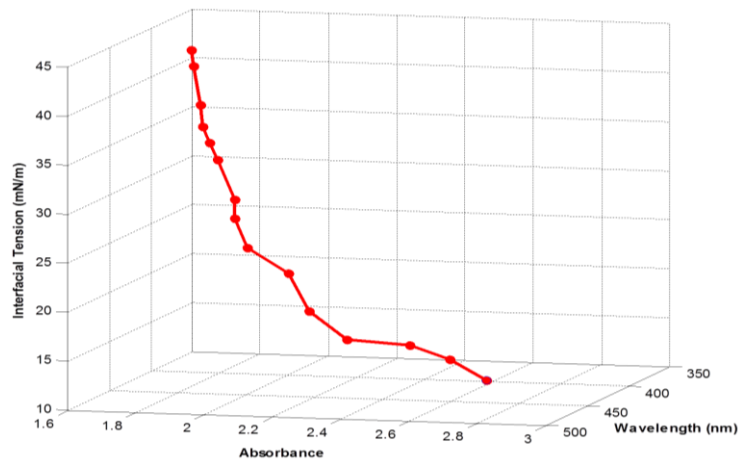


Figure 3-3 Correlation between IFT (mN/m), peak absorbance and maximum wavelength of oil spectral responses [155].

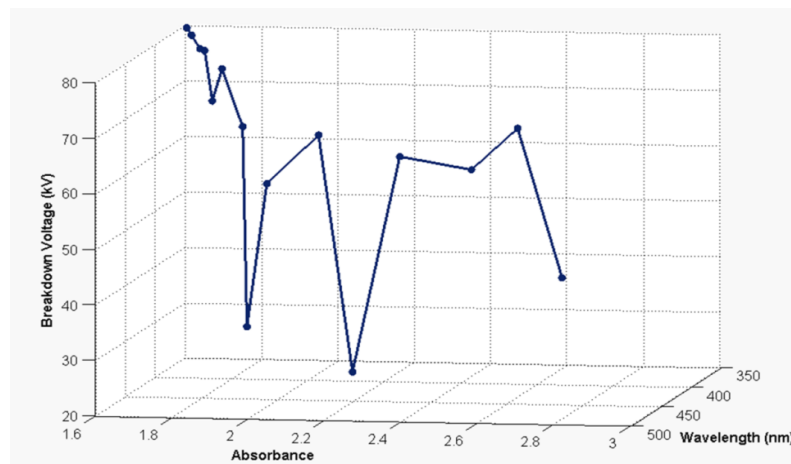


Figure 3-4 Correlation between breakdown voltage (kV), peak absorbance and maximum wavelength of oil spectral response [155].

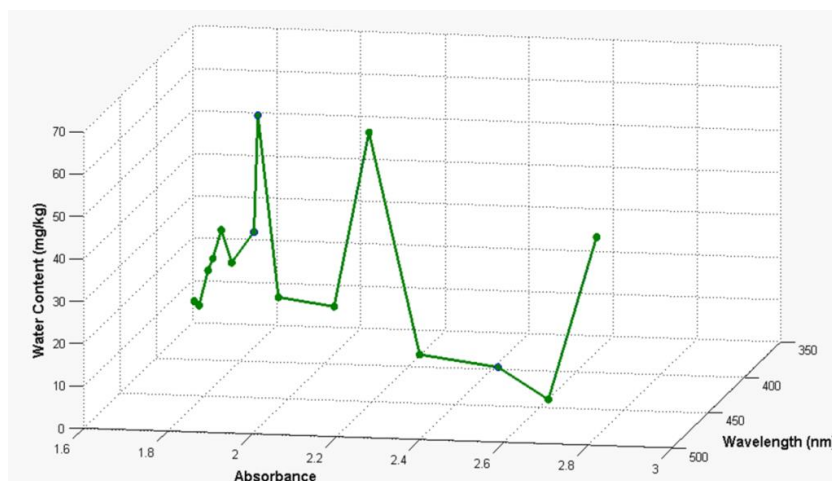


Figure 3-5 Correlation between water content (mg/kg), peak absorbance and maximum wavelength of oil spectral response [155].

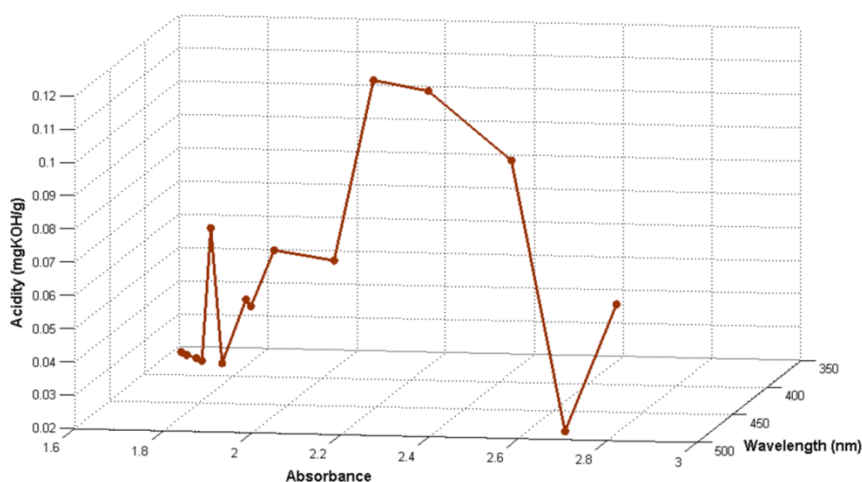


Figure 3-6 Correlation between acidity (mgKOH/g), peak absorbance and maximum wavelength of oil spectral response [155].

It is worth mentioning that all the investigated oil samples are of a mineral type. The correlation between IFT and spectral response of other types of transformer oil, such as silicone and ester oil, may vary due to different oil properties. While a new mineral oil exhibits an IFT value in the range of 40 to 50 mN/m, a new natural ester oil (FR3) has an IFT value around 24-26 mN/m, and new silicone oil has an IFT value of about 25mN/m [61, 149]. Fig.3-7 shows a comparison of the spectral response of various new oil types such as Natural Ester (FR3), Nynas Nytro 10GBN, Shell Diala BX, and Castrol Inhibited Transformer Oil.

The properties of these investigated oil types are given in the Appendix C. Fig. 3-7 shows that except for FR3 oil, new uninhibited and inhibited mineral oil exhibit a somewhat similar spectral response. This is attributed to the fact that uninhibited and inhibited mineral oil originate from hydrocarbon types of oil, which have the same characteristics.

The anti-oxidation additive in the inhibited oil has a negligible impact on the oil spectral response. FR3 is an ester-based oil which has a different chemical chain structure and group [150].

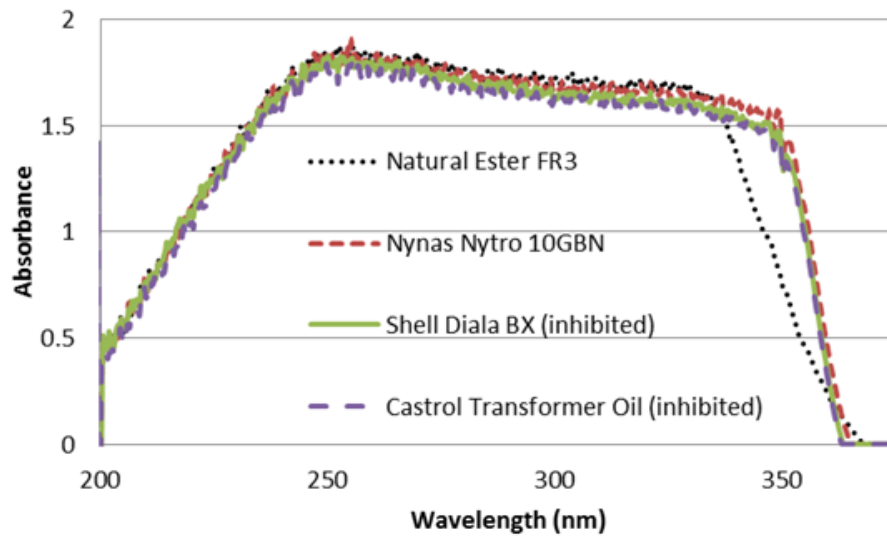


Figure 3-7 Spectral response of new transformer oil samples of different types [155].

3.5 Fuzzy Logic Modelling

Fuzzy logic is frequently used in modelling non-linear or complex systems [34]. It uses variables, usually in the form of words, which are manipulated using logic rules, such as “IF-THEN”. In contrast with other machine learning techniques such as neural network and support vector machine which influenced by the quantity and biasness of historical data used, the fuzzy logic can built a model by relies on the knowledge and experience of the expert, hence give more tolerant with imprecise data [34]. Moreover, fuzzy logic model is easy to interpret and modify compared to neural network model, therefore it was chosen in this thesis. Fuzzy logic system architecture consists of five main elements, namely fuzzification, membership function, fuzzy inference engine, fuzzy rules, and defuzzification, as shown in Fig. 3-8. A brief description of these five elements follows:

Membership functions. There are different types of membership function, such as triangular, trapezoidal and Gaussian. As an example, if men's height is divided into three levels, above 170cm being Tall, 170-150cm being Normal, and less than 150cm being Short, then Height is a fuzzy set and Tall, Normal and Short are the membership functions of that fuzzy set.

Fuzzification is the process of allocating the input data among the membership functions. Thus, in the above example, a man with a height of 140cm is allocated to the Short membership function of the Height fuzzy set.

Fuzzy Rules are conditional statements, e.g., “IF-THEN” or “IF-AND-THEN”, which associate one or more variables with each other. Thus IF (man is short) AND (man is heavy) THEN (man is overweight).

Inference engine converts the fuzzy inputs to the fuzzy outputs using pre-defined fuzzy rules.

Defuzzification is the process of converting the membership functions of a fuzzy set to an output with a quantitative value. A common defuzzification method is the centre of gravity (COG) method, defined by [34]:

$$Z_{COG} = \frac{\int z \cdot \mu_z(z) dz}{\int \mu_z(z) dz} \quad (3-2)$$

where Z_{COG} is the defuzzified output, μ_z is the membership function of the output fuzzy set determined from the input data and the developed fuzzy rules, and z is the output variable of the fuzzy system.

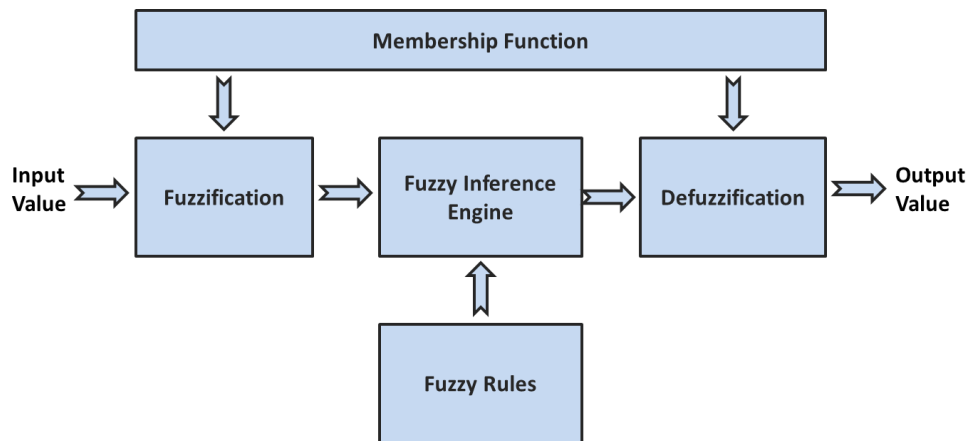


Figure 3-8 Basic fuzzy logic system architecture [140].

In this work, the input variables to the fuzzy logic model were the bandwidth (BW) and peak absorbance level (ABS) of the oil sample spectrum, and the output of the model was the estimated IFT of the oil sample.

The proposed fuzzy logic model was built using the MATLAB graphical user interface tool box. As shown in Fig.3-19, each input was fuzzified into five Gaussian membership functions: low, low-medium, medium, medium-high and high for peak absorbance: and small, small-medium, medium, medium-high and high for bandwidth. The IFT output variable was represented by the five triangular membership functions: very good, good, marginally critical, bad and very bad. Oil samples with IFTs greater than 40mN/m were considered very good, and oil samples with IFTs less than 17mN/m were considered very bad.

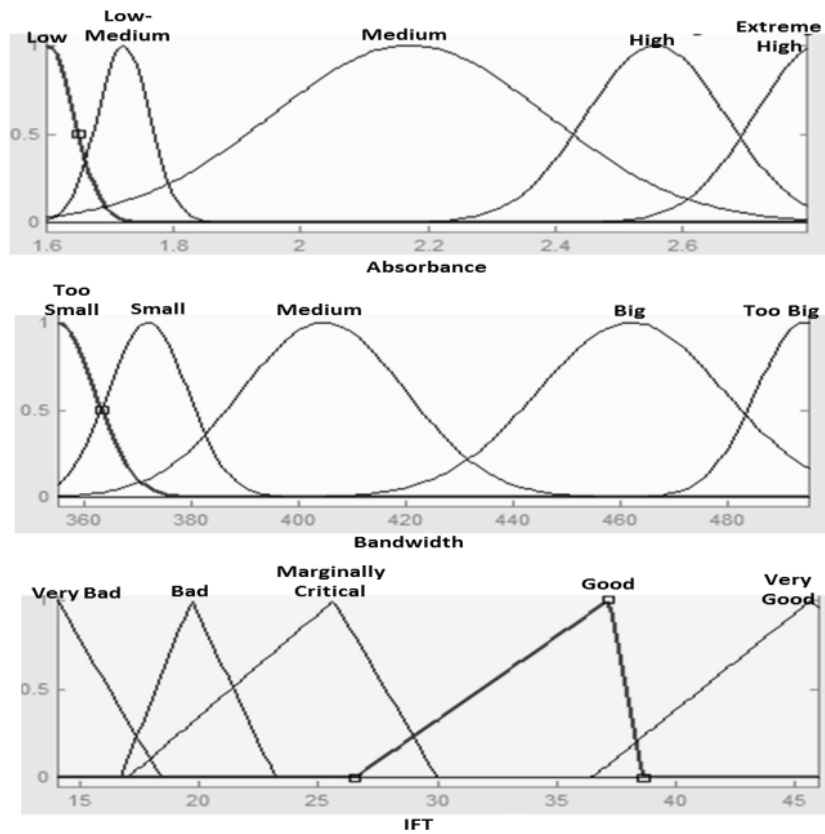


Figure 3-9 Absorbance, bandwidth and IFT membership functions [140].

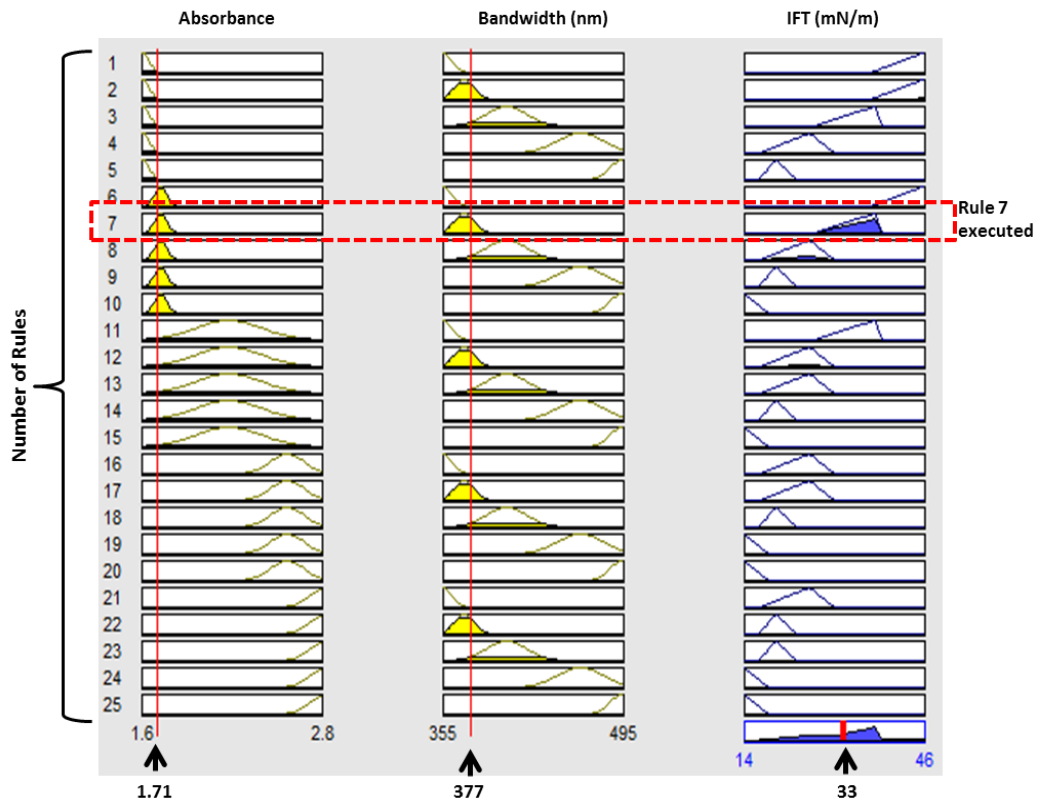


Figure 3-10 Graphical representation of the developed fuzzy logic rules correlating absorbance and bandwidth with IFT value [140].

Twenty-five fuzzy logic (IF-AND-THEN) rules were developed, based on the known correlations between IFT and the spectral parameters BW and ABS, as shown in Fig. 3-3. The fuzzy logic rules are illustrated graphically in Fig. 3-10; the IFT value can be obtained for any pair of peak absorbance and bandwidth values. Samples of these rules are as follows:

Rule 1: IF (ABS is low) AND (BW is low) THEN (IFT is very good)

Rule 2: IF (ABS is low) AND (BW is low-medium) THEN (IFT is very good)

Rule 3: IF (ABS is high) AND (BW is high) THEN (IFT is very bad).

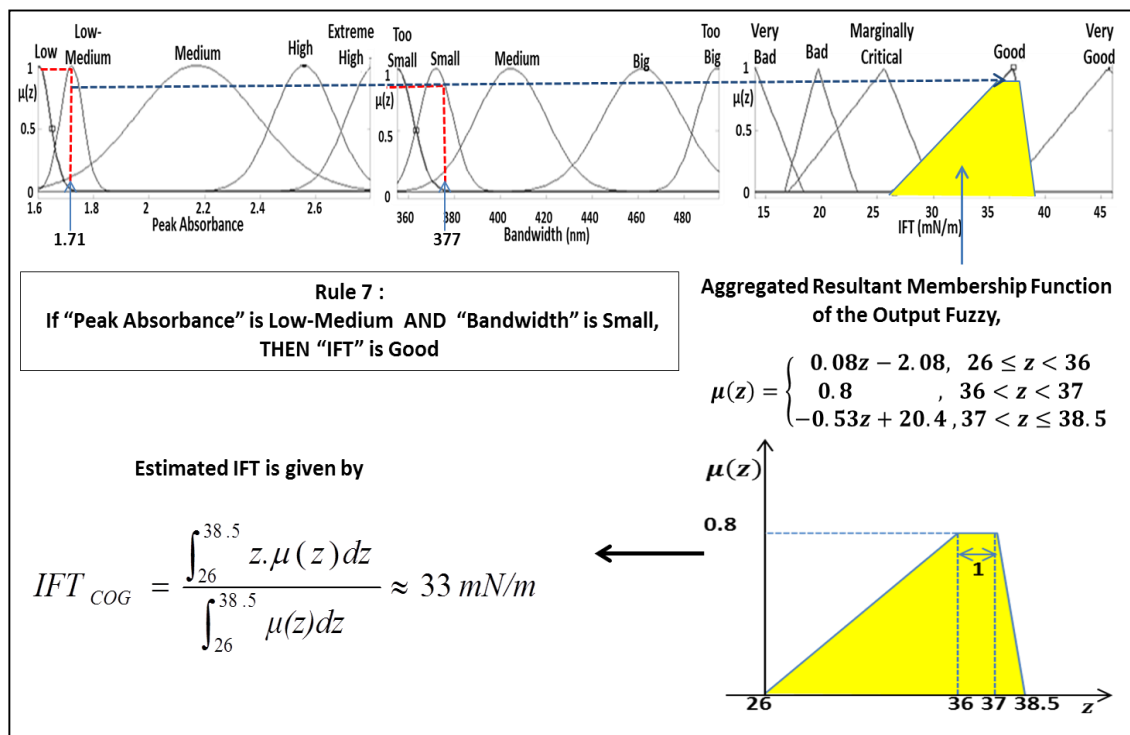


Figure 3-11 An example of the calculation of IFT based on Fig. 3-11 and (3-2) [140].

Thus if ABS = 1.71 and BW = 377nm, then Rule 7 (IF (ABS is low-medium) AND (BW is small-medium) THEN (IFT is good)) is executed, and an estimated IFT of 33mN/m is obtained using COG defuzzification, as shown in Fig. 3-11. The estimated IFT as a function of ABS and BW, according to the fuzzy logic model, is shown in Fig. 3-12. In the event whereas the measured ABS and BW goes below or beyond the range of membership functions, the lowest or highest value of that membership function will be consider as the inputs to the fuzzy logic model. For example, if the measured ABS and BW are 1.55 and 355nm, then the proposed fuzzy logic model will read it as 1.6 and 360nm respectively.

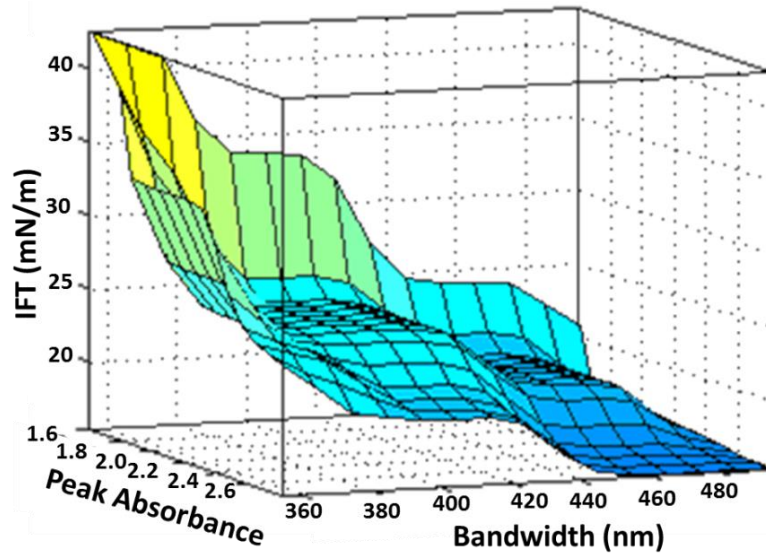


Figure 3-12 IFT as a function of bandwidth and peak absorbance, according to the fuzzy logic model [140].

3.6 Accuracy Analysis

Twenty oil samples collected from various transformers operating under different conditions were used to examine the accuracy of the proposed models. The twenty oil samples used to examine the developed model were selected to cover the all conditions of transformer oil samples starting from brand new oil that has excellent IFT number and passing with moderate deteriorated oil till significantly contaminated oil where the IFT value is within the critical range. The IFT of each sample was measured following ASTM D971.

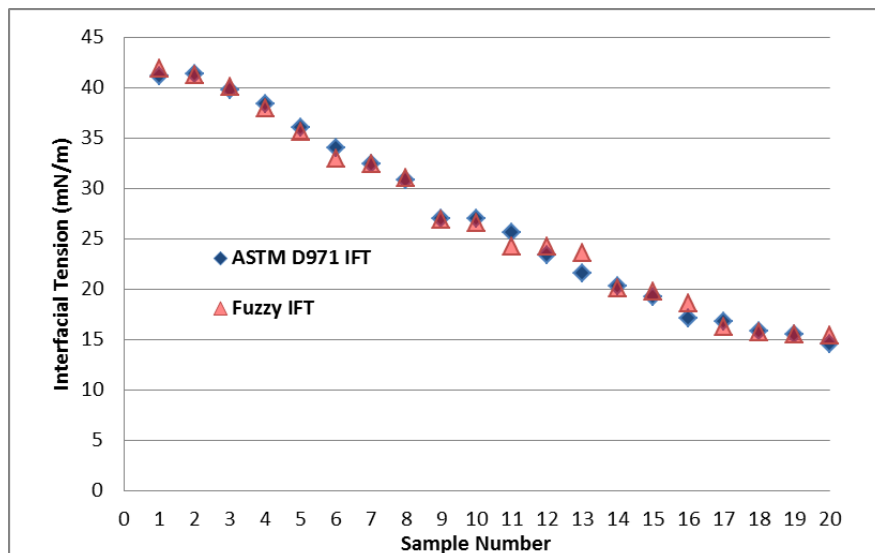


Figure 3-13 Comparison of ASTM D971 and fuzzy logic values of IFT for each of twenty oil samples.

The UV-Vis spectral response of each sample was also obtained, and BW and ABS used as input data to the fuzzy logic estimation model. The resulting IFT values were then compared with the ASTM D971 values (Fig. 3-13). The percentage difference A between $IFT_{ASTM\ D971}$ and IFT_{est} (Fuzzy IFT) is given by:

$$A = \left(\frac{IFT_{ASTMD971} - IFT_{est}}{IFT_{ASTMD971}} \right) \times 100 \quad (3-3)$$

where $IFT_{ASTMD971}$ is the IFT measured using ASTM D971 and IFT_{est} is the IFT obtained using the fuzzy logic model. Table 3-1 summarise the percentage differences between $IFT_{ASTM\ D971}$ and IFT_{est} (Fuzzy IFT) for twenty oil samples. Averaged over the twenty samples, A was 2.17% for the fuzzy logic model. The overall accuracy, i.e., the ratio of the number of correctly estimated IFT values (where A is less than 5%) to the total number of tested samples, was 90% for the fuzzy logic model.

Table 3-1 Comparison results between actual and estimated IFT for 20 oil samples

No.	ABS	BW (nm)	Actual IFT (mN/m)	Fuzzy Est.	% Fuzzy Error
1	1.62	359	41.20	41.90	1.70
2	1.66	359	41.40	41.25	0.36
3	1.64	364	39.80	40.10	0.75
4	1.72	362	38.40	38.01	1.02
5	1.67	369	36.00	35.60	1.11
6	1.69	374	34.00	33.00	2.94
7	1.71	374	32.40	32.40	0.00
8	1.74	377	30.80	31.10	0.97
9	1.78	381	27.00	26.85	0.56
10	1.80	381	27.00	26.60	1.48
11	1.83	393	25.60	24.20	5.47
12	1.91	411	23.40	24.20	3.42
13	2.07	427	21.60	22.60	4.63
14	1.89	425	20.30	20.10	0.99
15	2.21	460	19.20	19.80	3.13
16	2.36	477	17.10	18.20	6.43
17	2.55	479	16.80	16.30	2.98
18	2.68	485	15.80	15.70	0.63
19	2.72	488	15.50	15.50	0.00
20	2.81	494	14.50	15.20	4.83

3.7 Comparison Between ASTM D971 Ring Method and UV-Vis Spectroscopy

Table 3-2 summarises the advantages of the proposed technique over the current method used for measuring the IFT value of transformer insulating oil.

Table 3-2 Comparison between IFT measurement based on ASTM D971 method and proposed UV-Vis Spectroscopy.

Method	ASTM D971	UV-Vis
Advantages and Disadvantages	Requires a trained person to prepare the oil sample and conduct the measurement. Must be conducted in a laboratory environment and is time consuming. No possibility of on-line monitoring.	Does not require a trained person to conduct the measurement. Can be conducted on-site. Could be implemented online.
Cost	Up to US\$10,000 (depending on the model).	From US\$3,500 (depending on spectrophotometer features).
Running Costs	US\$120 to US\$150 per sample.	Negligible.

3.8 Conclusion

Objective 1 of this thesis was to develop a novel technique to estimate the interfacial tension of mineral transformer oil using UV-Vis spectroscopy. In addressing Objective 1 (a), the experimental results show that a strong correlation exists between the IFT value of transformer oil and its spectral response parameters, namely; bandwidth and peak absorbance. In addressing Objective 1 (b), a fuzzy logic model was developed to map this correlation. The results show that the proposed technique can estimate the IFT of transformer oil with a high degree of accuracy. This technique has many advantages over the current IFT measurement technique as it can be conducted instantly onsite, does not need specially trained personnel to conduct the measurements, incur negligible running costs and can be readily implemented online for continuous monitoring of the condition of the insulating oil.

Chapter 4 A New Method to Detect Dissolved Gases in Transformer Oil using NIR-IR Spectroscopy

4.1 Introduction

This chapter addresses the thesis' Objective 2: Developing a new technique to measure the dissolved gases in transformer oil using NIR-IR spectroscopy.

Dissolved gas analysis (DGA) has been widely used to assess the condition of power transformers. Due to high thermal and electrical stress on transformer insulation systems, paper and oil decomposition takes place and generates gases that dissolve in the oil and decrease its dielectric strength. Carbon monoxide (CO) and carbon dioxide (CO₂) are generated as a result of paper decomposition. Other gases, hydrogen (H₂), methane (CH₄), acetylene (C₂H₂), ethylene (C₂H₄), and ethane (C₂H₆) are generated due to oil decomposition. The type and concentration of dissolved gases in transformer oil identify various faults such as partial discharge, over-heating, and arcing within the transformer.

Typically, gas dissolved in transformer oil is analyzed using gas chromatography (GC). Even though GC provides a very high measurement accuracy and repeatability, it is only performed in a laboratory environment due to the complexity of the equipment [15]. Furthermore, an expert is required to conduct the test and interpret its results. Due to the long time, running costs and several standards that have to be applied, the extraction of oil samples from operating transformers, storing and transporting it to chemical laboratories, DGA using GC is usually performed once a year; however, more frequent testing is required when significant concentrations of fault gases are detected during transformer routine inspection. To overcome the limitations of GC, several online techniques such as hydrogen on-line monitoring [17] and photo-acoustic spectroscopy (PAS) [151] have been introduced. The hydrogen on-line monitoring technique was developed based on Teflon membrane technology and it can only trace H₂, CO, C₂H₂, and C₂H₄ gases [137]. Although the hydrogen on-line monitor can detect H₂ with 100% efficiency, the efficacy of detecting other gases is very low, whereas detection efficacy of 15% for CO, 8% for C₂H₂, and 1% for C₂H₄ has been reported [17]. Moreover, the accuracy of hydrogen on-line monitoring is questionable when ambient temperature is above 40°C [79].

By contrast, the PAS technique is able to identify most of the fault gases; however, this technique is sensitive to the wavenumber range of the optical filters used in the measurements and their absorption characteristics and at present PAS technology remains an immature technique that is still in the development phase [151].

Spectroscopy is a non-destructive test that utilizes an electromagnetic effect to determine the energy level and structure of atomic or molecular substances [135]. Each molecule absorbs electromagnetic radiation at various types of transition (electronic, rotational or vibrational) which leads to a change in nuclear spin and bond deformation [118]. Each transition mode requires a specific quantity of energy which results in different absorption characteristics within different regions of the electromagnetic spectrum. The near-infrared (NIR) to infrared (IR) spectral region lies approximately in the wave number range $12,800\text{cm}^{-1}$ to 667cm^{-1} which involves rotational and vibrational transition modes, while the ultraviolet (UV) to visible (Vis) spectral region lies within the range $50,000\text{cm}^{-1}$ to $13,000\text{cm}^{-1}$ which involves electronic transition mode [118]. Many gas molecules absorb NIR-IR radiation rather than UV-Vis radiation especially for colorless gases [23, 152]. Since each gas has a different number and type of atoms, bond angles and strengths, each gas has a unique absorption spectrum [22, 119]. According to the HITRAN (high-resolution transmission molecular absorption) database [153] and NIST (National Institute of Standards and Technology, United States) Atomic Spectra Database [154]: fault gases such as CO, CO₂, CH₄, and C₂H₂ can be traced within both the NIR and IR spectra, while C₂H₄, and C₂H₆ can only be detected within the IR spectrum, as shown in Fig.4-1 and Fig.4-2. The spectrum range for each fault gas is summarized in Table 4-1.

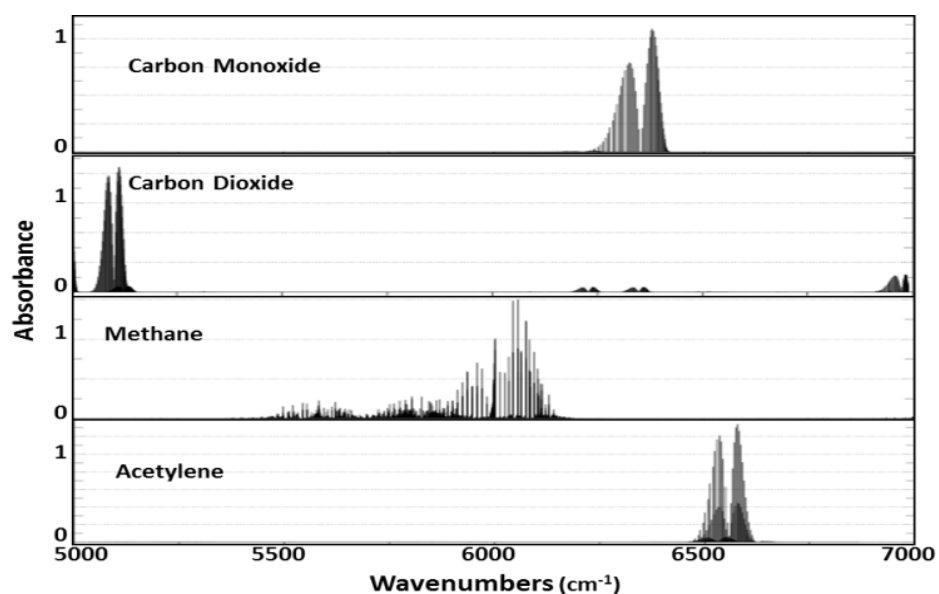


Figure 4-1 NIR absorption spectrum of CO, CO₂, CH₄, and C₂H₂ based on HITRAN database [153]

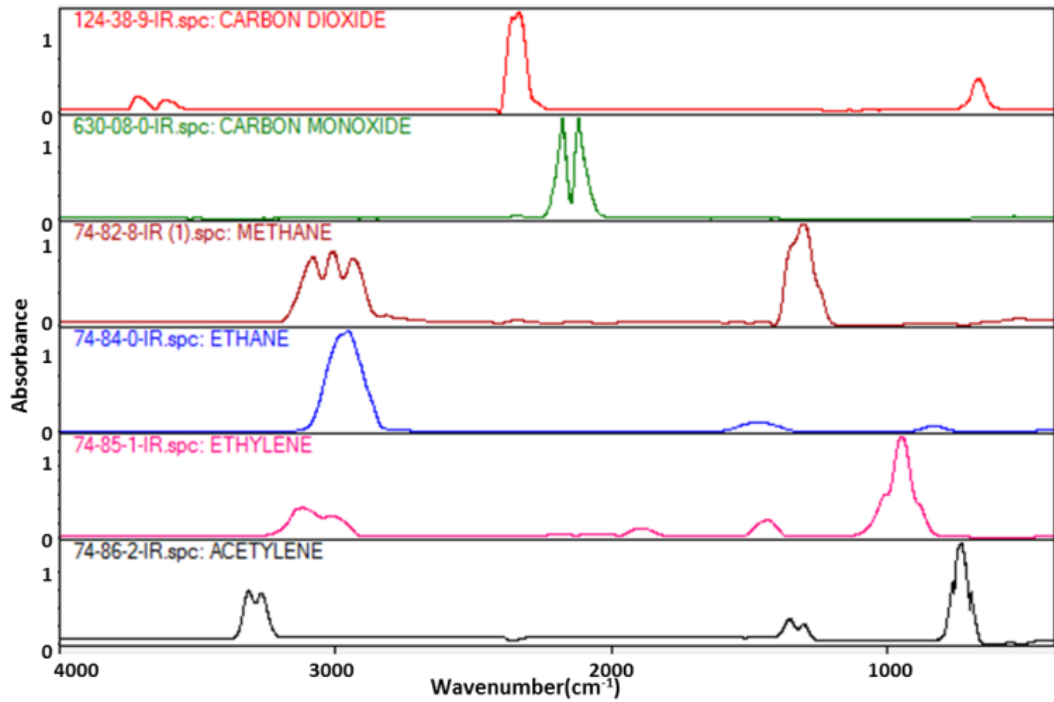


Figure 4-2 IR absorption spectrum of CO, CO₂, CH₄, C₂H₆, C₂H₄, and C₂H₂ based on HITRAN and NIST database [153, 154]

Table 4-1 Spectrum range for each fault gas

Gas	Band Interval (cm ⁻¹)	
	IR Spectrum	NIR Spectrum
CO	2000-2250	6100-6450
CO ₂	560-742; 2232-2405; 3540-3747	5000-5200; 6850-7000
CH ₄	1192-1411; 2721-3211	5800-6100
C ₂ H ₂	659-814; 1260-1393; 3157-3376	6500-6600
C ₂ H ₄	824-1134; 1345-1519; 1807-1951; 2900-3230	-
C ₂ H ₆	789-900; 1378-1548; 2845-3093	-

Objective 2 of this thesis proposes an alternative method to detect gases dissolved in transformer oil based on NIR-IR spectroscopy technology along with the fuzzy logic approach. The key advantage of proposing this technique over existing DGA measurement techniques is that the NIR-IR spectrum of the oil can be measured instantly onsite with relatively cheap equipment that does not call for an expert person to conduct the test and has the potential to be implemented online negligible running costs. In addition to measuring dissolved gases in transformer oil, spectroscopy technology can also be employed to assess insulation paper aging [19], moisture [18], additives and contaminants in oil [123], the furan concentration [21], and the oil interfacial tension number [155].

A fuzzy logic correlation model is developed based on the information gathered from the NIR-IR spectral response of various transformer oil samples that have been tested using GC in accordance with the ASTM D3612 standard to identify and quantify various dissolved gases in each sample. The accuracy of the model is assessed using another set of oil samples with a wide range of various gases concentrations.

4.2 Experimental

One hundred oil samples were prepared in the laboratory to include various fault gases (CO, CO₂, CH₄, C₂H₂, C₂H₄, C₂H₆) with low, intermediate, and high concentrations by injecting each particular gas into blank new oil of Shell Diala BX inhibited type in accordance with the ASTM D3612 standard [15]. 75mL of blank oil was placed in a gas-tight pre-calibrated 100mL syringe containing a lock valve that was connected to a standard gas bottle to allow the gas to mix with the oil and dissolve into it. A particular gas with different predetermined volumes was injected into the syringe to create several concentration levels. The desired gas volumes injected into the syringe were set based on the equation below [15].

$$C_{oi} = \frac{V_{sg} \times (P_a \div 760) \times (273 \div T_a)}{V_{bo} \times C_{sg_i} \times 10^4} \quad (4-1)$$

where C_{oi} is the concentration of gas (i) in the oil (ppm), P_a is the ambient pressure, T_a is the ambient temperature, C_{sg_i} is the percentage of gas-phase concentration of standard gas (i) in the bottle (as provided by the manufacturer), V_{sg} is the volume of the gas standard in the syringe, and V_{bo} is the volume of the blank oil in the syringe. The ambient pressure and temperature were maintained at 101.3kPa and 20°C during the process.

The actual concentrations of dissolved gases in oil samples were measured using GC in accordance with the ASTM D3612 guideline [15]. Absorption spectroscopy measurements at ambient temperature of 20°C were conducted on same samples, using two laboratory-grade spectrophotometers; FT-IR spectroscopy (4000-667cm⁻¹) and NIR spectroscopy (12,000-4,000cm⁻¹), in accordance with the ASTM E2412[156] and ASTM E1790 [157] standards.

Each gas was examined at a specific spectrum range, as listed in Table 4-1 and fault gases' concentrations obtained using GC were mapped with the spectral response attained for respective oil samples. The correlation between the gas concentrations in ppm and two spectral parameters – peak absorbance and area under the absorbance curve – were investigated, as will be elaborated below.

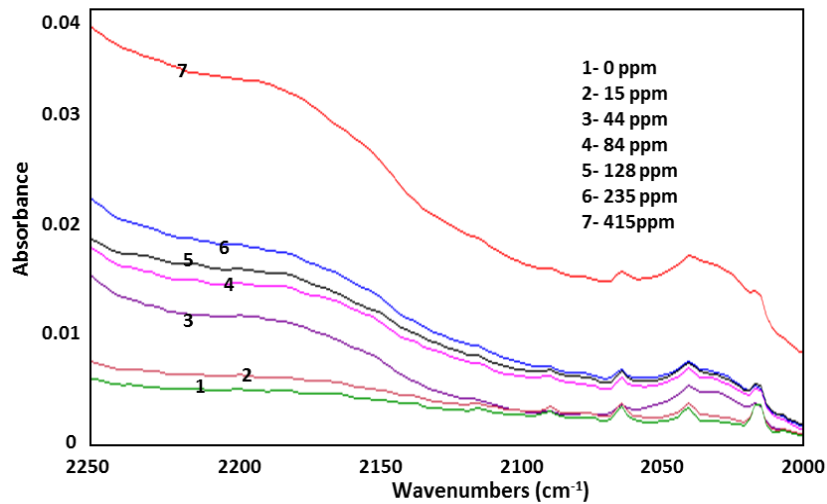


Figure 4-3 Absorbance spectra for various oil samples with different CO concentrations at 2250-2000cm⁻¹ region

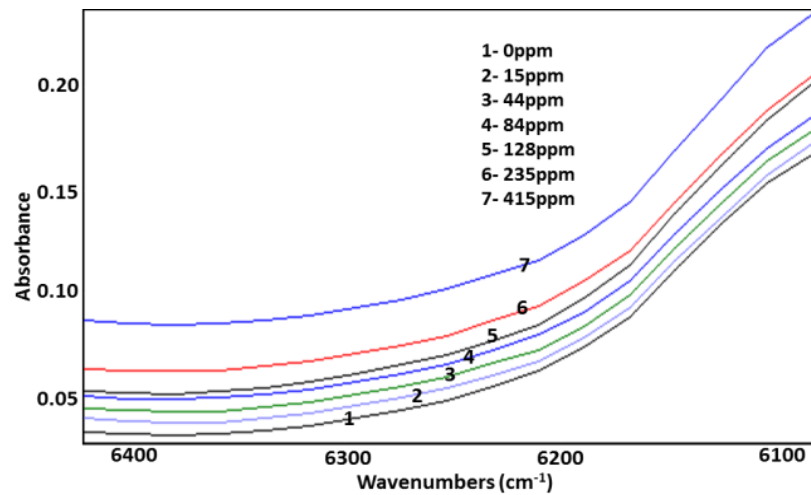


Figure 4-4 Absorbance spectra for various oil samples with different CO concentrations in the 6450-6100cm⁻¹ region

Fig.4-3 shows the spectral response obtained for seven oil samples of various CO gas concentrations within the IR spectrum range 2250-2000cm⁻¹, while Fig.4-4 shows the spectral response of the same gas within the NIR spectrum range 6450 to 6100cm⁻¹. Both results reveal a strong correlation between CO gas concentrations in ppm and their respective oil spectral responses; whereas new oil with 0ppm of CO was found to exhibit the lowest absorption level that increased consistently with the increase of CO concentration in oil.

Fig.4-5 and Fig.4-6 show the spectral responses obtained for various CO₂ concentrations within IR (2400-2250cm⁻¹) and NIR (7000-6850cm⁻¹) spectra respectively. Both figures reveal consistent correlation between oil spectral response and CO₂ concentration; the increase in gas concentration is corresponding to an increase in peak absorbance and area under the curve.

Two peaks are clearly seen within the IR region (Fig.4-5) at 2340cm^{-1} and 2360cm^{-1} . While no obvious global peak absorbance point can be observed within the NIR region (Fig.4-6), a common changeover point where the spectral responses start to decrease is observed at wave number 6968cm^{-1} .

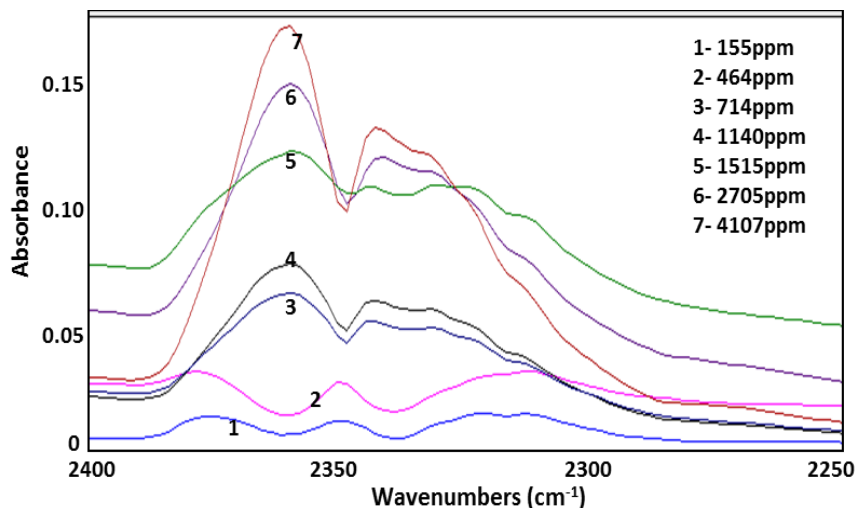


Figure 4-5 Absorbance spectra for various oil samples with different CO_2 concentrations in the $2400\text{-}2250\text{cm}^{-1}$ region

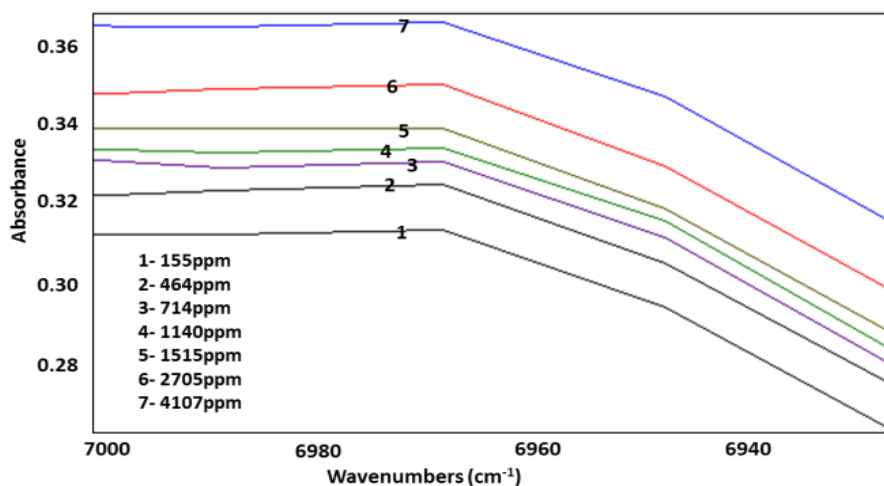


Figure 4-6 Absorbance spectra for various oil samples with different CO_2 concentrations in the $7000\text{-}6850\text{cm}^{-1}$ region

The NIR-IR spectral responses for oil samples containing various concentrations of CH_4 that can be traced in the wavenumber ranges of $3200 - 2721\text{cm}^{-1}$ and $6000 - 5800\text{cm}^{-1}$ are shown in Fig.4-7 and Fig.4-8, respectively. Both sets of results reveal a strong correlation of CH_4 concentrations and its oil spectral response. However, results obtained within the IR spectrum (see Fig.4-7) are more informative compared to the absorption spectral observed within the NIR spectrum (see Fig.4-8).

These differences may be understood in light of the fact that absorption within the IR spectrum is due to the fundamental harmonic of the gas molecule while the absorption in the NIR spectrum is due to the harmonic overtone of the fundamental harmonic of the molecule [118]. Fig. 4-7 also shows that all investigated oil samples had peak absorbance at 2923cm^{-1} .

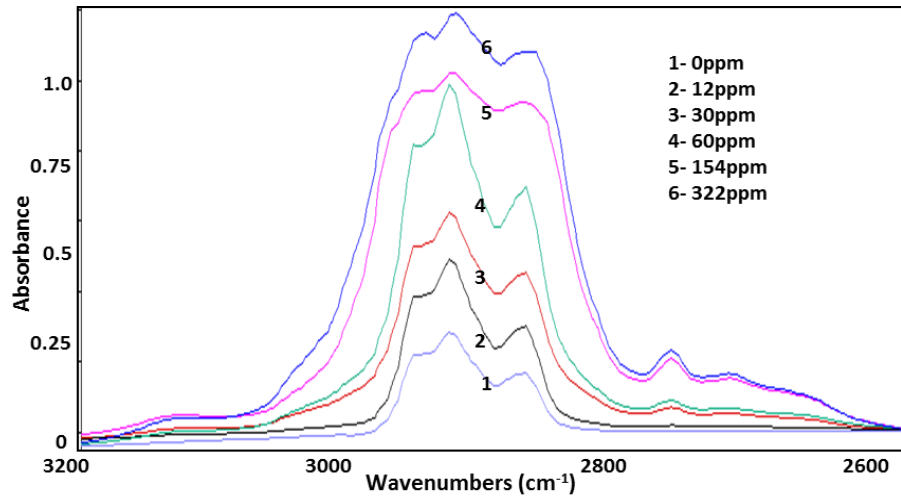


Figure 4-7 Absorbance spectra for various oil samples with different CH_4 concentrations in the $3200\text{-}2721\text{cm}^{-1}$ region

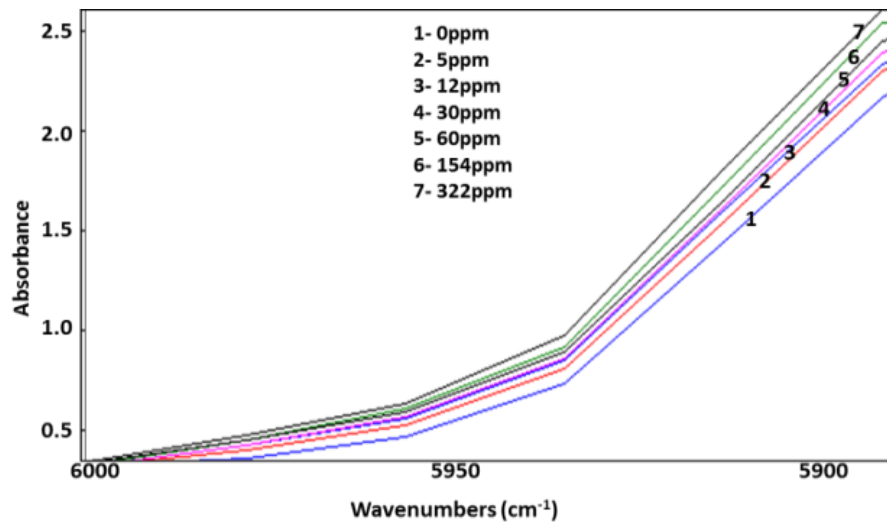


Figure 4-8 Absorbance spectra for various oil samples with different CH_4 concentrations in the $6000\text{-}5800\text{cm}^{-1}$ region

Spectral responses for C_2H_2 gas within the IR and NIR spectra are shown in Figs.4-9 and 4-10, respectively. As shown in Fig.4-9, the peak absorbance of oil spectral response within the $1400\text{-}1300\text{cm}^{-1}$ region is increasing with the increase of C_2H_2 concentration, and all samples show a maximum peak at wave number 1376cm^{-1} . On the other hand, it is quite difficult to identify a unique peak absorbance point at a particular wavenumber for the C_2H_2 NIR spectrum response, as shown in Fig.4-10; even though the trend is similar to the absorption trend shown in Fig.4-9.

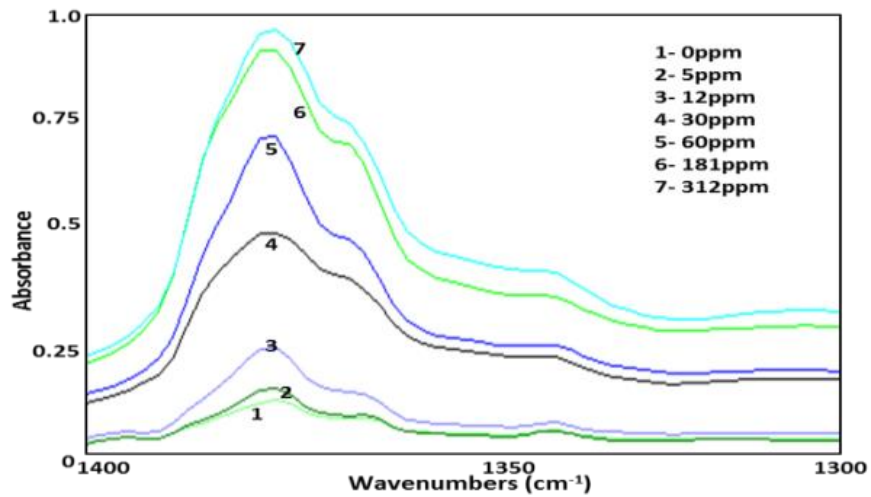


Figure 4-9 Absorbance spectra for various oil samples with different C_2H_2 concentrations in the $1400-1300cm^{-1}$ region

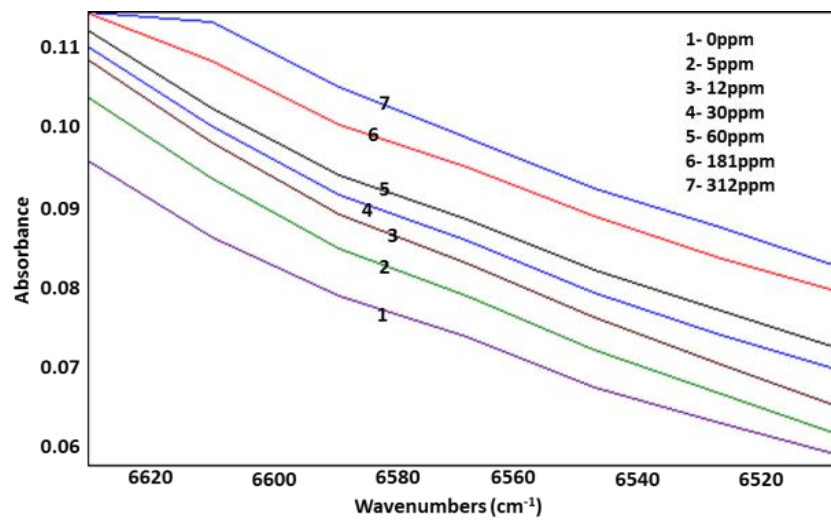


Figure 4-10 Absorbance spectra for various oil samples with different C_2H_2 concentrations in the $6600-6500cm^{-1}$ region

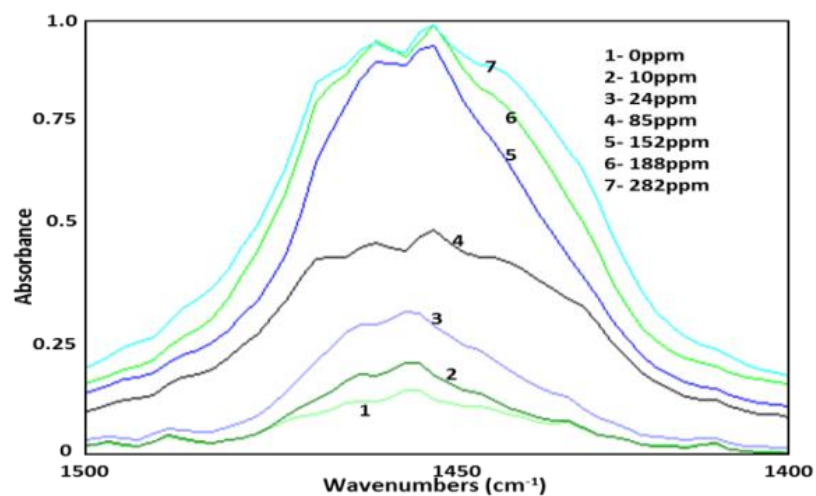


Figure 4-11 Absorbance spectra for various oil samples with different C_2H_6 concentrations in the $1500-1400cm^{-1}$ region

As mentioned earlier, according to the HITRAN database, C_2H_6 and C_2H_4 can only be traced within the IR spectrum. Fig.4-11 shows the spectral response obtained for various C_2H_6 concentrations within wavenumber range $1500-1400cm^{-1}$. Similar to other gases, a good correlation between oil spectral response and C_2H_6 concentration within the investigated spectrum range with a maximum absorbance at $1473cm^{-1}$ can be observed.

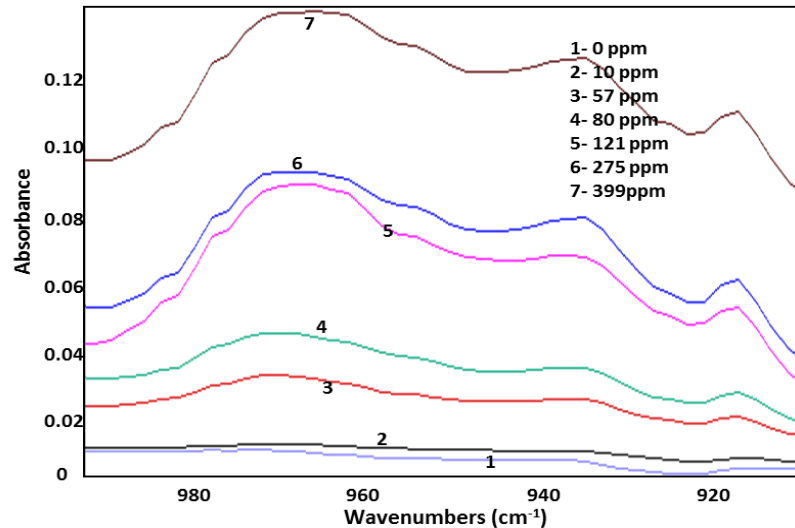


Figure 4-12 Absorbance spectra for various oil samples with different C_2H_4 concentrations in the $1000-900cm^{-1}$ region

Fig.4-12 shows the spectral response obtained for various C_2H_4 gas concentrations within the IR spectrum region, $1000-900cm^{-1}$. Within this region, absorbance characteristics increase with the increase of C_2H_4 concentration in oil and maximum peaks for all investigated samples occur at wavenumber $966cm^{-1}$.

The above results reveal that fault gases dissolved in transformer oil can be detected using NIR-IR spectroscopy as each gas will have a dominant impact at a unique wavenumber without any overlapping with the effects of other gases. Within a particular wavelength range, the spectral response of each gas increases as the level of gas concentration increases; and peak absorbance along with the area under the curve could be employed as dependent parameters to estimate the level of gas concentration. Due to the molecular transition modes characteristics at particular spectra, peak absorbance of each gas can be easily observed within the IR region.

Therefore, a correlation between the variable gas concentration level and the variables peak absorbance and spectral response area within the IR region has been demonstrated; and this correlation is used to develop a fuzzy logic estimation model, as explained below.

4.3 Fuzzy Logic Model Development

Fuzzy logic is used in modelling non-linear or complex systems based on the linguistic fuzzy “IF-THEN” rule [158]. Fuzzy logic system architecture comprises fuzzification, membership functions (MF), a fuzzy inference engine, fuzzy rules, and defuzzification [159]. The input variables in truth values are converted into different MFs based on each one’s value in fuzzification; after which the inference engine combines all MFs and interpret the information based on fuzzy rules to derive the fuzzy output that is determined using mean of maximum or centre of gravity methods [158].

For the present study, six fuzzy logic models were developed to map the correlation between various fault gases’ (CO, CO₂, CH₄, C₂H₂, C₂H₄, C₂H₆) concentration levels as an output; with the peak absorbance and spectral response area of the transformer oil as input variables. The proposed fuzzy logic models were built using the graphical user interface tool box provided by MATLAB. The development of the fuzzy model for CO concentration is described in detail below. The same procedure was used to develop the fuzzy logic models for the other gases using the relevant parameters.

The input variables to the fuzzy logic model to estimate the gas concentration dissolved in the transformer oil sample for CO are: the peak absorbance level at 2178cm⁻¹ and the spectral response area in the range of 2250-2000cm⁻¹ (as per Fig. 4-3). Spectral response area of transformer oil for CO can be calculated as:

$$Area = \int Abs \times d\lambda \quad (4-2)$$

where *Abs* is the peak absorbance at particular wavelength, and *dλ* is the wavelength interval. The output of the model is the estimated concentration of CO gas dissolved in oil sample in (ppm).

Five MFs of peak absorbance level, named “A1 to A5” and five MFs of spectral response area named “B1 to B5”, were developed based on the CO spectral responses shown in Fig.4-3. The output variable (estimated CO concentration in ppm) is represented by eight Gaussian MFs, named F1 to F8, as shown in Fig. 4-13. Fuzzy logic rules in the form of “IF-AND-THEN” were developed to correlate input and output parameters based on the correlation between spectral response parameters (peak absorbance and area) and CO concentration, as previously shown in Fig.4-3. This correlation was mapped using 16 developed fuzzy logic rules, as shown in Fig. 4-14. The developed fuzzy rules are given in Appendix F. The model was tested for input parameters, 0.0142 peak absorbance and a spectral response area of 2.36 that provided an output 128ppm of CO concentration.

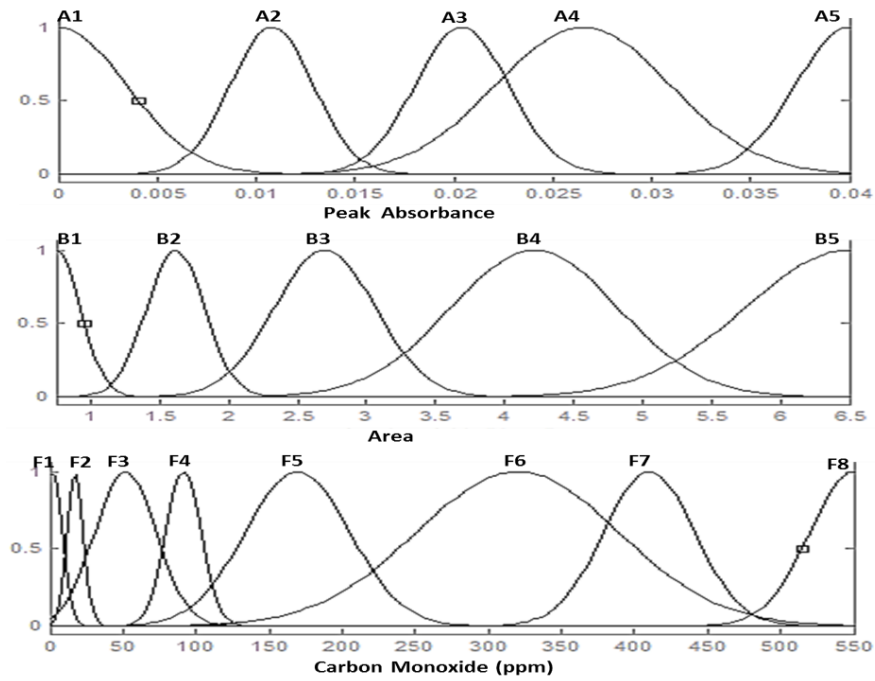


Figure 4-13 Input and output variables' MFs for CO fuzzy model

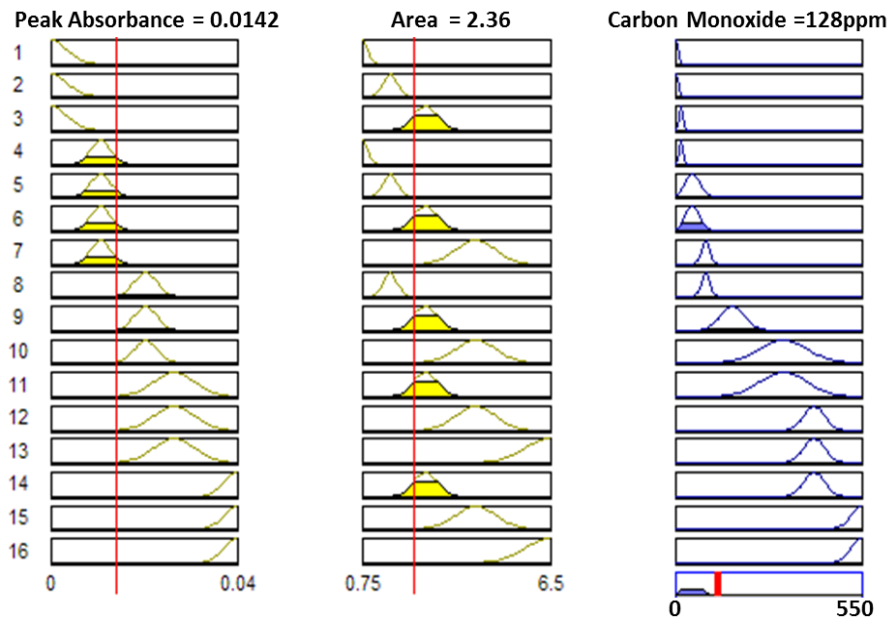


Figure 4-14 Developed fuzzy rules for CO estimation

This output is consistent with the correlation of CO concentration, peak absorbance and spectrum area as shown in Fig.4-3. Therefore, it should be possible for CO concentration for any set of input data to be estimated using the surface graph shown in Fig.4-15.

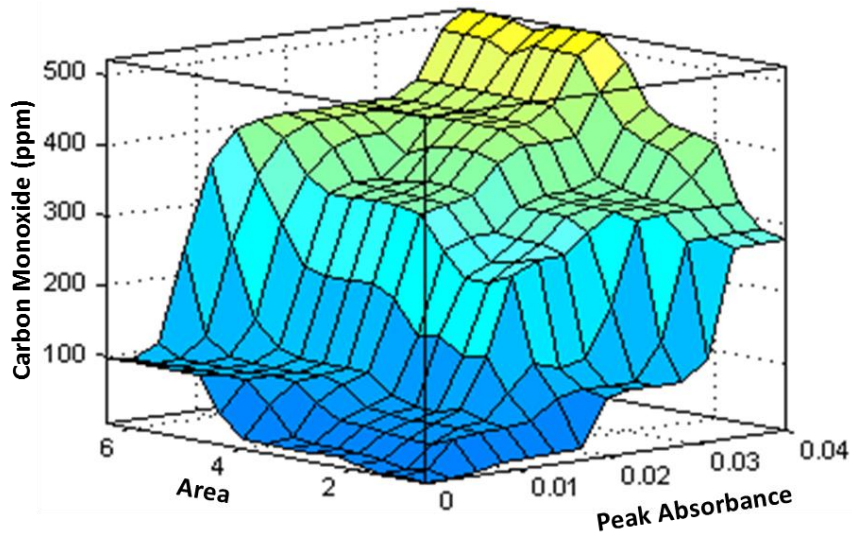


Figure 4-15 CO estimation surface graph

Another set of fuzzy rules correlates the peak absorbance at 2360cm^{-1} and spectrum area within $2400\text{-}2250\text{cm}^{-1}$ region, in accordance with Fig. 4-5; and this was developed to estimate the CO_2 concentration. Membership functions for peak absorbance and spectrum area were considered on the scale 0 to 0.25, and 0 to 13, respectively, as shown in Fig. 4-16. The output variable; CO_2 concentration, was set to be in the range 200 to 5200ppm.

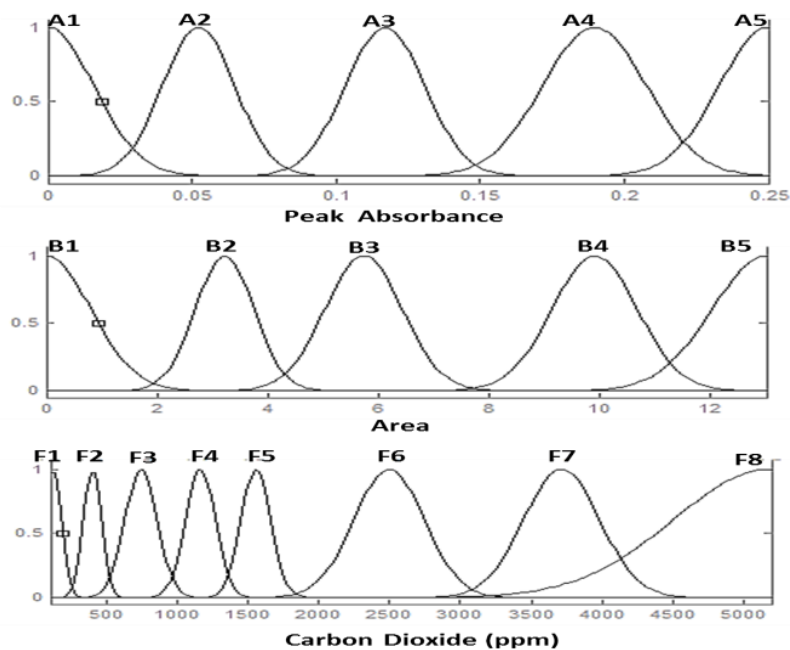


Figure 4-16 Input and output variables' MFs for CO_2 fuzzy model

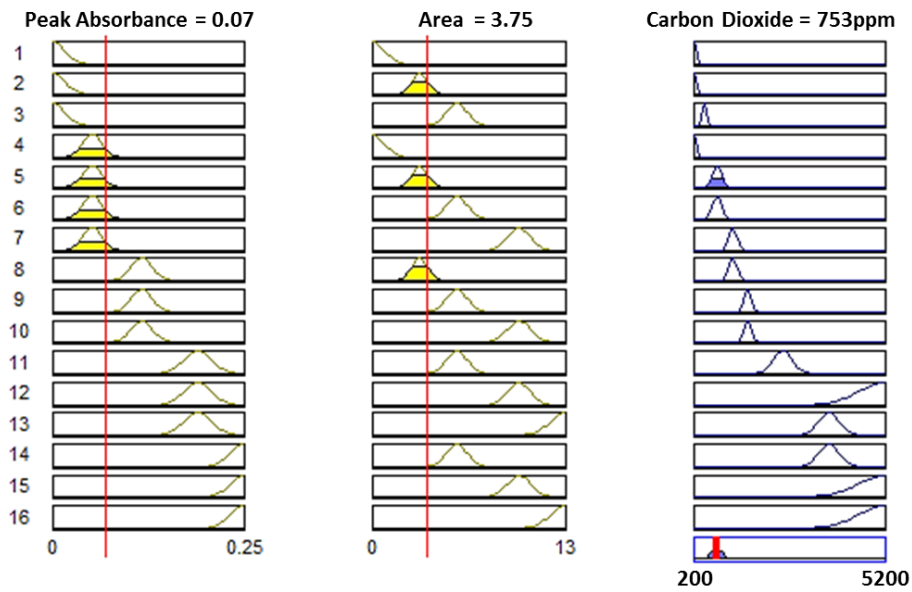


Figure 4-17 Developed fuzzy rules for CO₂ estimation

This correlation was mapped using 16 developed fuzzy logic rules as shown in Fig. 4-17. The model was tested for input parameters, 0.07 peak absorbance and a spectral response area of 3.75 that provided an output 753ppm of CO₂ concentration. This output is consistent with the correlation of CO₂ concentration, peak absorbance and spectrum area as shown in Fig.4-5. The surface graph mapping this correlation is shown in Fig.4-18.

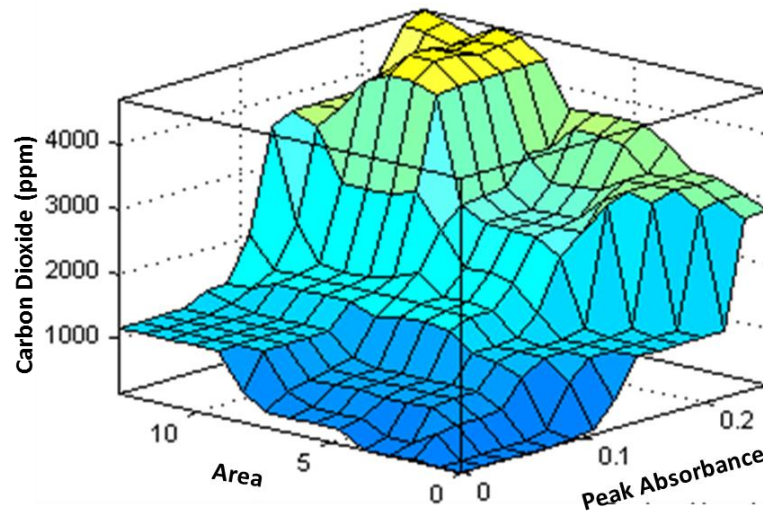


Figure 4-18 CO₂ estimation surface graph

A set of fuzzy rules to estimate CH₄ concentration in oil based on peak absorbance at 2923cm⁻¹ and spectral response area within the 3200-2731cm⁻¹ region was developed in accordance with Fig.4-7. Membership functions for peak absorbance and spectral response area were considered on the scales 0 to 2.25, and 0 to 280, respectively, as shown in Fig. 4-19. The CH₄ concentration was set to be in the range 0 to 400ppm.

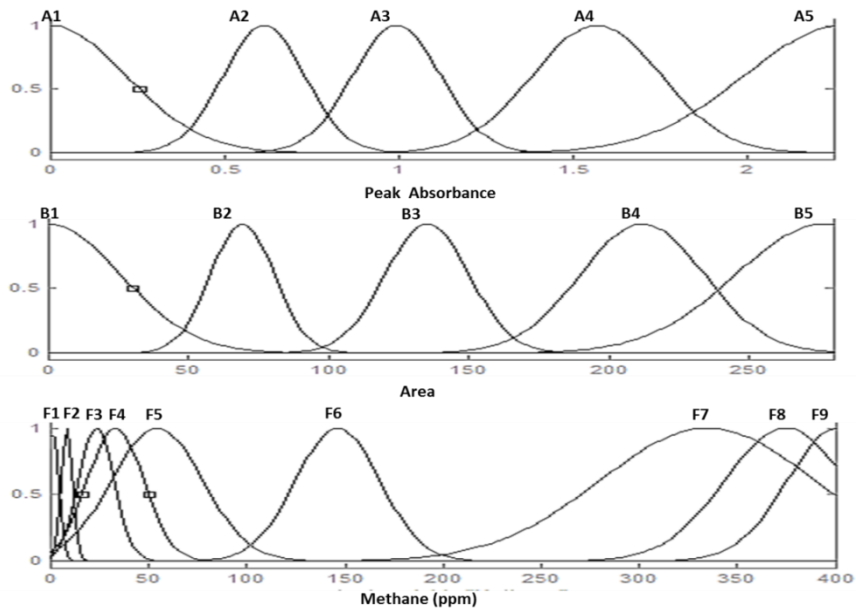


Figure 4-19 Input and output variables' MFs for CH₄ fuzzy model

This correlation was mapped using 16 developed fuzzy logic rules, as shown in Fig. 4-20. The model was tested for input parameters, 1.19 peak absorbance and spectral response area of 223 that provided an output 154ppm of CH₄ concentration. This output corresponds to the correlation of CH₄ concentration, peak absorbance and spectrum area as shown in Fig.4-7. This correlation is represented in a 3D graph in Fig. 4-21.

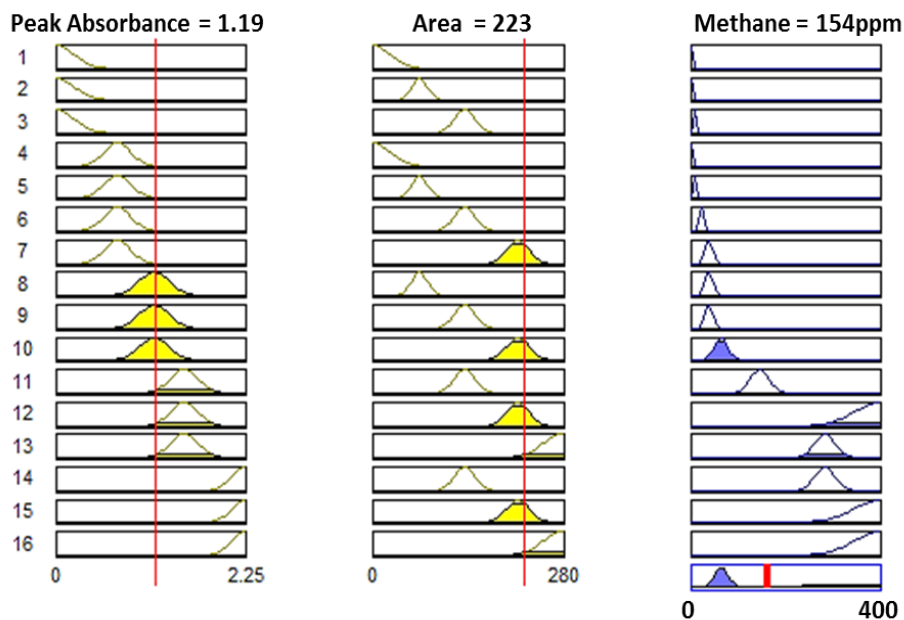


Figure 4-20 Developed fuzzy rules for CH₄ estimation

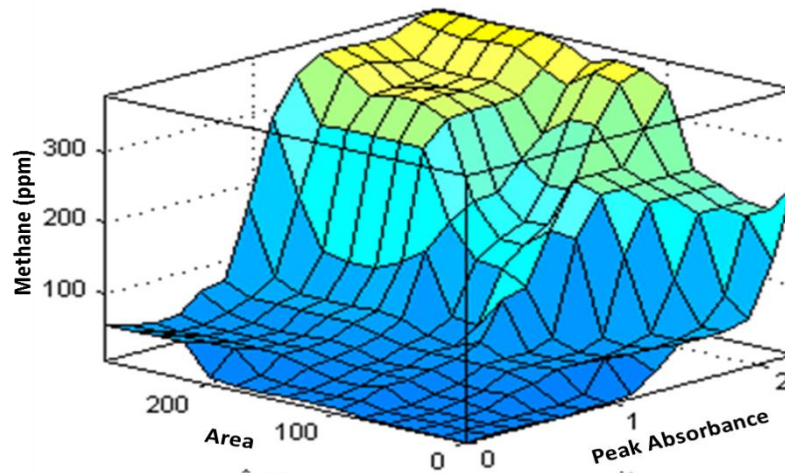


Figure 4-21 CH₄ estimation surface graph

The inputs to the C₂H₂ fuzzy estimation model are the peak absorbance at wavenumber 1376cm⁻¹ and the spectral response area within 1400-1300cm⁻¹. Input variable MFs were considered on the scale 0.1 to 1.2 and 0.9 to 13 for peak absorbance and area, respectively, as shown in Fig. 4-22. The C₂H₂ concentration was set in the range 0 to 400ppm.

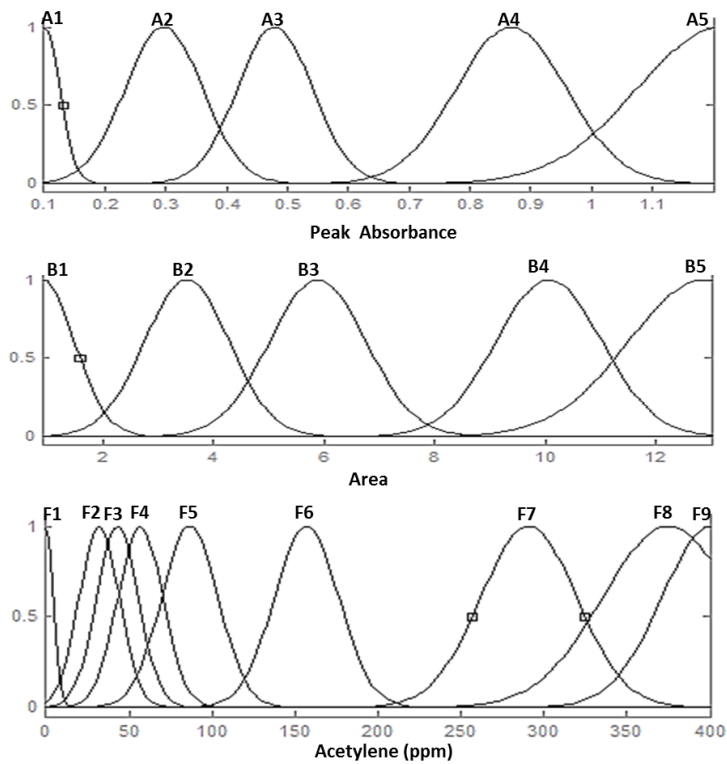


Figure 4-22 Input and output variables' MFs for C₂H₂ fuzzy model

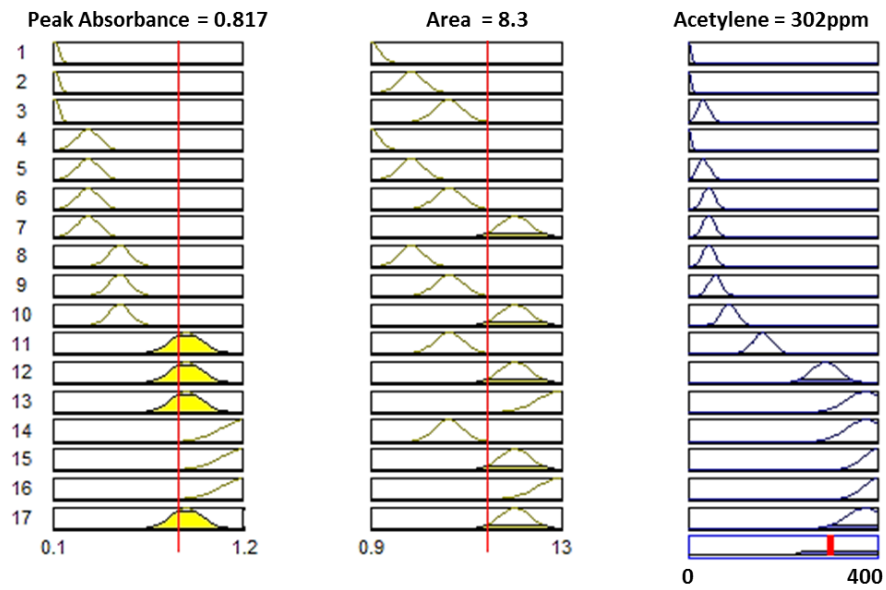


Figure 4-23 Developed fuzzy rules for C₂H₂ estimation

A set of fuzzy rules relating the input and the output variables for this model was developed in accordance with the results in Fig.4-9. This correlation was mapped using 17 developed fuzzy logic rules, as shown in Fig. 4-23. The model was tested for input parameters, 0.817 peak absorbance and a spectral response area of 8.3 that provided an output 302ppm of C₂H₂ concentration.

This output corresponds to the correlation of C₂H₂ concentration, peak absorbance and spectrum area as shown in Fig.4-9. This latter correlation is represented in the 3D graph Fig. 4-24.

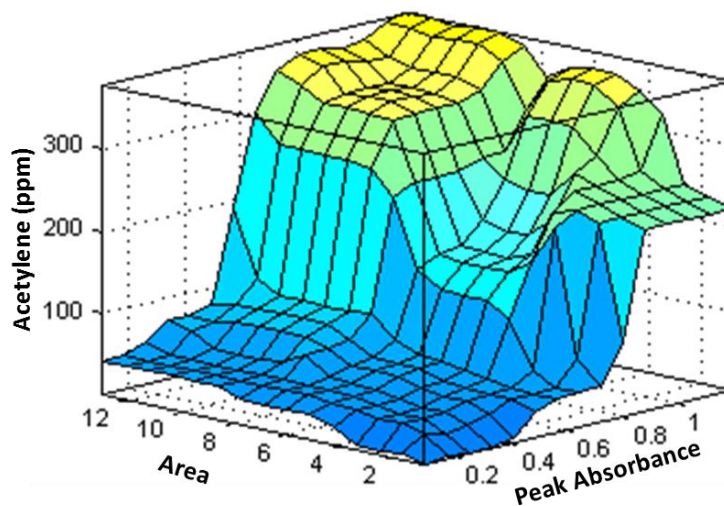


Figure 4-24 C₂H₂ estimation surface graph

The C₂H₆ fuzzy estimation model was developed using the spectral response peak absorbance at 1473cm⁻¹ and spectral response area in the range 1500-1400cm⁻¹. The MF of peak absorbance and spectrum area were considered on the scale 0.1 to 1.2, and 0.3 to 4.5, respectively; while the output was considered on the scale 0 to 350ppm, as shown in Fig. 4-25. The correlation developed by the fuzzy rules is as shown in Fig.4-26.

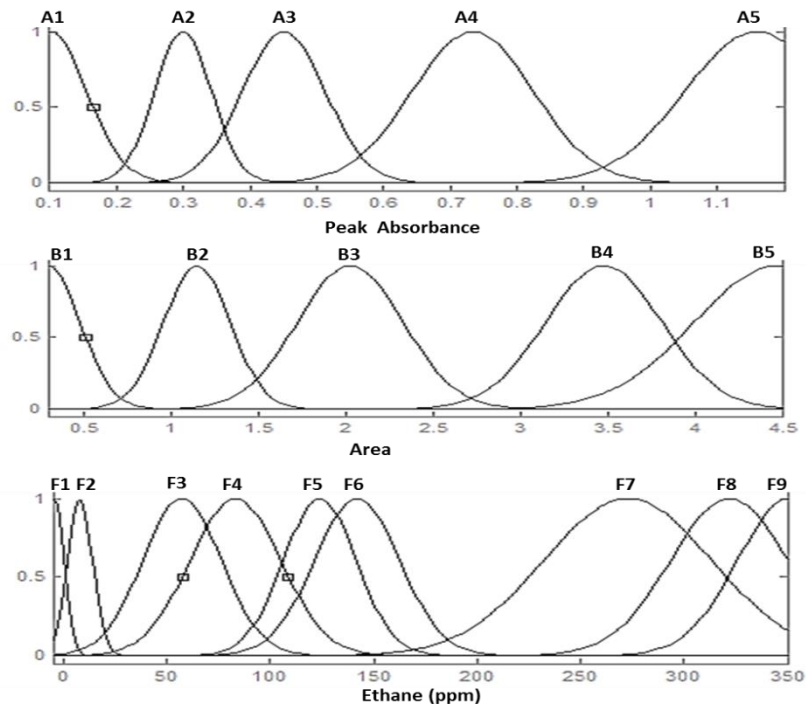


Figure 4-25 Input and output variables' MFs for C₂H₆ fuzzy model

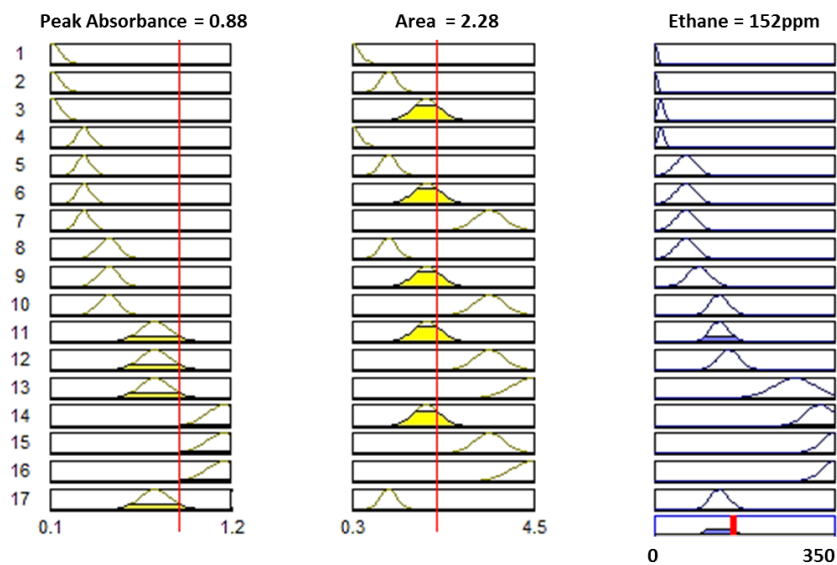


Figure 4-26 Developed fuzzy rules for C₂H₆ estimation

This correlation for C_2H_6 variables was mapped using 17 developed fuzzy logic rules. The model was tested for input parameters, 0.88 peak absorbance and a spectral response area of 2.28 that provided an output 152ppm of C_2H_6 concentration. This output corresponds with the correlation of C_2H_6 concentration, peak absorbance and spectrum area, as shown in Fig.4-11. This latter correlation is represented in the 3D graph, Fig. 4-27.

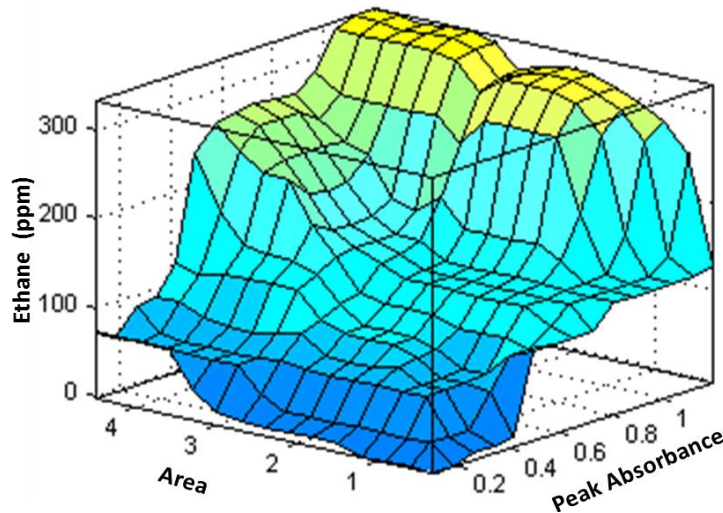


Figure 4-27 C_2H_6 estimation surface graph

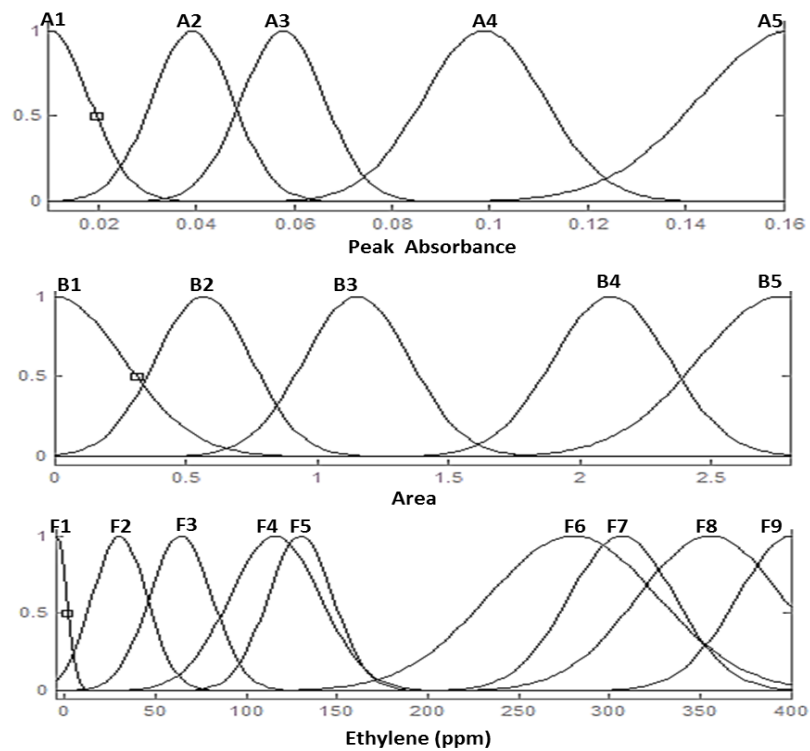


Figure 4-28 Input and output variables' MFs for C_2H_4 fuzzy model

The fuzzy logic to estimate C₂H₄ concentration in oil was developed based on the peak absorbance at 966cm⁻¹ and area within the range 1000-900cm⁻¹ as inputs to the model where MF of peak absorbance and spectral response area were considered on the scale 0.01 to 0.16 and 0 to 2.8, respectively, as shown in Fig. 4-28. The output of the model was considered on the scale 0 to 400ppm.

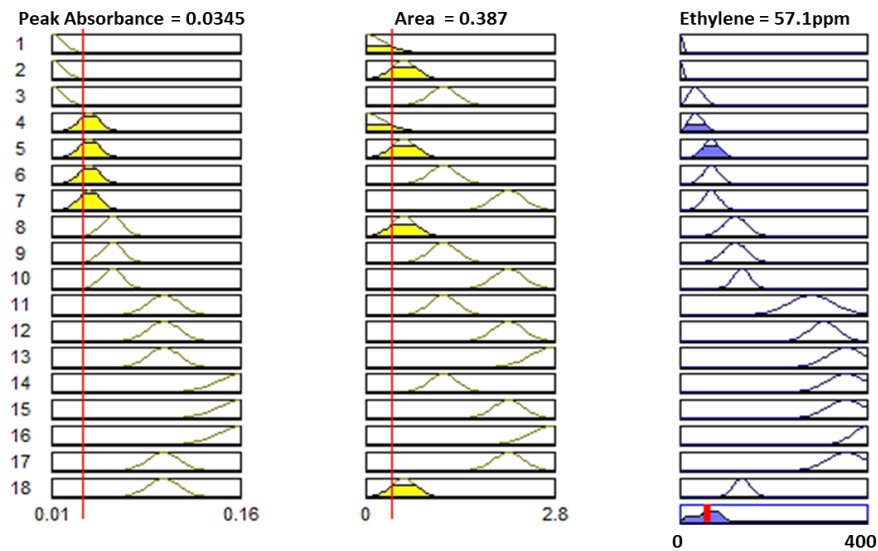


Figure 4-29 Developed fuzzy rules for C₂H₄ estimation

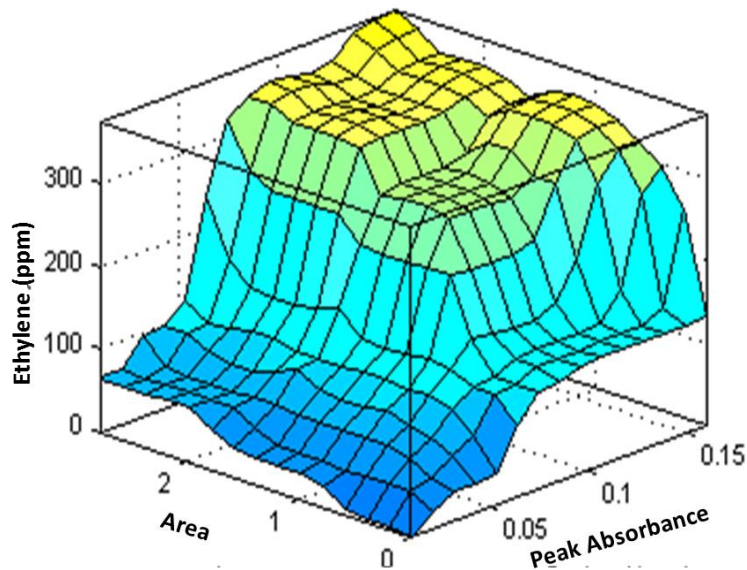


Figure 4-30 C₂H₄ estimation surface graph

This correlation for C₂H₄ was mapped using 18 developed fuzzy logic rules as shown in Fig. 4-29. The model was tested for input parameters, 0.0345 peak absorbance and a spectral response area of 0.387 that provided an output of 57.1ppm of C₂H₄ concentration.

This output corresponds with the correlation of C₂H₄ concentration, peak absorbance and spectrum area as shown in Fig.4-12. The C₂H₄ concentration for any set of input variables could be estimated through the 3D surface graph shown in Fig. 4-30. The proposed overall fuzzy logic estimation model for all gases is shown in Fig.4-31.

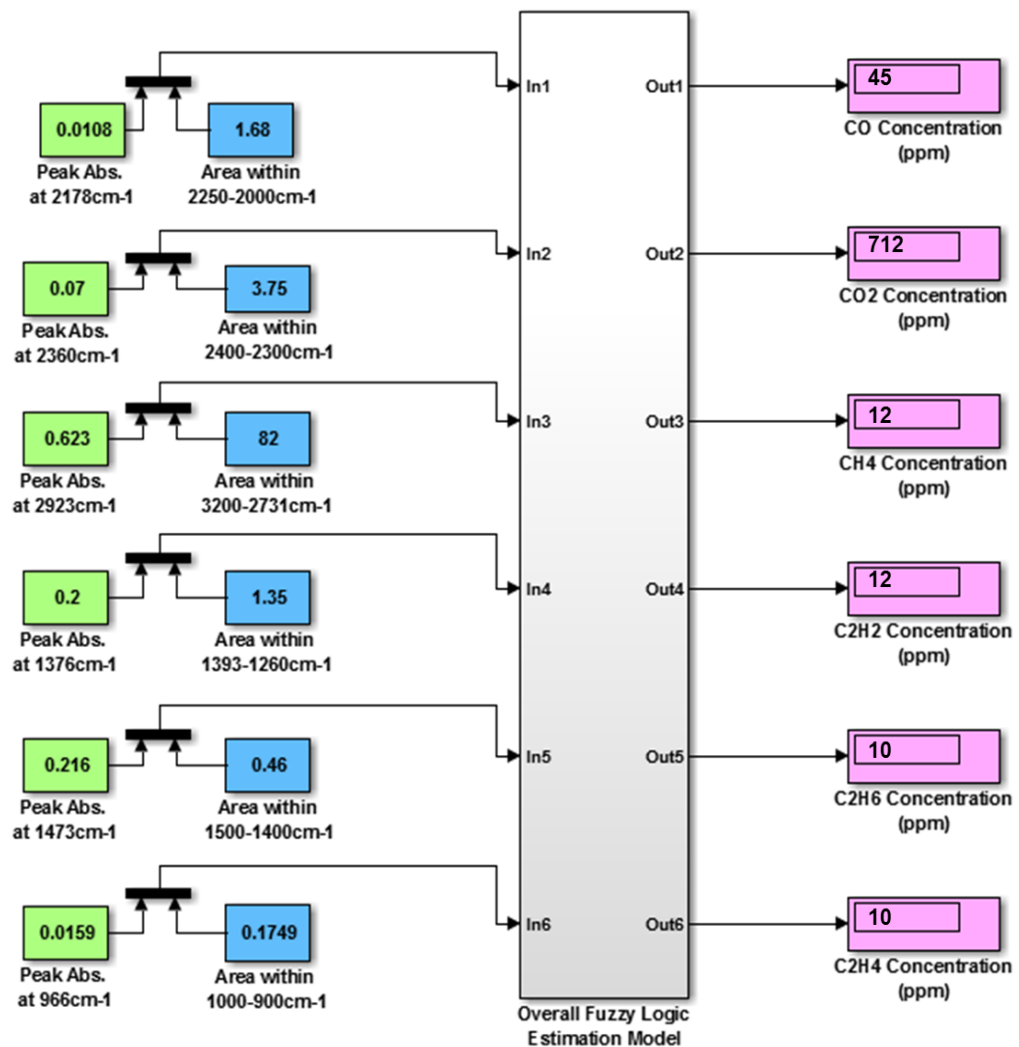


Figure 4-31 The proposed overall fuzzy logic estimation model

4.4 Accuracy Analysis

Twenty oil samples that were collected from various transformers of different ratings, life span and operating conditions were used to examine the accuracy of the proposed dissolved gases fuzzy logic estimation model. DGA using GC was performed on each oil sample to accurately quantify the concentration of dissolved gases in the collected samples. Absorption Spectral responses for the same oil samples were then measured within the wavenumber range 12,000cm⁻¹ to 667cm⁻¹ (NIR to IR band).

The peak absorbance and area of oil spectral response at designated wavenumber ranges were extracted and provided to the developed fuzzy logic estimation model. The estimated gas concentration value was compared with the actual value of gas concentration obtained using GC as shown in Table 4-2. As can be seen in Table 4-2, the fuzzy logic model provides a gas concentration that is very close to the measured value using the GC technique. The root mean square error (RMSE) between gas concentration using GC, \hat{Y} and estimation concentration by the fuzzy model, Y is given by:

$$RMSE = \sqrt{\frac{\sum_{i=1}^n (\hat{Y}_i - Y_i)^2}{n}} \quad (4-2)$$

where n is the total number of samples.

On the other hand, the mean absolute percentage error (MAPE) between GC concentration and fuzzy model estimated value can be calculated as:

$$MAPE = \frac{\sum_{i=1}^n \left| \frac{\hat{Y}_i - Y_i}{\hat{Y}_i} \right|}{n} \times 100 \quad (4-3)$$

RMSE and MAPE for the investigated 20 oil samples for all six gases are shown in Table 4-2, where the maximum RMSE and MAPE for the proposed model were less than 4 and 3%, respectively. A brief comparison between the proposed NIR-IR spectroscopy method and the existing GC, hydrogen on-line monitor and PAS techniques is given in Table 4-3.

4.5 Conclusion

Objective 2 of this thesis proposed a new technique to estimate the concentration of dissolved fault gases in transformer oil using NIR-IR spectroscopy. Experimental results show that six fault gases can be identified using spectroscopy within the spectrum range 7000cm^{-1} to 667cm^{-1} . Each gas will have a dominant impact on the oil spectral response within a particular spectrum range without overlapping with the effects of other gases.

The results show that a strong correlation exists between each gas concentration and its spectral response parameters; namely, peak absorbance and area at particular band. The fuzzy logic models that were developed to map these correlations can estimate the dissolved gas concentration in transformer oil with a high degree of accuracy.

The results suggest the superiority of this study's proposed technique over the current gas chromatography measurement technique due to its ability to be conducted instantly on site without the need for trained personnel. Also, unlike the gas chromatography technique, the proposed technique in this study incurs only negligible running costs, and can be readily implemented on-line for continuous monitoring of the transformer oil condition. Moreover, the proposed technique can also be used to estimate other condition monitoring parameters such as the oil interfacial value, the furan content, moisture level, and the additive and contamination level in transformer oil.

Table 4-2 Comparison between actual (GC) and estimated (fuzzy model) gas concentration for 20 oil samples

Sample No.	Carbon Monoxide		Carbon Dioxide		Methane		Acetylene		Ethane		Ethylene	
	Actual (GC)	Estimate (Fuzzy)	Actual (GC)	Estimate (Fuzzy)	Actual (GC)	Estimate (Fuzzy)	Actual (GC)	Estimate (Fuzzy)	Actual (GC)	Estimate (Fuzzy)	Actual (GC)	Estimate (Fuzzy)
1	60	58.8	304	304.1	36	36.4	65	65.1	118	114.3	90	87.2
2	66	66.5	332	330.3	3	3.0	0	0.0	22	22.9	8	8.3
3	231	221.8	2500	2505.3	18	17.9	33	34.0	65	66.2	45	45.8
4	512	505.3	2705	2701.5	20	20.6	6	6.2	10	10.2	1	1.0
5	388	390.7	2991	2996.4	21	22.3	12	11.9	10	10.1	2	2.0
6	8	8.2	464	464.4	8	8.0	10	10.1	72	70.6	132	130.9
7	140	141.4	786	779.7	2	2.1	0	0.0	0	0.0	30	31.3
8	448	444.4	4107	4102.9	157	155.6	233	228.3	30	30.0	11	10.9
9	52	54.2	714	714.9	4	4.2	0.5	0.5	175	172.7	7	7.4
10	60	59.4	903	905.9	26	26.0	35	34.7	231	232.6	55	53.6
11	44	46.5	1141	1140.7	5	5.1	0	0.0	312	321.4	6	6.1
12	36	33.8	1824	1833.1	7	6.9	3	3.0	334	334.0	5	5.3
13	41	40.2	1989	1989.6	17	17.2	30	31.7	397	402.6	50	51.8
14	287	291.3	2187	2192.0	110	107.3	48	45.1	106	106.4	39	39.4
15	36	36.3	1728	1728.2	80	81.7	112	114.2	48	49.9	74	73.4
16	306	301.1	1751	1749.6	70	73.5	45	45.7	80	81.4	145	146.5
17	131	133.0	373	373.7	15	15.5	0	0.0	28	26.1	48	48.8
18	188	190.1	1021	1017.9	146	147.6	38	37.7	111	112.6	86	79.1
19	466	469.7	1068	1067.9	49	49.7	17	17.7	100	97.9	4	3.9
20	126	123.7	1334	1330.1	211	213.0	173	173.0	112	113.6	270	280.8
RMSE	3.46		3.69		1.31		1.41		2.85		3.03	
MAPE(%)	2.08		0.207		2.11		2.52		1.97		2.85	

Table 4-3 Comparison of GC, hydrogen on-line monitor, PAS and the proposed spectroscopy methods

Method	GC	Hydrogen On-line Monitor	PAS	NIR-IR Spectroscopy
Test method	<ul style="list-style-type: none"> -A trained person is required to prepare the oil sample and conduct the measurement. -Measurement must be conducted in a laboratory environment with a lot of standards that have to be followed and is time consuming. -There is no possibility of on-line monitoring. 	<ul style="list-style-type: none"> -Can be implemented on-line. - Unable to provide the concentration of all fault gases as it can only detect H₂, CO, C₂H₂, and C₂H₄. -Accuracy is influenced by the ambient temperature and detection sensitivity of the membrane sensor used in the measurement. 	<ul style="list-style-type: none"> -Can be implemented on-line. -Accuracy is influenced by external temperature and pressure and is also affected by vibration. - Unable to detect H₂. - Mechanical rotating control (optical filter and chopper) is subject to high probability of fault for long operational time. 	<ul style="list-style-type: none"> -A trained person is not required to conduct the measurement. -Measurement can be conducted instantly on site and could be implemented on-line. -Can be used to monitor other parameters such as paper degradation, (furan), interfacial tension, moisture, oxidation products, additives and contamination in oil. -Accuracy is influenced by the ambient temperature so is unable to detect H₂.
Price of Equipment	-From US\$80,000 (depending on model and extraction method used).	- From US\$13,000 (depending on model).	-From US\$20,000 (depending on PAS features).	-From US\$10,000 (depending on spectrophotometer features).
Running costs	-US\$150 to US\$180 per sample (transportation cost is not included).	-Negligible.	-Negligible.	-Negligible.

Chapter 5 Power Transformer Asset Management and Remnant Life

5.1 Introduction

This chapter addresses Objective 3 of the thesis: Developing an expert model to estimate the remnant life and asset management decision of power transformers based on routine insulating oil tests.

Statistics show that the bulk of power transformer fleets within developed countries such as United States, United Kingdom, and Australia are approaching or have already exceeded their design lifetimes as they were installed prior to 1985 [8]. With the current global economic crisis, the mindset within the electricity utility industry is centered on getting the most usage out of existing equipment rather than installing replacements. An aging population of large power transformers requires more reliable monitoring systems and diagnostics to detect incipient faults, and to provide an efficient predictive maintenance plan that can extend the operational life of the asset and minimise the possibility of catastrophic failures [38].

Several papers investigating the correlation between some condition monitoring parameters such as furan, dissolved gases, water content, and temperature with the transformer's remnant life using mathematical-based approaches can be found in the literature [55, 59, 111, 138]. However, due to the complexity in developing a mathematical model for such a non-linear problem, researchers have limited their models to only one or two parameters without giving attention to all the accelerating aging factors, thereby risking making an incorrect estimation for the transformer's remnant life [160]. IEEE Std. C57.91-2011 [161] and IEC Standard 60076-7 [162] proposed mathematical models to estimate a transformer's remnant life based on hot-spot temperature within the transformer. Two other parameters: water content in paper and dissolved oxygen in oil, are considered in one proposed remnant life mathematical-based model [42]. A further two parameters; 2-furfural (2-FAL) concentration in oil, and the degree of polymerization (DP) of paper insulation which reflects the remaining life of solid insulation and hence a transformer have also been found to correlate [59].

In addition to the inaccuracy of these mathematical-based models due to neglecting other key parameters that contribute to transformer aging, the validity of measurements using the proposed parameters in these models such as hot spot temperature and water content in paper is questionable.

To overcome the limitations of mathematical-based approaches in estimating transformer remnant life, some models based on artificial intelligence (AI) have been developed. An AI-based model using gene expression programming (GEP) and dissolved gas analysis (DGA) parameters was developed to identify the criticality of power transformer and asset management [25]. Also, another study proposed a fuzzy logic-based model using furan and carbon oxides to assess the transformer ageing condition [163].

Although more condition monitoring parameters have been considered in AI-based models, none of the proposed models considered all of the key factors affecting the transformer life, such as rise in operating temperature, oxygen level, and water content in paper. Moreover, most of the existing transformer remnant life estimation models were developed without incorporating a reliable asset management decision model. An AI-based asset management model was developed using expert machine learning and three condition monitoring parameters; DGA, polarization and depolarization current (PDC), and dielectric frequency domain spectroscopy (FDS) [164]. However, the parameters (PDC and FDS) used by this model are not regularly measured through transformer's routine inspections.

A transformer remnant life and asset decision fuzzy logic model was proposed [165], which considered several condition monitoring parameters such as partial discharge (PD), leakage reactance, dielectric dissipation factor (DDF), and frequency response analysis (FRA); however, the model cannot be implemented online as several input parameters can only be measured offline. Moreover, not all parameters required by the model, such as FRA, are available during routine inspection of transformers. Statistical analysis for transformers' failure-rate population is used in [166], [167] to estimate the transformer remaining life based on analytical model. However, this approach is affected by various environmental conditions and maintenance procedure which reduce the accuracy of the developed estimation model.

Another approach to assess transformer condition using a health index (HI) or a score table is proposed in [12, 168]. The HI-based technique is developed based on a pre-defined weighting factor for each parameter and uses historical data which calls for expert personnel. This means results from HI-based techniques can be inconsistent when developed by various experts and used by various utilities [169].

This thesis proposes a new fuzzy logic approach that utilizes data gathered mainly from insulating oil routine assessment such as furan, DGA, interfacial tension (IFT), water content, and operating temperature in evaluating the remnant life and health condition of power transformer.

The key advantage of the proposed model in this paper over previously published models is that all input parameters proposed in the model can potentially be measured on-line or on-site which facilitates a proper and timely maintenance action based on the model output [21, 137, 151, 155, 170]. The model also considers the rate of increase of key parameters that significantly affect transformer health condition, such as 2-FAL, carbon monoxide (CO), and IFT. The generation rate of furan's derivatives in transformer oil have been found to be more important in identifying paper health condition than its absolute level [55]. The CO increment rate in insulating oil along with the CO₂/CO ratio provide valuable information about paper degradation activity [28]. On the other hand, the IFT decrement rate has been found to be more effective than the oil acid number increment rate in identifying oil contamination criticality [171].

5.2 Transformer Health Condition

The quality of the insulation system within power transformers that comprises dielectric insulation paper and oil reflects the overall health condition of the transformer. The combination of heat (pyrolysis), moisture (hydrolysis) and air (oxidation) within operating transformers cause oil and paper decomposition which result in a number of gases that relates to the cause and effect of various faults [8]. Faults such as overheating, partial discharge and sustained arcing produce a range of gases such as hydrogen (H₂), methane (CH₄), acetylene (C₂H₂), ethylene (C₂H₄), and ethane (C₂H₆) that dissolve in insulating oil and can be quantified using DGA. The concentration of these gases in transformer oil can aid in identifying the criticality level of the transformer health condition [137].

Chemical products such as carbon oxides and furan derivatives are formed due to paper insulation degradation and can be detected through dissolved gas in oil and furan analyses, respectively. As transformer operational life is strongly correlated to the age of paper insulation, carbon oxides and furan in oil are widely used as indicators to predict the transformer remnant life and paper aging criticality [138]. However, any oil treatment will eliminate carbon oxides and furan contents, hence limiting the reliability of these gases in estimating the transformer's remaining life [38]. It takes approximately 3 years for furan concentration to retain its original value before oil reclamation [110].

High operating temperature, water content in paper and oxygen dissolved in oil accelerate the degradation of paper insulation. Studies show that the rate of aging of a transformer with a high level of oxygen (above 16,500ppm) and wet paper insulation is 40 times the aging rate of a similar transformer with a low level of oxygen (below 7000ppm) and dry paper insulation [111]. Additionally, the transformer's remnant operational life is halved for every 6 to 8°C increment of the operating temperature [161, 162].

On the other hand, the quality of insulating oil influences the performance and the service life of the transformer [10]. During the oil aging process, oil gets contaminated with dissolved decay products such as organic acids, peroxides, aldehydes, and ketone formed as a result of the chemical reaction between mineral oil molecules and oxygen dissolved in oil [106]. The acids formed due to this oxidation process attack the metal tank, forming sludge that reduces the dielectric strength of the oil. Meanwhile, the acids also attack the cellulosic chain of the paper, causing accelerating insulation degradation [12]. Sludge and contamination development in insulating oil can be identified by measuring the IFT value of the oil. Oil is considered severely contaminated and sludge is expected to increase when the IFT value drops to 22mN/m [12].

DGA, Furan analysis, water content, and IFT are normally performed during routine transformer inspection. Conventionally, these analyses are conducted in a laboratory environment. Recently, several analytical techniques have been developed which allowed these parameters be measured on-line or on-site. Dissolved gases in insulating oil can be measured on-line by using Photo-Acoustic Spectroscopy (PAS) or a hydrogen on-line monitoring [137].

Meanwhile, the use of UV-Vis spectroscopy to measure the Furan (2-FAL) concentration and the IFT value of the transformer oil, which can be performed on site and has the potential to be implemented on-line, has been proposed by Abu-Siada, Lai and Islam (2012) [21] and Bakar, Abu-Siada, Islam and El-Naggar (2015) [155]. Instead of using the Karl Fischer titration technique to measure water content in oil, Martin, Perkasa and Lelekakis (2013) [170] proposed the use of water-activity probes immersed in transformer oil to measure the water concentration.

Table 5-1 summarizes the parameters used for the asset management and remnant life model proposed for Objective 3 of this thesis.

Table 5-1 Proposed parameters for transformer remnant life and asset management decision model

Category	Parameters
Remnant Life Estimation	Furan, Water Content, Oxygen, Operating Temperature Rise
Paper Aging Criticality	Furan, Carbon Oxides
Faults Criticality	Fault gases (CH ₄ , C ₂ H ₂ , C ₂ H ₄ , C ₂ H ₆)
Contamination Criticality	IFT
Relative Accelerated Aging Criticality	Water Content, Oxygen, Operating Temperature Rise

5.3 Proposed Approach

An asset management decision model was designed as proposed in the flow chart of Fig.5-1. Four criticalities comprising faults criticality, paper aging criticality, contamination criticality, and relative accelerating aging are examined to allow a proper maintenance action on the transformer. As shown in Fig.5-1, the faults criticality is examined based on DGA data to determine the health condition of the transformer which accords with IEEE Std. C57.104 guidelines [28]. If the faults criticality check is positive, further analyses on individual dissolved gases are to be performed to find the fault causes. The condition of paper insulation is examined through the furan and carbon oxides data in accordance with the guidelines reported in [12].

If paper aging is found to be critical, the trend of increases of the critical factor is to be monitored through observing the increment of the monitored parameters per a particular period that depends on the significance of the measured parameters, and operational load reduction is recommended. The contamination level in oil is to be examined through the IFT value, as recommended in the IEEE Std. C62-1995 [11]. If the contamination level is found to be critical, oil is recommended for reclamation.

The relative accelerated aging factor is examined through transformer operating temperature, water content in paper and oxygen in oil. If this factor is found to be critical in accordance with [12], oil is recommended for rehabilitation through oil degassing or dry-out. In cases where all investigated criticality factors are normal, the transformer is reported as healthy and is to be scheduled for the next routine inspection.

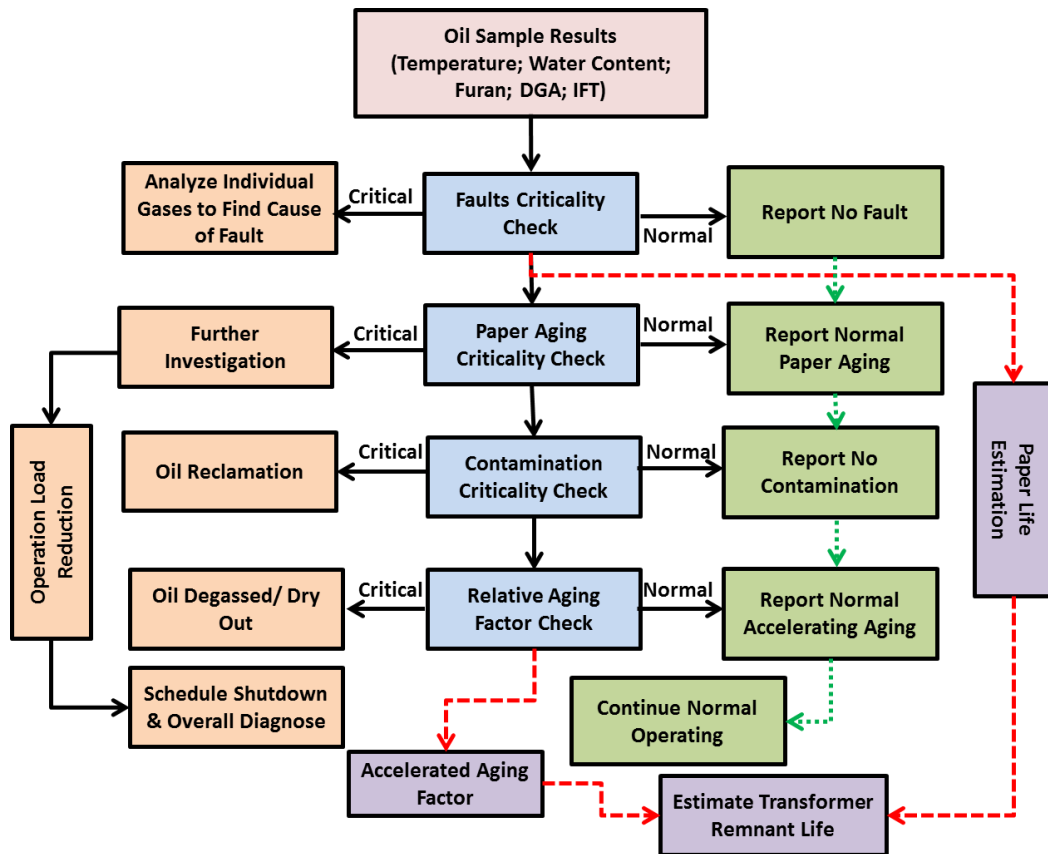


Figure 5-1 Flow chart of the proposed approach

Paper aging criticality is used to estimate the remaining operational life of paper insulation in accordance with the recommendation published in [12]. Accelerated aging factor is determined by relative accelerated aging factor criticality as presented in [106]. Transformer remnant life is obtained by integrating the estimated paper remaining life and accelerated aging factors, as shown in Fig.5-1.

5.4 Fuzzy Logic Model Development

A fuzzy logic model to implement the flow chart shown in Fig. 5-1 was developed based on the pre-known correlations between paper aging, faults, oil contamination level, and relative accelerating aging factors with transformer health condition and oil maintenance recommendations. A fuzzy decision trees concept was constructed based on a “top-down” method, as shown in Fig.5-2.

The root node of the model is the transformer health condition, while paper aging, faults, contamination criticalities, and relative accelerating aging are the internal nodes. Furan, CO₂/CO ratio, fault gases (CH₄, C₂H₄, C₂H₄, and C₂H₆), IFT, operating temperature, water content in paper, and Oxygen dissolved in oil are the leaf nodes or input variables to the model.

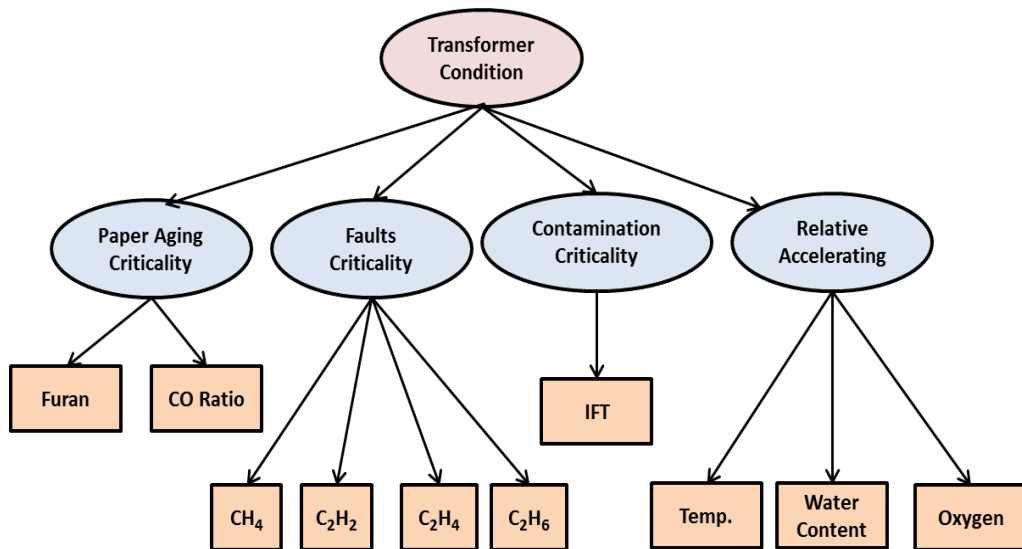


Figure 5-2 Fuzzy decision tree concept

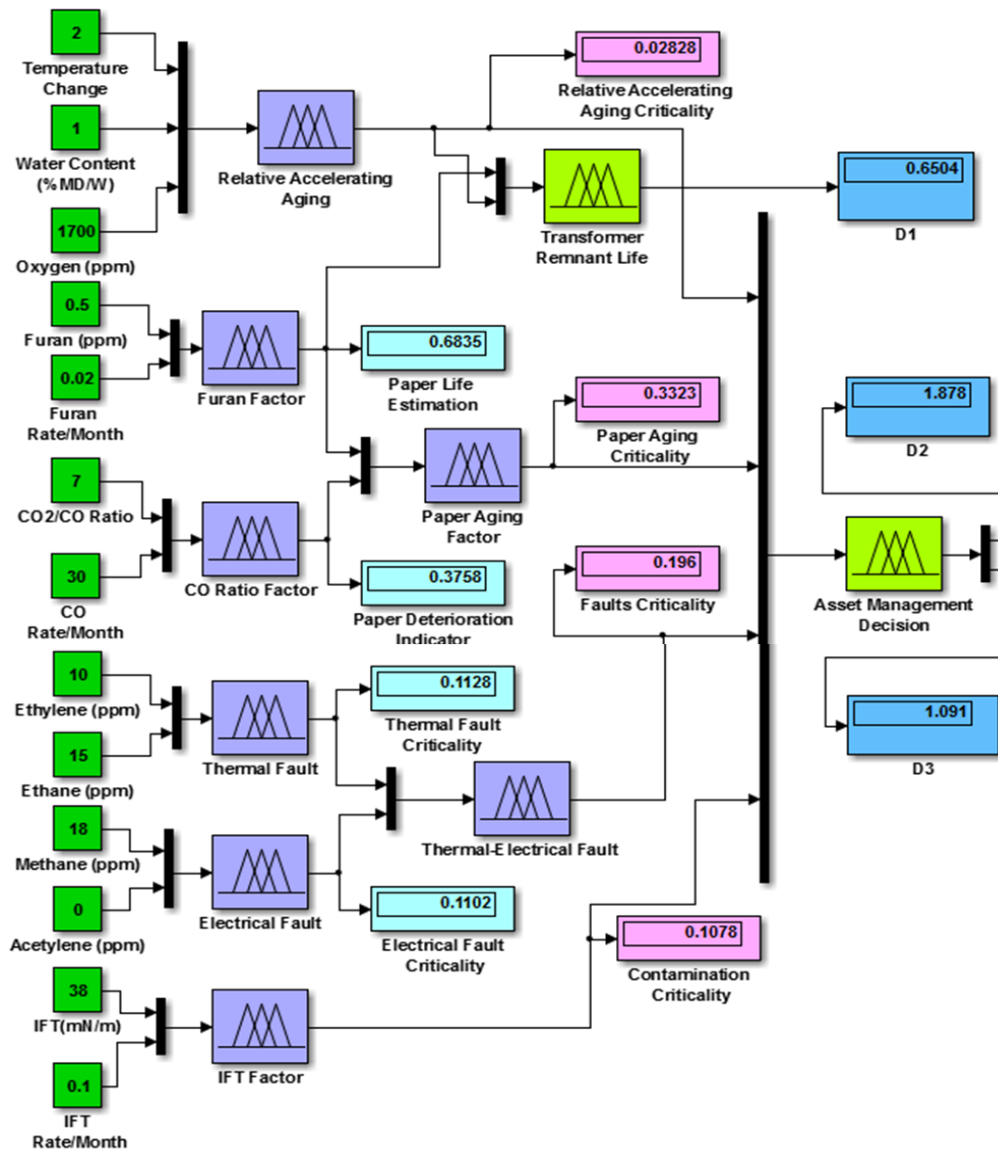


Figure 5-3 Proposed fuzzy logic asset management decision model

The proposed overall fuzzy logic asset management decision model is shown in Fig.5-3. The development of the fuzzy sub-model for the furan factor is described in detail below. The same procedure was used to develop the fuzzy models for the other factors.

5.4.1 Furan Criticality

Furan concentration (2-furfural) is generated by paper degradation, and is normally used to estimate the paper remaining life. A fuzzy model was developed to estimate the paper's remaining life where furan concentration and furan generation rate/month are the inputs to the model in parts per million (ppm) and ppm/month respectively, while the output variable is the estimated paper remaining life which is normalized on a scale 0 to 1, whereas 1 reflects new paper with 100% remaining life, and 0 reflects the end of the paper's life.

There are five membership functions (MF) based on Furan concentration in oil; "Normal", "Moderate", "Accelerated", "Extensive", and "End Life", and five sets based on Furan rate/month named "Low", "Low-Medium", "Medium", "Medium-High", and "High"; these were developed based on the correlation between Furan and paper condition [12], as shown in Fig.5-4. The output is represented by five triangular MFs named "Normal", "Accelerated", "Excessive", "High Risk", and "End Life".

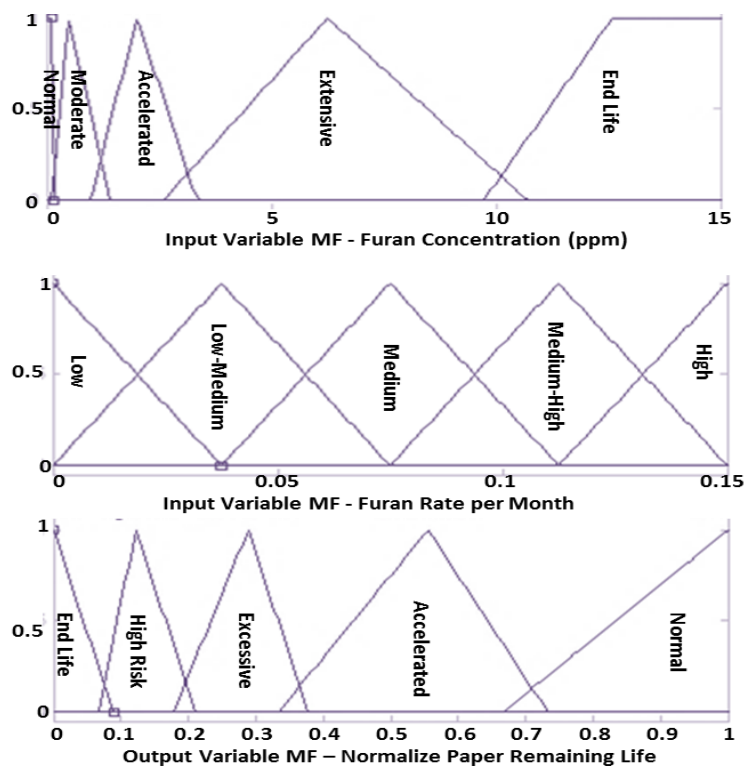


Figure 5-4 Input and output variables' MF for furan fuzzy model

Fuzzy-logic rules in the form of “IF-AND-THEN” were developed to correlate input and output parameters based on the correlation between furan concentration / rate of increment per month and paper remaining life [12], as shown in Fig.5-5 which shows the 25 rules developed to map this correlation.

The model was tested for input parameters, 0.5ppm furan concentration and an increment rate of 0.02ppm/month. The model output is 0.684 i.e. the estimated remaining life of paper insulation is 68.4% of its designed life which is normally 40 years [12]. This output is consistent with the correlation of paper degree of polymerisation (DP), furan and paper life developed in [12]. The paper life estimation for any set of input data (furan and furan increment rate) can be estimated using the surface graph shown in Fig.5-6.

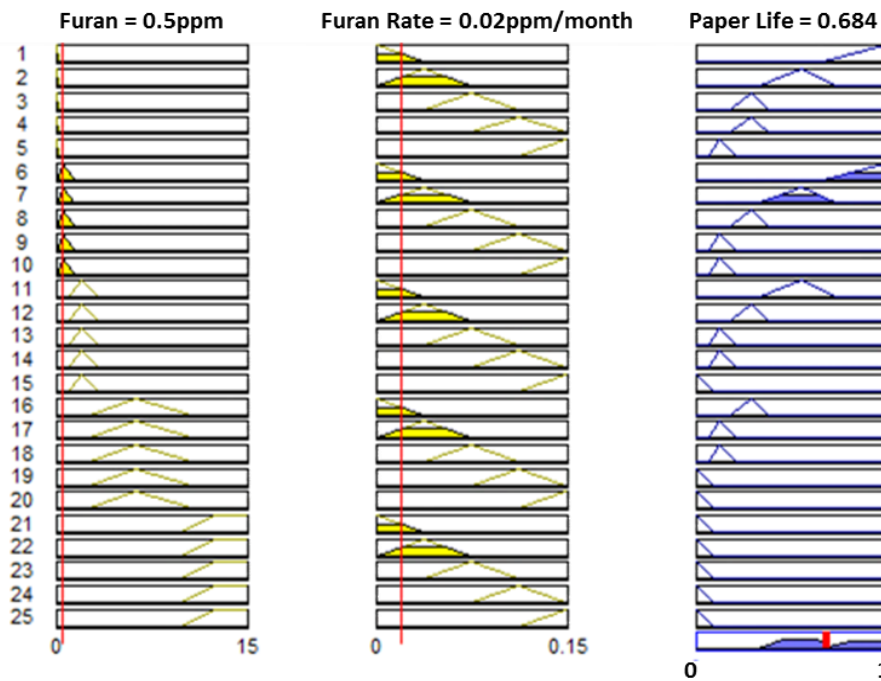


Figure 5-5 Developed fuzzy rules for paper life estimation based on furan

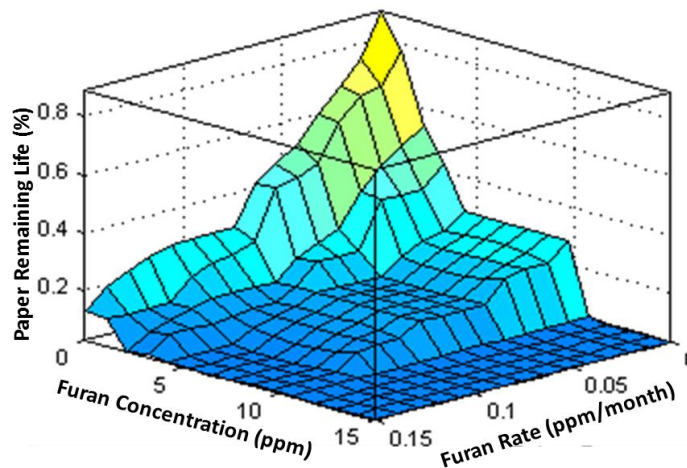


Figure 5-6 Paper life estimation surface graph

5.4.2 CO Ratio Criticality

CO and CO₂ are the main gases evolved from paper degradation. A set of fuzzy rules correlating CO₂/CO ratio and CO generation rate/month, with paper deterioration was developed in accordance with IEEE Std. C57.104 recommendations [28]. Membership functions for CO₂/CO ratio and CO generation rate/month are considered on the scale 0 to 15, and 0 to 350ppm/month respectively as shown in Fig.5-7. The output variable; paper deterioration, is assumed to be in the range 0 to 1. Output approaching 1 indicates significant paper deterioration while output close to 0 reflects normal paper condition.

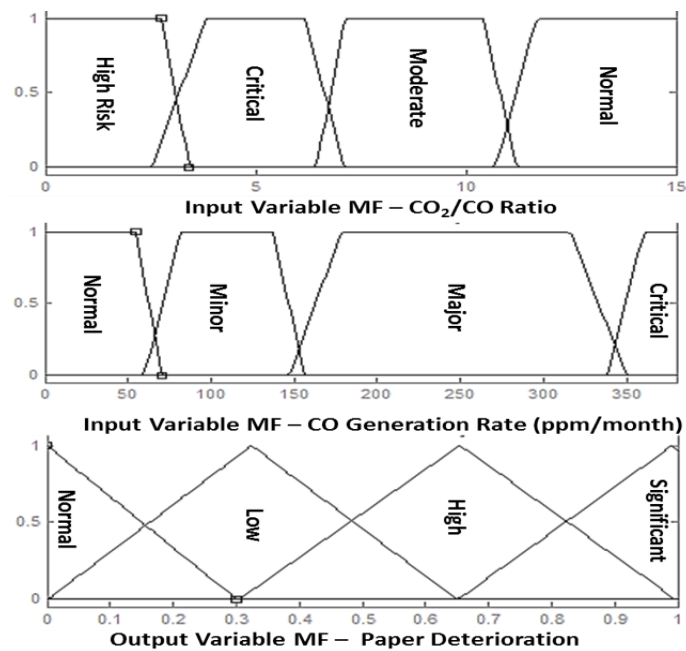


Figure 5-7 Input and output variables' MF for CO ratio fuzzy model

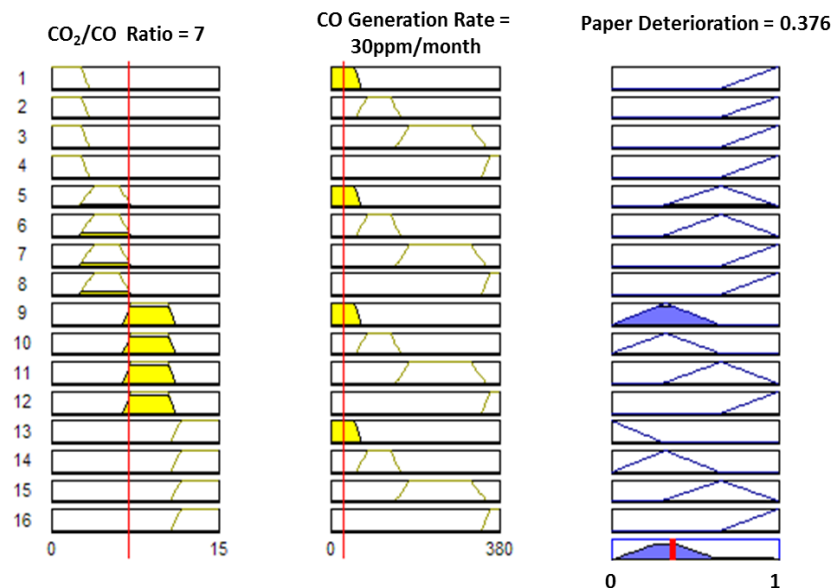


Figure 5-8 Developed fuzzy rules for paper deterioration based on CO ratio

The model is tested with inputs, CO₂/CO ratio (7) and CO generation rate (30ppm/month). The fuzzy logic numerical output is 0.376, which corresponds to moderate deterioration paper condition as shown in Fig.5-8. This result aligns well with the recommendation in [12]. The paper deterioration for any set of input data (CO₂/CO ratio and CO generation rate) can be estimated using the surface graph shown in Fig.5-9.

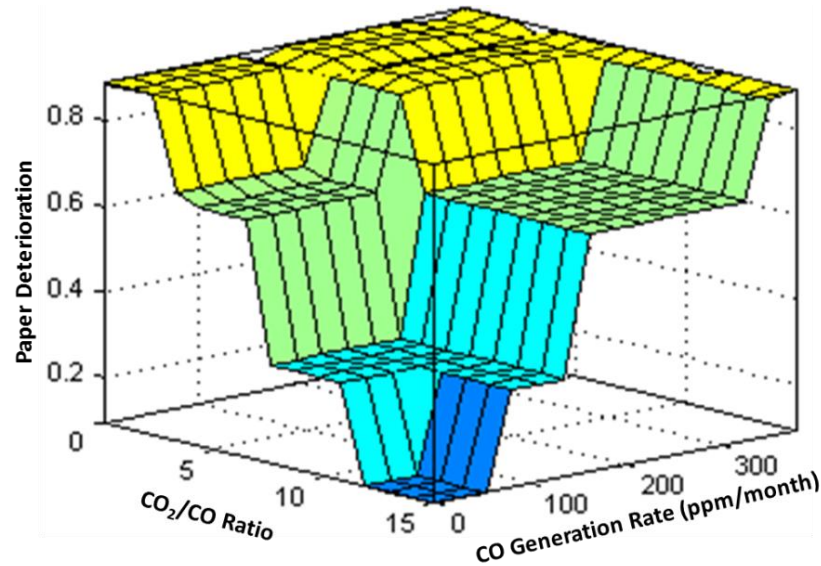


Figure 5-9 Paper deterioration surface graph

5.4.3 Paper Aging Criticality

The overall paper aging criticality is obtained by integrating the furan and CO ratio factors fuzzy models as shown in Fig.5-3. The input to the model are the same outputs of the Furan and CO ratio fuzzy models and the output representing paper aging criticality is assumed to be in range 0 to 1 (normal to significant criticality) as shown in Fig.5-10.

A set of fuzzy rules relates the input and the output variables for overall paper aging model is developed in accordance with FIST 3-31 guidelines, as shown in Fig.5-11 [12]. The model is tested with output values obtained from Furan and CO Ratio fuzzy models; 0.684 and 0.376, respectively. A paper aging criticality of 0.332 is resulted. This value is corresponding to moderate paper aging activity.

The overall paper aging criticality for any set of input variable can be estimated through the 3D surface graph shown in Fig. 5-12.

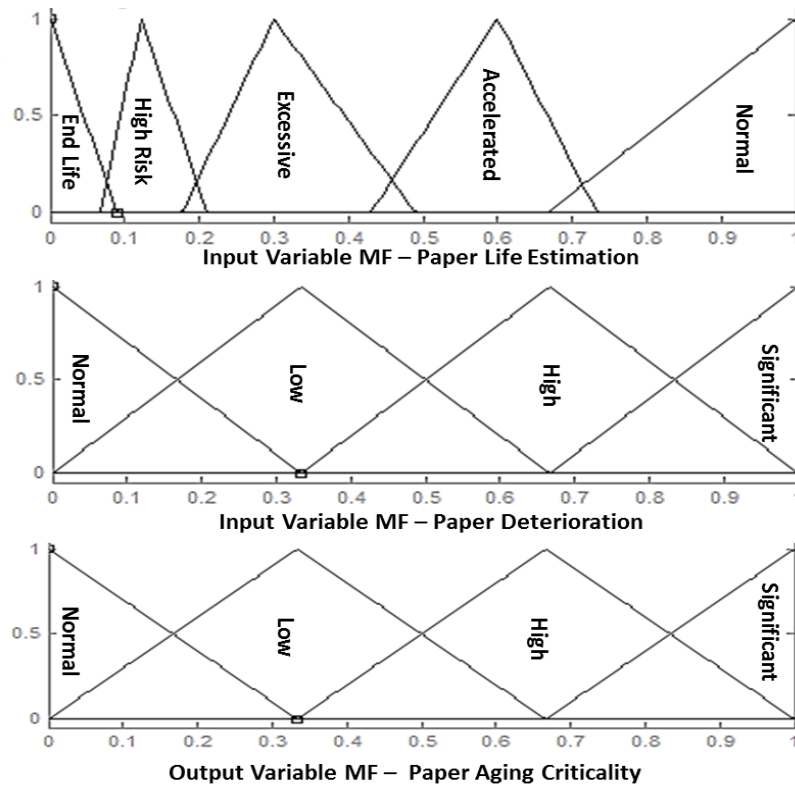


Figure 5-10 Input and output variables' MF for paper aging criticality fuzzy model

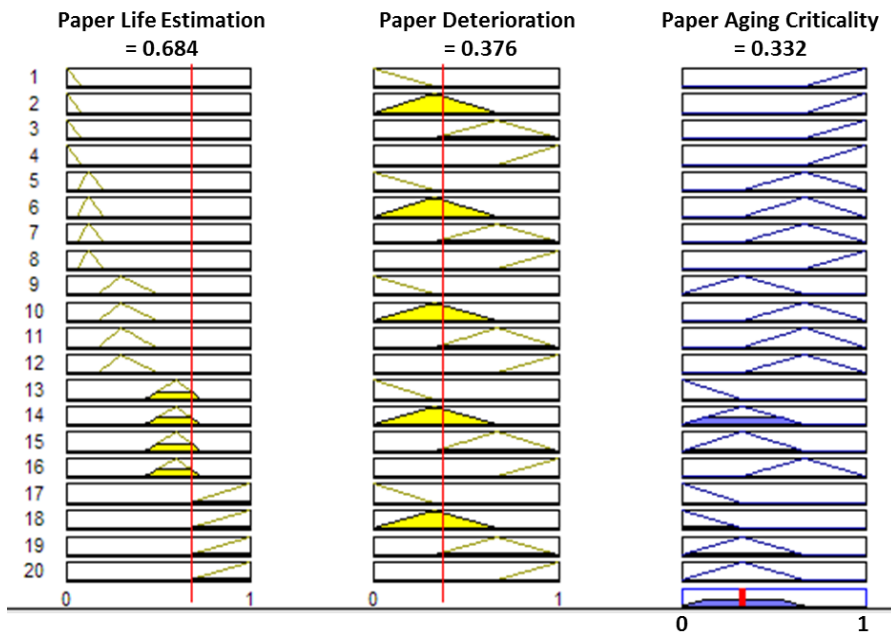


Figure 5-11 Developed fuzzy rules for paper aging criticality

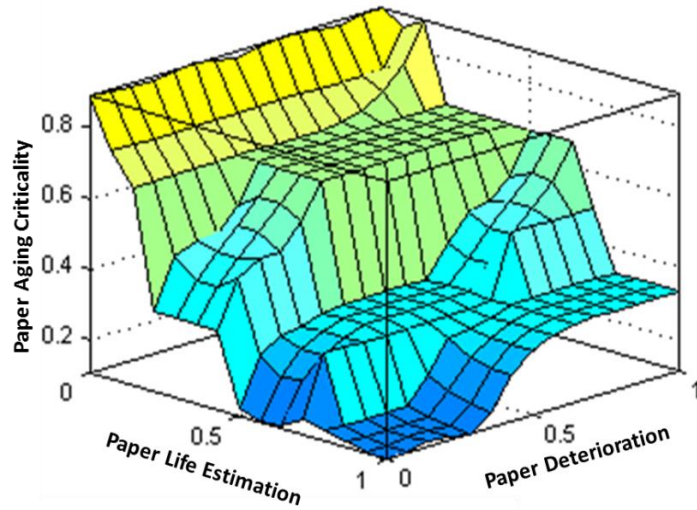


Figure 5-12 Paper aging criticality surface graph

5.4.4 Relative Accelerating Aging Criticality

A fuzzy logic model was developed using operating temperature rise, oxygen in oil, and water content in paper insulation parameters as inputs to the model where the output is the accelerating aging factor based on the correlations of these factors with paper aging [106].

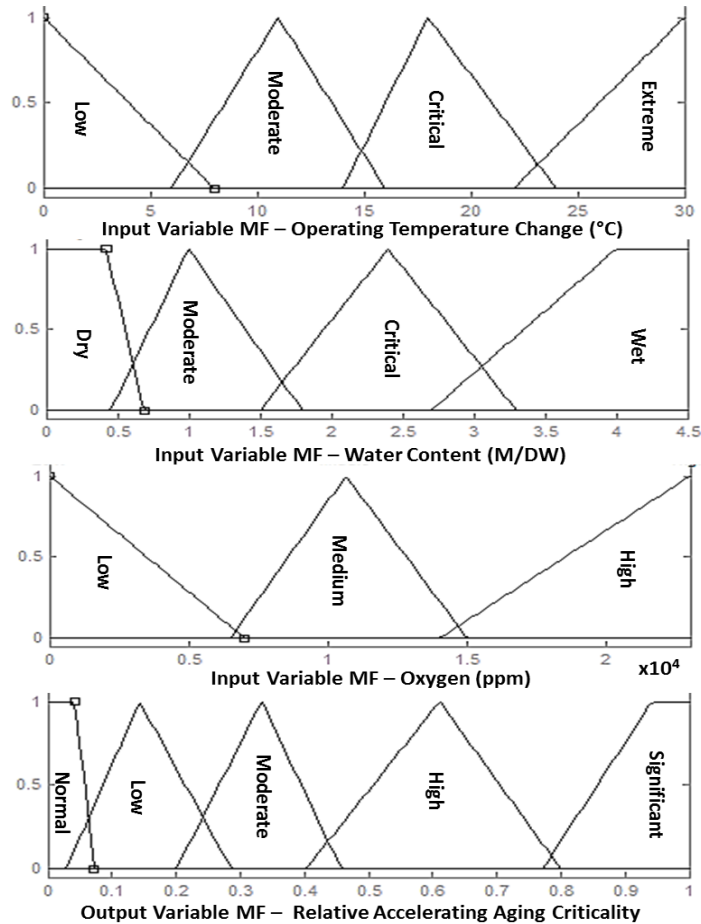


Figure 5-13 Input and output variables' MF for relative accelerating aging fuzzy model

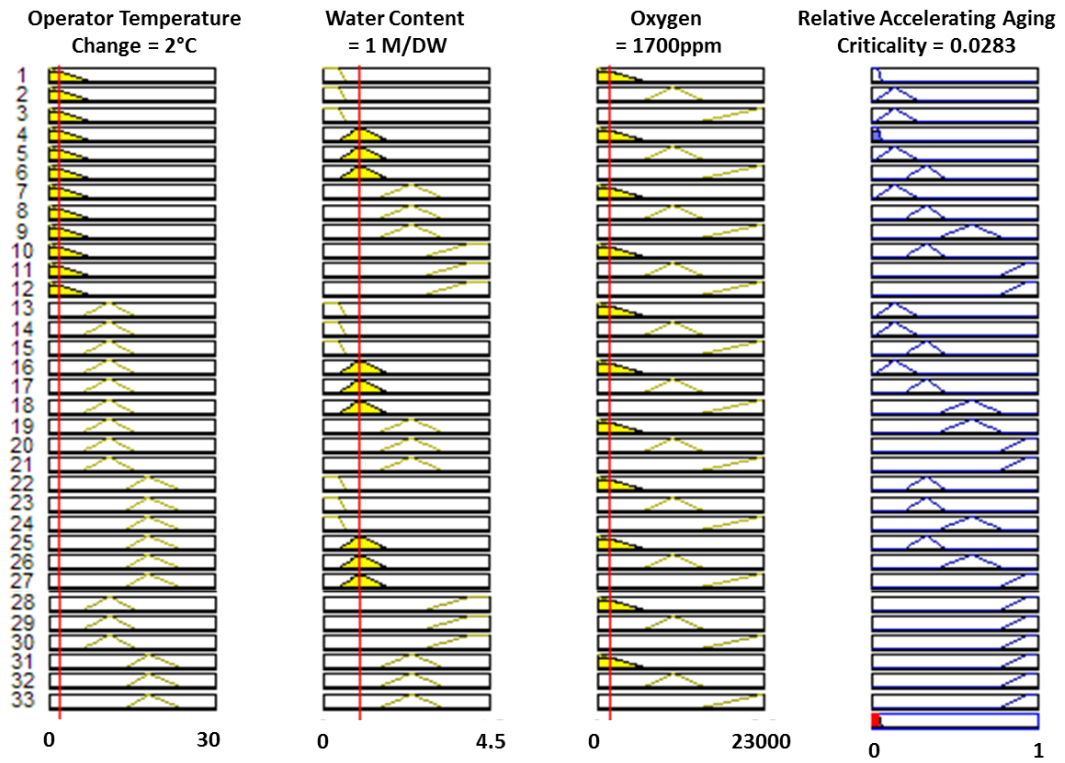


Figure 5-14 Developed fuzzy rules for relative accelerating aging

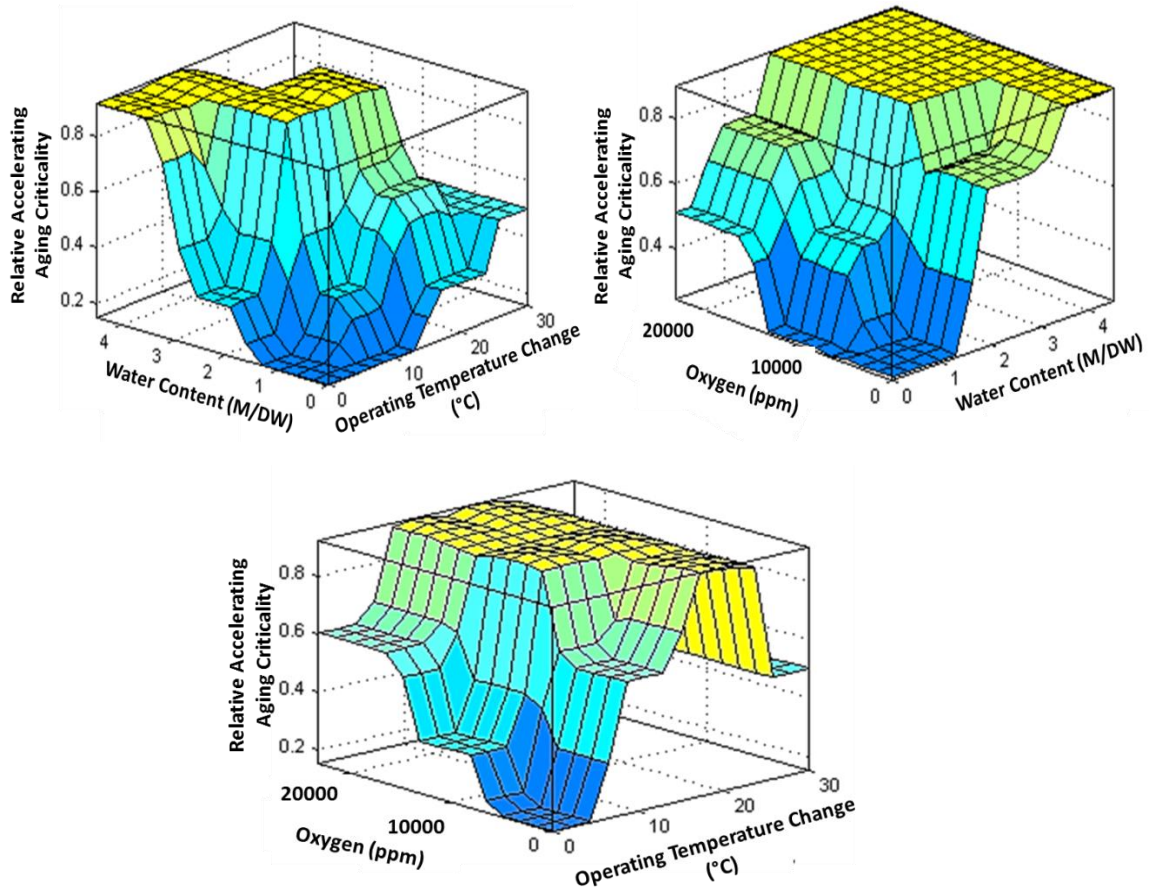


Figure 5-15 Relative accelerating aging surface graph

The MF of operating temperature rise, oxygen, and water content are considered on the scale 0 to 30°C, 0 to 23,000ppm, and 0 to 4.5% moisture by dry weight (M/DW) of paper insulation respectively, as shown in Fig.5-13. The output of the model is considered on the range 0 to 1 (normal to significant criticality).

A set of fuzzy rules which correlate inputs and output variables is shown in Fig. 5-14. The model is tested with inputs, operating temperature rise (2°C), water content (1M/DW), and oxygen (1700ppm). The fuzzy logic numerical output is 0.028, which corresponds to normal accelerating aging factor. The relative accelerating aging criticality for any set of input variable can be estimated through the 3D surface graph shown in Fig. 5-15.

5.4.5 Thermal Fault Criticality

C₂H₄ and C₂H₆ are the main gases generated by oil decomposition due to thermal stress. A thermal fault fuzzy model is developed to assess the oil thermal criticality where C₂H₄ and C₂H₆ concentrations in ppm are the inputs to the model, while the output represents the thermal fault criticality.

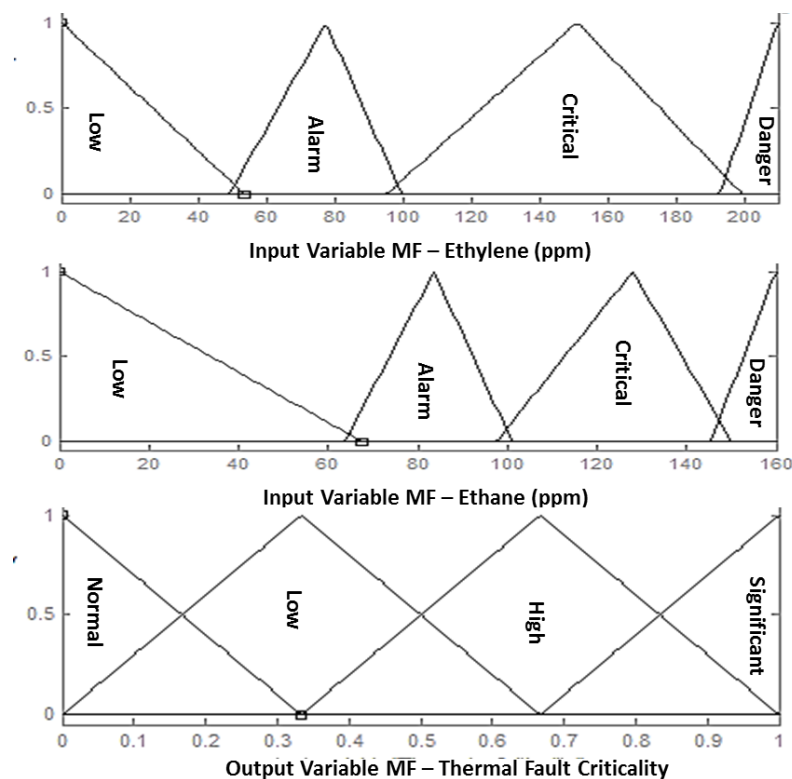


Figure 5-16 Input and output variables' MF for thermal fault fuzzy model

Input variable membership functions are considered on the scale 0 to 210ppm and 0 to 160ppm for C₂H₄ and C₂H₆ respectively. The output membership functions are measured on the scale 0 to 1 (normal to significant criticality) as shown in Fig.5-16.

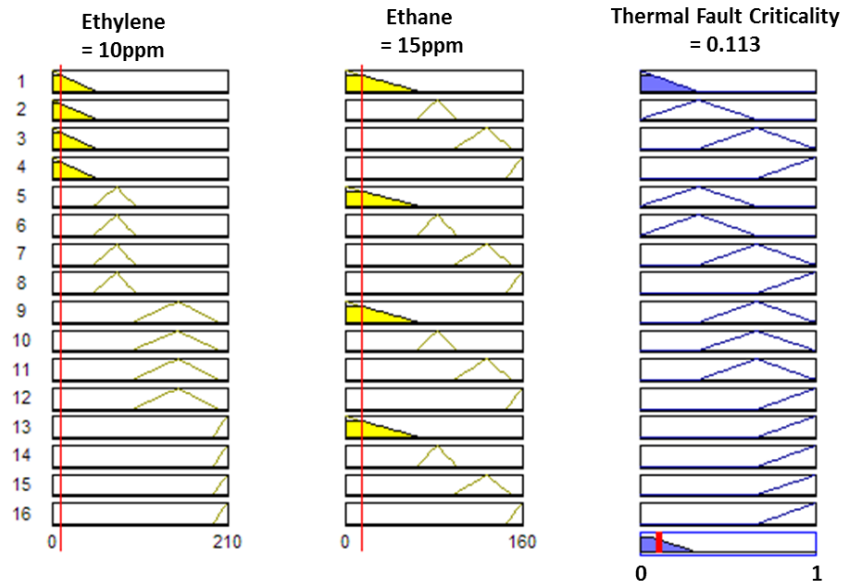


Figure 5-17 Developed fuzzy rules for thermal fault criticality based on ethylene and ethane

The fuzzy rules for thermal fault model are developed in accordance with IEEE Std. C57.104 recommendation [28] as shown in Fig.5-17. The model is tested with inputs, C_2H_4 (10ppm) and C_2H_6 (15ppm). The fuzzy logic numerical output is 0.1128, which corresponds to less significant thermal fault condition. This result agrees with the IEEE Std. C57.104 guidelines [28].

The thermal fault criticality for any set of input variable can be estimated through the 3D surface graph shown in Fig. 5-18.

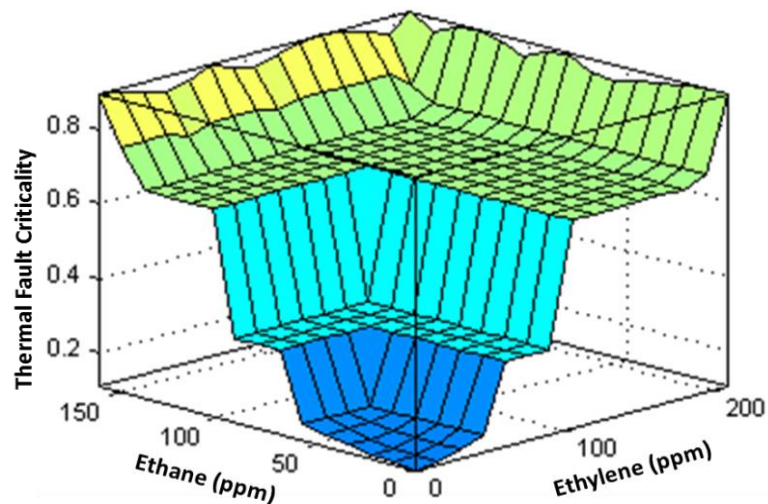


Figure 5-18 Thermal fault surface graph

5.4.6 Electrical Fault Criticality

CH₄ and C₂H₂ are the main gases generated by oil decomposition due to partial discharge or arcing faults. An electrical fault fuzzy model was developed to assess the electric fault criticality where CH₄ and C₂H₂ are the inputs to the model in ppm, and the output is the electrical fault criticality. Input variable membership functions were considered on the scale 0 to 1100ppm and 0 to 90ppm for CH₄ and C₂H₂ respectively, as shown in Fig. 5-19. The output membership functions were measured on the scale 0 to 1 (normal to significant criticality).

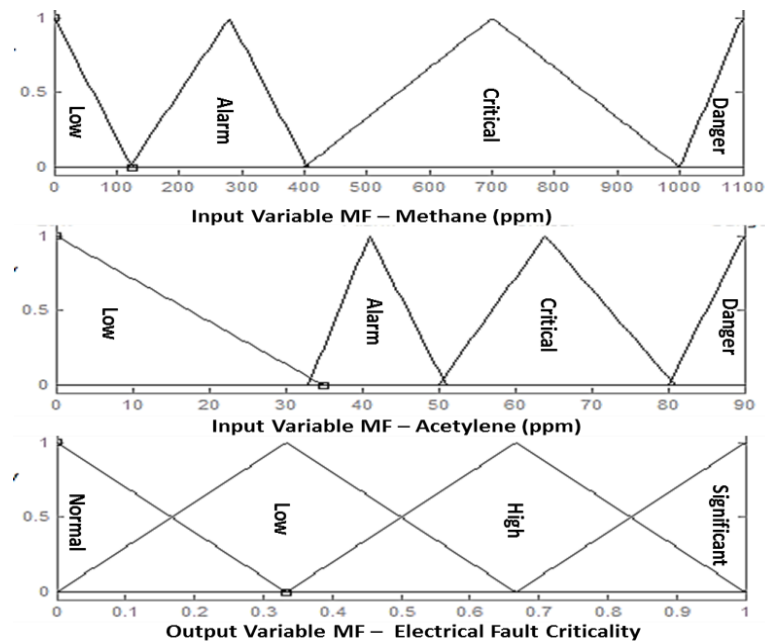


Figure 5-19 Input and output variables' MF for electrical fault fuzzy model

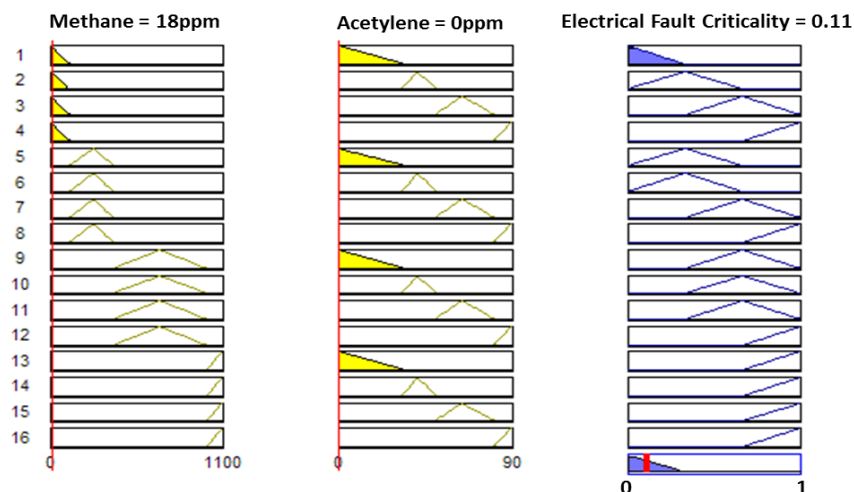


Figure 5-20 Developed fuzzy rules for electrical fault criticality based on methane and acetylene

The fuzzy rules for electrical fault model were developed in accordance with the IEEE Std. C57.104 recommendation [28] as shown in Fig. 5-20. The model was tested with inputs, CH₄ (18ppm) and C₂H₂ (0ppm). The fuzzy logic numerical output is 0.1102, which corresponds to a less significant electrical fault condition. This result is consistent with the IEEE Std. C57.104 guidelines [28]. The electrical fault criticality for any set of input variable can be estimated through the 3D surface graph shown in Fig. 5-21.

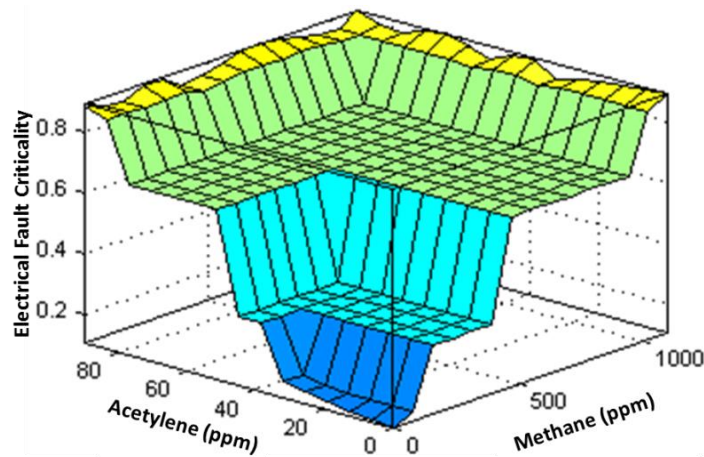


Figure 5-21 Electrical fault surface graph

5.4.7 Overall Thermal-Electrical Fault Criticality

The overall thermal electrical fault criticality can be assessed by integrating thermal and electrical fault criticalities fuzzy models.

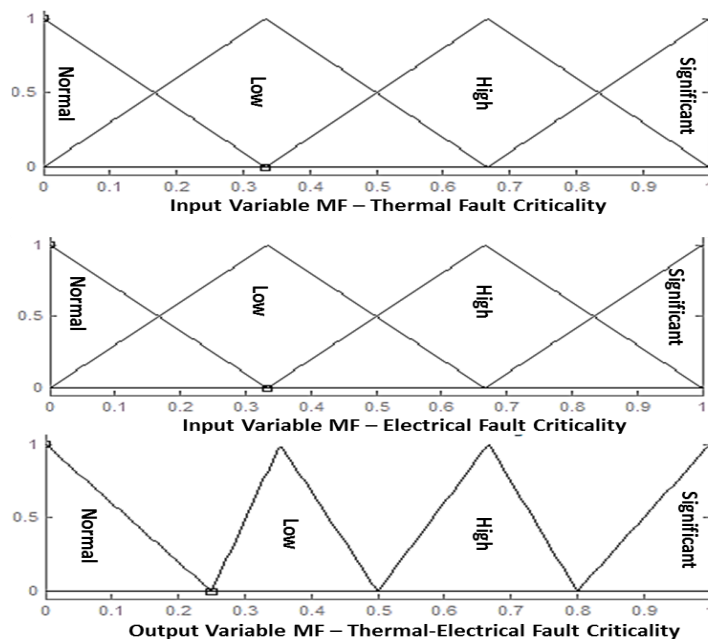


Figure 5-22 Input and output variables' MF for overall thermal-electrical fault fuzzy model

The inputs to the overall thermal-electrical fault criticality model are the outputs of the two aforementioned models while the output representing the overall fault criticality is assumed to be in the range 0 to 1 (normal to significant criticality), as shown in Fig. 5-22.

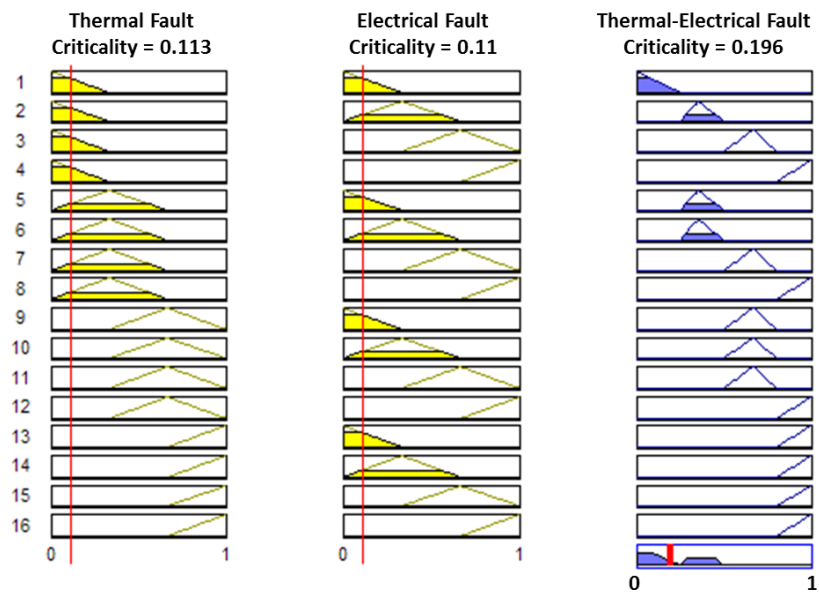


Figure 5-23 Developed fuzzy rules for overall thermal-electrical fault criticality

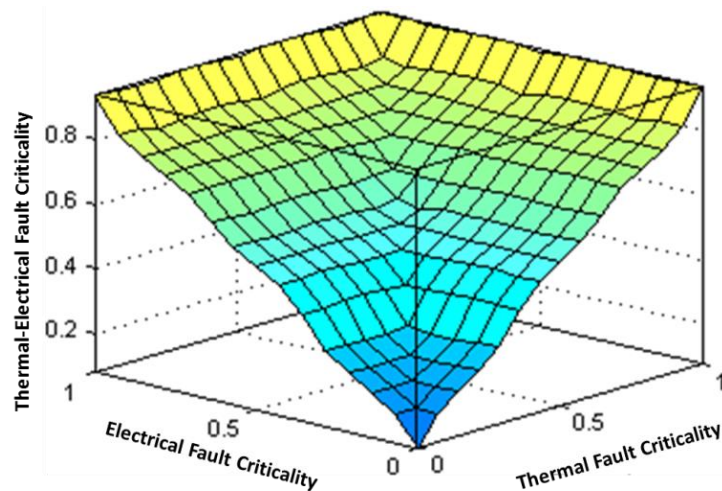


Figure 5-24 Overall thermal-electrical fault surface graph

A set of fuzzy rules developed to correlate between inputs and output variables is shown in Fig. 5-23. The model was tested with the output values obtained from thermal and electrical fault fuzzy models, 0.1128 and 0.1102, respectively. The final output of the fuzzy logic model is 0.1078, which corresponds with a less significant thermal-electrical fault activity. This output is consistent with the IEEE Std. C57.104 as all fault gases are well below the designated minimum threshold fault limit [28]. The overall thermal-electrical fault criticality for any set of input variable can be estimated through the 3D surface graph shown in Fig. 5-24.

5.4.8 IFT Criticality

A fuzzy logic model was developed using IFT and IFT decrement rate as inputs to the model where output is the IFT criticality that reflects the contaminations in transformer oil. Membership functions for IFT and IFT decrement rate are considered on the scale 15 to 45mN/m and 0 to 1.5 mN/m per month, respectively while the IFT criticality output membership functions are considered on the scale 0 (no contamination) to 1 (significant contamination) as shown in Fig. 5-25.

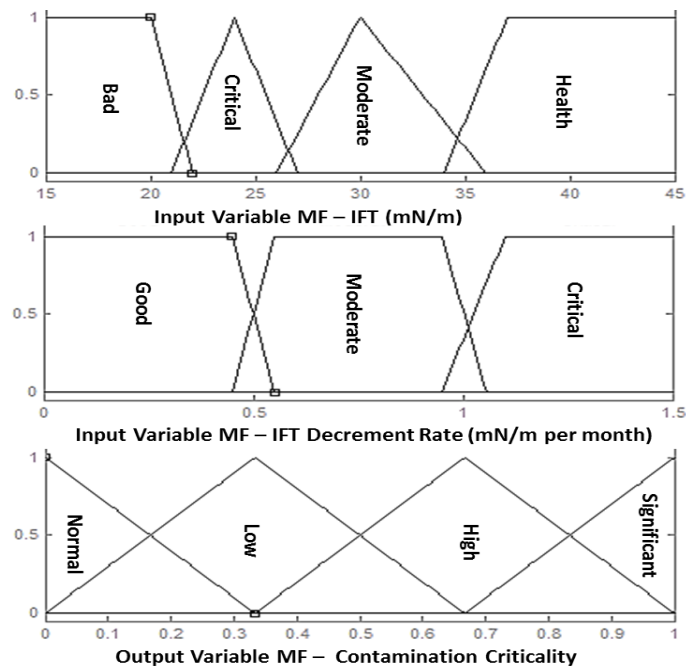


Figure 5-25 Input and output variables' MF for IFT criticality fuzzy model

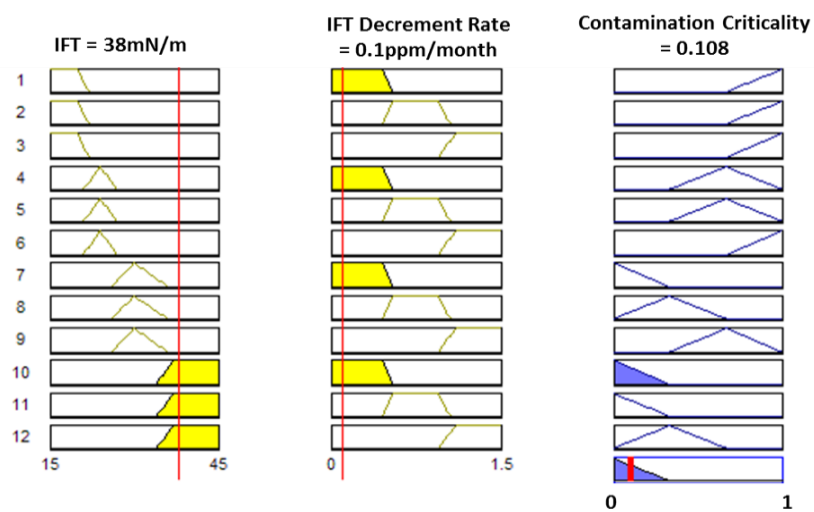


Figure 5-26 Developed fuzzy rules for contamination criticality based on IFT

A set of fuzzy rules relating the input and output variables for the IFT criticality model was developed in accordance with the guidelines reported in FIST 3-31 [12], as shown in Fig. 5-26. The IFT criticality fuzzy model is tested with inputs, IFT (38mN/m) and IFT decrement rate (0.1mN/m per month). The fuzzy logic model output is 0.107, which corresponds to the minor contamination level detected in the oil. The IFT criticality for any set of input variable can be estimated through the 3D surface graph shown in Fig. 5-27.

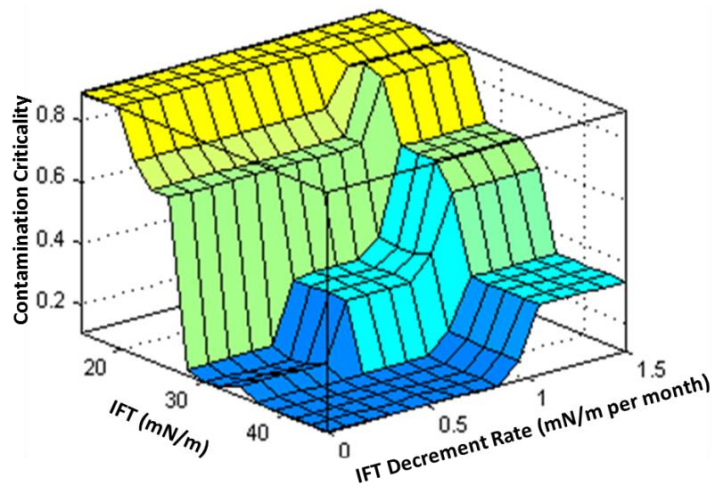


Figure 5-27 Contamination criticality surface graph

5.4.9 Remnant Life Estimation

The transformer remnant life can be estimated by integrating the furan and relative accelerating aging criticalities, as shown previously in Fig.5-3.

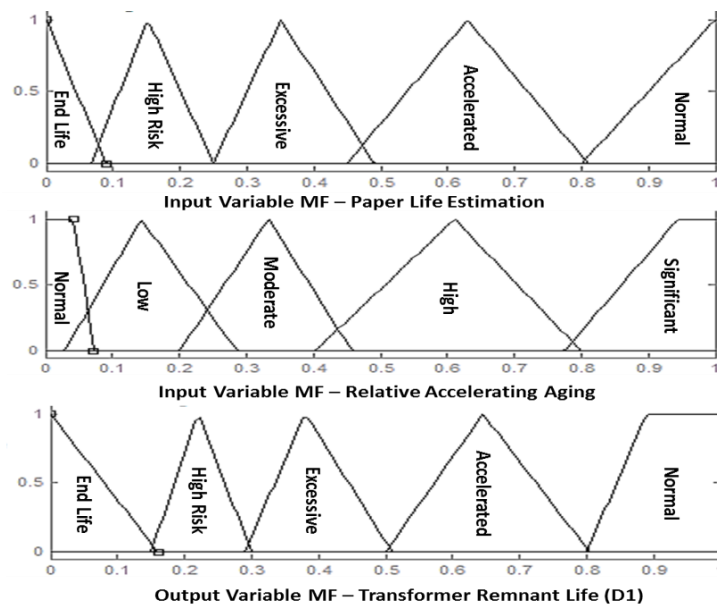


Figure 5-28 Input and output variables' MF for transformer remnant life (D1) fuzzy model

The inputs to the model are the same outputs of the furan and relative accelerating aging fuzzy models and the membership functions of the output which represents the transformer remnant life (D_1) are normalized on a scale 0 to 1, whereas 1 reflects a new transformer with 100% remaining life, and 0 reflects the end of the transformer's life, as shown in Fig. 5-28.

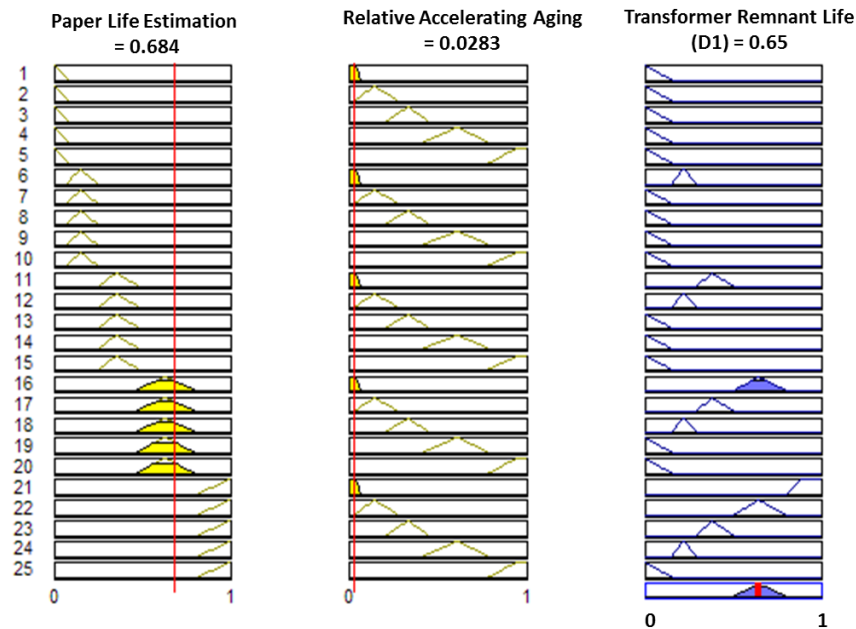


Figure 5-29 Developed fuzzy rules for transformer remnant life estimation (D_1)

A set of fuzzy rules that relate the input and output variables for the model was developed in accordance with the published recommendations [111], as shown in Fig.5-29. The model was tested with the output values obtained from furan and relative accelerating aging fuzzy models, 0.684 and 0.028, respectively. The fuzzy model output is 0.65, which corresponds to 65% of transformer remaining life. The transformer remnant life for any set of input variables can be estimated through the 3D surface graph shown in Fig. 5-30.

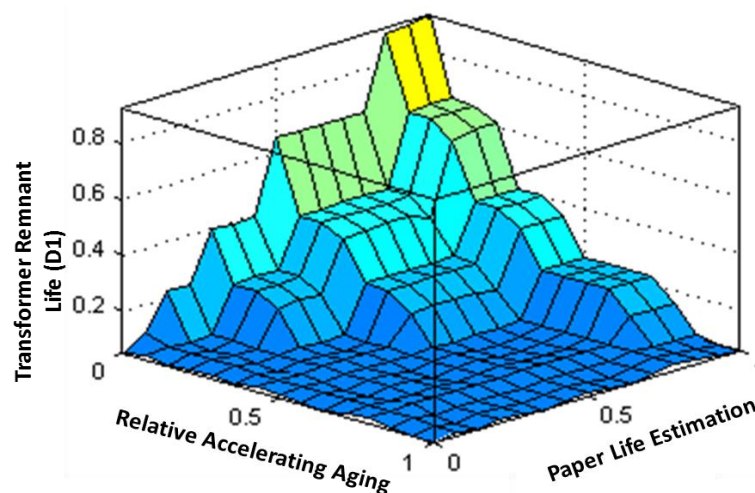


Figure 5-30 Transformer remnant life (D_1) surface graph

5.4.10 Asset Management Model

An asset management decision model was developed by integrating paper aging, faults, contamination, and relative accelerated aging criticalities, as shown in Fig.5-3.

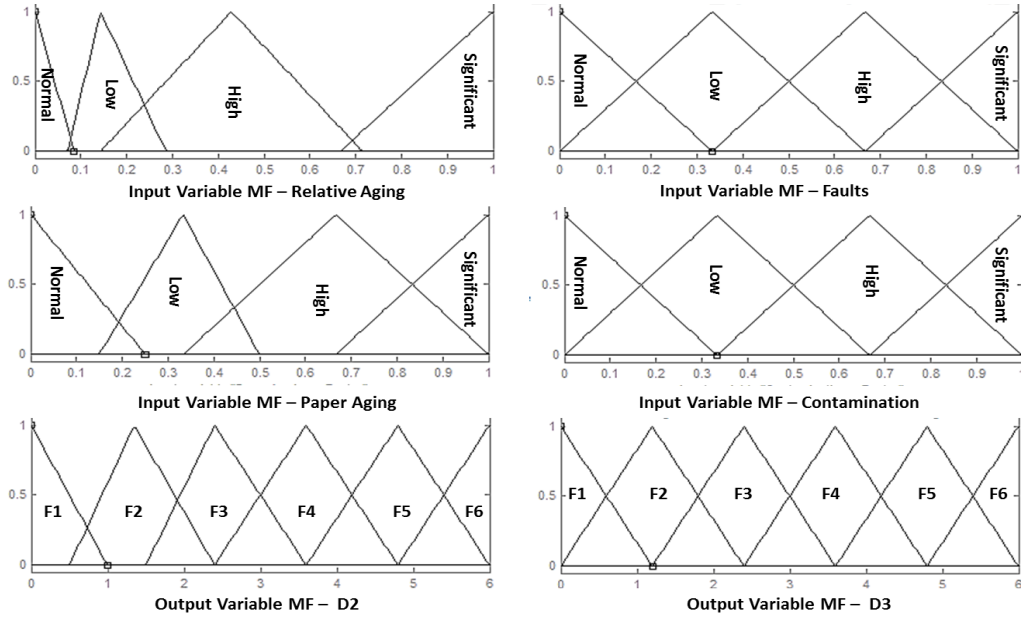


Figure 5-31 Input and output variables' MF for asset management decision fuzzy model

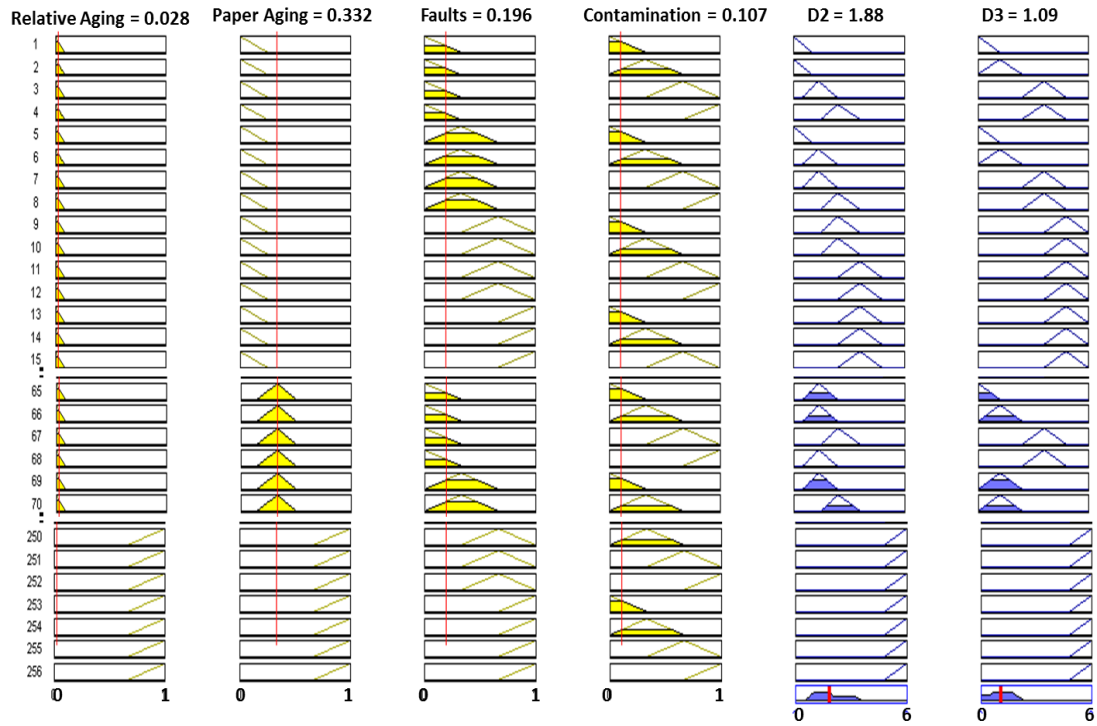


Figure 5-32 Developed fuzzy rules for asset management decision (D_2 and D_3)

Inputs to the model are the outputs of the mentioned models. Two output decisions are made based on these factors; transformer operation condition (D_2), and recommendation for oil maintenance (D_3). Both output decisions are mapped on a scale 0 to 6 as shown in Fig. 5-31. Fuzzy rules developed to correlate between input and output variables are shown in Fig. 5-32. The overall asset management decision fuzzy model was tested with the output values obtained from the four aforementioned models, paper aging (0.332), faults (0.196), contamination (0.107), and relative accelerated aging criticalities (0.028). The fuzzy model outputs are 1.88 and 1.09 for D_2 and D_3 , respectively.

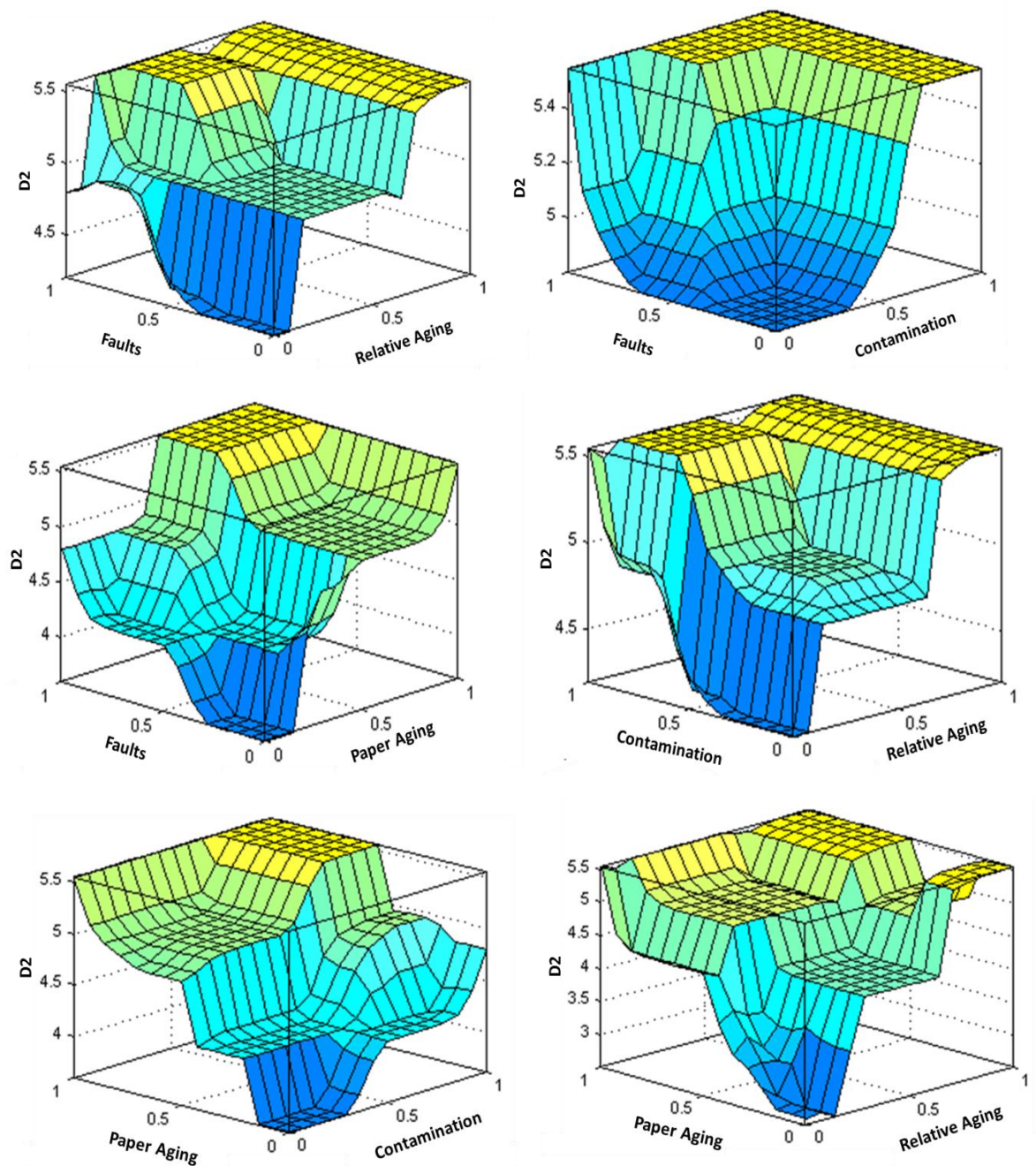


Figure 5-33 Asset management decision (D_2) surface graph

The asset management decision, D_2 and D_3 , for any set of input variable can be estimated through the 3D surface graph shown in Figs. 5-33 and 5-34, respectively.

Eighteen transformer asset management decision codes that are associated with the combination of D_2 and D_3 were developed to represent the criticality of the transformer along with asset management decision. Table 5-2 provides the proposed asset management decision code corresponding to various numerical numbers resulted from the asset management fuzzy logic model (D_2 and D_3). The overall results of the asset management model decisions in Fig.5-3 are consistent with the code 4 shown in Table 5-2, which corresponds to a transformer in good condition.

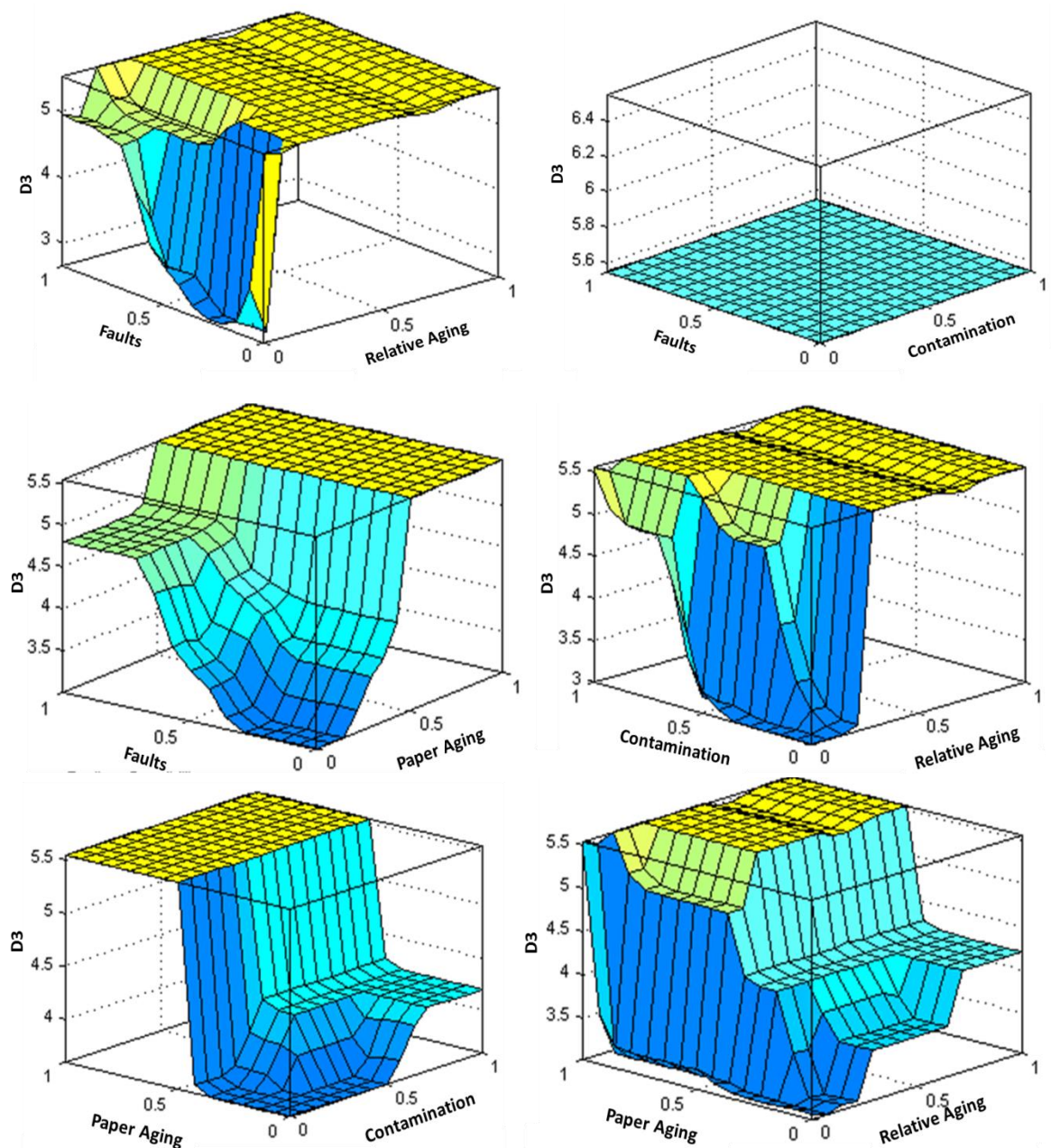


Figure 5-34 Asset management decision (D_3) surface graph

Table 5-2 Proposed transformer asset management decision code

Code No.	Model Output		Trans. Condition	Recommended decision
	D ₂	D ₃		
1	$0 \leq D_2 < 1$	$0 \leq D_3 < 1$	Very good	Continue normal operation.
2	$0 \leq D_2 < 1$	$1 \leq D_3 < 2$	Good	Continue normal operation.
3	$1 \leq D_2 < 2$	$0 \leq D_3 < 1$	Good	Continue normal operation.
4	$1 \leq D_2 < 2$	$1 \leq D_3 < 2$	Good	Exercise caution. Monitor the trend of all factors.
5	$1 \leq D_2 < 2$	$2 \leq D_3 < 3$	Average	Exercise caution. Monitor the trend of all factors. Degassing/dry-out recommended.
6	$1 \leq D_2 < 2$	$3 \leq D_3 < 4$	Average	Exercise caution. Monitor the trend of all factors. Reclamation recommended.
7	$2 \leq D_2 < 3$	$1 \leq D_3 < 2$	Average	Exercise extra caution. Specific trend monitoring on critical factor. Plan for predictive maintenance.
8	$2 \leq D_2 < 3$	$2 \leq D_3 < 3$	Average	Exercise extra caution. Specific trend monitoring on critical factor. Degassing/dry-out recommended.
9	$2 \leq D_2 < 3$	$3 \leq D_3 < 4$	Average	Exercise extra caution. Specific trend monitoring on critical factor. Reclamation recommended.
10	$3 \leq D_2 < 4$	$2 \leq D_3 < 3$	Poor	Exercise extreme caution. Specific trend monitoring on critical factor with restricted load operation. Degassing/dry-out recommended.
11	$3 \leq D_2 < 4$	$3 \leq D_3 < 4$	Poor	Exercise extreme caution. Specific trend monitoring on critical factor with restricted load operation. Reclamation recommended
12	$3 \leq D_2 < 4$	$4 \leq D_3 < 5$	Poor	Exercise extreme caution. Fault detected. Analyse individual gases to find cause of fault. Schedule for total condition monitoring diagnoses.
13	$4 \leq D_2 < 5$	$2 \leq D_3 < 3$	Bad	Exercise extreme caution. Specific trend monitoring on critical factor. Reduce load operation to below 70%. Plan outage. Degassing/dry-out recommended.
14	$4 \leq D_2 < 5$	$3 \leq D_3 < 4$	Bad	Exercise extreme caution. Specific trend monitoring on critical factor. Reduce load operation to below 70%. Plan outage. Reclamation recommended.
15	$4 \leq D_2 < 5$	$4 \leq D_3 < 5$	Bad	Exercise extreme caution. Fault detected. Analyse individual gases to find cause of fault. Urgent total condition monitoring diagnoses required.
16	$4 \leq D_2 < 5$	$5 \leq D_3 < 6$	Bad	Exercise extreme caution. Specific trend monitoring on critical factor. Reduce load operation to below 60%. Plan outage. Consider removal from service.
17	$5 \leq D_2 < 6$	$4 \leq D_3 < 5$	Very bad	Exercise extreme caution. Fault detected. Analyse individual gases to find cause of fault. Immediate action required. Consider removal from service.
18	$5 \leq D_2 < 6$	$5 \leq D_3 < 6$	Very bad	Exercise extreme caution. Reduce load operation to below 50%. Immediate action required. Consider removal from service.

5.5 Validation of The Proposed Model

To examine the accuracy of the proposed model, insulating oil analyses of 50 power transformers of different rating and life span with pre-known health conditions, where 20 data from previously published research papers [139, 169] along with 30 collected field data were tested using the proposed model shown in Fig.5-3 to compare the model's output with the actual condition of the transformers. Table 5-3 shows the overall model output for 16 oil samples. Results obtained from the proposed fuzzy logic model were compared with the actual condition of the transformer, as shown in Table 5-3. Clarification of the actual health conditions of the investigated transformers are given in Table S.1 in Appendix S.

The model outputs, (D_2, D_3) for the first two transformers were less than 1, (0.98,0.97) for sample 1 and (0.9,0.9) for sample 2 which correspond to code 1 in Table 5-2. This code indicates that all investigated critical factors are within normal limits and the transformer condition is considered "very good". This result is consistent with the guidelines for the IEEE Std. 57.106 [116] and FIST 3-31 [12] as all input parameters are within safety limits. It also matches with the actual condition of the two transformers.

The model output for samples 3 and 4 reveals code 4 which indicates one or more of the investigated critical factors were over normal limits. The very low CO_2/CO ratio may influence the decision for sample 3. On the other hand, sample 4 which was taken from a 22 year old transformer indicates 2-FAL more than 0.1ppm, revealing incipient paper aging acceleration. Exercise caution monitoring on overall factors is recommended.

As stated in Table S.1 in the Appendix S, samples 5 and 6 are obtained from aged transformers with very contaminated insulating oil. The model outputs for both samples reflect code 6, which indicates either paper degradation is accelerated or contamination level has entered the critical zone. Oil reclamation is recommended.

The model outputs for sample 7 is (2.6, 1.9) which are corresponding to code 7. This code reflects paper accelerated aging with moderate faults factor criticality as C_2H_6 concentration exceeds its safety limit. Specific trend monitoring on critical factor is required, and predictive maintenance is recommended. Paper insulation of transformer 8 is reported to be nearly wet and moderately contaminated. The fuzzy output model for sample 8 (2.7, 3.5) is corresponding to code 9 which requires specific trend monitoring on critical factor. Code 9 reveals accelerated paper aging and either relative accelerating aging and/or oil contamination is critical. Oil reclamation is recommended.

Transformers 9 and 10 are found to be faulty where the model output results is (3.6, 4.8) which is corresponding to code 12. The model results agree with the actual condition of the two transformers as presented in Table S.1, whereas transformer 9 is detected with arcing in oil and transformer 10 is detected with tap changer failure. Further investigation on individual dissolved gases is recommended to find the cause of fault.

The fuzzy model output for sample 11 coincides with code 11, which indicates accelerated paper aging with high criticalities of relative accelerating aging and contamination. Transformer 11 is reported to have wet paper insulation and highly contaminated insulating oil. Extreme caution monitoring on related factors with restricted load operation is necessary and oil reclamation is recommended.

Fuzzy output for sample 12 coincide with code 10 which indicates significant criticality of relative accelerated aging factor. Oil is recommended for degassing/dry-out depending on water content and oxygen level.

The model output for sample 13 (4.3, 3.6) was associated with code 14 which indicates significant transformer criticality. A transformer under this code requires specific trend monitoring on critical factors with load reduction below 70%. Oil reclamation and plan for outage are recommended for this transformer.

Code 15 was the fuzzy model output for sample 14 which reflects high thermal fault and excessive paper degradation. A transformer in this category is considered highly critical. Further assessment on individual dissolved gases is recommended to find the cause of fault. Immediate overall transformer condition diagnoses are suggested.

Samples 15 and 16 were associated with code 18 of the fuzzy model output. With extreme paper degradation and highly contaminated insulating oil, transformers 15 and 16 are considered to be in a high risk condition. A transformer under this code should be taken out of service immediately to prevent any potential catastrophic failure.

The overall results of the transformer criticality measures proposed by this model are highly consistent with the actual condition of the investigated 50 power transformers, as shown in Fig.5-35. The proposed model was able to accurately match 48 out of 50 transformer's actual conditions, which represents 96% overall agreement with real conditions.

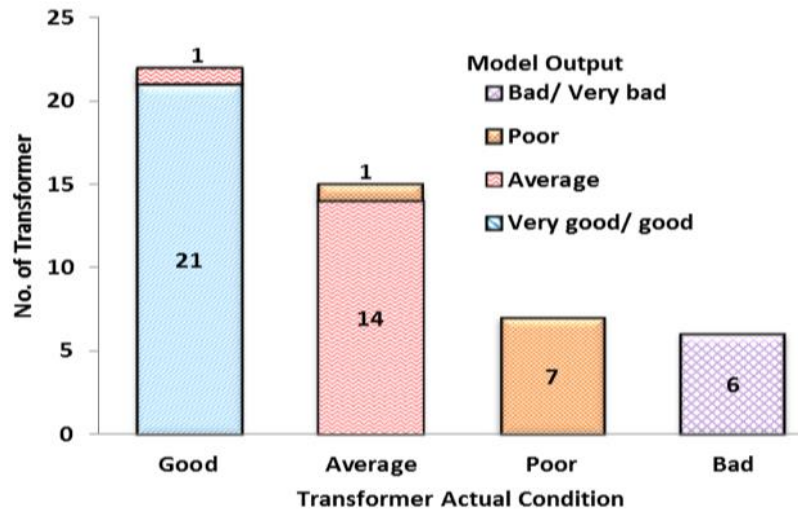


Figure 5-35 Comparison between proposed model and real transformer condition

The transformer remnant life estimation model output (D_i) has a good correlation with transformer criticality, as shown in Fig.5-36. Transformers in good condition have an average transformer remnant life above 80%, while the majority of transformers in an average condition are estimated to have a remnant life within 60% to 80%. Average transformers in bad condition will have a remnant life less than 25%, as shown in Fig.5-36.

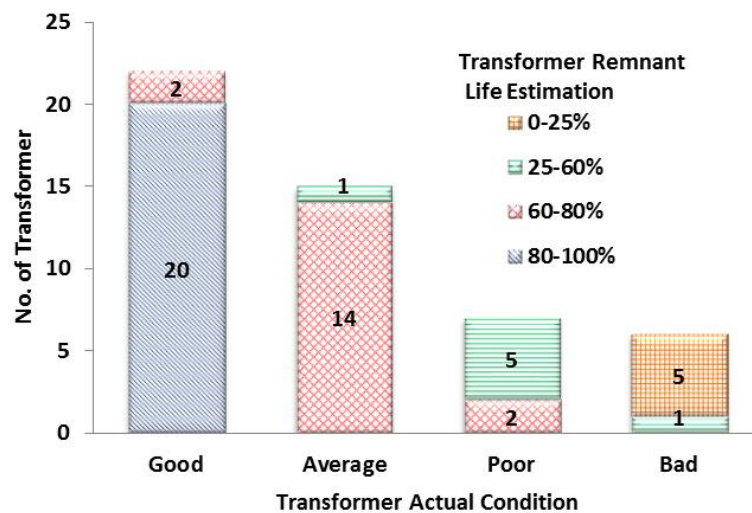


Figure 5-36 Relationship between model transformer remnant life estimation and transformer real condition

5.6 Conclusion

This chapter has addressed Objective 3: Developing an expert model to estimate the remnant life and asset management decision of power transformers based on routine insulating oil tests.

A new fuzzy logic approach to predicting the remnant life of power transformers and to provide a proper asset management decision tool based on insulating oil routine inspection was developed. All input parameters used in the proposed model can be measured on site and / or on-line. Eighteen codes which reflect the overall fuzzy logic output have been developed to cover all criticality conditions of an operating power transformer and recommend an appropriate asset management decision based on the proposed model. Accuracy of the overall model was assessed through historical data of fifty transformers of different ages, ratings and pre-known operating conditions. Results of the model were found to be consistent with real transformer conditions. The development of the model is expected to be beneficial for quick and reliable insulation condition assessment, and for assisting inexperienced engineers in proposing a proper management decision based on current transformer condition.

Table 5-3 Fuzzy logic model output with criticality code proposed

Sample	Temp. Rise	Water Content	Oxygen	Furan	Furan Rate	CO ₂ /CO Ratio*	CO Rate	Ethylene	Ethane	Methane	Acetylene	IFT	IFT Rate	Model Output (D ₁)	Model Output (D ₂)	Model Output (D ₃)	Code Apply	Model Condition	Actual Condition
1	1	0.6	500	<0.01	0	18	5	2	3	4	0	40	0.2	91%	0.98	0.97	1	VG	G
2	1	0.45	180	<0.01	0	10	0	0	0	0	0	42	0.1	93%	0.9	0.9	1	VG	G
3	1	0.8	800	<0.01	0	2	22	2	4	22	0	40	0.2	89%	1.8	1.2	4	G	G
4	1	0.45	1050	0.23	0.01	10	5	9	1	1	0	40	0.2	67%	1.8	1.2	4	G	G
5	2	1	1510	0.61	0.01	10.6	10	2	2	3	3	16	0.8	63%	1.87	3.6	6	A	A
6	2	0.8	1200	0.25	0.01	10	5	3	1	2	0	20	0.5	65%	1.8	3.6	6	A	A
7	2	0.85	158	0.12	0.02	10	5	7	90	23	0	32	0.5	63%	2.6	1.9	7	A	A
8	1	2	1817	1.05	0.05	11	8	31	9	29	0	28	0.8	38%	2.7	3.5	9	A	A
9	2	0.9	1515	0.3	0.01	10	10	458	14	286	884	32	0.4	63%	3.6	4.8	12	P	P
10	2	1	780	0.11	0.01	10	10	13	1	3	73	25	0.5	63%	3.6	4.8	12	P	P
11	2	2.6	3250	0.24	0.01	10	10	2	0	2	0	18	0.5	38%	3.7	3.6	11	P	P
12	2	3	4715	0.29	0.01	10	10	1	0	1	0	28	0.5	32%	3.2	2.1	10	P	P
13	2	3	5112	0.99	0.05	4.9	10	8	7	34	0	14	1	31%	4.3	3.6	14	B	B
14	2	0.85	30280	1.38	0.05	10	5	150	18	55	22	41	0.2	22%	4.8	4.8	15	B	B
15	2	1.1	2680	4.46	0.1	5.8	20	7	10	39	0	20	0.5	19%	5.2	5.5	18	VB	B
16	2	1.8	1700	5.53	0.1	3	40	15	18	22	0	19	0.5	7%	5.6	5.6	18	VB	B

*CO₂/CO ratio only applicable when the accumulated values of CO₂ and CO exceeds 2,500ppm and 350ppm respectively. Else, CO₂/CO ratio is set as 10.

Chapter 6 Conclusions and Future Research

6.1 Conclusions

This research presented a novel use of absorption spectroscopy using a Fuzzy logic approach in estimating the IFT and the concentration of dissolved key gases in transformer oil.

Research on fifty-five transformer mineral oil samples (Shell Diala BX type) that were collected from in-service transformers of various ratings, operating conditions and life spans shows the interfacial tension of transformer oil can be measured using UV-Vis spectroscopy. The peak absorbance and maximum bandwidth of oil spectral response show a significant correlation with the oil IFT value whereas the peak absorbance and maximum bandwidth of the oil spectral response increases as the IFT of the oil decreases. Oil sample with an IFT greater than 40 mN/m exhibits lowest peak absorbance and narrowest bandwidth, while oil sample with an IFT less than 14 mN/m exhibits highest peak absorbance and widest bandwidth. Fuzzy logic technique was used to map this correlation and was tested with another twenty oil samples. Validation of the fuzzy logic model developed shows a high degree of accuracy in estimating IFT value of transformer oil whereas the average percentage difference between actual IFT (ASTM D971) and estimated model of 20 samples is 2.17%, while the overall accuracy is 90%.

Experimental results on one hundred oil samples show that the concentration of key gases such as CO, CO₂, CH₄, C₂H₂, C₂H₄, and C₂H₆ can be measured using NIR-IR spectroscopy. Each gas has a dominant impact on the oil spectral response within a particular spectrum range without overlapping with the effect of other gases. Oil spectral response parameters; peak absorbance and area at a particular wavelength range show a strong correlation with the concentration of each gas whereas the peak absorbance and area increases as the concentration of gas in oil increases. Fuzzy logic technique was used to map correlation between each gas concentration and its oil spectral response and was tested with twenty oil samples taken from in-service transformers. The Fuzzy logic models developed to map these correlations show a high degree of accuracy in estimating gas concentration in transformer oil whereas the maximum RMSE and MAPE for the twenty investigated oil samples were less than 4 and 3% respectively.

The advantages of the absorption spectroscopy technique proposed in this research over current IFT and DGA measurement techniques are that it can be conducted instantly on site without the need for an expert person to run the test, and it only incurs negligible running costs. Furthermore, this technique could also be implemented on-line for continuous monitoring of transformer oil condition. Moreover, absorption spectroscopy can be employed to examine transformer paper degradation, furan concentration, moisture, and the additive and contamination level in transformer oil.

A transformer remnant life and asset management decision model based on insulating oil routine inspection proposed in this research shows results consistent with real transformer conditions. The proposed model was able to match accurately 48 out of 50 transformer's actual conditions, which represents 96% of the overall accuracy of proposed model. In this model, eighteen codes were introduced to cover all criticality conditions of a transformer and provide an appropriate asset management decision. The key advantage of the remnant life estimation and asset management decision model proposed in this thesis is that all input parameters used in the model can be measured on-site and/or on-line, hence it offers more reliable and timely transformer condition monitoring and asset management.

The proposed asset management model in this research is expected to be beneficial for quick and consistent insulation condition assessment, and could assist inexperienced engineers in proposing a proper asset management decision based on current transformer condition.

6.2 Future Research Recommendation

It is expected that the accuracy of the developed fuzzy logic models in this thesis including IFT estimation, dissolved gases measurements, transformer remnant life estimation and asset management decision could be improved through:

- Using more field data from various transformers of different operating conditions, ratings and health conditions.
- Employing an adaptive neuro-fuzzy inference system (ANFIS). ANFIS is a hybrid intelligent system of artificial neural network (ANN) and fuzzy logic which utilizes the ANN learning methods to tune the parameters of a Fuzzy Inference Systems (FIS). The main advantage of ANFIS is that it can adapt and learn the information on-line. Hence historical data can be used to improve the accuracy and reliability of the developed model.
- Implementing a hardware/software tool to test the developed methods in this research on in-service transformers.

-Improve the paper degradation assessment through adopting a reliable chemical marker such as the concentration of Methanol in transformer oil. The current technique for measuring methanol in transformer oil uses gas chromatography. However, this technique cannot be implemented on-line. On the other hand, absorption spectroscopy is widely used to examine the methanol concentration in other applications especially in organic chemistry. Therefore, development of an alternative method to detect methanol in transformer oil using absorption spectroscopy can be considered in future research.

References

- [1] Office of Electricity Delivery and Energy Reliability, "Large Power Transformers and The U.S. Electric Grid," *The US Department of Energy*, April 2014.
- [2] W. Bartley, "Analysis of Transformer Failures," presented at the 36th Annual Conference Stockholm, 2003.
- [3] W. P. Australia, "Western Power: State of the Infrastructure Report 2014/15," 2016.
- [4] "IEEE Guide for Selecting and Using Reliability Predictions Based on IEEE 1413," *IEEE Std 1413.1-2002*, p. 0_1, 2003.
- [5] A. Abu-Siada and S. Islam, "A Novel Online Technique to Detect Power Transformer Winding Faults," *IEEE Transactions on Power Delivery*, vol. 27, pp. 849-857, Apr 2012.
- [6] D. J. Woodcock and J. C. Wright, "Power transformer design enhancements made to increase operational life," in *Sixty-Sixth Annual International Conference of Doble Clients*, 1999.
- [7] Y. Shirasaka, H. Murase, S. Okabe, and H. Okubo, "Cross-sectional comparison of insulation degradation mechanisms and lifetime evaluation of power transmission equipment," *IEEE Transactions on Dielectrics and Electrical Insulation*, vol. 16, pp. 560-573, 2009.
- [8] M. Arshad and S. M. Islam, "Significance of cellulose power transformer condition assessment," *IEEE Transactions on Dielectrics and Electrical Insulation*, vol. 18, pp. 1591-1598, 2011.
- [9] A. Schaut, S. Autru, and S. Eeckhoudt, "Applicability of methanol as new marker for paper degradation in power transformers," *IEEE Transactions on Dielectrics and Electrical Insulation*, vol. 18, pp. 533-540, 2011.
- [10] M. Wang, A. J. Vandermaar, and K. D. Srivastava, "Review of condition assessment of power transformers in service," *IEEE Electrical Insulation Magazine*, vol. 18, pp. 12-25, 2002.
- [11] "IEEE Guide for Diagnostic Field Testing of Electric Power Apparatus - Part 1: Oil Filled Power Transformers, Regulators, and Reactors," *IEEE Std 62-1995*, pp. 1-64, 1995.
- [12] D. Hydroelectric Research and Technical Services Group, Colorado, "Facilities, Illustrations, Standards and Techniques; Transformer Diagnostic" *US Department of Interior Bureau of Reclamation*, vol. 3-31, pp. 1-62, June 2003.
- [13] "Standard Test Method for Interfacial Tension of Oil Against Water by the Ring Method," *ASTM D971 – 12 Standard*, 2012.
- [14] B. Pahlavanpour, M. Eklund, and K. Sundkvist, "Revised IEC standard for maintenance of in-service insulating oil," in *Weidmann Third Annual Technical Conference, Sacramento, USA*, 2004.
- [15] "Standard Test Method for Analysis of Gases Dissolved in Electrical Insulating Oil by Gas Chromatography," *ASTM D3612-02 (Reapproved 2009)*, 2009.
- [16] D. Skelly, "Photo-acoustic spectroscopy for dissolved gas analysis: Benefits and Experience," in *International Conference on Condition Monitoring and Diagnosis 2012*, pp. 29-43.
- [17] M. Webb, "Anticipating failures by dissolved-gas monitoring," *Power Engineering Journal*, vol. 1, pp. 295-298, 1987.
- [18] O. Koreh, K. Torkos, M. Bashir Mahara, J. Boressay, and V. Izvekov, "Study of water clusters in insulating oils by Fourier transform infrared spectroscopy," *IEEE Transactions on Dielectrics and Electrical Insulation*, vol. 5, pp. 896-902, 1998.
- [19] M. Ali, A. M. Emsley, H. Herman, and R. J. Heywood, "Spectroscopic studies of the ageing of cellulosic paper," *Polymer*, vol. 42, pp. 2893-2900, 2001.

- [20] P. J. Baird, H. Herman, G. C. Stevens, and P. N. Jarman, "Non-destructive measurement of the degradation of transformer insulating paper," *IEEE Transactions on Dielectrics and Electrical Insulation*, vol. 13, pp. 309-318, 2006.
- [21] A. Abu-Siada, S. P. Lai, and S. M. Islam, "A Novel Fuzzy-Logic Approach for Furan Estimation in Transformer Oil," *IEEE Transactions on Power Delivery*, vol. 27, pp. 469-474, 2012.
- [22] M. A. van Agthoven, G. Fujisawa, P. Rabbito, and O. C. Mullins, "Near-Infrared Spectral Analysis of Gas Mixtures," *Applied Spectroscopy*, vol. 56, pp. 593-598, 2002/05/01 2002.
- [23] E. Canè and A. Trombetti, "High Resolution Gas Phase IR Spectroscopy Applications," in *Encyclopedia of Spectroscopy and Spectrometry (Second Edition)*, L. Editor-in-Chief: John, Ed., ed Oxford: Academic Press, 1999, pp. 877-883.
- [24] A. E. B. Abu-Elanien and M. M. A. Salama, "Survey on the Transformer Condition Monitoring," in *Large Engineering Systems Conference on Power Engineering*, 2007, pp. 187-191.
- [25] A. Abu-Siada and S. Islam, "A new approach to identify power transformer criticality and asset management decision based on dissolved gas-in-oil analysis," *IEEE Transactions on Dielectrics and Electrical Insulation*, vol. 19, pp. 1007-1012, 2012.
- [26] R. Tamura, H. Anetai, T. Ishii, and T. Kawamura, "Diagnostic of ageing deterioration of insulating paper," *JIEE Proc Pub A*, vol. 101, p. 30, 1981.
- [27] J. P. van Bolhuis, E. Gulski, and J. J. Smit, "Monitoring and diagnostic of transformer solid insulation," *IEEE Transactions on Power Delivery*, vol. 17, pp. 528-536, 2002.
- [28] "IEEE Guide for the Interpretation of Gases Generated in Oil-Immersed Transformers - Redline," *IEEE Std C57.104-2008* pp. 1-45, 2009.
- [29] A. Abu-Siada, P. Lai Sin, and S. Islam, "Remnant life estimation of power transformer using oil UV-Vis spectral response," in *Power Systems Conference and Exposition, 2009. PSCE '09. IEEE/PES*, 2009, pp. 1-5.
- [30] T. K. Saha and P. Purkait, "Understanding the impacts of moisture and thermal ageing on transformer's insulation by dielectric response and molecular weight measurements," *IEEE Transactions on Dielectrics and Electrical Insulation*, vol. 15, pp. 568-582, 2008.
- [31] A. M. Emsley and G. C. Stevens, "Review of chemical indicators of degradation of cellulosic electrical paper insulation in oil-filled transformers," *IEE Proceedings - Science, Measurement and Technology*, vol. 141, pp. 324-334, 1994.
- [32] J. Jalbert, R. Gilbert, P. Tétreault, B. Morin, and D. Lessard-Déziel, "Identification of a chemical indicator of the rupture of 1,4- β -glycosidic bonds of cellulose in an oil-impregnated insulating paper system," *Cellulose*, vol. 14, pp. 295-309, 2007.
- [33] IEC, "Measurement of the Average Viscometric Degree of Polymerization of New and Aged Cellulosic Electrically Insulating Materials," *IEC 60450 Standard*, April 2004. Amendment 1 - May 2007.
- [34] "Standard Test Method for Measurement of Average Viscometric Degree of Polymerization of New and Aged Electrical Papers and Boards," *ASTM D4243 -99 (Reapproved 2009)*, 2009.
- [35] R. J. Heywood, A. M. Emsley, and M. Ali, "Degradation of cellulosic insulation in power transformers. I. Factors affecting the measurement of the average viscometric degree of polymerisation of new and aged electrical papers," *IEE Proceedings Science, Measurement and Technology*, vol. 147, pp. 86-90, 2000.
- [36] Y. Wang, Z. Huan, and J. Zhang, "Expediting cellulose insulation aging evaluation and life prediction through degree of polymerization measurements," in *Second International Conference on Properties and Applications of Dielectric Materials, 1988. Proceedings.*, 1988, pp. 328-331 vol.1.
- [37] P. Pahlavanpour, Eklund, and M. A. Martins, "Insulating paper ageing and furfural formation," in *Electrical Insulation Conference and Electrical Manufacturing ; Coil Winding Technology Conference, 2003. Proceedings*, 2003, pp. 283-288.
- [38] "IEEE Guide for the Evaluation and Reconditioning of Liquid Immersed Power Transformers," *IEEE Std C57.140-2006*, pp. c1-67, 2007.

- [39] A. Emsley and G. Stevens, "Kinetics and mechanisms of the low-temperature degradation of cellulose," *Cellulose*, vol. 1, pp. 26-56, 1994.
- [40] K. E. P. C. I. O. (Japan), "Transformer condition monitoring diagnostic technologies to detect deterioration and faults," *E-Journal of Advanced Maintenance*, vol. 3, p. 5, 2011.
- [41] D. H. Shroff and A. W. Stannett, "A review of paper aging in power transformers," *IEE Proceedings Generation, Transmission and Distribution*, vol. 132, pp. 312-319, 1985.
- [42] A. M. Emsley, R. J. Heywood, M. Ali, and X. Xiao, "Degradation of cellulosic insulation in power transformers .4. Effects of ageing on the tensile strength of paper," *IEE Proceedings - Science, Measurement and Technology*, vol. 147, pp. 285-290, 2000.
- [43] T. K. Saha, "Review of modern diagnostic techniques for assessing insulation condition in aged transformers," *IEEE Transactions on Dielectrics and Electrical Insulation*, vol. 10, pp. 903-917, 2003.
- [44] H.-C. Sun, Y.-C. Huang, and C.-M. Huang, "A review of dissolved gas analysis in power transformers," *Energy Procedia*, vol. 14, pp. 1220-1225, 2012.
- [45] A. de Pablo, "Furfural and ageing: how are they related," in *IEE Colloquium on Insulating Liquids 1999*, pp. 1-4.
- [46] "IEEE Guide for the Interpretation of Gases Generated in Oil-Immersed Transformers," *IEEE Std C57.104-1991*, p. 0_1, 1992.
- [47] S. Corporation, "Serveron White Paper : DGA Diagnostic Methods," 2007.
- [48] M. Duval, F. Langdeau, P. Gervais, and G. Belanger, "Influence of paper insulation on acceptable gas-in-oil levels in transformers," in *Conference on Electrical Insulation and Dielectric Phenomena, 1989. Annual Report.*, 1989, pp. 358-362.
- [49] H. Kan and T. Miyamoto, "Proposals for an improvement in transformer diagnosis using dissolved gas analysis (DGA)," *IEEE Electrical Insulation Magazine*, vol. 11, pp. 15-21, 1995.
- [50] H. Kan, T. Miyamoto, Y. Makino, S. Namba, and T. Hara, "Absorption of CO₂ and CO gases and furfural in insulating oil into paper insulation in oil-immersed transformers," in *IEEE International Symposium on Electrical Insulation*, 1994, pp. 41-44.
- [51] R. Gilbert, J. Jalbert, S. Duchesne, P. Tétreault, B. Morin, and Y. Denos, "Kinetics of the production of chain-end groups and methanol from the depolymerization of cellulose during the ageing of paper/oil systems. Part 2: Thermally-upgraded insulating papers," *Cellulose*, vol. 17, pp. 253-269, 2010.
- [52] J. Scheirs, G. Camino, M. Avidano, and W. Tumiatti, "Origin of furanic compounds in thermal degradation of cellulosic insulating paper," *Journal of Applied Polymer Science*, vol. 69, pp. 2541-2547, 1998.
- [53] "Standard Test Method for Furanic Compounds in Electrical Insulating Liquids by High-Performance Liquid Chromatography (HPLC)," *ASTM D5837-12*, 2012.
- [54] M. K. Domun, "Condition monitoring of power transformers by oil analysis techniques," in *Condition Monitoring and Remanent Life Assessment in Power Transformers, IEE Colloquium on*, 1994, pp. 2/1-2/3.
- [55] A. M. Emsley, X. Xiao, R. J. Heywood, and M. Ali, "Degradation of cellulosic insulation in power transformers. Part 2: formation of furan products in insulating oil," *IEE Proceedings on Science, Measurement and Technology*, vol. 147, pp. 110-114, 2000.
- [56] P.J.Burton, M. Carballeira, M. Duval, C. W. Fuller, J.Samat, and E. Spicar, "Application of liquid chromatography to analysis of electrical Insulating Materials," presented at the CIGRE, Intern. Conf. Large High Voltage Electric Systems, Paris, France, 1988.
- [57] B. Pahlavanpour, M. A. Martins, and A. de Pablo, "Experimental investigation into the thermal-ageing of Kraft paper and mineral insulating oil," in *IEEE International Symposium on Electrical Insulation*, 2002, pp. 341-345.
- [58] A. Cheim and C. Dupont, "A new transformer aging model and its correlation to 2FAL," in *Cigré Transformer Colloquium*, 2003.
- [59] L. Cheim, "Furan analysis for liquid power transformers," *IEEE Electrical Insulation Magazine*, vol. 28, p. 8, 2012.

- [60] J. Jalbert, R. Gilbert, Y. Denos, and P. Gervais, "Methanol: A Novel Approach to Power Transformer Asset Management," *IEEE Transactions on Power Delivery*, vol. 27, pp. 514-520, 2012.
- [61] M. A. G. Martins, "Vegetable oils, an alternative to mineral oil for power transformers-experimental study of paper aging in vegetable oil versus mineral oil," *IEEE Electrical Insulation Magazine*, vol. 26, pp. 7-13, 2010.
- [62] N. Yamagata, K. Miyagi, and E. Oe, "Diagnosis of thermal degradation for thermally upgraded paper in mineral oil," in *International Conference on Condition Monitoring and Diagnosis, 2008. CMD 2008.*, 2008, pp. 1000-1004.
- [63] W. McDermid and D. H. Grant, "Use of furan-in-oil analysis to determine the condition of oil filled power transformers," in *International Conference on Condition Monitoring and Diagnosis, 2008*, pp. 479-481.
- [64] K. Spurgeon, W. H. Tang, Q. H. Wu, Z. J. Richardson, and G. Moss, "Dissolved gas analysis using evidential reasoning," *IEE Proceedings - Science, Measurement and Technology*, vol. 152, p. 110, 2005.
- [65] J. Jalbert, S. Duchesne, E. Rodriguez-Celis, P. Tetreault, and P. Collin, "Robust and sensitive analysis of methanol and ethanol from cellulose degradation in mineral oils," *J Chromatogr A*, vol. 1256, pp. 240-5, Sep 21 2012.
- [66] H.-T. Y. C. C. Liao, "Adaptive Fuzzy Diagnosis System for Dissolved Gas Analysis," *IEEE Transactions on Power Delivery*, vol. 14, p. 1342, 1999.
- [67] "IEEE Guide for the Detection and Determination of Generated Gases in Oil-Immersed Transformers and Their Relation to the Serviceability of the Equipment," *ANSI/IEEE Std C57.104-1978*, p. 0_1, 1978.
- [68] "IEEE Guide for the Interpretation of Gases Generated in Oil-Immersed Transformers," *IEEE Std C57.104-2008 (Revision of IEEE Std C57.104-1991)*, pp. C1-27, 2009.
- [69] M. Duval, "New techniques for dissolved gas-in-oil analysis," *IEEE Electrical Insulation Magazine*, vol. 19, pp. 6-15, 2003.
- [70] A. de Pablo, W. Ferguson, A. Mudryk, and D. Golovan, "On-line condition monitoring of power transformers: A case history," in *Electrical Insulation Conference (EIC), 2011*, 2011, pp. 285-288.
- [71] G. L. Martin, "The Hydran^(R) a system for the detection and monitoring of failure conditions in power transformers," in *IEE Colloquium on Monitors and Condition Assessment Equipment (Digest No. 1996/186)*, 1996, pp. 3/1-3/5.
- [72] A. Stadler, "Analyzing UV/Vis/NIR and Photo-Acoustic Spectra: A Note to the Band Gap of Tix Si1 - xO2," *IEEE Transactions on Semiconductor Manufacturing*, vol. 26, pp. 156-161, 2013.
- [73] O. D. Sparkman, Z. E. Penton, and F. G. Kitson, "Gas Chromatography," in *Gas Chromatography and Mass Spectrometry (Second edition)*, ed Amsterdam: Academic Press, 2011, pp. 15-83.
- [74] "Standard Guide for Sampling, Test Methods, and Specifications for Electrical Insulating Oils of Petroleum Origin," *ASTM D117-10*, 2010.
- [75] "Standard Practice for Sampling Gas from a Transformer Under Positive Pressure," *ASTM D2759-00*, 2010.
- [76] "Standard Practices for Sampling Electrical Insulating Liquids," *ASTM D923-07*, 2007.
- [77] E. Forgács and T. Cserhádi, "CHROMATOGRAPHY | Principles," in *Encyclopedia of Food Sciences and Nutrition (Second Edition)*, C. Editor-in-Chief: Benjamin, Ed., ed Oxford: Academic Press, 2003, pp. 1259-1267.
- [78] S. Okabe, S. Kaneko, M. Kohtoh, and T. Amimoto, "Analysis results for insulating oil components in field transformers," *IEEE Transactions on Dielectrics and Electrical Insulation*, vol. 17, pp. 302-311, 2010.
- [79] J. L. Kirtley, W. H. Hagman, B. C. Lesieutre, M. J. Boyd, E. P. Warren, H. P. Chou, *et al.*, "Monitoring the health of power transformers," *IEEE Computer Applications in Power*, vol. 9, pp. 18-23, 1996.
- [80] D. Jie, I. Khan, Z. D. Wang, and I. Cotton, "Comparison of HYDRAN and laboratory DGA results for electric faults in ester transformer fluids," in *Conference on Electrical*

- Insulation and Dielectric Phenomena, 2007. CEIDP 2007. Annual Report, 2007, pp. 731-734.*
- [81] Q. Zhu, Y. Yin, Q. Wang, Z. Wang, and Z. Li, "Study on the Online Dissolved Gas Analysis Monitor based on the Photoacoustic Spectroscopy," in *International Conference on Condition Monitoring and Diagnosis (CMD), 2012, 2012, pp. 433-436.*
 - [82] C. Haisch and R. Niessner, "Light and sound-Photoacoustic spectroscopy," *Spectroscopy Europe*, vol. 14/5, 2002.
 - [83] W. Fu, C. Weigen, P. Xiaojuan, and S. Jing, "Study on the gas pressure characteristics of photoacoustic spectroscopy detection for dissolved gases in transformer oil," in *International Conference on High Voltage Engineering and Application (ICHVE), 2012, 2012, pp. 286-289.*
 - [84] N. A. Muhamad, B. T. Phung, T. R. Blackburn, and K. X. Lai, "Comparative Study and Analysis of DGA Methods for Transformer Mineral Oil," in *Power Tech, 2007 IEEE Lausanne, 2007, pp. 45-50.*
 - [85] R. R. Rogers, "IEEE and IEC Codes to Interpret Incipient Faults in Transformers, Using Gas in Oil Analysis," *IEEE Transactions on Electrical Insulation*, vol. EI-13, pp. 349-354, 1978.
 - [86] S. A. Ward, "Evaluating transformer condition using DGA oil analysis," in *Conference on Electrical Insulation and Dielectric Phenomena, 2003. Annual Report. , 2003, pp. 463-468.*
 - [87] V. Miranda and A. R. G. Castro, "Improving the IEC table for transformer failure diagnosis with knowledge extraction from neural networks," *IEEE Transactions on Power Delivery*, vol. 20, pp. 2509-2516, 2005.
 - [88] M. Duval and A. dePabla, "Interpretation of gas-in-oil analysis using new IEC publication 60599 and IEC TC 10 databases," *IEEE Electrical Insulation Magazine*, vol. 17, pp. 31-41, 2001.
 - [89] M. Duval, "A review of faults detectable by gas-in-oil analysis in transformers," *IEEE Electrical Insulation Magazine*, vol. 18, pp. 8-17, 2002.
 - [90] M. Duval and J. Dukarm, "Improving the reliability of transformer gas-in-oil diagnosis," *IEEE Electrical Insulation Magazine*, vol. 21, pp. 21-27, 2005.
 - [91] M. Duval, "The duval triangle for load tap changers, non-mineral oils and low temperature faults in transformers," *IEEE Electrical Insulation Magazine*, vol. 24, pp. 22-29, 2008.
 - [92] A. Abu-Siada, S. Hmood, and S. Islam, "A new fuzzy logic approach for consistent interpretation of dissolved gas-in-oil analysis," *IEEE Transactions on Dielectrics and Electrical Insulation*, vol. 20, pp. 2343-2349, 2013.
 - [93] K. F. Thang, R. K. Aggarwal, D. G. Esp, and A. J. McGrail, "Statistical and neural network analysis of dissolved gases in power transformers," in *Dielectric Materials, Measurements and Applications, 2000. Eighth International Conference on (IEE Conf. Publ. No. 473), 2000, pp. 324-329.*
 - [94] A. K. Mehta, R. N. Sharma, S. Chauhan, and S. Saho, "Transformer diagnostics under dissolved gas analysis using Support Vector Machine," in *International Conference on Power, Energy and Control (ICPEC), 2013, 2013, pp. 181-186.*
 - [95] N. A. Muhamad, B. T. Phung, and T. R. Blackburn, "Comparative study and analysis of DGA methods for mineral oil using fuzzy logic," in *International Power Engineering Conference, 2007, 2007, pp. 1301-1306.*
 - [96] D. R. Morais and J. G. Rolim, "A hybrid tool for detection of incipient faults in transformers based on the dissolved gas analysis of insulating oil," *IEEE Transactions on Power Delivery*, vol. 21, pp. 673-680, 2006.
 - [97] C. Pan, W. Chen, and Y. Yun, "Fault diagnostic method of power transformers based on hybrid genetic algorithm evolving wavelet neural network," *IET Electric Power Applications*, vol. 2, pp. 71-76, 2008.
 - [98] A. Shintemirov, W. Tang, and Q. H. Wu, "Power Transformer Fault Classification Based on Dissolved Gas Analysis by Implementing Bootstrap and Genetic

- Programming," *IEEE Transactions on Systems, Man, and Cybernetics, Part C: Applications and Reviews*, vol. 39, pp. 69-79, 2009.
- [99] H.-X. Wang, Q.-P. Yang, and Q.-M. Zheng, "Artificial neural network for transformer insulation aging diagnosis," in *Third International Conference on Electric Utility Deregulation and Restructuring and Power Technologies*, 2008, pp. 2233-2238.
- [100] W. Tang, S. Almas, and Q. H. Wu, "Transformer Dissolved Gas Analysis Using Least Square Support Vector Machine and Bootstrap," in *Control Conference, 2007. CCC 2007. Chinese*, 2007, pp. 482-486.
- [101] K. Bacha, S. Souahlia, and M. Gossa, "Power transformer fault diagnosis based on dissolved gas analysis by support vector machine," *Electric Power Systems Research*, vol. 83, pp. 73-79, 2012.
- [102] Z. J. Richardson, J. Fitch, W. H. Tang, J. Y. Goulermas, and Q. H. Wu, "A Probabilistic Classifier for Transformer Dissolved Gas Analysis With a Particle Swarm Optimizer," *IEEE Transactions on Power Delivery*, vol. 23, pp. 751-759, 2008.
- [103] D. Hydroelectric Research and Technical Services Group, Colorado, "Facilities, Illustrations, Standards and Techniques; Transformer Maintenance," *US Department of Interior Bureau of Reclamation*, vol. 3-30, pp. 1-81, October 2000.
- [104] T. O. Rouse, "Mineral insulating oil in transformers," *IEEE Electrical Insulation Magazine*, vol. 14, pp. 6-16, 1998.
- [105] X. Zhang and E. Gockenbach, "Asset-Management of Transformers Based on Condition Monitoring and Standard Diagnosis [Feature Article]," *IEEE Electrical Insulation Magazine*, vol. 24, pp. 26-40, 2008.
- [106] N. Lelekakis, J. Wijaya, D. Martin, and D. Susa, "The effect of acid accumulation in power-transformer oil on the aging rate of paper insulation," *IEEE Electrical Insulation Magazine*, vol. 30, pp. 19-26, 2014.
- [107] IEC, "Insulating liquids - Determination of acidity - Part 2: Colourimetric titration," *IEC 62021-2 Standard*, 2007.
- [108] "Standard Test Method for Acid and Base Number by Color-Indicator Titration " *ASTM D974-12*, 2012.
- [109] "Standard Test Method for Acid Number of Petroleum Products by Potentiometric Titration," *ASTM D644-01*, 2001.
- [110] D. Martin, T. Saha, T. Gray, and K. Wyper, "Determining water in transformer paper insulation: effect of measuring oil water activity at two different locations," *IEEE Electrical Insulation Magazine*, vol. 31, pp. 18-25, 2015.
- [111] L. E. Lundgaard, W. Hansen, D. Linhjell, and T. J. Painter, "Aging of oil-impregnated paper in power transformers," *IEEE Transactions on Power Delivery*, vol. 19, pp. 230-239, 2004.
- [112] IEC, "Insulating Liquids- Oil-impregnated paper and pressboard- Determination of water by automatic coulometric Karl Fischer titration," *IEC 60814 Standard*, 1997.
- [113] "Standard Test Method for Water in Insulating Liquids by Coulometric Karl Fischer Titration," *ASTM D1533-12*, 2012.
- [114] "Standard Test Method for Dielectric Breakdown Voltage of Insulating Liquids Using VDE Electrodes," *ASTM D1816-12*, 2012.
- [115] IEC, "Insulating liquids - Determination of the breakdown voltage at power frequency - Test method," *IEC 60156 Standard*, 1995.
- [116] "IEEE Guide for Acceptance and Maintenance of Insulating Oil in Equipment," *IEEE Std C57.106-2002 (Revision of IEEE Std C57.106-1991)*, pp. 0_1-27, 2002.
- [117] "Standard Test Method for Dissipation Factor (or Power Factor) and Relative Permittivity (Dielectric Constant) of Electrical Insulating Liquids," *ASTM D924-15*, 2015.
- [118] J. Mohan, *Organic Spectroscopy: Principles and Applications*: CRC ; New Delhi, 2000.
- [119] L. H. J. Lajunen, *Spectrochemical Analysis by Atomic Absorption and Emission*. Cambridge, UK: The Royal Society of Chemistry, 1992.
- [120] H.-H. Perkampus, *UV-VIS Spectroscopy and Its Applications*: Springer-Verlag Berlin Heidelberg, 1992.

- [121] C. Burgess, A. Knowles, and U. S. Group, *Standards in absorption spectrometry*: Chapman and Hall, 1981.
- [122] M. J. Shenton, H. Herman, R. J. Heywood, and G. C. Stevens, "The use of spectroscopy with chemometrics to assess the condition and predict the lifetime of paper and oil used as transformer insulation," in *Eighth International Conference on Dielectric Materials, Measurements and Applications, 2000. (IEE Conf. Publ. No. 473)*, 2000, pp. 346-351.
- [123] J. P. Percherancier and P. J. Vuarchex, "Fourier transform infrared (FT-IR) spectrometry to detect additives and contaminants in insulating oils," *IEEE Electrical Insulation Magazine*, vol. 14, pp. 23-29, 1998.
- [124] F. R. van de Voort, J. Sedman, R. Cocciardi, and S. Juneau, "An automated FTIR method for the routine quantitative determination of moisture in lubricants: An alternative to Karl Fischer titration," *Talanta*, vol. 72, pp. 289-295, 4/15/ 2007.
- [125] M. M. Hamada, M. A. A. Wahab, A. G. Zeitoun, and G. Ismail, "Infrared spectroscopy and ferrographic analysis of deposits in oil," in *High Voltage Engineering, 1999. Eleventh International Symposium on (Conf. Publ. No. 467)*, 1999, pp. 356-359 vol.3.
- [126] A. Georgiev, I. Karamancheva, and L. Topalova, "Determination of oxidation products in transformer oils using FT-IR spectroscopy," *Journal of Molecular Structure*, vol. 872, pp. 18-23, 1/15/ 2008.
- [127] Y. Liu, "Vibrational spectroscopic investigation of Australian cotton cellulose fibres: Part 1. A Fourier transform Raman study," *Analyst*, vol. 123, pp. 633-636, 1998.
- [128] H. H. Patrick J. Baird, Gary C. Stevens, "On-Site Analysis of Transformer Paper Insulation Using Portable Spectroscopy for Chemometric Prediction of Aged Condition," *IEEE Transactions on Dielectrics and Electrical Insulation*, vol. 15, p. 1089, 2008.
- [129] P. J. Baird, H. Herman, G. C. Stevens, and P. N. Jarman, "Spectroscopic measurement and analysis of water and oil in transformer insulating paper," *IEEE Transactions on Dielectrics and Electrical Insulation*, vol. 13, pp. 293-308, 2006.
- [130] P. J. S. Baird, H. Herman, and G. C. Stevens, "Non-destructive and in-situ analysis of insulating materials in high-voltage power transformers," in *Solid Dielectrics, 2004. ICSD 2004. Proceedings of the 2004 IEEE International Conference on*, 2004, pp. 719-722 Vol.2.
- [131] "Standard Test Method for Determination of the Relative Content Of Dissolved Decay Products in Mineral Insulating Oils by Spectrophotometry," *ASTM D6802 - 02(2010)* 2010.
- [132] A. Abu-Siada, "Correlation of furan concentration and spectral response of transformer oil-using expert systems," *IET Science, Measurement & Technology*, vol. 5, pp. 183-188, 2011.
- [133] S. P. Lai, A. Abu-Siada, S. M. Islam, and G. Lenco, "Correlation between UV-Vis spectral response and furan measurement of transformer oil," in *International Conference on Condition Monitoring and Diagnosis, 2008*, 2008, pp. 659-662.
- [134] J. Workman Jr, "UV-VIS Spectroscopy Charts," in *The Handbook of Organic Compounds*, ed Burlington: Academic Press, 2001, p. 63.
- [135] H. Kaur, *Spectroscopy*. Meerut, IND: Global Media, 2009.
- [136] C. Burgess, "UV-VIS spectroscopy : UV-VIS Spectroscopy and its Application, by H.-H. Perkampus (Translators: H. Charlotte Grinter and T.L. Threlfall) Springer, Berlin, 1992, DM 168 (244 pp.), ISBN: 0-387-5542 1 - 1," *TrAC Trends in Analytical Chemistry*, vol. 12, p. x, 1993.
- [137] N. A. Bakar, A. Abu-Siada, and S. Islam, "A review of dissolved gas analysis measurement and interpretation techniques," *IEEE Electrical Insulation Magazine*, vol. 30, pp. 39-49, 2014.
- [138] N. A. Bakar, A. Abu-Siada, and S. Islam, "A review on chemical diagnosis techniques for transformer paper insulation degradation," in *Australasian Universities Power Engineering Conference, AUPEC 2013*, 2013.

- [139] A. Abu-Siada, S. Hmood, and S. Islam, "A new fuzzy logic Approach for consistent interpretation of dissolved gas-in-oil analysis," *IEEE Transactions on Dielectrics and Electrical Insulation*, vol. 20, pp. 2343-2349, Dec 2013.
- [140] N. A. Bakar, and A. Abu-Siada, "A novel method of measuring transformer oil interfacial tension using UV-Vis spectroscopy," *IEEE Electrical Insulation Magazine*, vol. 32, pp. 7-13, 2016.
- [141] ASTM, "Standard Test Method for Interfacial Tension of Oil Against Water by the Ring Method," *D971 – 12*, 2012.
- [142] H. Malik, A. K. Yadav, Tarkeshwar, and R. K. Jarial, "Make use of UV/VIS spectrophotometer to determination of dissolved decay products in mineral insulating oils for transformer remnant life estimation with ANN," in *India Conference (INDICON), 2011 Annual IEEE*, 2011, pp. 1-6.
- [143] M. Duval, and L. Lamarre, "The Duval pentagon - a new complementary tool for the interpretation of dissolved gas analysis in transformers," *IEEE Electrical Insulation Magazine*, vol. 30, pp. 9-12, 2014.
- [144] N. A. Bakar, A. Abu-Siada, N. Das, and S. Islam, "Effect of conducting materials on UV-Vis spectral response characteristics," *Universal Journal of Electrical and Electronic Engineering*, pp. 81-86, 2013.
- [145] L. D. Field, S. Sternhell, and J. R. Kalman, *Organic Structures from Spectra*, 4th ed.: Wiley, 2011.
- [146] ASTM, "Standard Practice for Describing and Measuring Performance of Ultraviolet and Visible Spectrophotometers," *ASTM E275*, 2013.
- [147] J. Wada, G. Ueta, S. Okabe, and T. Amimoto, "Inhibition technique of transformer insulating oil degradation-evaluation of the effectiveness of oxidation degradation inhibitors," *IEEE Transactions on Dielectrics and Electrical Insulation*, vol. 20, pp. 1641-1648, 2013.
- [148] ASTM, "Standard Practice for Describing and Measuring Performance of Ultraviolet, Visible, and Near-Infrared Spectrophotometers,," *ASTM E275-01*, vol. 03.06, pp. 72-81, 2001.
- [149] T. V. Oommen, "Vegetable oils for liquid-filled transformers," *IEEE Electrical Insulation Magazine*, vol. 18, pp. 6-11, 2002.
- [150] B. Matharage, M. Fernando, M. Bandara, G. Jayantha, and C. Kalpage, "Performance of coconut oil as an alternative transformer liquid insulation," *IEEE Transactions on Dielectrics and Electrical Insulation*, vol. 20, pp. 887-898, 2013.
- [151] M. Zhixin and W. Jingyu, "Detection of dissolved gas in oil-insulated electrical apparatus by photoacoustic spectroscopy," *IEEE Electrical Insulation Magazine*, vol. 31, pp. 7-14, 2015.
- [152] M. B. Esler, D. W. T. Griffith, S. R. Wilson, and L. P. Steele, "Precision trace gas analysis by FT-IR spectroscopy. 1. Simultaneous analysis of CO₂, CH₄, N₂O, and CO in air," *Analytical Chemistry*, vol. 72, pp. 206-215, 2000.
- [153] L. S. Rothman, I. E. Gordon, D. C. Benner, P. F. Bernath, M. Birk, and e. al., "The HITRAN 2012 molecular spectroscopic database," *Journal of Quantitative Spectroscopy and Radiative Transfer*, vol. 130, pp. 4-50, 2013.
- [154] A. Kramida, Y. Ralchenko, J. Reader, and NIST-ASD-Team. NIST Atomic Spectra Database (Version 5.2) [Online]. Available: www.nist.gov/pml/data/asd.cfm
- [155] N. A. Bakar, A. Abu-Siada, S. Islam, and M. F. El-Naggar, "A new technique to measure interfacial tension of transformer oil using UV-Vis spectroscopy," *IEEE Transactions on Dielectrics and Electrical Insulation*, vol. 22, pp. 1275-1282, 2015.
- [156] ASTM, "Standard Practice for Condition Monitoring of Used Lubricants by Trend Analysis Using Fourier Transform Infrared (FT-IR) Spectrometry," *ASTM E2412*, 2010.
- [157] ASTM, "Standard Practice for Near Infrared Qualitative Analysis," *ASTM E1790-04(2010)*, 2010.
- [158] T. J. Ross, *Fuzzy logic with engineering applications*: John Wiley & Sons, 2009.
- [159] K. Tanaka, *An Introduction to Fuzzy Logic for Practical Applications*. New York, USA: Springer, 1996.

- [160] D. Martin, C. Yi, C. Ekanayake, M. Hui, and T. Saha, "An Updated Model to Determine the Life Remaining of Transformer Insulation," *IEEE Transactions on Power Delivery*, vol. 30, pp. 395-402, 2015.
- [161] "IEEE Guide for Loading Mineral-Oil-Immersed Transformers and Step-Voltage Regulators," *IEEE Std C57.91-2011* pp. 1-123, 2012.
- [162] "Power transformers - Part 7: Loading guide for oil-immersed power transformers," *IEC 60076-7:2005 Std*, 2005.
- [163] Z. Qian and Z. Yan, "Fuzzy synthetic method for life assessment of power transformer," *IEE Proceedings -Science, Measurement and Technology*, vol. 151, pp. 175-180, 2004.
- [164] T. K. Saha and P. Purkait, "Investigation of an expert system for the condition assessment of transformer insulation based on dielectric response measurements," *IEEE Transactions on Power Delivery*, vol. 19, pp. 1127-1134, 2004.
- [165] M. Arshad, S. Islam, and A. Khaliq, "Fuzzy logic approach in power transformers management and decision making," *IEEE Transactions on Dielectrics and Electrical Insulation*, vol. 21, pp. 2343-2354, 2014.
- [166] L. Chmura, P. H. F. Morshuis, J. J. Smit, and A. Janssen, "Life-data analysis for condition assessment of high-voltage assets," *IEEE Electrical Insulation Magazine*, vol. 31, pp. 33-43, 2015.
- [167] R. A. Jongen, P. H. F. Morshuis, E. Gulski, J. J. Smit, J. Maksymiuk, and A. L. J. Janssen, "Application of statistical methods for making maintenance decisions within power utilities," *IEEE Electrical Insulation Magazine*, vol. 22, pp. 24-35, 2006.
- [168] A. Jahromi, R. Piercy, S. Cress, J. Service, and W. Fan, "An approach to power transformer asset management using health index," *IEEE Electrical Insulation Magazine*, vol. 25, pp. 20-34, 2009.
- [169] A. E. B. Abu-Elanien, M. M. A. Salama, and M. Ibrahim, "Calculation of a Health Index for Oil-Immersed Transformers Rated Under 69 kV Using Fuzzy Logic," *IEEE Transactions on Power Delivery*, vol. 27, pp. 2029-2036, 2012.
- [170] D. Martin, C. Perkasa, and N. Lelekakis, "Measuring Paper Water Content of Transformers: A New Approach Using Cellulose Isotherms in Nonequilibrium Conditions," *IEEE Transactions on Power Delivery*, vol. 28, pp. 1433-1439, 2013.
- [171] M. Kohtoh, S. Kaneko, S. Okabe, and T. Amimoto, "Aging effect on electrical characteristics of insulating oil in field transformer," *IEEE Transactions on Dielectrics and Electrical Insulation*, vol. 16, pp. 1698-1706, 2009.

"Every reasonable effort has been made to acknowledge the owners of copyright material. I would be pleased to hear from any copyright owner who has been omitted or incorrectly acknowledge."

Appendix A Properties of 55 Transformers Used for IFT

No.	Manufacturer	Year	Rating	Ratio	Oil Type	Volume
1	British Thompson Houston Co Ltd	1936	1000 kVA	3300/415	Diala BX	1,614 LTS
2	STANDARD WAYGOOD (GEC)	1973	1.9 MVA	11000/415	Diala BX	2412 LTS
3	PARSON PEEBLES	1973	585 MVA	22000/358000	Diala BX	65,918 LTS
4	WESTINGHOUSE ELECTRIC	1973	56kVA	50000/415	Diala BX	680 LTS
5	WESTINGHOUSE ELECTRIC	1973	56kVA	70000/415	Diala BX	680 LTS
6	TYREE	1974	2.4 MVA	11000/415	Diala BX	2503 LTS
7	TYREE	1974	2.4 MVA	11000/415	Diala BX	2503 LTS
8	ENGLISH ELEC (GEC)	1974	1.16 MVA	6600/415	Diala BX	2,227 LTS
9	TYREE	1975	2.4 MVA	11000/415	Diala BX	2,325 LTS
10	TYREE	1975	2.4 MVA	11000/415	Diala BX	2,325 LTS
11	WESTINGHOUSE ELECTRIC	1975	56kVA	70000/415	Diala BX	680 LTS
12	TYREE	1977	2.4 MVA	11000/415	Diala BX	2,325 LTS
13	PARSON PEEBLES	1978	585 MVA	22000/358000	Diala BX	66,735 LTS
14	TYREE	1979	2.4 MVA	11000/415	Diala BX	2,325 LTS
15	TYREE	1979	2.4 MVA	11000/415	Diala BX	2,325 LTS
16	TYREE	1979	2.4 MVA	11000/415	Diala BX	2,325 LTS
17	WILSON	1979	1.25 kVA	3300/415	Diala BX	1,330 LTS
18	WILSON	1979	1.25 Kva	3300/415	Diala BX	1,330 LTS
19	TYREE	1979	22.5MVA	22000/11000	Diala BX	9,220 LTS
20	TYREE	1979	22.5MVA	22000/11000	Diala BX	9,220 LTS
21	TYREE	1979	12/19MVA	22000/3300	Diala BX	7,000 LTS
22	TYREE	1979	12/19MVA	22000/3300	Diala BX	7,000 LTS
23	WESTINGHOUSE ELECTRIC	1979	56kVA	70000/415	Diala BX	680 LTS
24	WESTINGHOUSE ELECTRIC	1979	56 Kva	50000/415	Diala BX	680 LTS
25	WESTINGHOUSE ELEC,AUST	1980	1.5 MVA	66000/425	Diala BX	2,364 LTS
26	WILSON	1980	750kVA	11000/415	Diala BX	940 LTS
27	WILSON	1980	750 kVA	11000/415	Diala BX	940 LTS
28	ABB Power Transmission (Tyree)	1981	6 MVA	66000/3300	Diala BX	6645 LTS
29	ABB Power Transmission (Tyree)	1981	6 MVA	66000/3300	Diala BX	6645 LTS
30	ABB Power Transmission (Tyree)	1981	150 KVA	3300/415	Diala BX	725 LTS
31	ABB Power Transmission (Tyree)	1985	45 MVA	23000/10000	Diala BX	19,640 LTS
32	ABB Power Transmission (Tyree)	1985	45 MVA	23000/10000	Diala BX	19,640 LTS
33	Toshiba	1985	7500 KVA	23000/11000	Diala BX	6,250 LTS
34	ABB Power Transmission (Tyree)	1986	15 MVA	11000/3300	Diala BX	7,640 LTS
35	ABB Power Transmission (Tyree)	1986	22 MVA	66000/11000	Diala BX	17,645 LTS
36	ABB Power Transmission (Tyree)	1986	45 MVA	23000/10000	Diala BX	19,640 LTS
37	ABB Power Transmission (Tyree)	1986	45 MVA	23000/10000	Diala BX	19,640 LTS
38	Toshiba	1986	7500 KVA	23000/11000	Diala BX	6,250 LTS
39	ALSTROM (GEC)	1990	28/55 MVA	3000/1100/371	Diala BX	26,820 LTS
40	ALSTROM (GEC)	1990	28/55 MVA	3000/1100/371	Diala BX	26820 LTS
41	ABB Power Transmission (Tyree)	1991	390 MVA	23000/330000	Diala BX	106,830 LTS
42	ALSTOM (GEC Alstom)	1991	390 MVA	23000/330000	Diala BX	78,920 LTS
43	ALSTOM (GEC Alstom)	1991	390 MVA	23000/330000	Diala BX	78,920 LTS
44	ABB Power Transmission (Tyree)	1992	390 MVA	23000/330000	Diala BX	88,548 LTS
45	CASTLET AUST,	1994	56kVA	95000/415	Diala BX	680 LTS
46	CASTLET AUST,	1994	95kVA	95000/415	Diala BX	400 LTS
47	KRAFT	2000	59 kVA	70000/415	Diala BX	270 LTS
48	KRAFT	2000	59kVA	70000/415	Diala BX	270 LTS
49	ABB	2002	500kVA	11,000/415	Diala BX	883 LTS
50	KRAFT	2004	59kVA	70000/415	Diala BX	270 LTS
51	WILSON	2008	30MVA	22000/11900	Diala BX	14,390 LTS
52	WILSON	2008	19MVA	22000/3600	Diala BX	15,436 LTS
53	WILSON	2009	25MVA	11900/3600	Diala BX	17200 LTS
54	Wilson Transformer Co	2009	60 MVA	132000/11900	Diala BX	25700 LTS
55	AREVA	2010	585MVA	22000/358000	Diala BX	83740 LTS

Appendix B Repeatability Test Results of IFT Measurement

No.	Test 1			Test 2			Test 3			Average		
	IFT (mN/m)	ABS	BW (nm)	IFT (mN/m)	ABS	BW (nm)	IFT (mN/m)	ABS	BW (nm)	IFT (mN/m)	ABS	BW (nm)
1	41.2	1.63	359	41.1	1.62	358	41.2	1.62	359	41.17	1.62	358.67
2	41.4	1.66	360	41.4	1.66	359	41.4	1.66	359	41.40	1.66	359.33
3	39.7	1.64	365	39.8	1.65	364	39.8	1.64	364	39.77	1.64	364.33
4	38.5	1.73	364	38.4	1.72	361	38.4	1.71	362	38.43	1.72	362.33
5	36.1	1.67	369	36	1.68	369	36	1.67	368	36.03	1.67	368.67
6	34	1.69	374	34	1.69	375	34.1	1.68	374	34.03	1.69	374.33
7	32.4	1.71	374	32.4	1.71	374	32.4	1.71	374	32.40	1.71	374.00
8	30.8	1.74	376	30.8	1.73	377	30.8	1.75	377	30.80	1.74	376.67
9	27	1.78	381	27	1.78	381	27	1.79	381	27.00	1.78	381.00
10	27	1.82	381	27	1.8	381	27	1.8	382	27.00	1.81	381.33
11	25.6	1.83	393	25.6	1.83	393	25.6	1.83	393	25.60	1.83	393.00
12	23.4	1.91	412	23.4	1.91	410	23.4	1.91	411	23.40	1.91	411.00
13	21.6	2.07	427	21.6	2.07	427	21.6	2.07	427	21.60	2.07	427.00
14	20.3	1.89	425	20.2	1.89	425	20.3	1.88	425	20.27	1.89	425.00
15	19.2	2.21	460	19.2	2.21	460	19.2	2.21	460	19.20	2.21	460.00
16	17.1	2.36	477	17.1	2.36	476	17.2	2.36	477	17.13	2.36	476.67
17	16.8	2.54	479	16.8	2.56	478	16.8	2.55	479	16.80	2.55	478.67
18	15.8	2.68	484	15.8	2.69	485	15.8	2.68	485	15.80	2.68	484.67
19	15.5	2.72	488	15.6	2.71	488	15.5	2.72	489	15.53	2.72	488.33
20	14.5	2.81	494	14.5	2.81	494	14.5	2.8	493	14.50	2.81	493.67

Appendix C Properties of various oil types used for the results of Figure 3-8

Oil Types	FR3	Nyro 10GBN	Shell Diala BX	Castrol
Chemical Types	Ester	Uninhibited Mineral	Inhibited Mineral	Inhibited Mineral
Interfacial Tension (mN/m)	24	40.5	42	41.8
Breakdown Voltage (kV)	70	76	76	76
Water Content (mg/kg)	61.6	8	8	8
Acidity (mgKOH/g)	0.06	0.02	0.02	0.02

Appendix D Fuzzy Rules: IFT Estimation Model

1. If (Absorbance is Low) and (Bandwidth(nm) is Too_Small) then (IFT is Very_Good) (1)
2. If (Absorbance is Low) and (Bandwidth(nm) is Small) then (IFT is Very_Good) (1)
3. If (Absorbance is Low) and (Bandwidth(nm) is Medium) then (IFT is Good) (1)
4. If (Absorbance is Low) and (Bandwidth(nm) is Big) then (IFT is Marginally_Critical) (1)
5. If (Absorbance is Low) and (Bandwidth(nm) is Too_Big) then (IFT is Bad) (1)
6. If (Absorbance is Low-Medium) and (Bandwidth(nm) is Too_Small) then (IFT is Very_Good) (1)
7. If (Absorbance is Low-Medium) and (Bandwidth(nm) is Small) then (IFT is Good) (1)
8. If (Absorbance is Low-Medium) and (Bandwidth(nm) is Medium) then (IFT is Marginally_Critical) (1)
9. If (Absorbance is Low-Medium) and (Bandwidth(nm) is Big) then (IFT is Bad) (1)
10. If (Absorbance is Low-Medium) and (Bandwidth(nm) is Too_Big) then (IFT is Very_Bad) (1)
11. If (Absorbance is Medium) and (Bandwidth(nm) is Too_Small) then (IFT is Good) (1)
12. If (Absorbance is Medium) and (Bandwidth(nm) is Small) then (IFT is Marginally_Critical) (1)
13. If (Absorbance is Medium) and (Bandwidth(nm) is Medium) then (IFT is Marginally_Critical) (1)
14. If (Absorbance is Medium) and (Bandwidth(nm) is Big) then (IFT is Bad) (1)
15. If (Absorbance is Medium) and (Bandwidth(nm) is Too_Big) then (IFT is Very_Bad) (1)
16. If (Absorbance is High) and (Bandwidth(nm) is Too_Small) then (IFT is Marginally_Critical) (1)
17. If (Absorbance is High) and (Bandwidth(nm) is Small) then (IFT is Marginally_Critical) (1)
18. If (Absorbance is High) and (Bandwidth(nm) is Medium) then (IFT is Bad) (1)
19. If (Absorbance is High) and (Bandwidth(nm) is Big) then (IFT is Very_Bad) (1)
20. If (Absorbance is High) and (Bandwidth(nm) is Too_Big) then (IFT is Very_Bad) (1)
21. If (Absorbance is High) and (Bandwidth(nm) is Too_Small) then (IFT is Marginally_Critical) (1)
22. If (Absorbance is High) and (Bandwidth(nm) is Small) then (IFT is Bad) (1)
23. If (Absorbance is High) and (Bandwidth(nm) is Medium) then (IFT is Bad) (1)
24. If (Absorbance is High) and (Bandwidth(nm) is Big) then (IFT is Very_Bad) (1)
25. If (Absorbance is High) and (Bandwidth(nm) is Too_Big) then (IFT is Very_Bad) (1)

Appendix E FTIR Repeatability Test Results

	Sample No.	ppm	Measurement 1		Measurement 2		Measurement 3		Average	
			ABS	Area	ABS	Area	ABS	Area	ABS	Area
Carbon Dioxide	1	155	0.016	1.29	0.016	1.28	0.016	1.29	0.016	1.287
	2	464	0.021	2.07	0.02	2.07	0.02	2.07	0.020	2.070
	3	714	0.07	3.75	0.07	3.76	0.07	3.75	0.070	3.753
	4	1140	0.0822	4.17	0.082	4.17	0.082	4.17	0.082	4.170
	5	1515	0.121	7.3	0.121	7.3	0.12	7.3	0.121	7.300
	6	2705	0.15	7.6	0.15	7.62	0.15	7.6	0.150	7.607
	7	4107	0.175	7.92	0.174	7.94	0.175	7.94	0.175	7.933
Methane	1	0	0.27	26	0.27	26	0.26	27	0.267	26.333
	2	5	0.49	50	0.48	51	0.48	50	0.483	50.333
	3	12	0.622	81	0.623	82	0.623	82	0.623	81.667
	4	30	0.987	123	0.987	123	0.987	123	0.987	123.000
	5	60	1.027	190	1.029	189	1.027	189	1.028	189.333
	6	154	1.192	224	1.194	223	1.192	223	1.193	223.333
	7	322	1.48	235	1.49	235	1.48	235	1.483	235.000
Acetylene	1	0	0.1	0.93	0.1	0.93	0.1	0.93	0.100	0.930
	2	5	0.128	1	0.128	1.02	0.128	1	0.128	1.007
	3	12	0.2	1.36	0.2	1.35	0.202	1.35	0.201	1.353
	4	30	0.424	4.42	0.427	4.43	0.426	4.44	0.426	4.430
	5	60	0.612	4.98	0.614	4.99	0.612	4.98	0.613	4.983
	6	181	0.76	7.35	0.79	7.35	0.79	7.35	0.780	7.350
	7	312	0.818	8.32	0.817	8.3	0.817	8.3	0.817	8.307
Ethane	1	0	0.157	0.45	0.156	0.44	0.158	0.45	0.157	0.447
	2	10	0.218	0.48	0.216	0.46	0.216	0.46	0.217	0.467
	3	24	0.331	0.62	0.333	0.64	0.332	0.62	0.332	0.627
	4	85	0.476	1.9044	0.476	1.9044	0.475	1.9044	0.476	1.904
	5	152	0.88	2.279	0.88	2.278	0.88	2.278	0.880	2.278
	6	188	0.901	3.32	0.9	3.321	0.901	3.321	0.901	3.321
	7	282	0.912	3.587	0.91	3.587	0.91	3.5867	0.911	3.587
Ethylene	1	0	0.0133	0.43	0.0134	0.45	0.0134	0.45	0.013	0.443
	2	10	0.0159	0.46	0.0159	0.45	0.0159	0.46	0.016	0.457
	3	57	0.033	0.61	0.033	0.61	0.034	0.62	0.033	0.613
	4	80	0.0456	1.9054	0.0455	1.9044	0.0455	1.9044	0.046	1.905
	5	121	0.89	2.28	0.88	2.277	0.88	2.278	0.883	2.278
	6	275	0.093	3.323	0.092	3.321	0.091	3.321	0.092	3.322
	7	339	0.137	3.587	0.137	3.587	0.137	3.5867	0.137	3.587
Carbon Monoxide	1	0	0.0045	0.28	0.0045	0.29	0.0047	0.28	0.005	0.283
	2	15	0.0056	0.65	0.0056	0.64	0.0056	0.65	0.006	0.647
	3	44	0.0108	1.68	0.0108	1.68	0.0108	1.68	0.011	1.680
	4	84	0.0123	2.04	0.0123	2.02	0.0123	2.02	0.012	2.027
	5	128	0.0142	2.36	0.0144	2.36	0.0142	2.36	0.014	2.360
	6	235	0.0192	3.02	0.0192	3.02	0.0192	3.02	0.019	3.020
	7	415	0.0263	4.85	0.0261	4.82	0.0263	4.8	0.026	4.823

Appendix F Fuzzy Rules: CO Concentration Estimation Model

1. If (Peak__Absorbance is A1) and (Area is B1) then (Carbon__Monoxide is F1) (1)
2. If (Peak__Absorbance is A1) and (Area is B2) then (Carbon__Monoxide is F1) (1)
3. If (Peak__Absorbance is A1) and (Area is B3) then (Carbon__Monoxide is F2) (1)
4. If (Peak__Absorbance is A2) and (Area is B1) then (Carbon__Monoxide is F2) (1)
5. If (Peak__Absorbance is A2) and (Area is B2) then (Carbon__Monoxide is F3) (1)
6. If (Peak__Absorbance is A2) and (Area is B3) then (Carbon__Monoxide is F3) (1)
7. If (Peak__Absorbance is A2) and (Area is B4) then (Carbon__Monoxide is F4) (1)
8. If (Peak__Absorbance is A3) and (Area is B2) then (Carbon__Monoxide is F4) (1)
9. If (Peak__Absorbance is A3) and (Area is B3) then (Carbon__Monoxide is F5) (1)
10. If (Peak__Absorbance is A3) and (Area is B4) then (Carbon__Monoxide is F6) (1)
11. If (Peak__Absorbance is A4) and (Area is B3) then (Carbon__Monoxide is F6) (1)
12. If (Peak__Absorbance is A4) and (Area is B4) then (Carbon__Monoxide is F7) (1)
13. If (Peak__Absorbance is A4) and (Area is B5) then (Carbon__Monoxide is F7) (1)
14. If (Peak__Absorbance is A5) and (Area is B3) then (Carbon__Monoxide is F7) (1)
15. If (Peak__Absorbance is A5) and (Area is B4) then (Carbon__Monoxide is F8) (1)
16. If (Peak__Absorbance is A5) and (Area is B5) then (Carbon__Monoxide is F8) (1)

Appendix G Fuzzy Rules: CO₂ Concentration Estimation Model

1. If (Peak_Absorbance is A1) and (Area is B1) then (Carbon_Dioxide is F1) (1)
2. If (Peak_Absorbance is A1) and (Area is B2) then (Carbon_Dioxide is F1) (1)
3. If (Peak_Absorbance is A1) and (Area is B3) then (Carbon_Dioxide is F2) (1)
4. If (Peak_Absorbance is A2) and (Area is B1) then (Carbon_Dioxide is F1) (1)
5. If (Peak_Absorbance is A2) and (Area is B2) then (Carbon_Dioxide is F3) (1)
6. If (Peak_Absorbance is A2) and (Area is B3) then (Carbon_Dioxide is F3) (1)
7. If (Peak_Absorbance is A2) and (Area is B4) then (Carbon_Dioxide is F4) (1)
8. If (Peak_Absorbance is A3) and (Area is B2) then (Carbon_Dioxide is F4) (1)
9. If (Peak_Absorbance is A3) and (Area is B3) then (Carbon_Dioxide is F5) (1)
10. If (Peak_Absorbance is A3) and (Area is B4) then (Carbon_Dioxide is F5) (1)
11. If (Peak_Absorbance is A4) and (Area is B3) then (Carbon_Dioxide is F6) (1)
12. If (Peak_Absorbance is A4) and (Area is B4) then (Carbon_Dioxide is F8) (1)
13. If (Peak_Absorbance is A4) and (Area is B5) then (Carbon_Dioxide is F7) (1)
14. If (Peak_Absorbance is A5) and (Area is B3) then (Carbon_Dioxide is F7) (1)
15. If (Peak_Absorbance is A5) and (Area is B4) then (Carbon_Dioxide is F8) (1)
16. If (Peak_Absorbance is A5) and (Area is B5) then (Carbon_Dioxide is F8) (1)

Appendix H Fuzzy Rules: CH₄ Concentration Estimation Model

1. If (Peak__Absorbance is A1) and (Area is B1) then (Mathane is F1) (1)
2. If (Peak__Absorbance is A1) and (Area is B2) then (Mathane is F1) (1)
3. If (Peak__Absorbance is A1) and (Area is B3) then (Mathane is F2) (1)
4. If (Peak__Absorbance is A2) and (Area is B1) then (Mathane is F1) (1)
5. If (Peak__Absorbance is A2) and (Area is B2) then (Mathane is F2) (1)
6. If (Peak__Absorbance is A2) and (Area is B3) then (Mathane is F3) (1)
7. If (Peak__Absorbance is A2) and (Area is B4) then (Mathane is F4) (1)
8. If (Peak__Absorbance is A3) and (Area is B2) then (Mathane is F4) (1)
9. If (Peak__Absorbance is A3) and (Area is B3) then (Mathane is F4) (1)
10. If (Peak__Absorbance is A3) and (Area is B4) then (Mathane is F5) (1)
11. If (Peak__Absorbance is A4) and (Area is B3) then (Mathane is F6) (1)
12. If (Peak__Absorbance is A4) and (Area is B4) then (Mathane is F7) (1)
13. If (Peak__Absorbance is A4) and (Area is B5) then (Mathane is F8) (1)
14. If (Peak__Absorbance is A5) and (Area is B3) then (Mathane is F8) (1)
15. If (Peak__Absorbance is A5) and (Area is B4) then (Mathane is F9) (1)
16. If (Peak__Absorbance is A5) and (Area is B5) then (Mathane is F9) (1)
17. If (Peak__Absorbance is A4) and (Area is B4) then (Mathane is F8) (1)

Appendix I Fuzzy Rules: C₂H₂ Concentration Estimation Model

1. If (Peak__Absorbance is A1) and (Area is B1) then (Acythelene is F1) (1)
2. If (Peak__Absorbance is A1) and (Area is B2) then (Acythelene is F1) (1)
3. If (Peak__Absorbance is A1) and (Area is B3) then (Acythelene is F2) (1)
4. If (Peak__Absorbance is A2) and (Area is B1) then (Acythelene is F1) (1)
5. If (Peak__Absorbance is A2) and (Area is B2) then (Acythelene is F2) (1)
6. If (Peak__Absorbance is A2) and (Area is B3) then (Acythelene is F3) (1)
7. If (Peak__Absorbance is A2) and (Area is B4) then (Acythelene is F3) (1)
8. If (Peak__Absorbance is A3) and (Area is B2) then (Acythelene is F3) (1)
9. If (Peak__Absorbance is A3) and (Area is B3) then (Acythelene is F4) (1)
10. If (Peak__Absorbance is A3) and (Area is B4) then (Acythelene is F5) (1)
11. If (Peak__Absorbance is A4) and (Area is B3) then (Acythelene is F6) (1)
12. If (Peak__Absorbance is A4) and (Area is B4) then (Acythelene is F7) (1)
13. If (Peak__Absorbance is A4) and (Area is B5) then (Acythelene is F8) (1)
14. If (Peak__Absorbance is A5) and (Area is B3) then (Acythelene is F8) (1)
15. If (Peak__Absorbance is A5) and (Area is B4) then (Acythelene is F9) (1)
16. If (Peak__Absorbance is A5) and (Area is B5) then (Acythelene is F9) (1)
17. If (Peak__Absorbance is A4) and (Area is B4) then (Acythelene is F8) (1)

Appendix J Fuzzy Rules: C₂H₆ Concentration Estimation Model

1. If (Peak__Absorbance is A1) and (Area is B1) then (Ethane is F1) (1)
2. If (Peak__Absorbance is A1) and (Area is B2) then (Ethane is F1) (1)
3. If (Peak__Absorbance is A1) and (Area is B3) then (Ethane is F2) (1)
4. If (Peak__Absorbance is A2) and (Area is B1) then (Ethane is F2) (1)
5. If (Peak__Absorbance is A2) and (Area is B2) then (Ethane is F3) (1)
6. If (Peak__Absorbance is A2) and (Area is B3) then (Ethane is F3) (1)
7. If (Peak__Absorbance is A2) and (Area is B4) then (Ethane is F3) (1)
8. If (Peak__Absorbance is A3) and (Area is B2) then (Ethane is F3) (1)
9. If (Peak__Absorbance is A3) and (Area is B3) then (Ethane is F4) (1)
10. If (Peak__Absorbance is A3) and (Area is B4) then (Ethane is F5) (1)
11. If (Peak__Absorbance is A4) and (Area is B3) then (Ethane is F5) (1)
12. If (Peak__Absorbance is A4) and (Area is B4) then (Ethane is F6) (1)
13. If (Peak__Absorbance is A4) and (Area is B5) then (Ethane is F7) (1)
14. If (Peak__Absorbance is A5) and (Area is B3) then (Ethane is F8) (1)
15. If (Peak__Absorbance is A5) and (Area is B4) then (Ethane is F9) (1)
16. If (Peak__Absorbance is A5) and (Area is B5) then (Ethane is F9) (1)
17. If (Peak__Absorbance is A4) and (Area is B2) then (Ethane is F5) (1)

Appendix K Fuzzy Rules: C₂H₄ Concentration Estimation Model

1. If (Peak__Absorbance is A1) and (Area is B1) then (Ethylene is F1) (1)
2. If (Peak__Absorbance is A1) and (Area is B2) then (Ethylene is F1) (1)
3. If (Peak__Absorbance is A1) and (Area is B3) then (Ethylene is F2) (1)
4. If (Peak__Absorbance is A2) and (Area is B1) then (Ethylene is F2) (1)
5. If (Peak__Absorbance is A2) and (Area is B2) then (Ethylene is F3) (1)
6. If (Peak__Absorbance is A2) and (Area is B3) then (Ethylene is F3) (1)
7. If (Peak__Absorbance is A2) and (Area is B4) then (Ethylene is F3) (1)
8. If (Peak__Absorbance is A3) and (Area is B2) then (Ethylene is F4) (1)
9. If (Peak__Absorbance is A3) and (Area is B3) then (Ethylene is F4) (1)
10. If (Peak__Absorbance is A3) and (Area is B4) then (Ethylene is F5) (1)
11. If (Peak__Absorbance is A4) and (Area is B3) then (Ethylene is F6) (1)
12. If (Peak__Absorbance is A4) and (Area is B4) then (Ethylene is F7) (1)
13. If (Peak__Absorbance is A4) and (Area is B5) then (Ethylene is F8) (1)
14. If (Peak__Absorbance is A5) and (Area is B3) then (Ethylene is F8) (1)
15. If (Peak__Absorbance is A5) and (Area is B4) then (Ethylene is F8) (1)
16. If (Peak__Absorbance is A5) and (Area is B5) then (Ethylene is F9) (1)
17. If (Peak__Absorbance is A4) and (Area is B4) then (Ethylene is F8) (1)
18. If (Peak__Absorbance is A4) and (Area is B2) then (Ethylene is F5) (1)

Appendix L Fuzzy Rules: Furan Criticality Model

-
1. If (Furan is Normal) and (Furan__Rate is Low) then (Paper__Life is Normal) (1)
 2. If (Furan is Normal) and (Furan__Rate is Low-Medium) then (Paper__Life is Accelerated) (1)
 3. If (Furan is Normal) and (Furan__Rate is Medium) then (Paper__Life is Excessive) (1)
 4. If (Furan is Normal) and (Furan__Rate is Medium-High) then (Paper__Life is Excessive) (1)
 5. If (Furan is Normal) and (Furan__Rate is High) then (Paper__Life is HighRisk) (1)
 6. If (Furan is Moderate) and (Furan__Rate is Low) then (Paper__Life is Normal) (1)
 7. If (Furan is Moderate) and (Furan__Rate is Low-Medium) then (Paper__Life is Accelerated) (1)
 8. If (Furan is Moderate) and (Furan__Rate is Medium) then (Paper__Life is Excessive) (1)
 9. If (Furan is Moderate) and (Furan__Rate is Medium-High) then (Paper__Life is HighRisk) (1)
 10. If (Furan is Moderate) and (Furan__Rate is High) then (Paper__Life is HighRisk) (1)
 11. If (Furan is Accelerated) and (Furan__Rate is Low) then (Paper__Life is Accelerated) (1)
 12. If (Furan is Accelerated) and (Furan__Rate is Low-Medium) then (Paper__Life is Excessive) (1)
 13. If (Furan is Accelerated) and (Furan__Rate is Medium) then (Paper__Life is HighRisk) (1)
 14. If (Furan is Accelerated) and (Furan__Rate is Medium-High) then (Paper__Life is HighRisk) (1)
 15. If (Furan is Accelerated) and (Furan__Rate is High) then (Paper__Life is EndLife) (1)
 16. If (Furan is Extensive) and (Furan__Rate is Low) then (Paper__Life is Excessive) (1)
 17. If (Furan is Extensive) and (Furan__Rate is Low-Medium) then (Paper__Life is HighRisk) (1)
 18. If (Furan is Extensive) and (Furan__Rate is Medium) then (Paper__Life is HighRisk) (1)
 19. If (Furan is Extensive) and (Furan__Rate is Medium-High) then (Paper__Life is EndLife) (1)
 20. If (Furan is Extensive) and (Furan__Rate is High) then (Paper__Life is EndLife) (1)
 21. If (Furan is EndLife) and (Furan__Rate is Low) then (Paper__Life is EndLife) (1)
 22. If (Furan is EndLife) and (Furan__Rate is Low-Medium) then (Paper__Life is EndLife) (1)
 23. If (Furan is EndLife) and (Furan__Rate is Medium) then (Paper__Life is EndLife) (1)
 24. If (Furan is EndLife) and (Furan__Rate is Medium-High) then (Paper__Life is EndLife) (1)
 25. If (Furan is EndLife) and (Furan__Rate is High) then (Paper__Life is EndLife) (1)

Appendix M Fuzzy Rules: CO Ratio Criticality Model

1. If (CO2/CO__Ratio is High__Risk) and (CO__Rate is Normal) then (Paper__Deterioration is Significant) (1)
2. If (CO2/CO__Ratio is High__Risk) and (CO__Rate is Minor) then (Paper__Deterioration is Significant) (1)
3. If (CO2/CO__Ratio is High__Risk) and (CO__Rate is Major) then (Paper__Deterioration is Significant) (1)
4. If (CO2/CO__Ratio is High__Risk) and (CO__Rate is Critical) then (Paper__Deterioration is Significant) (1)
5. If (CO2/CO__Ratio is Critical) and (CO__Rate is Normal) then (Paper__Deterioration is High) (1)
6. If (CO2/CO__Ratio is Critical) and (CO__Rate is Minor) then (Paper__Deterioration is High) (1)
7. If (CO2/CO__Ratio is Critical) and (CO__Rate is Major) then (Paper__Deterioration is Significant) (1)
8. If (CO2/CO__Ratio is Critical) and (CO__Rate is Critical) then (Paper__Deterioration is Significant) (1)
9. If (CO2/CO__Ratio is Moderate) and (CO__Rate is Normal) then (Paper__Deterioration is Low) (1)
10. If (CO2/CO__Ratio is Moderate) and (CO__Rate is Minor) then (Paper__Deterioration is Low) (1)
11. If (CO2/CO__Ratio is Moderate) and (CO__Rate is Major) then (Paper__Deterioration is High) (1)
12. If (CO2/CO__Ratio is Moderate) and (CO__Rate is Critical) then (Paper__Deterioration is Significant) (1)
13. If (CO2/CO__Ratio is Normal) and (CO__Rate is Normal) then (Paper__Deterioration is Normal) (1)
14. If (CO2/CO__Ratio is Normal) and (CO__Rate is Minor) then (Paper__Deterioration is Low) (1)
15. If (CO2/CO__Ratio is Normal) and (CO__Rate is Major) then (Paper__Deterioration is High) (1)
16. If (CO2/CO__Ratio is Normal) and (CO__Rate is Critical) then (Paper__Deterioration is Significant) (1)

Appendix N Fuzzy Rules: Paper Aging Criticality Model

1. If (Paper__Life is EndLife) and (Paper__Deterioration is Normal) then (Ageing__Criticality is Significant) (1)
2. If (Paper__Life is EndLife) and (Paper__Deterioration is ModerateLow) then (Ageing__Criticality is Significant) (1)
3. If (Paper__Life is EndLife) and (Paper__Deterioration is High) then (Ageing__Criticality is Significant) (1)
4. If (Paper__Life is EndLife) and (Paper__Deterioration is Significant) then (Ageing__Criticality is Significant) (1)
5. If (Paper__Life is HighRisk) and (Paper__Deterioration is Normal) then (Ageing__Criticality is High) (1)
6. If (Paper__Life is HighRisk) and (Paper__Deterioration is ModerateLow) then (Ageing__Criticality is High) (1)
7. If (Paper__Life is HighRisk) and (Paper__Deterioration is High) then (Ageing__Criticality is High) (1)
8. If (Paper__Life is HighRisk) and (Paper__Deterioration is Significant) then (Ageing__Criticality is Significant) (1)
9. If (Paper__Life is Excessive) and (Paper__Deterioration is Normal) then (Ageing__Criticality is Low) (1)
10. If (Paper__Life is Excessive) and (Paper__Deterioration is ModerateLow) then (Ageing__Criticality is High) (1)
11. If (Paper__Life is Excessive) and (Paper__Deterioration is High) then (Ageing__Criticality is High) (1)
12. If (Paper__Life is Excessive) and (Paper__Deterioration is Significant) then (Ageing__Criticality is High) (1)
13. If (Paper__Life is Accelerated) and (Paper__Deterioration is Normal) then (Ageing__Criticality is Normal) (1)
14. If (Paper__Life is Accelerated) and (Paper__Deterioration is ModerateLow) then (Ageing__Criticality is Low) (1)
15. If (Paper__Life is Accelerated) and (Paper__Deterioration is High) then (Ageing__Criticality is Low) (1)
16. If (Paper__Life is Accelerated) and (Paper__Deterioration is Significant) then (Ageing__Criticality is High) (1)
17. If (Paper__Life is Normal) and (Paper__Deterioration is Normal) then (Ageing__Criticality is Normal) (1)
18. If (Paper__Life is Normal) and (Paper__Deterioration is ModerateLow) then (Ageing__Criticality is Normal) (1)
19. If (Paper__Life is Normal) and (Paper__Deterioration is High) then (Ageing__Criticality is Low) (1)
20. If (Paper__Life is Normal) and (Paper__Deterioration is Significant) then (Ageing__Criticality is Low) (1)

Appendix O Fuzzy Rules: Relative Accelerating Aging Criticality Model

1. If (Temp__Change is Low) and (Moisture is Dry) and (Oxygen is Low) then (Relative__Aging is Normal) (1)
2. If (Temp__Change is Low) and (Moisture is Dry) and (Oxygen is Medium) then (Relative__Aging is Low) (1)
3. If (Temp__Change is Low) and (Moisture is Dry) and (Oxygen is High) then (Relative__Aging is Low) (1)
4. If (Temp__Change is Low) and (Moisture is Moderate) and (Oxygen is Low) then (Relative__Aging is Normal) (1)
5. If (Temp__Change is Low) and (Moisture is Moderate) and (Oxygen is Medium) then (Relative__Aging is Low) (1)
6. If (Temp__Change is Low) and (Moisture is Moderate) and (Oxygen is High) then (Relative__Aging is Moderate) (1)
7. If (Temp__Change is Low) and (Moisture is Critical) and (Oxygen is Low) then (Relative__Aging is Low) (1)
8. If (Temp__Change is Low) and (Moisture is Critical) and (Oxygen is Medium) then (Relative__Aging is Moderate) (1)
9. If (Temp__Change is Low) and (Moisture is Critical) and (Oxygen is High) then (Relative__Aging is High) (1)
10. If (Temp__Change is Low) and (Moisture is Wet) and (Oxygen is Low) then (Relative__Aging is Moderate) (1)
11. If (Temp__Change is Low) and (Moisture is Wet) and (Oxygen is Medium) then (Relative__Aging is Significant) (1)
12. If (Temp__Change is Low) and (Moisture is Wet) and (Oxygen is High) then (Relative__Aging is Significant) (1)
13. If (Temp__Change is Moderate) and (Moisture is Dry) and (Oxygen is Low) then (Relative__Aging is Low) (1)
14. If (Temp__Change is Moderate) and (Moisture is Dry) and (Oxygen is Medium) then (Relative__Aging is Low) (1)
15. If (Temp__Change is Moderate) and (Moisture is Dry) and (Oxygen is High) then (Relative__Aging is Moderate) (1)
16. If (Temp__Change is Moderate) and (Moisture is Moderate) and (Oxygen is Low) then (Relative__Aging is Low) (1)
17. If (Temp__Change is Moderate) and (Moisture is Moderate) and (Oxygen is Medium) then (Relative__Aging is Moderate) (1)
18. If (Temp__Change is Moderate) and (Moisture is Moderate) and (Oxygen is High) then (Relative__Aging is High) (1)
19. If (Temp__Change is Moderate) and (Moisture is Critical) and (Oxygen is Low) then (Relative__Aging is High) (1)
20. If (Temp__Change is Moderate) and (Moisture is Critical) and (Oxygen is Medium) then (Relative__Aging is Significant) (1)
21. If (Temp__Change is Moderate) and (Moisture is Critical) and (Oxygen is High) then (Relative__Aging is Significant) (1)
22. If (Temp__Change is Critical) and (Moisture is Dry) and (Oxygen is Low) then (Relative__Aging is Moderate) (1)
23. If (Temp__Change is Critical) and (Moisture is Dry) and (Oxygen is Medium) then (Relative__Aging is Moderate) (1)
24. If (Temp__Change is Critical) and (Moisture is Dry) and (Oxygen is High) then (Relative__Aging is High) (1)
25. If (Temp__Change is Critical) and (Moisture is Moderate) and (Oxygen is Low) then (Relative__Aging is Moderate) (1)
26. If (Temp__Change is Critical) and (Moisture is Moderate) and (Oxygen is Medium) then (Relative__Aging is High) (1)
27. If (Temp__Change is Critical) and (Moisture is Moderate) and (Oxygen is High) then (Relative__Aging is Significant) (1)
28. If (Temp__Change is Moderate) and (Moisture is Wet) and (Oxygen is Low) then (Relative__Aging is Significant) (1)
29. If (Temp__Change is Moderate) and (Moisture is Wet) and (Oxygen is Medium) then (Relative__Aging is Significant) (1)
30. If (Temp__Change is Moderate) and (Moisture is Wet) and (Oxygen is High) then (Relative__Aging is Significant) (1)
31. If (Temp__Change is Critical) and (Moisture is Critical) and (Oxygen is Low) then (Relative__Aging is Significant) (1)
32. If (Temp__Change is Critical) and (Moisture is Critical) and (Oxygen is Medium) then (Relative__Aging is Significant) (1)
33. If (Temp__Change is Critical) and (Moisture is Critical) and (Oxygen is High) then (Relative__Aging is Significant) (1)

Appendix P Fuzzy Rules: Thermal Fault Criticality Model

1. If (Ethylene is Low) and (Ethane is Low) then (Thermal__Criticality is Normal) (1)
2. If (Ethylene is Low) and (Ethane is Alarm) then (Thermal__Criticality is Low) (1)
3. If (Ethylene is Low) and (Ethane is Critical) then (Thermal__Criticality is High) (1)
4. If (Ethylene is Low) and (Ethane is Danger) then (Thermal__Criticality is Significant) (1)
5. If (Ethylene is Alarm) and (Ethane is Low) then (Thermal__Criticality is Low) (1)
6. If (Ethylene is Alarm) and (Ethane is Alarm) then (Thermal__Criticality is Low) (1)
7. If (Ethylene is Alarm) and (Ethane is Critical) then (Thermal__Criticality is High) (1)
8. If (Ethylene is Alarm) and (Ethane is Danger) then (Thermal__Criticality is Significant) (1)
9. If (Ethylene is Critical) and (Ethane is Low) then (Thermal__Criticality is High) (1)
10. If (Ethylene is Critical) and (Ethane is Alarm) then (Thermal__Criticality is High) (1)
11. If (Ethylene is Critical) and (Ethane is Critical) then (Thermal__Criticality is High) (1)
12. If (Ethylene is Critical) and (Ethane is Danger) then (Thermal__Criticality is Significant) (1)
13. If (Ethylene is Danger) and (Ethane is Low) then (Thermal__Criticality is Significant) (1)
14. If (Ethylene is Danger) and (Ethane is Alarm) then (Thermal__Criticality is Significant) (1)
15. If (Ethylene is Danger) and (Ethane is Critical) then (Thermal__Criticality is Significant) (1)
16. If (Ethylene is Danger) and (Ethane is Danger) then (Thermal__Criticality is Significant) (1)

Appendix Q Fuzzy Rules: Electrical Fault Criticality Model

1. If (Methane is Low) and (Acetylene is Low) then (Electrical__Criticality is Normal) (1)
2. If (Methane is Low) and (Acetylene is Alarm) then (Electrical__Criticality is Low) (1)
3. If (Methane is Low) and (Acetylene is Critical) then (Electrical__Criticality is High) (1)
4. If (Methane is Low) and (Acetylene is Danger) then (Electrical__Criticality is Significant) (1)
5. If (Methane is Alarm) and (Acetylene is Low) then (Electrical__Criticality is Low) (1)
6. If (Methane is Alarm) and (Acetylene is Alarm) then (Electrical__Criticality is Low) (1)
7. If (Methane is Alarm) and (Acetylene is Critical) then (Electrical__Criticality is High) (1)
8. If (Methane is Alarm) and (Acetylene is Danger) then (Electrical__Criticality is Significant) (1)
9. If (Methane is Critical) and (Acetylene is Low) then (Electrical__Criticality is High) (1)
10. If (Methane is Critical) and (Acetylene is Alarm) then (Electrical__Criticality is High) (1)
11. If (Methane is Critical) and (Acetylene is Critical) then (Electrical__Criticality is High) (1)
12. If (Methane is Critical) and (Acetylene is Danger) then (Electrical__Criticality is Significant) (1)
13. If (Methane is Danger) and (Acetylene is Low) then (Electrical__Criticality is Significant) (1)
14. If (Methane is Danger) and (Acetylene is Alarm) then (Electrical__Criticality is Significant) (1)
15. If (Methane is Danger) and (Acetylene is Critical) then (Electrical__Criticality is Significant) (1)
16. If (Methane is Danger) and (Acetylene is Danger) then (Electrical__Criticality is Significant) (1)

Appendix R Fuzzy Rules: Overall Thermal-Electrical Fault Criticality Model

1. If (Thermal is Normal) and (Electrical is Normal) then (Faults__Probability2 is Normal) (1)
2. If (Thermal is Normal) and (Electrical is Low) then (Faults__Probability2 is Low) (1)
3. If (Thermal is Normal) and (Electrical is High) then (Faults__Probability2 is High) (1)
4. If (Thermal is Normal) and (Electrical is Significant) then (Faults__Probability2 is Significant) (1)
5. If (Thermal is Low) and (Electrical is Normal) then (Faults__Probability2 is Low) (1)
6. If (Thermal is Low) and (Electrical is Low) then (Faults__Probability2 is Low) (1)
7. If (Thermal is Low) and (Electrical is High) then (Faults__Probability2 is High) (1)
8. If (Thermal is Low) and (Electrical is Significant) then (Faults__Probability2 is Significant) (1)
9. If (Thermal is High) and (Electrical is Normal) then (Faults__Probability2 is High) (1)
10. If (Thermal is High) and (Electrical is Low) then (Faults__Probability2 is High) (1)
11. If (Thermal is High) and (Electrical is High) then (Faults__Probability2 is High) (1)
12. If (Thermal is High) and (Electrical is Significant) then (Faults__Probability2 is Significant) (1)
13. If (Thermal is Significant) and (Electrical is Normal) then (Faults__Probability2 is Significant) (1)
14. If (Thermal is Significant) and (Electrical is Low) then (Faults__Probability2 is Significant) (1)
15. If (Thermal is Significant) and (Electrical is High) then (Faults__Probability2 is Significant) (1)
16. If (Thermal is Significant) and (Electrical is Significant) then (Faults__Probability2 is Significant) (1)

Appendix S Fuzzy Rules: IFT Criticality Model

-
1. If (IFT is Bad) and (IFT__Rate is Good) then (Contamination is Significant) (1)
 2. If (IFT is Bad) and (IFT__Rate is Moderate) then (Contamination is Significant) (1)
 3. If (IFT is Bad) and (IFT__Rate is Critical) then (Contamination is Significant) (1)
 4. If (IFT is Critical) and (IFT__Rate is Good) then (Contamination is High) (1)
 5. If (IFT is Critical) and (IFT__Rate is Moderate) then (Contamination is High) (1)
 6. If (IFT is Critical) and (IFT__Rate is Critical) then (Contamination is Significant) (1)
 7. If (IFT is Moderate) and (IFT__Rate is Good) then (Contamination is Normal) (1)
 8. If (IFT is Moderate) and (IFT__Rate is Moderate) then (Contamination is Low) (1)
 9. If (IFT is Moderate) and (IFT__Rate is Critical) then (Contamination is High) (1)
 10. If (IFT is Health) and (IFT__Rate is Good) then (Contamination is Normal) (1)
 11. If (IFT is Health) and (IFT__Rate is Moderate) then (Contamination is Normal) (1)
 12. If (IFT is Health) and (IFT__Rate is Critical) then (Contamination is Low) (1)

Appendix T Fuzzy Rules: Remnant Life Estimation Model

1. If (Paper__Life is EndLife) and (Relative_Aging is Normal) then (Transformer__Life is EndLife) (1)
2. If (Paper__Life is EndLife) and (Relative_Aging is Low) then (Transformer__Life is EndLife) (1)
3. If (Paper__Life is EndLife) and (Relative_Aging is Moderate) then (Transformer__Life is EndLife) (1)
4. If (Paper__Life is EndLife) and (Relative_Aging is High) then (Transformer__Life is EndLife) (1)
5. If (Paper__Life is EndLife) and (Relative_Aging is Significant) then (Transformer__Life is EndLife) (1)
6. If (Paper__Life is HighRisk) and (Relative_Aging is Normal) then (Transformer__Life is HighRisk) (1)
7. If (Paper__Life is HighRisk) and (Relative_Aging is Low) then (Transformer__Life is EndLife) (1)
8. If (Paper__Life is HighRisk) and (Relative_Aging is Moderate) then (Transformer__Life is EndLife) (1)
9. If (Paper__Life is HighRisk) and (Relative_Aging is High) then (Transformer__Life is EndLife) (1)
10. If (Paper__Life is HighRisk) and (Relative_Aging is Significant) then (Transformer__Life is EndLife) (1)
11. If (Paper__Life is Excessive) and (Relative_Aging is Normal) then (Transformer__Life is Excessive) (1)
12. If (Paper__Life is Excessive) and (Relative_Aging is Low) then (Transformer__Life is HighRisk) (1)
13. If (Paper__Life is Excessive) and (Relative_Aging is Moderate) then (Transformer__Life is EndLife) (1)
14. If (Paper__Life is Excessive) and (Relative_Aging is High) then (Transformer__Life is EndLife) (1)
15. If (Paper__Life is Excessive) and (Relative_Aging is Significant) then (Transformer__Life is EndLife) (1)
16. If (Paper__Life is Accelerated) and (Relative_Aging is Normal) then (Transformer__Life is Accelerated) (1)
17. If (Paper__Life is Accelerated) and (Relative_Aging is Low) then (Transformer__Life is Excessive) (1)
18. If (Paper__Life is Accelerated) and (Relative_Aging is Moderate) then (Transformer__Life is HighRisk) (1)
19. If (Paper__Life is Accelerated) and (Relative_Aging is High) then (Transformer__Life is EndLife) (1)
20. If (Paper__Life is Accelerated) and (Relative_Aging is Significant) then (Transformer__Life is EndLife) (1)
21. If (Paper__Life is Normal) and (Relative_Aging is Normal) then (Transformer__Life is Normal) (1)
22. If (Paper__Life is Normal) and (Relative_Aging is Low) then (Transformer__Life is Accelerated) (1)
23. If (Paper__Life is Normal) and (Relative_Aging is Moderate) then (Transformer__Life is Excessive) (1)
24. If (Paper__Life is Normal) and (Relative_Aging is High) then (Transformer__Life is HighRisk) (1)
25. If (Paper__Life is Normal) and (Relative_Aging is Significant) then (Transformer__Life is EndLife) (1)

Appendix V Transformer Condition

V.1 Pre-known Condition of Sixteen Transformers

Sample	Real Age (Years)	Trans. Status	Description
1	4	Good	New and healthy transformer
2	2	Good	New and healthy transformer
3	18	Good	Healthy transformer, but CO exceed limits
4	22	Good	Aged and healthy transformer.
5	35	Average	Aged transformer with average paper degradation. Oil is contaminated.
6	28	Average	Aged transformer with average paper degradation. Oil is contaminated.
7	30	Average	Aged transformer with average paper degradation. No faults detected, but Ethane exceeds safety limits.
8	23	Average	Aged transformer with accelerated paper degradation. Paper is nearly wet and oil is moderately contaminated.
9	38	Poor	Faulty transformer (arcing in oil). Average paper degradation.
10	25	Poor	Faulty transformer (Failed tap changer). Normal paper degradation. Acetylene level is very high. Oil is contaminated.
11	42	Poor	Aged transformer with average paper degradation. High Oxygen concentration. Oil is too contaminated.
12	49	Poor	Aged transformer with average paper degradation. Paper is wet and highly risk for failure.
13	56	Bad	Aged transformer with accelerated paper degradation. Paper is wet and highly risk for failure. Oil is very contaminated.
14	50	Bad	Faulty transformer (Thermal faults exceeding 700°C). Excessive paper degradation. Very high Oxygen concentration.
15	63	Bad	Aged transformer with excessive paper degradation. Oil is contaminated.
16	36	Bad	Aged transformer with excessive paper degradation. Paper is nearly wet and oil is contaminated.

Appendix W Validation Results of Transformer Remnant Life Model

Sample	Temp. Rise	Water Content	Oxygen	Furan	Furan K _{rate}	CO ₂ /CO Ratio*	CO Rate	Ethylene	Ethane	Methane	Acetylene	IFT	IFT Rate	Model Output (D ₁)	Model Output (D ₂)	Model Output (D ₃)	Code Apply	Model Condition	Actual Condition
1	1	0.6	500	<0.01	0	18	5	2	3	4	0	40	0.2	91%	0.98	0.97	1	VG	G
2	1	0.45	180	<0.01	0	10	0	0	0	0	0	42	0.1	93%	0.9	0.9	1	VG	G
3	1	0.8	800	<0.01	0	2	22	2	4	22	0	40	0.2	89%	1.8	1.2	4	G	G
4	1	0.45	1050	0.23	0.01	10	5	9	1	1	0	40	0.2	67%	1.8	1.2	4	G	G
5	1	0.65	800	<0.01	0	10	10	2	4	10	0	40	0.2	89%	1.8	1.2	4	G	G
6	1	0.85	1105	<0.01	0	10	5	10	0	4	0	40	0.2	89%	1.8	1.2	4	G	G
7	1	0.45	520	<0.01	0	11	0	0	0	0	0	42	0.1	93%	0.9	0.9	1	VG	G
8	1	0.65	900	<0.01	0	10	3	0	0	2	0	42	0.1	91%	1.8	0.9	3	G	G
9	2	0.8	988	0.01	0	9	5	2	2	10	0	39	0.1	89%	1.8	1.2	4	G	G
10	2	0.8	860	<0.01	0	10	5	2	5	10	0	39	0.1	91%	1.8	1.2	4	G	G
11	1	0.45	750	<0.01	0	11	0	0	5	10	0	42	0.1	93%	0.9	0.9	1	VG	G
12	1	1	880	0.01	0	8	5	5	9	15	0	37	0.1	85%	0.9	1.8	2	G	G
13	1	0.85	1021	<0.01	0	10	5	0	0	10	0	40	0.1	91%	1.2	1.2	4	G	G
14	2	0.85	880	0.02	0	9	5	12	0	10	0	40	0.1	89%	1.2	1.2	4	G	G
15	1	0.65	900	<0.01	0	10	4	0	0	0	0	43	0	93%	0.9	0.9	1	VG	G
16	1	0.65	880	<0.01	0	10	0	0	1	5	0	42	0	93%	0.9	0.9	1	VG	G
17	2	0.95	880	<0.01	0	9	5	0	1	1	0	40	0.1	91%	0.9	0.9	1	VG	G
18	1	0.65	1450	<0.01	0	8	3	0	5	5	0	40	0.1	91%	0.9	1.8	2	G	G
19	2	1	1511	0.01	0	9	10	10	0	23	0	39	0.1	87%	1.8	1.8	4	G	G
20	2	1	850	0.01	0	11	4	2	1	12	0	38	0.1	87%	1.2	1.8	4	G	G
21	2	0.98	1131	0.01	0	7	10	5	0	15	0	38	0.1	87%	1.8	1.8	4	G	G
22	2	1.2	1890	0.01	0	6	15	0	0	15	0	36	0.1	91%	2.2	1.2	5	A	G
23	2	1	1510	0.61	0.01	10.6	10	2	2	3	3	16	0.8	63%	1.87	3.6	6	A	A
24	2	0.8	1200	0.25	0.01	10	5	3	1	2	0	20	0.5	65%	1.8	3.6	6	A	A
25	2	0.85	158	0.12	0.02	10	5	7	90	23	0	32	0.5	63%	2.6	1.9	7	A	A
26	1	2	1817	1.05	0.05	11	8	31	9	29	0	28	0.8	38%	2.7	3.5	9	A	A
27	2	1.1	1620	0.61	0.01	9	8	5	5	3	0	18	0.8	63%	1.87	3.6	6	A	A
28	2	0.85	980	0.32	0.01	11	15	9	3	12	0	23	0.5	65%	1.8	3.6	6	A	A
29	2	0.85	1580	0.1	0.01	10	10	11	78	33	0	35	0.5	64%	2.6	1.9	7	A	A
30	1	1.8	1827	1.1	0.05	9	10	35	21	38	0	26	0.8	44%	2.7	3.5	9	A	A
31	2	1.4	2101	0.05	0	10	5	10	5	13	0	39	0.1	89%	2.2	1.2	5	A	A
32	1	0.85	890	<0.01	0	10	3	5	5	18	0	26	0.4	89%	1.8	3.6	6	A	A
33	1	1.1	981	0.1	0.01	9	5	11	7	21	0	26	0.4	75%	1.8	3.6	6	A	A
34	2	1.2	1988	0.21	0.01	8	5	15	15	32	0	28	0.5	68%	1.8	3.6	6	A	A
35	2	1.8	1892	0.1	0.01	6	10	10	8	15	0	32	0.4	68%	2.2	2.2	8	A	A
36	1	1.2	912	0.1	0.01	3	13	11	15	29	0	30	0.4	58%	2.2	2.2	8	A	A
37	2	1.6	1511	0.25	0.01	8	10	15	18	35	0	28	0.5	63%	3.2	2.2	10	P	A
38	2	0.9	1515	0.3	0.01	10	10	458	14	286	884	52	0.4	63%	3.6	4.8	12	P	P
39	2	1	780	0.11	0.01	10	10	13	1	3	73	25	0.5	63%	3.6	4.8	12	P	P
40	2	2.6	3250	0.24	0.01	10	10	2	0	2	0	18	0.5	38%	3.7	3.6	11	P	P
41	2	3	4715	0.29	0.01	10	10	1	0	1	0	28	0.5	32%	3.2	2.1	10	P	P
42	2	1	890	0.15	0.01	9	10	8	1	3	45	28	0.5	63%	3.6	4.8	12	P	P
43	2	2.2	2850	0.35	0.01	10	10	12	5	10	0	20	0.5	38%	3.7	3.6	11	P	P
44	1	3	4511	0.41	0.01	8	10	5	5	10	0	30	0.5	32%	3.2	2.1	10	P	P
45	2	3	5112	0.99	0.05	4.9	10	8	7	34	0	14	1	31%	4.3	3.6	14	B	B
46	2	0.85	30280	1.38	0.05	10	5	150	18	55	22	41	0.2	22%	4.8	4.8	15	B	B
47	2	1.1	2680	4.46	0.1	5.8	20	7	10	39	0	20	0.5	19%	5.2	5.5	18	VB	B
48	2	1.8	1700	5.53	0.1	3	40	15	18	22	0	19	0.5	7%	5.6	5.6	18	VB	B
49	2	2.8	11021	1.23	0.05	6	18	14	10	66	0	16	1	31%	4.3	3.6	14	B	B
50	2	3	28800	1.56	0.05	5	10	98	35	78	35	38	0.2	28%	4.8	4.8	15	B	B